UNIVERSITY OF LONDON THESIS

Degree PhD Year 2007 Name of Author SAAD, Mai Mohamed Abd El-Aziz El-Anwar

Molecular Genetics of Autosomal Recessive Retinitis Pigmentosa

A THESIS SUBMITTED TO THE UNIVERSITY OF LONDON

FOR THE DEGREE OF DOCTOR OF PHILOSOPHY

Mai Mohamed Abd El-Aziz El-Anwar Saad

MB ChB, M Sc

DEPARTMENT OF MOLECULAR GENETICS

INSTITUTE OF OPHTHALMOLOGY

UNIVERSITY COLLEGE LONDON

BATH STREET

LONDON

2007

ProQuest LLC
789 East Eisenhower Parkway
P.O. Box 1346
Ann Arbor, MI 48106-1346

Declaration

I, Mai Mohamed Abd El-Aziz El-Anwar Saad, declare that, unless otherwise sated, this thesis entitled "Molecular Genetics of Autosomal Recessive Retinitis Pigmentosa" and submitted to the University of London for the degree of Doctor of Philosophy is entirely my own original work and composition and has not been submitted for a degree at any other university.

Signed

Mai Mohamed Abd El-Aziz El-Anwar Saad MB ChB MSc

Date:

ABSTRACT

Autosomal recessive retinitis pigmentosa (arRP) is one of the commonest forms of monogenic retinal degeneration (RD). To date, 24 loci have been implicated in the pathogenesis of arRP. The genes for five of these loci (RP22, RP25, RP28, RP29 and RP32), still remain to be identified. This thesis mainly focused on the cloning of a major gene (RP25); however identifying novel loci for recessive RP constituted a significant objective.

Originally the RP25 locus was mapped to chromosome 6p12.1-q15, a region that spans 34 Mb, by our collaborators in Seville in seven Spanish families. Initially, a whole-genome scan in these families was undertaken using GeneChip 10K array. The data obtained confirmed the initial findings of linkage to the RP25 region. To date, 61 out of 111 genes within the interval (~55%) have been excluded as disease causing by direct sequence analysis. A large number of single nucleotide polymorphisms (SNPs), of which a significant percentage was novel were identified. We have also postulated that both RP25 and Leber congenital amaurosis 5 (LCA5), a severe form of RD, could be due to the same genetic defect since they genetically overlap. Therefore, seventeen LCA families were genotyped to identify new LCA5 families that may further refine the RP25 interval by identifying novel crossovers. However, the gene for LCA5 has been recently cloned and sequence analysis of the RP25 families rules out this gene as causative of RP25.

To investigate if copy number variations (CNVs) exist within the RP25 interval, a comparative genome hybridisation (CGH) was performed on one of the RP25 families (RP5). A clone from the tiling path, chr6tp-19C7, within 6q12 was observed

to be deleted in all affected members of this family indicating that one of the genes within this interval could be responsible for the RP25 phenotype.

A novel approach utilising the 10K GeneChip for identifying the disease locus in three non-consanguineous Chinese families with arRP was implemented. The studied families were probably linked to the RP25 locus; proposing that this approach could be a useful tool for genetic mapping in cases of rare and genetically heterogeneous recessive traits.

Finally, in parallel, a genomewide linkage search in a consanguineous family with arRP was undertaken. Linkage to a 10-cM interval on chromosome 10q23.1-23.3 was observed where a good candidate gene, protocadherin-21 (*PCDH21*), is located. A homozygous 1-bp deletion was identified in this family in addition to two other novel mutations in two different patients raising the possibility that *PCDH21* is likely to be a novel gene for RP.

Dedication

I dedicate my thesis to my parents and my sisters, Lamiss and Maha whom their continuous emotional support was always a great motivation for me. I also dedicate it to my talented husband, Mohamed El-Ashry, who was always supportive and helpful. I also have a very special dedication to my little sons, Ahmed and Mahmoud, who sometimes came along over the weekends to finish off some work and even though still very young, they love science.

Acknowledgments

First of all thanks to ALLAH to whom I owe everything in my life and for giving me the strong determination to finish off this piece of work.

I would like to thank my supervisors, Shomi Bhattacharya and Alison Hardcastle for all the support, guidance and encouragement throughout the project. Shomi, I am deeply grateful for your understanding and support during every single step of this work. I have to say that it is not only science I have learnt but priceless knowledge and experience on how to lead a project and be successful at the end. Alison, I am grateful for your help and support.

I would like to thank Guillermo Antiñolo for collaboration and supporting my work. I also like to thank Isabel Barragan, the dearest friend, whom I shared all the strategies and the non-stop thinking and ideas all the way through the project. It has been a great pleasure to work alongside during the time you spent here in London. I also have to acknowledge my colleague Ciara O'driscoll, who recently started working on this project, your great enthusiasm has been a positive step towards the success of the project. Thanks also to Leen Abu Safieh and Rowaida Taha.

I have to extend my gratitude to every one in my group Christina, Naushin, Venita, Cecilia, Brotati, Amna, Francesca, Kinga, Beverlay and Quincy. I also acknowledge the library staff, Debbie Heatlie and Desta Pokre for their emotional support and their help in renewing my books and keeping my fines to the minimum.

I wish to particularly thank Christina Chakarova and Naushin Waseem for your emotional support in the downs times. Your support has been always appreciated. A big thank you to Brotati Veritch who has been always vigilant on my pictures particularly the flow chart one.

Last but not least to my husband, Mohamed El-Ashry, to my sons, Ahmed and Mahmoud and my nanny, Soad. Truly, I can say that without your support this thesis would not come to the light. Thank you ever and forever.

PUBLICATIONS AND PRESENTATIONS ARISING FROM THIS WORK

Publications

1. **Abd El-Aziz, M.M.**, El-Ashry, M.F., Chan, W.M., Chong, K.L., Barragán, I., Antiñolo, G., Pang, C.P. and Bhattacharya, S.S. (2007) A novel genetic study of Chinese families with autosomal recessive retinitis pigmentosa. *Ann. Hum. Genet.* **71**(3): 281-294.

2. **Abd El-Aziz, M.M.**, Patel, R.J., El-Ashry, M.F., Barragán, I., Marcos, I., Borrego, S., Antiñolo, G. and Bhattacharya SS. (2006) Exclusion of four candidate genes, *KHDRBS2*, *PTP4A1*, *KIAA1411* and *OGFRL1*, as causative of autosomal recessive retinitis pigmentosa. *Ophthalmic Res.* **38**(1): 19-23.

3. **Abd El-Aziz, M.M.**, El-Ashry, M.F., Barragan, I., Marcos, I., Borrego, S., Antinolo, G. and Bhattacharya SS. (2005) Molecular genetic analysis of two functional candidate genes in the autosomal recessive retinitis pigmentosa, RP25, locus. *Curr Eye Res.* **30**(12):1081-1087.

4. Barragán I, Borrego S, **Abd El-Aziz MM**, El-Ashry MF, Abu-Safieh L., Bhattacharya SS, Antiñolo G.1. Genetic analysis of *FAM46A* in Spanish families with autosomal recessive retinitis pigmentosa: Characterisation of novel VNTRs. Accepted for publication in *Ann. Hum. Genet.*

5. Henderson RH*, **Abd El-Aziz MM***, El-Ashry MF, O'Driscoll C, El-Jinini A, Pierce K, Zaidi M, Moore AT, Bhattacharya SS, Webster AR. Protocadherin-21 (*PCDH21*), a Novel Gene for Juvenile-Onset Recessive Retinitis Pigmentosa. A manuscript submitted to the *AJHG* * Joint first authors.

Presentations

1. **Abd El-Aziz MM**, Patel RJ, El-Ashry MF, Barragan I, Marcos I, Borrego S, Antinolo G, Bhattacharya SS. (2005) Mutation screening of four candidate genes, *KHDRBS2*, *PTP4A1*, *KIAA1411* and *OGFRL1*, in the autosomal recessive retinitis pigmentosa (RP25) critical interval. *Invest. Ophthalmol. Vis. Sci.* 46(4): ARVO E-Abstract 1808.

2. **Abd El-Aziz MM**, El-Ashry MM, Abu Safieh L, Chan WM, Pang CP, Bhattacharya SS. (2006) Linkage of Chinese families with autosomal recessive retinitis pigmentosa to the RP25 Locus. *Invest. Ophthalmol. Vis. Sci.* ARVO E-Abstract (3273/B743).

Table of Contents

CHAPTER 3

IDENTIFICATION OF THE CAUSATIVE GENE FOR THE RP25 LOCUS

CHAPTER 4

A NOVEL GENETIC STUDY OF CHINESE FAMILIES WITH ARRP

CHAPTER 5

PROTOCADHERIN-21 (*PCDH21*), A NOVEL GENE FOR AUTOSOMAL RECESSIVE RETINAL DEGENERATION

LIST OF TABLES

Page no.

LIST OF FIGURES

LIST OF ABBREVIATIONS

A: Adenine

ABI: Applied Biosystems Incorporated

aCGH: Array-based comparative genome hybridisation

Ach: Acetylcholine

ALMS1: Alstorm syndrome

ad: Autosomal dominant

adMD: Autosomal dominant macular dystrophy

AMD: Age related macular degeneration

ar: Autosomal recessive

BACs: Bacterial artificial chromosomes

bp: Base pair

BBS: Bardet-Biedl syndrome

BCAMD: Benign concentric annular macular dystrophy

C: Cytosine

Ca^{2+}: Calcium

CD: Circular dichroism

cDNA: Complementary deoxyribonucleic acid

CEPH: The Centre d'Etudes du Polymorphisme Humaine (Paris)

cGMP: Cyclic guanine monophosphate

cGMP-PDE: cGMP-phosphodiesterase

CHLC: Co-operative Human Linkage Centre

CKN: Cockayne syndrome

CNVs: Copy number variations

COH1: Cohen syndrome

cM: CentiMorgan

CNS: Central nervous system

CSNB: Congenital stationary night blindness

CORD: Cone-rod dystrophy

DA: Dopamine

DNA: Deoxyribonucleic acid

dNTP: Deoxynucleotide triphosphate

dHPLC: Denaturing high performance liquid chromatography

ECs: Extracellular domains

EDTA: Ethylenediamine-tetra acetic acid

EGF: Epidermal growth factor

ERG: Electroretinography

ESTs: Expressed sequence tags

FA: Fundus albipunctatus

G: Guanine

GABA: γ-aminobutyric acid

GDB: Genome database

HGMP: Human Genome Mapping Project

HIV-1: Human Immunodeficiency Virus-1

HS: Hierarchical shotgun approach

IOP: Intra-ocular pressure

IPM: Interphotoreceptor matrix

JBTS1: Joubert syndrome

Kb: Kilobase

LCA: Leber congenital amaurosis

LD: Linkage disequilibrium

LOD: Likelihood of the odds

Mb: Megabase

MCDR1: North Carolina macular dystrophy

MHC: Major histocompatibility complex

Na^+: Sodium

mRNA: Messenger ribonucleic acid

NCBI: National Centre of Biotechnology Information

NEIBank: The National Eye Institute Bank

NIH: National Institute of Health

NO: Nitric oxide

OMIM: Online Mendelian Inheritance in Man

ORF: Open reading frame

PBCRA: Progressive bifocal chorioretinal atrophy

PCR: Polymerase Chain Reaction

PIC: Polymorphic Information content

PKC: Protein kinase

PTT: Protein truncation test

RFLP: Restriction Fragment Length Polymorphism

RDs: Retinal dystrophies

RPA: Retinitis punctata albescens

RPE: Retinal pigment epithelium

RNA: Ribonucleic acid

ROS: rod outer segment

SAGE: Serial Analysis of Gene Expression

SNPs: Single Nucleotide Polymorphisms

SSCP: Single strand confirmation polymorphism

STGD: Stargardt's disease

STGD3: Autosomal dominant Stargardt-like disease

STRPs: Short Tandem Repeat Polymorphisms

θ: Theta, recombination fraction

T: Thymine

TBE: Tri-borate-EDTA Buffer

TCAG: Database for genome variants

T: Transducin

USH1: Usher syndrome type I

UTRs: Untranslated regions

VNTRs: Variable number tandem repeats

WGS: whole-genome shotgun

Z: Lod score

Amino acids codes

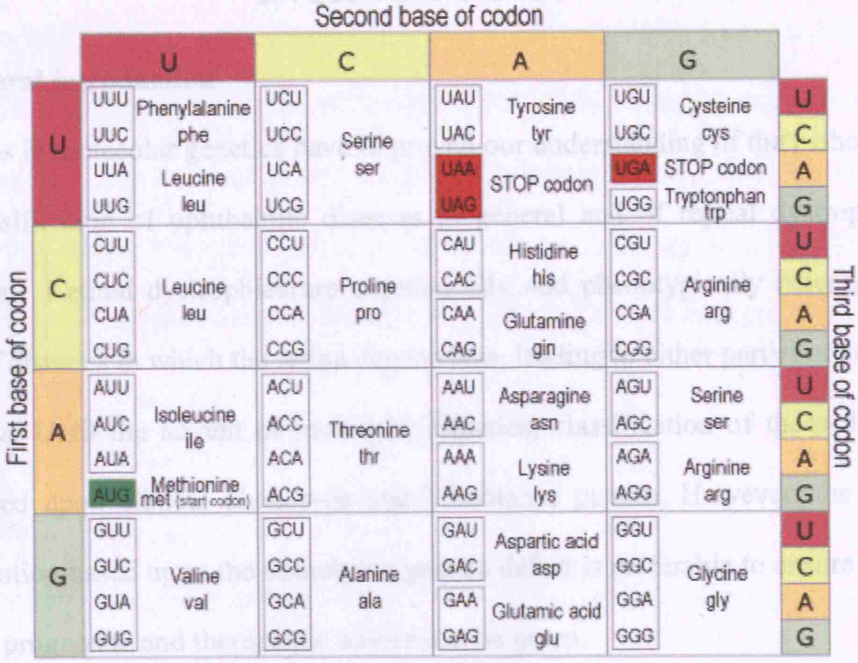

Amino acid names

Single-letter code	Abbreviation	Full name	Single-letter code	Abbreviation	Full name
A	Ala	Alanine	Q	Gln	Glutamine
R	Arg	Arginine	E	Glu	Glutamatic acid
N	Asn	Asparagine	G	Gly	Glysine
D	Asp	Aspartic acid	H	His	Histidine
C	Cys	Cysteine	I	Ile	Isoleucine
L	Leu	Leucine	S	Ser	Serine
K	Lys	Lysine	T	Thr	Threonine
M	Met	Methionine	W	Trp	Tryptophan
F	Phe	Phenylalanine	Y	Tyr	Tyrosine
P	Pro	Proline	V	Val	Valine

CHAPTER ONE

INTRODUCTION

1.1 General introduction

Advances in molecular genetics have improved our understanding of the pathogenesis and classification of ophthalmic diseases in general and of retinal dystrophies in particular. Retinal dystrophies are a genetically and phenotypically heterogeneous group of diseases in which the retina degenerates, leading to either partial or complete blindness. Until the advent of molecular genetics, classification of these disorders was based upon clinical phenotype and inheritance pattern. However, the present classification based upon the underlying genetic defect is preferable to ensure the best genetic, prognostic and therapeutic advice can be given.

A better understanding of normal retinal physiology and pathobiology can be achieved through identification of retinal disease genes. Subsequently, it is possible to develop cell culture techniques and animal models to study the functions of the relevant genes. This will ultimately lead to the innovation of better methods for the treatment of retinal dystrophies using chemical agents, gene therapy or stem cell therapy.

The work in this thesis concerns the identification of a major gene (RP25) in seven Spanish families with autosomal recessive retinitis pigmentosa (arRP). This was followed by implementing a novel approach utilising the 10K GeneChip array for identifying the disease locus in three non-consanguineous Chinese families with arRP. Finally, in parallel, a linkage to a 10-cM interval on chromosome 10q23.1-23.3 in a consanguineous family with recessive RP was identified. A good candidate gene,

protocadherin-21 (*PCDH21*), was localised within this interval and our findings suggest that it is likely to be a novel gene for recessive RP.

Therefore in the following sections an overview of the genetic concepts behind the project is described in more detail with explanation of the strategies employed for the identification of the RP25 gene and for genetic mapping of new families to known genes or novel loci. The reader will also be introduced to the development, structure, and function of the retina, and to the pathological and genetic background of retinal dystrophy.

1.2 Retina

The retina is the simplest and best-studied part of the central nervous system (CNS) and has characteristic features, making it an ideal tissue for scientists to study. Moreover, it is the only place in the body where blood vessels at the arteriolar level can be seen, making it a window for diagnosis of CNS and cardiovascular system diseases.

1.2.1 Gross anatomy

The retina is the innermost layer of the eye ball and it has two main components, a sensory layer and a pigmented layer. The neural retina is a thin, delicate layer of nervous tissue that has a surface area of about 266 mm^2. The major landmarks of the retina are the optic disc, the retinal blood vessels, the area centralis with the fovea and foveola and the peripheral retina. The macula is located roughly in the center of the retina, temporal to the optic nerve. The fovea is the very centre of the macula and is highly sensitive part of the retina responsible for detailed central vision. It allows us

to appreciate details and perform tasks that require central vision such as reading (Bron *et al.*, 2003) (Figure 1.1).

In the normal human eye, the optic disc is a circular to slightly oval structure that measures approximately 1.5 mm in diameter. The area centralis or central retina is divided into the fovea which marks the approximate centre of the area centralis and the foveola which represents the area of highest visual acuity in the retina. This is due to both its avascular nature and to the sole presence of cone photoreceptor cells. The peripheral retina is divided into four regions: the near periphery, the mid-periphery, the far periphery and the ora serrata. The near periphery occupies a circumscribed region of 1.5 mm around the area centralis, and the mid-periphery is 3 mm-wide zone around the near periphery. The far periphery is a region that extends 10 mm and 16 mm on the temporal and nasal sides of the optic disc, respectively. The most anterior region of the retina is the orra serrata, which consists of dentate fringe, and which denotes the termination of the retina (Sigelman and Ozanics, 1982) (Figure 1.1).

1.2.2 Microscopic anatomy

Cross-section by light microscopy shows that the retina is composed of 10 layers (Figure 1.2).

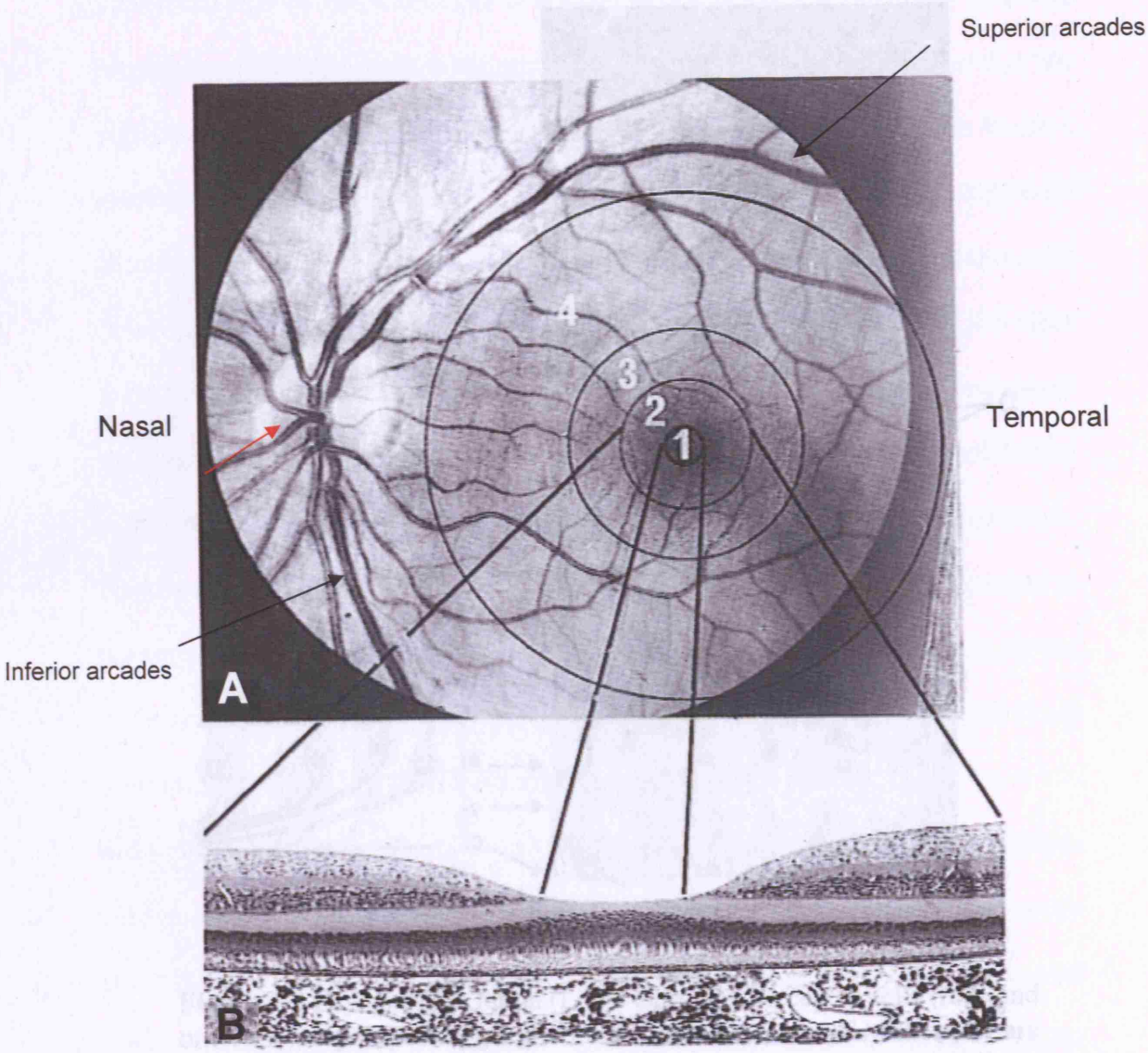

Figure 1.1 (A) Fundus photograph of left human Eye showing topographic demarcation of the area centralis (Macula, is the region between superior and inferior aracades) and its sub-divisions (inner circles) (1) foveola; (2) fovea; (3) parafovea; (4) perifovea. Red arrow points to the optic disc. (B) Transverse section of the foveal retina matched to the fundus photograph shown in (A) (adapted from Bron *et al.*, 2003).

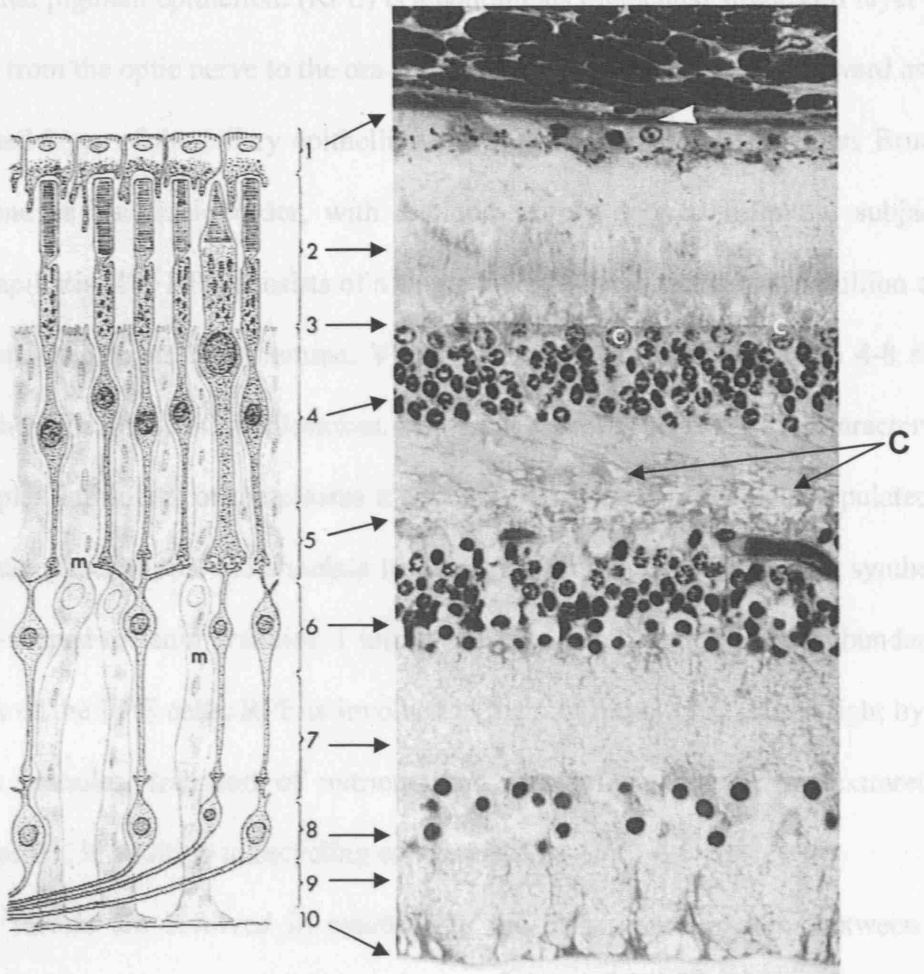

Figure 1.2 Layers of the retina (Left). Only photoreceptor cells (rods and one cone), bipolar cells, ganglion cells, and the fibres of Müller (m) are illustrated. The numbers refer to the layers 1. retinal pigment epithelium; 2. photoreceptor inner/outer segment of rods and cones; 3. external limiting membrane; 4. outer nuclear layer; 5. outer plexiform layer; 6. inner nuclear layer; 7. inner plexiform layer; 8. ganglion cell layer; 9. nerve fibre layer; and 10. internal limiting membrane. (Right) photomicrograph of same area (×400). At top is the inner portion of the choroids with choriocapillaries (white arrow head). Cone nuclei are indicated (c) (reproduced from Leeson and Leeson, 1976).

1.2.2.1 The retinal pigment epithelium

The retinal pigment epithelium (RPE) is a continuous pigmented single cell layer that extends from the optic nerve to the ora serrata, from which it continues forward as the pigmented layer of the ciliary epithelium (Bron *et al.,* 2003). The RPE has Bruch's membrane as its basal border, with a blood supply derived from the subjacent choriocapillaris. The RPE consists of a single layer of approximately 4-6 million cells firmly attached to its basal lamina. Viewed from above, RPE cells have 4-8 sides giving the appearance of cobblestones. The basal aspect of RPE cells is characterised by complex infoldings of the plasma membrane. This region of cells is populated by numerous mitochondria and annulate lamellae, which are active in protein synthesis. Spindle-shaped melanin granules, 1 μm in diameter and 2-3 μm long, are abundant at the apex of the RPE cells. RPE is involved in the absorption of scattered light by the melanin granules, transport of nutrients and metabolites through the extraretinal blood barrier, in addition to recycling of vitamin A.

Several factors are involved in maintaining the close approximation between the photoreceptor cell layer and the RPE layer. Passive forces, such as intraocular pressure (IOP), osmotic pressure, fluid transport across the RPE and the presence of the vitreous help preserve the position of the neural retina (Kita and Marmor, 1992). Meanwhile, interdigitations between the RPE microvilli and the photoreceptor outer segments provide a physical closeness between the two layers. Likewise, the material that occupies the space between the two layers provides adhesive forces (Hageman *et al.,* 1995). This material is known as interphotoreceptor matrix (IPM) and it has been postulated that it provides means for the exchange of metabolites and for interactions between the two layers (Sigelman and Ozanics, 1982). In addition, it may be partly

responsible for orienting the photoreceptor outer segments for optimum light capture (Hollyfield *et al.,* 1989).

1.2.2.2 Photoreceptor cells

The photoreceptors are highly specialised cells that convert light into nerve signals by a process called phototransduction. There are between 77 and 107 million (average 92 millions) rods which are responsible for vision in dim light and 4 to 5 million (average 4.6 millions) cones which are responsible for vision in bright illumination in the human eye. Human cone cells contain three different opsins sensitive to three different regions of the light spectrum in contrast to rods that contain the same opsin. The photoreceptor cells consist of a cell body, an outer and an inner segment, an inner fiber and sometimes an outer fibre connecting the cell body to the outer and inner segments. The outer segment is separated from the inner by a narrow connecting stalk, which actually has the structure of a cilium arising from a basal body in the inner segment. The outer segment of rods is made up of approximately 600 to 1000 discs systematically piled on each other. The rod outer segments are highly specialised for capturing photons, and they contain all the molecules necessary for converting light into an electrical impulse (Baylor, 1987). In cone cells the photopigment is not stored in membranous discs but rather in invaginations of the cytoplasmic membrane (Eckmiller, 1990). Moreover, the outer segments are short in comparison with rods and are broader at the proximal end than at the apical end (Figure 1.3).

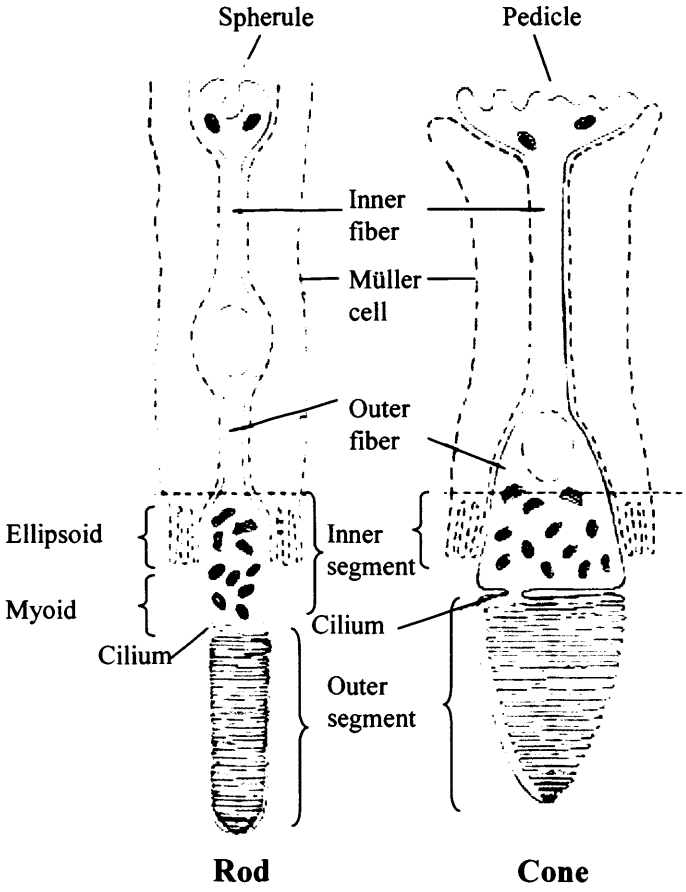

Figure 1.3 A diagrammatic representation of the photoreceptor cells. Portions of Müller cells (dotted lines) are shown adjoining the rods and cones (adapted from Krause and Cutts, 1981).

1.2.2.3 External limiting membrane

The outer limiting membrane is not a true membrane however it is a narrow zone with numerous zonulae adherence between Müller cells and photoreceptor cells. This structure has the potential to act as a metabolic barrier to the passage of some large molecules (Cohen, 1992).

1.2.2.4 Outer nuclear layer

The outer nuclear layer is created by the cell bodies of the photoreceptor cells. In the retinal periphery the rod cell bodies outnumber those of the cones and the opposite is true for the centre of the retina.

1.2.2.5 Outer plexiform layer

The outer plexiform layer is formed by the synapses between photoreceptor cells, bipolar cells and horizontal cells.

1.2.2.6 Inner nuclear layer

The inner nuclear layer contains four types of cells: horizontal cells which are located in the distal part of the nuclear layer, amacrine cells which are the most proximal part of this layer, bipolar and Müller cells which occupy the outer intermediate and the inner intermediate parts of the layer, respectively.

1.2.2.7 Inner plexiform layer

The inner plexiform layer is the place where bipolar, amacrine, and ganglion cells synapse. It contains the synapse between the first and the second-order neuron in the visual pathway.

1.2.2.8 Ganglion cell layer

Ganglion cell layer contains ganglion cells and numerous displaced amacrine cells.

1.2.2.9 Nerve fibre layer

This layer contains the axons of ganglion cells as they converge from all parts of the retina on their way to the optic nerve.

1.2.2.10 Internal limiting membrane

Internal limiting membrane forms the innermost boundary of the retina and is formed by the Müller cells end feet.

1.2.3 Ultrastructure of the neural retina

The neural retina consists of six neuron types: photoreceptor cells, horizontal cells bipolar cells, amacrine cells, interplexiform cells and ganglion cells. The neurons are in close contact with and are supported by the radial glial cells, which are called the Müller cells (Figure 1.4).

1.2.3.1 Photoreceptor cells

The rods and cones are at the distal end of the retina. The proximal ends of the photoreceptors contain the synaptic machinery that releases glutamate, an excitatory, chemical neurotransmitter that interacts with glutamate receptors found in the second-order neuron, the bipolar cells and horizontal cells.

1.2.3.2 Horizontal cells

The horizontal cells receive input from the photoreceptors and transfer information into the inner plexiform layer where they contact amacrine and ganglion cells. They have one long process or axon and several short dendrites with branching terminals; the processes spread out parallel to the retinal surface. Three types of horizontal cells have been described: HI, HII and HIII (Kolb *et al.,* 1992) (Figure 1.4).

1.2.3.3 Bipolar cells

Bipolar cells relay information from photoreceptor cells to ganglion cells or amacrine cells. The nucleus of the bipolar cell is large and contains little cell body cytoplasm. Only one variety of rod bipolar cells has been described in mammals, including humans, which is easily identified by its high content of the enzyme protein kinase C (PKC) (Kolb *et al.,* 1993). Primate cone bipolar cells can be divided into 8-10 different types according to their dendritic branching pattern, the number of cone cells contacted and the shape of their processes in the inner plexiform layer (Euler and Wassle, 1995).

1.2.3.4 Amacrine cells

The amacrine cell has a large body, a lobulated nucleus, and a single process with extensive branches that extend towards the vitreous. The amacrine cell plays an important role in modulating the information that reaches the ganglion cells, owing to the extremely broad spread of its process (Witkorsky, 1994). Three groups of amacrine cells have been described according to the extent of the field covered by the branching process. They also contain a variety of neurotransmitters, including γ-aminobutyric acid (GABA), glycine, acetylcholine (Ach), dopamine (DA), 5-hydroxytryptamine (serotonin) and nitric oxide (NO). Most amacrine cells contain glycine or GABA, two structurally related inhibitory neurotransmitters, and are referred to as glycinergic or GABA-ergic amacrine cells. Approximately 40% of all amacrine cells are likely to be GABA-ergic. Even though, many functions of amacrine cells are probably not well understood, in some species feed-forward inhibition onto the ganglion cells forms a prominent action of amacrine cells. Glycine and GABA both contribute to inhibition observed in retinal ganglion cells.

1.2.3.5 Ganglion cells

The final common pathway for expressing retinal processing is the ganglion cell, whose axon goes to the brain. Ganglion cells can be bipolar (e.g. a single dendrite) or multipolar. Classifications can be made on the basis of the branching pattern of the dendrite, which may be either stratified, with horizontal branches arranged in one to three layers, or diffuse, branching like a tree. Eighteen types of ganglion cells have been identified (Kolb *et al.,* 1992).

1.2.3.6 Interplexiform cells

Interplexiform cell has large cell body and is found among the layer of amacrine cells. It provides feedback from inner retinal layers to the photoreceptors. They use GABA or dopamine as their neurotransmitter (Witkorsky, 1994).

1.2.3.7 Neuroglial cells

Neuroglial cells, though not involved in the transfer of neural signals, provide structure and support and play a role in neural tissue reaction to injury or infection. Four types of glial cells exist in the retina: 1) the Müller cells, which are the most numerous; 2) the astrocytes that mainly appear in the innermost parts of the retina; 3) the microglial cells, which are phagocytic; and 4) glial cells that surround ganglion cell axons.

1.2.3.8 Müller cells

Müller cells are large neuroglial cells that extend throughout most of the retina. The apex of the cell is in the photoreceptor layer, and the basal aspect is at the inner retinal surface. They play a supportive role in providing structure (Figure 1.4).

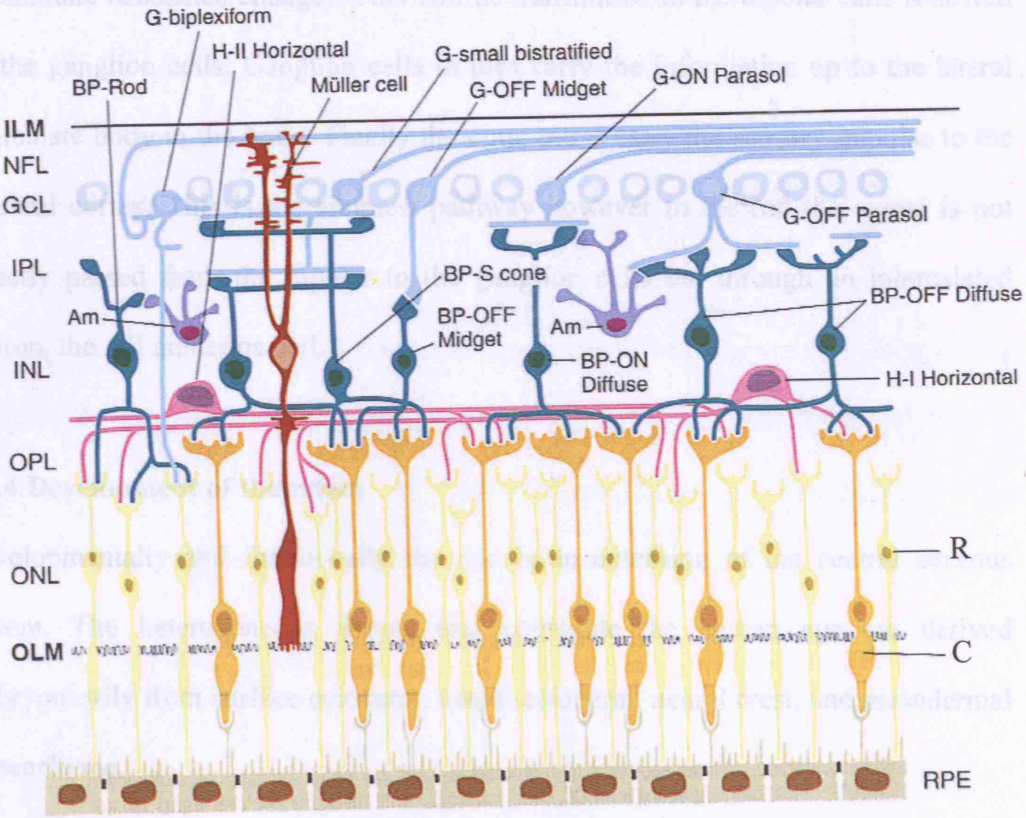

Figure 1.4 Schematic diagram of the cell types and histologic layers in the primate retina. The basic relationship is shown between rod (R) and cone (C) photoreceptors, as well as different types of bipolar cells (BP), horizontal (H) cells, and amacrine (Am) and ganglion (G) neurons (adapted from Rodiek, 1998).

1.2.3 Visual Pathway

The visual pathway starts when the external information or light (photon) is taken by the photoreceptor cells where it will be converted into a suitable cellular event (membrane resistance change). This will be transmitted to the bipolar cells followed by the ganglion cells. Ganglion cells in turn carry the information up to the lateral geniculate body in the brain. Finally the optic tracts carry the sensory impulse to the cerebral cortex. This is the simplest pathway however in the rod the signal is not directly passed from the bipolar to the ganglion cells but through an intercalated neuron, the AII amacrine cell.

1.2.4 Development of the retina

Developmentally and functionally the eye is an extension of the central nervous system. The heterogeneous tissues that constitute the human eye are derived embryonically from surface ectoderm, neural ectoderm, neural crest, and mesodermal mesenchyme.

The first signs of the developing eyes in the human appear by the third week of gestation (the 2.6 mm stage). Two pits appear in the transverse neural folds which within few days will develop into the optic vesicles (the 3.2 mm stage) and are connected to the brain by the optic stalks. During the next stage of ocular development (4-6 week postovulatory), the optic vesicles enlarge and folds in on itself, becoming the optic cup and the lens ectoderm invaginates into the vesicle. The inner wall lining the cup gives rise to the neural retina, and the outer wall produces the RPE. The optic stalk gives rise to the glia of the optic nerve (Figure 1.5).

By the time the optic cup is formed (the 10 mm stage), the retinal differentiation is already in progress. Cell division in the outer wall of the optic cup occurs only in one plane, creating a single layer of cells.

By the 12 mm stage, two nuclear layers, called the inner and outer neuroblastic layers, are established at the posterior pole of the retina. A narrow acellular strip the Chievitz transient fibre layer separates them. The proliferating cells synthesise their DNA on the vitreal side of this neuroblastic cell mass. After synthesising the DNA, they move toward the sclera and divide at the apical side of the neuroblastic cell mass. If the daughter cells do not leave the mitotic cycle, they move back to the vitreal side to synthesise more DNA. Cells that leave the cell cycle migrate to locations determined at their birth and start to differentiate. By the end of eight weeks (30 mm stage), a single layered pigmented epithelium can be identified.

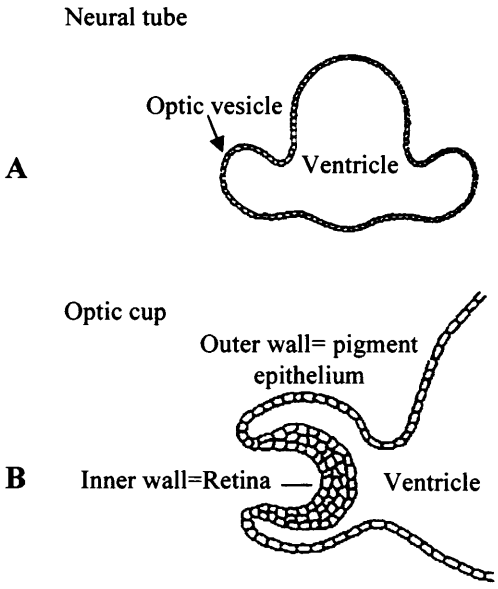

Figure 1.5 Schematic diagrams showing (A) optic vesicle, which develops from the neural tube, and (B) the invagination of an optic vesicle to form an optic cup (adapted from Dowling, 1987).

The development of the retinal nuclear and plexiform layers and the cellular differentiations of various cell types begin in the central retina and spread peripherally. The ganglion cell layer appears first by the formation of the inner plexiform layer. Its development starts at 12 weeks and it is well established by the fifth month. The outer plexiform layer forms at the fourth month, and cells located between the outer and the inner plexiform layers then consolidate to form the inner nuclear layer, obliterating all of the Chievitz transient fibre layer except a remnant at the macula which also disappears when the macula matures (Figure 1.6).

By the sixth month of gestation, there are up to nine rows of ganglion cells in the macular region. This region then starts thinning, and ganglion cells and other cells of the inner retina become displaced centrifugally and develop elongated processes. The displacement results in depression at the centre of the macula. Migration of ganglion cells, cells of the inner nuclear layer, and Müller cells toward the periphery thus form the foveal pit. The foveal pit is fully formed by about 11 to 15 months postnatally.

At the time of birth, the cone density of the human fovea is only 20% of the adult value, which it reaches only 4-5 years after birth. As the fovea matures, the cone cells become thinner and therefore more compactly packed.

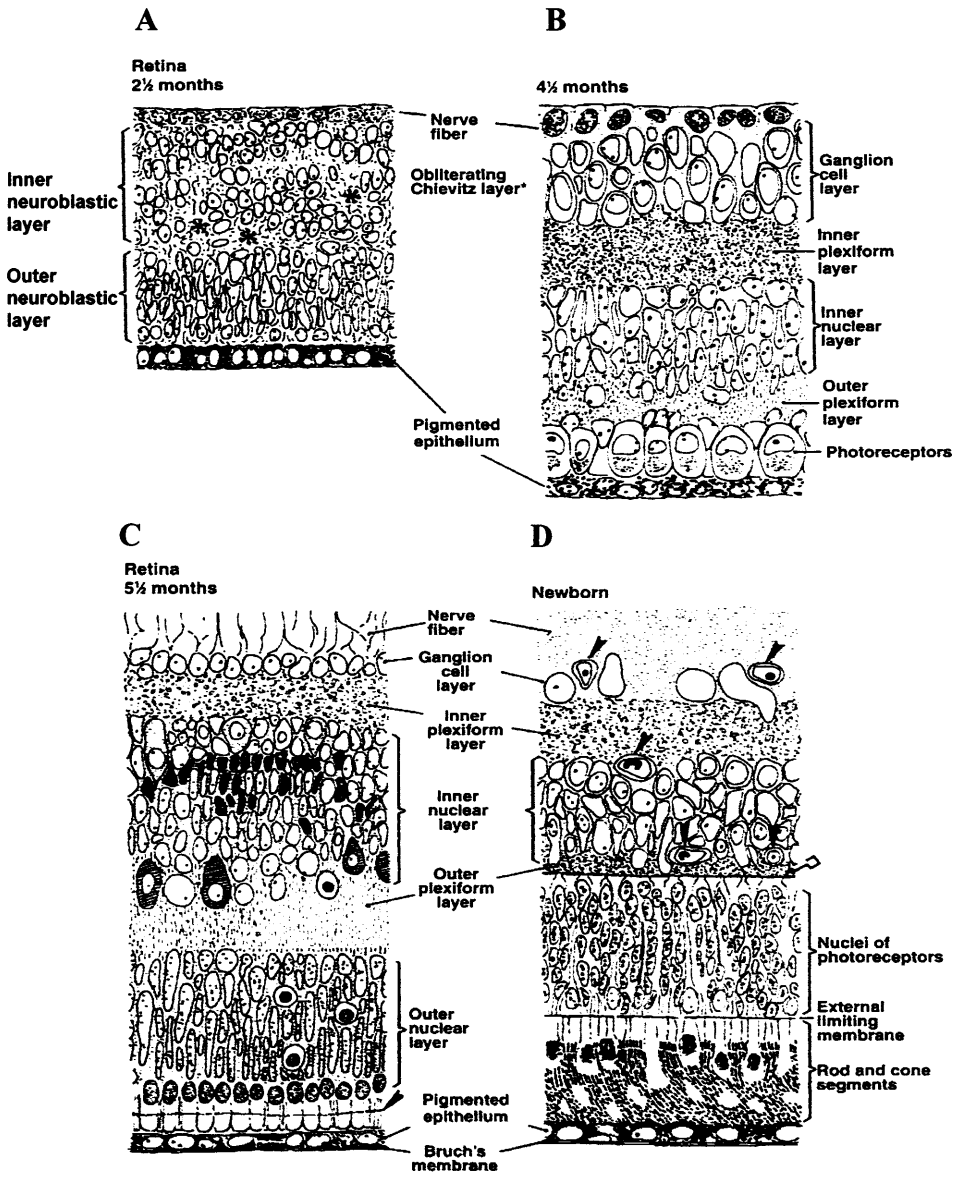

Figure 1.6 The developing retina. The region of the posterior pole is represented in sagittal section in each diagram. (**A**) At 2.5 months, the transient fibre layer of Chievitz is being obliterated slowly by shifting of the nuclear elements and realignment of their processes. (**B**) At midterm (4.5 months), retinal lamination is complete. (**C**) At 5.5 months, the ganglion cells have thinned out to one or two layers. (**D**) The newborn retina has an adult configuration, with vascularistion (arrow heads) reaching the outer limits of the inner nuclear layer (adapted from Cook *et al.*, 1994).

1.2.5 Phototransduction

Phototransduction is the process of conversion of light energy into electrical signals by photoreceptor cells. In rods the light sensitive molecule is rhodopsin, which consists of a protein named opsin and a chromophore, the 11-cis-retinaldehyde derived from vitamin A. In the rod outer segment (ROS) membrane, cyclic guanine monophosphate (cGMP) binds to a cGMP-gated cation channel in the dark, keeping it open and enabling sodium (Na^+) and calcium (Ca^{2+}) ions to flow into the ROS (Figure 1.7). When light enters the retina, an absorbed photon isomerises the 11-cis-retinal to all-trans-retinal resulting in conformational changes in the opsin molecule and in the formation of Meta II rhodopsin R*. Meta II rhodopsin is crucial for the phototransduction process where it initiates the visual cascade by binding transducin (T) and catalysing the exchange of GDP for GTP on its α-subunit, thus converting tranducin into an active form (T*). Activated transducin in turn activates cGMP-phosphodiesterase (cGMP-PDE), which brings about the hydrolysis of channel bound cGMP to 5'-GMP. The resulting rapid decrease in intracellular cGMP levels causes the cGMP-gated channels to close and the rod cell becomes hyperpolarised (Figure 1.8). Termination of the light-response cascade is mediated by inactivation of R* by phosphorylation catalysed by rhodopsin kinase and is then bound by arrestin, which prevents further interaction with transducin. Tranducin and PDE are inactivated by the hydrolysis of GTP to GDP. Guanylate cyclase, the enzyme responsible for the synthesis of cGMP from GTP, is activated by the decrease in intracellular Ca^{2+} after photoexcitation. As the cGMP concentration increases, the cGMP-gated channels re-open, and the photoreceptor cell is returned to its depolarised state.

In cones the phototranduction process is similar to that in rods, with three main differences: (1) Even though the chromophore in all cones is the 11-cis-retinal, the opsins have different structures. This will lead to different absorption spectra and light sensitivity; (2) The cone light sensitivity is about 100 to 1000 times lower than that of the rods, but the response kinetics is several times faster; (3) The voltage of the cGMP gated channels is different from that of the rod, and it exhibits strong inward rectification at negative potentials. Defects in the majority of phototransduction cascade proteins have been reported to be responsible for some types of retinal dystrophy (http://www.sph.uth.tmc.edu/retnet/disease.htm). In the following section, clinical and genetic description of retinal dystrophies will be described.

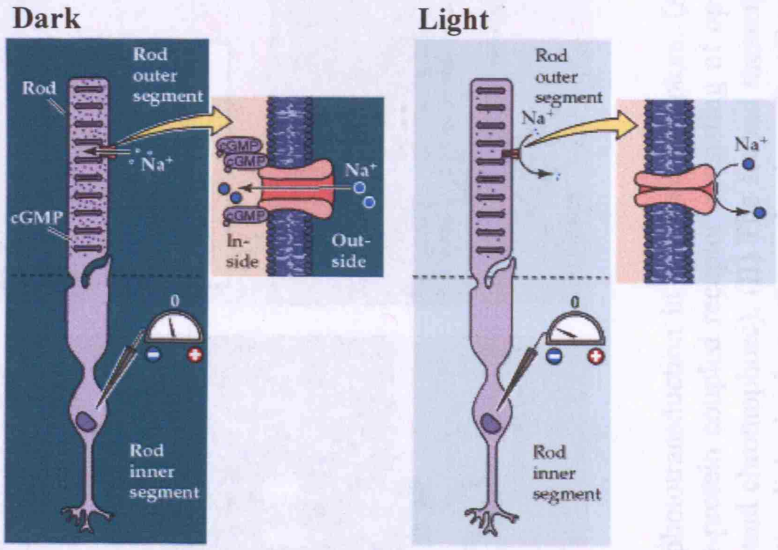

Figure 1.7 Diagrammatic representation of the visual transduction cascade. Cyclic GMP-gated channels in the outer segment membrane are responsible for the light-induced changes in the electrical activity of photoreceptors (adapted from Purves *et al.*, 2001).

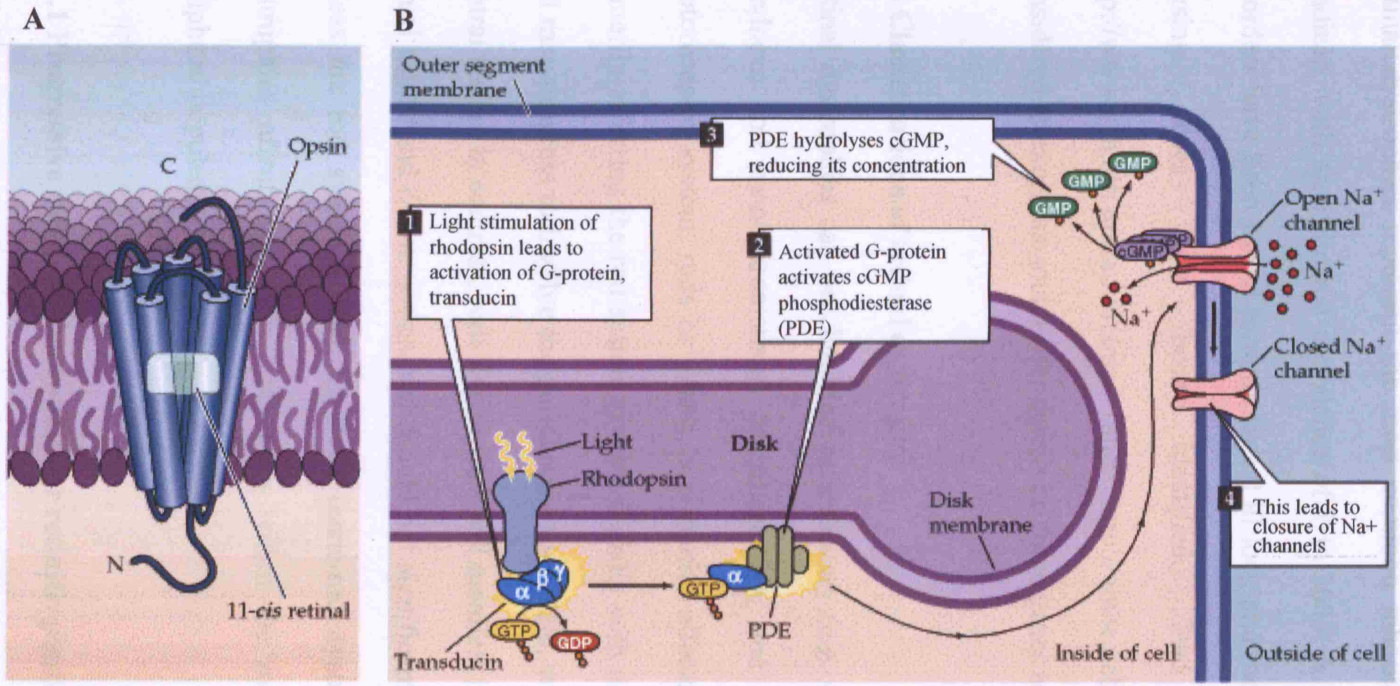

Figure 1.8 Details of phototransduction in rod photoreceptors. (A) The molecular structure of rhodopsin, the pigment in rods. Rhodopsin is a G-protein coupled receptor consisting of opsin (a seven transmembrane domain protein) and 11-cis-retinal (a covalently bound chromophore). (B) The second messenger cascade of phototransduction. 1. Light stimulation of rhodopsin in the receptor disks leads to the activation of a G-protein (transducin). 2. The GTP-bound alpha subunit of transducin activates a phosphodiesterase (PDE). 3. The activated phosphodiesterase hydrolyzes cGMP into GMP, reducing its concentration in the outer segment and leading to the closure of sodium channels in the outer segment membrane. (Neuroscience, Purves *et al.*, 2001)

1.3 Retinal Dystrophy

Retinal dystrophies represent the most common inherited form of human visual handicap, with an estimated prevalence of 1 in 3000. A variety of inherited retinal disorders have been linked to more than 150 loci, and more than 100 of the disease causing genes have been identified. Two electronic databases, http://www.sph.uth.tmc.edu/retnet/ and http://www.ncbi.nlm.nih.gov/Omim, are considered as excellent sources for details on these genes and loci.

1.4 Classifications of retinal dystrophy

Retinal dystrophies can be classified as stationary (e.g. congenital stationary night blindness, rod monochromatism) or progressive, and also according to which photoreceptor system, rods or cones, is primarily affected (Bird, 1995). Disorders primarily affecting the rod system present initially with night blindness (nyctalopia) and may progress to involve the peripheral visual field, with relative preservation of central vision. In contrast, cone dystrophies will manifest initially with loss of central visual acuity and colour vision and should not significantly affect peripheral vision unless the rod system is also involved (cone-rod dystrophy, [CORD]). Macular dystrophies affect both rods and cones within the macula, whilst leaving the peripheral populations intact.

1.4.1 Progressive rod-cone dystrophies or retinitis pigmentosa

Retinitis pigmentosa (RP, OMIM #268000) is a term used to refer to a genetically and clinically heterogeneous group of photoreceptor degenerations affecting approximately 1:3000 people and responsible for visual loss of 1.5 million individual

worldwide. Diagnostic features common to most cases of RP include night blindness, attenuated retinal vessels, waxy pallor of the optic disc, and bone spicule-like pigmentation in the fundus (Figure 1.9 B and C) in comparison to the normal picture of fundus (Figure 1.9 A). The genetics of RP is complex with autosomal dominant, autosomal recessive, X-linked, digenic and mitochondrial patterns of inheritance.

1.4.1.1 Autosomal dominant RP

Autosomal dominant RP (adRP) accounts for ~20% of all RP cases and is characterised by significant allelic and non allelic heterogeneity. The majority of the genes causing adRP are photoreceptor specific. *Rhodopsin* (*RHO*) was the first gene shown to cause dominant RP and is responsible for 30% of all cases of adRP (Farrar *et al.,* 1990; Dryja *et al.,* 1990 and 1991). Mutations in *RDS/peripherin*, a component of the photoreceptor outer disc membrane, have been shown to cause a wide range of retinal dystrophies including digenic RP (Farrar *et al.,* 1991; Kajiwara *et al.,* 1991). Mutations in the neural-retinal specific leucine zipper transcription factor gene (*NRL*) which shows its highest level of expression in the photoreceptor cells cause adRP. Meanwhile, *HPRP3*, *PRPC8* and *PRP31* genes which are responsible for RP18, RP13 and RP11, respectively were found to be ubiquitously expressed and are highly conserved between yeast and humans. These genes are involved in regulating mRNA processing and splicing.

1.4.1.2 Autosomal recessive RP

Autosomal recessive RP (arRP) accounts for ~15-30% of all cases of RP. To date, 24 loci have been identified for arRP. The majority of these genes are involved in the pathway of phototransduction (*CNGA1*, *PDE6A*, *PDE6B*, *SAG*) or in the pathway of vitamin A metabolism and its recycling in the eye (*RLBP1*, *ABCA4*, *LRAT*).

1.4.1.3 X-linked RP

X-linked RP (xlRP) is a severe form of RP that affects males in their first decade of life (Figure 1.9 D). xlRP is genetically heterogeneous form of RP with at least 5 loci reported: RP2, RP3, RP6, RP23 and RP24. The RP2 gene was found to be responsible for about 15-20% of xlRP families (Hardcastle *et al.,* 1999). However, RP3 (*RPGR*) accounts for nearly 70% of affected xlRP families (Vervoort *et al.,* 2000).

1.4.1.4 Digenic RP

Digenic inheritance, the interplay of mutations in two different genes resulting in a heritable eye disorder, is an important genetic concept. Mutations in *ROM1* only have not been proven to be pathogenic. However, when present in association with a specific *RDS/peripherin* missense mutation, *ROM1* mutations result in RP (Kajiwara *et al.,* 1994).

1.4.1.5 Mitochondrial RP

RP due to mitochondrial inheritance is a very rare condition. It has been reported that C12258A mutation in the mitochondrial Transfer RNA, mitochondrial, serine, 2 (*MTTS2*) was associated with progressive sensorineural hearing loss and RP (Mansergh *et al.,* 1999). Mutations in the (ATP synthase 6) *MT-ATP6* gene have also been reported to cause neuropathy, ataxia, and RP (Holt *et al.,* 1990; Moslemi *et al.,* 2005). The *MT-ATP6* gene provides instructions for making a protein that is essential for normal mitochondrial function. Hence, mutations in *MT-ATP6* could alter the structure or function of ATP synthesis, leading to reduction of the ability of the mitochondria to make ATP. However, it remains unclear how this disruption in mitochondrial energy production leads to muscle weakness, vision loss, and the other specific features of neuropathy, ataxia, and RP (NARP) syndrome.

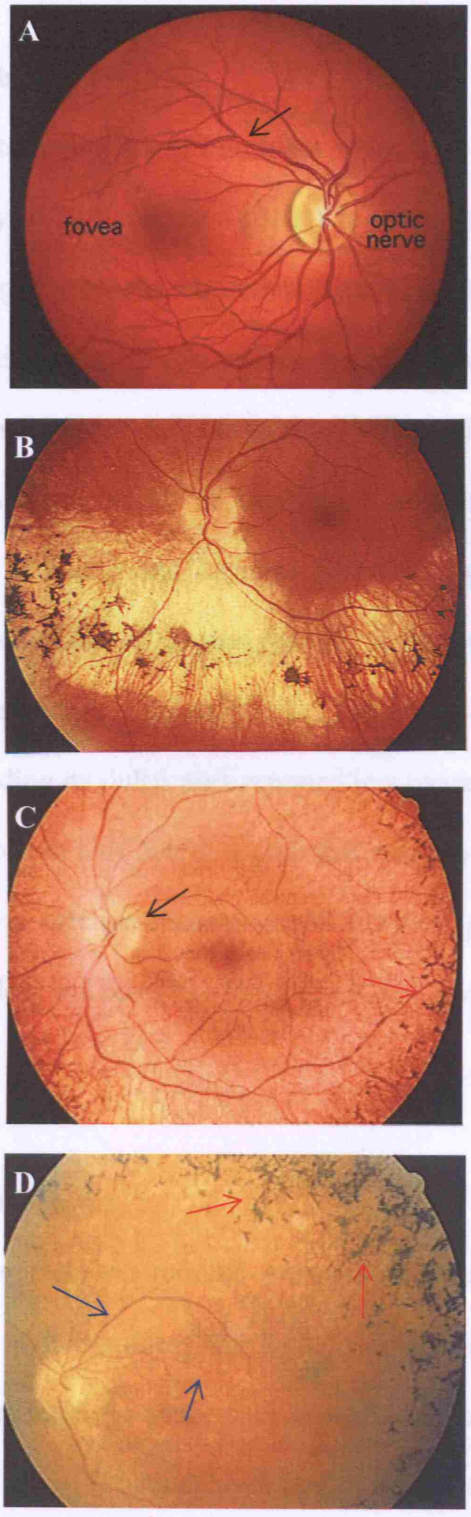

Figure 1.9 Fundus appearance of (**A**): Normal retina with the major landmarks of the fundus; fovea, optic disc and retinal blood vessels (arrow) (**B**): Autosomal dominant sectorial RP preserving part of the retina; (**C**): Advanced autosomal recessive RP with waxy pallor of the optic disc (black arrow) and mild bone spicule like pigmentation (red arrow); and (**D**): X linked RP with extensive bone spicule like pigmentation (red arrows) and arteriolar narrowing (blue arrows) (adapted from Ryan, 2001).

1.4.2 Stationary night blindness

1.4.2.1 Congenital stationary night blindness

Congenital stationary night blindness (CSNB) is a non-progressive retinal disorder characterised by a negative-type electroretinography (ERG) in which the amplitude of the b-wave (originating from the inner retina) is smaller than that of the a-wave (representing the photoreceptor cells) even though the retina appears normal (Figure 1.10 A). Three monogenic modes of inheritance have been described: autosomal dominant, autosomal recessive and X-linked recessive. Two forms of the dominant CSNB, CSNBAD1 and CSNBAD2, were reported to be caused by mutations in *RHO* and *PDE6B* genes, respectively (Sieving *et al.,* 1995; Gal *et al.,* 1994). Mutations in the *GRM6* gene encoding mGluR6 were reported in a recessive form of CSNB (Dryja *et al.,* 2005). Mutations in *CACNA1F*, a gene that maps to Xp11.23, encoding the α-1F subunit of an L-type calcium channel and *NYX* (nyctalopin) gene on Xp11.4, were linked to the incomplete and complete forms of xlCSN, respectively (Bech-Hansen *et al.,* 1998, 2000).

1.4.2.2 Fundus albipunctatus

Fundus albipunctatus (FA) or retinitis punctata albescens (RPA) is a form of congenital stationary night blindness with an autosomal recessive inheritance pattern. The fundus has a characteristic appearance of numerous small yellow-white dotlike lesions at the level of the RPE with delayed course of dark adaptation (Figure 1.10 B) (Marmor, 1977). Mutations in the gene encoding retinal dehydrogenase type 5 (*RDH5*) were identified in most patients with FA (Yamamoto *et al.,* 1999; Gonzalez-Fernandez *et al.,* 1999).

1.4.2.3 Oguchi disease

Oguchi disease is a rare autosomal recessive form of stationary night blindness. Patients with this disease show a distinctive golden-brown fundus colouration that develops as the retina adapts to light with abnormal slow dark adaptation (Maw *et al.*, 1995) (Figure 1.10 C). Oguchi disease was reported to be caused by mutations in either *arrestin* (*S-antigen*) or rhodopsin kinase (*RHOK*) (Fuchs *et al.*, 1995; Yamamoto *et al.*, 1997).

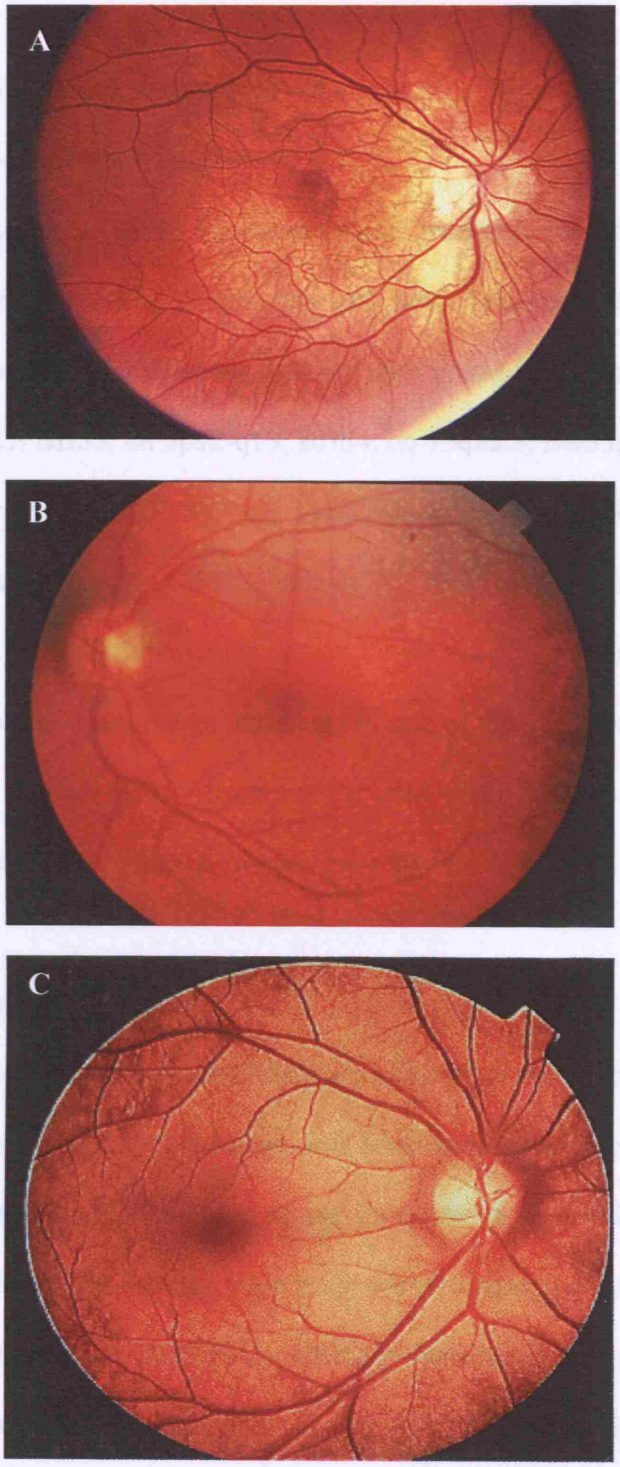

Figure 1.10 (**A**) Fundus photograph of a CSNB type 2 patient with an unusual golden to rust coloration of the fundus that is reversed with long dark adaptation (adapted from retina.umh.es/Webvision/imageswv/); (**B**) Fundus photograph of a patient with fundus albipunctatus showing numerous small yellow-white dotlike lesions at the level of the RPE (adapted from Yamamoto *et al.,* 1999); (**C**) Fundus photo of a patient with the golden metallic reflex characteristic of Oguchi disease (adapted from Usui *et al.,* 2000).

1.4.3 Syndromic retinal dystrophies

1.4.3.1 Bardet-Biedl syndrome

Bardet-Biedl syndrome or BBS is an autosomal recessive condition characterised by obesity, mental retardation, polydactyly and retinal degeneration (Figure 1.11 A). BBS is a genetically heterogeneous disorder with linkage to 12 loci BBS1, on 11q13; BBS2, on 16q21; BBS3, on 3p12-q13; BBS4, on 15q22.3; BBS5, on 2q31; BBS6, on 20p12; BBS7, on 4q27; BBS8 on 14q32.11; BBS9, on 7p14; BBS10, on 12q; BBS11, on 9q33.1; and BBS12, on 4q27. Recently, Katsanis et al. (2001) demonstrated a triallelic inheritance pattern where the clinical manifestation of some forms of BBS requires recessive mutations in one of the BBS loci plus an additional mutation in a second locus. However, Burghes et al. (2001) suggested the term recessive inheritance with a modifier of penetrance.

1.4.3.2 Usher syndrome

Usher syndrome is a recessive condition in which retinal dystrophy (Figure 1.11 B) is associated with neurosensory deafness. It is considered to be the most common cause of deaf-blindness in humans and accounts for 3-6% of deaf children. Clinically the condition can be classified into three main types: Usher syndrome type I (USH1), type II (USH2), and type III (USH3). USH1 is characterised by profound congenital deafness, absent vestibular responses, and onset of RP by the age of 10. However, patients with USH2 have normal vestibular responses, onset of RP is by the late teens, and they demonstrate moderate to severe congenital deafness (Kimberling *et al.*, 1995). Finally USH3 is characterised by progressive hearing loss and occasional vestibular dysfunction. To date, five genes (*MYO7A*, *USH1C*, *CDH23*, *PCDH15* and

USH1G) and two loci are known for USH1, two genes (*USH2A* and *VLGR1*) for USH2 and one gene (*USH3A*) and one locus for USH3 (Reiners *et al.,* 2006).

1.4.3.3 Alstorm syndrome

Alstorm syndrome or ALMS1 is an autosomal recessive multisystem disorder associated with obesity, diabetes, and retinal degeneration. Unlike BBS, polydactyly is absent and intelligence is often normal. Frameshift and nonsense mutations have been described in *ALMS1* gene on chromosome 2p13 (Collin *et al.,* 2002; Hearn *et al.,* 2002).

1.4.3.4 Cockayne syndrome

Cockayne syndrome or CKN is a recessive disorder resulting from defective DNA repair. Patients with CKN have a characteristic facial appearance with a beaked nose, sunken eyes and early onset cataract is common. In addition, there is a progressive retinal dystrophy associated with peripheral retinal degeneration. Two loci, CKN1 and CKN2, have been reported as causative for CKN syndrome. Cockayne syndrome type A (CSA) is caused by mutation in the gene encoding the group 8 excision-repair cross-complementing protein (*ERCC8*) on chromosome 5q11 (Henning *et al.,* 1995; Cao *et al.,* 2004).

1.4.3.5 Cohen syndrome

Cohen syndrome or COH1 is an autosomal recessive disease that is characterised by non-progressive mild to severe psychomotor retardation, motor clumsiness, microcephaly, characteristic facial features, progressive retinochoroidal dystrophy,

myopia, intermittent isolated neutropenia and a cheerful disposition (Norio *et al.*, 1984). The disease locus for COH1 has been mapped to chromosome 8q22-q23. Recently, mutations in a novel gene, *COH1*, encoding a transmembrane protein with a presumed role in vesicle-mediated sorting and intracellular protein transport was reported to be responsible for Cohen syndrome (Kolehmainen *et al.*, 2003).

1.4.3.6 Joubert syndrome

Joubert syndrome or JBTS1 is a rare autosomal recessive syndrome with complete or partial cerebellar vermian agenesis. JBTS1 patients can be divided into two groups based on the presence or absence of retinal dystrophy. Patients with retinal dystrophy are more likely to have renal cysts. Recently, four genes associated with JBTS have been identified: *NPHP1* at 2q13 (Parisi *et al.*, 2004), *AHI1* at 6q23.3 (Ferland *et al.*, 2004), *CEP290* (*NPHP6*) at 12q21.3 (Sayer *et al.*, 2006) and the Meckel-Gruber syndrome-associated gene *TMEM67* (*MKS3*) at 8q22.1 (Baala *et al.*, 2007).

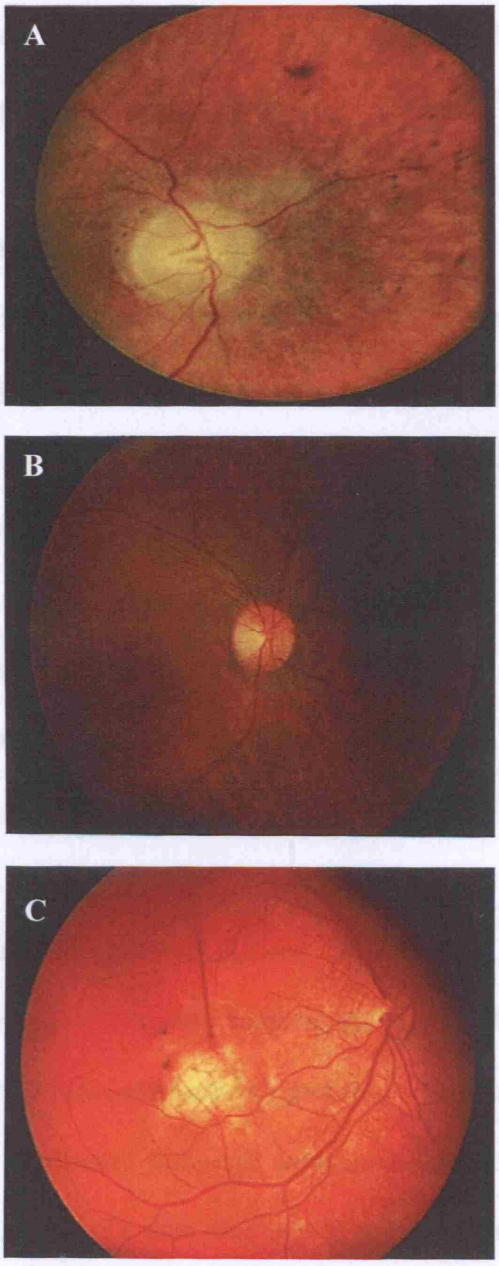

Figure 1.11 (**A**) Fundus photograph showing retinal degeneration in Bardet Beidl syndrome showing bull's eye type macular degeneration (**B**) Fundus of an Usher's syndrome patient with typical picture of RP showing attenuation of retinal blood vessels and waxy pallor of the optic disc (**C**) Fundus photograph of cone dystrophy showing macular degeneration but relative preservation of peripheral retina (adapted from Callanan, 1998).

1.4.4 Cone dystrophies

Cone dystrophies can be classified into achromatopsia, blue cone monochromatic color blindness and progressive cone dystrophy (Figure 1.11 C).

1.4.5 Macular dystrophies

This classification includes all disorders that affect the macula for example, age related macular degeneration (AMD), Best's disease (Figure 1.12 A), Stargardt's disease (STGD) (Figure 1.12 B), North Carolina macular dystrophy (MCDR1) and adult vitelliform dystrophy.

1.4.6 Miscellaneous retinal dystrophies

These include chorioderemia, CORD, enhanced S-cone syndrome and Leber congenital amaurosis.

1.4.6.1 Leber congenital amaurosis (LCA)

LCA is a clinically and genetically heterogeneous retinal disorder that begins to manifest in infancy and is accompanied by profound visual loss (Figure 1.12 C). LCA is mainly a recessive disease although autosomal dominant pedigrees have been identified (Francois, 1968). To date nine loci have been identified for LCA of which seven genes, *AIPL1*, *CRB1*, *CRX*, *GUCY2D*, *RPE65*, *RPGRIP1* and *Lebercillin* have been cloned. The other two loci implicated in LCA include LCA3 on 14q24 (Stockton *et al.*, 1998) and LCA9 on 1p36 (Keen *et al.*, 2003) for which the genes are yet to be identified.

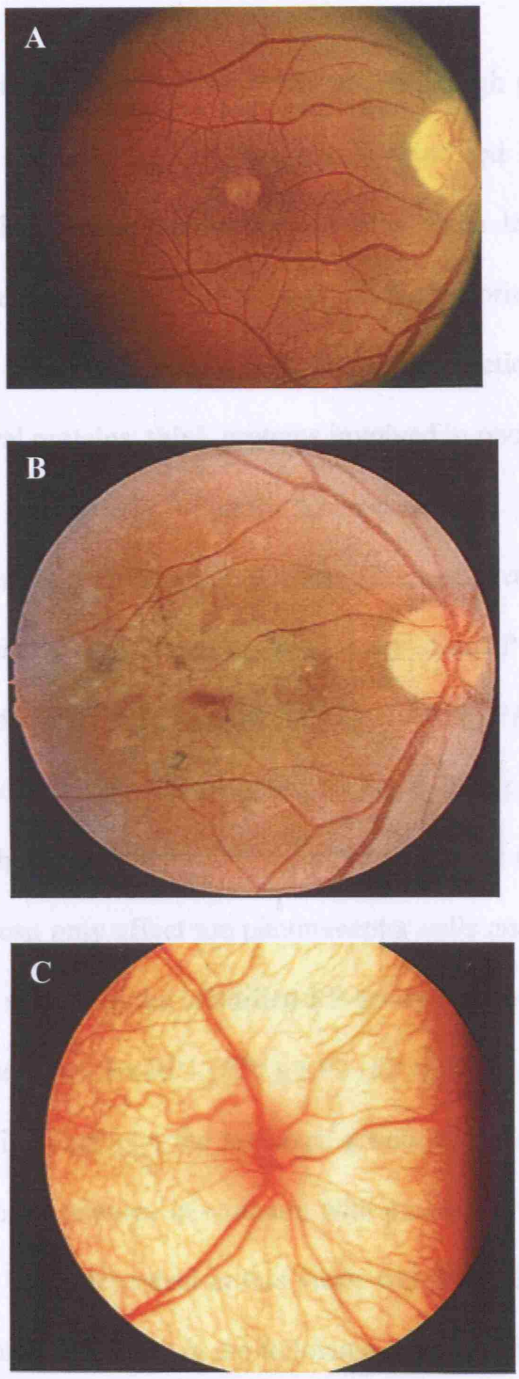

Figure 1.12 (**A**) Fundus photograph of a patient with Best's disease, a small vitelliform lesion is beneath the fovea; (**B**) Fundus photograph of a patient with Stargardt's disease affecting the macula (adapted from Ryan, 2001); (**C**) Fundus photography of a patient with Leber's congenital amaurosis showing a relatively normal appearance apart from a very pale fundus (adapted from Callanan, 1988).

1.5 Genetics of RP

RP is a paradigm of monogenic diseases with extremely high genetic heterogeneity (Hims *et al.,* 2003). This complexity has clearly hindered the identification of causative genes, particularly in the recessive forms, since large nuclear families suitable for linkage studies are rare. The products of the majority of RP genes can be placed into one of four categories: first, phototransduction proteins; second, photoreceptor structural proteins; third, proteins involved in photoreceptor and retinal pigment epithelium (particularly vitamin A) metabolism; and fourth, proteins regulating gene expression (transcription factors) (Bessant *et al.,* 2001). However, a fifth class has now been established as a major cause of adRP which is the splicing factors. Four of the identified adRP genes, *PRPF3*, *PRPF8*, *PRPF31* and *Pim-1*, are known to encode proteins that are involved in the splicing of introns from pre-mRNAs. Even though, these splicing factors are ubiquitously expressed they have a crucial function that can only affect the photoreceptor cells and their mutations lead to RP. Additionally, several of the identified RP genes encode products of unknown function, including the genes for RP1 (*RP1*), RP2 (*RP2*), RP3 (*RPGR*), RP12 (*CRB1*) and RP14 (*TULB1*). Interestingly, the predicted products of *RP2*, *RPGR*, *CRB1* and *TULP1*, all seem to have features in common with proteins involved in intracellular trafficking. Since the work described in this thesis will focus upon arRP, genetics of this form will be discussed in depth in the following sub-section.

1.5.1 Genetics of recessive RP

Autosomal recessive RP is the commonest form of RP worldwide accounting for ~39% of cases in Spain (Ayuso *et al.,* 1995). The mutations responsible for arRP have been reported in 19 genes including ATP binding cassette subfamily A member 4 (*ABCA4*) (Martinez-Mir *et al.,* 1998), retinal pigment epithelium specific protein 65 KD (*RPE65*) (Morimura *et al.,* 1998), crumbs Drosophila homolog of 1 (*CRB1*) (den Hollander *et al.,* 2001), Usherin (*USH2A1*) (Rivolta *et al.,* 2000), MER tyrosine kinase proto-oncogene (*MERTK*) (Gal *et al.,* 2000), ceramide kinase like (*CERKL*) (Tuson *et al.,* 2004), arrestin (*SAG*) (Nakazwa *et al.,* 1998), rhodopsin (*RHO*) (Rosenfeld *et al.,* 1992), the alpha and beta subunits of phosphodiestrase (*PDE6B* and *PDE6A*) (McLaughlin *et al.,* 1993, Huang *et al.,* 1995), the alpha and beta subunits of the rod cyclic GMP-gated channel protein (*CNGA1* and *CNGB1*) (Dryja *et al.,* 1995; Bareil *et al.,* 2001; Zhang *et al.,* 2004), lecithin retinol acyltransferase (*LRAT*) (Thompson *et al.,* 2001), tubby like protein 1 (*TULP1*) (Hagstrom *et al.,* 1998), G protein coupled receptor retinal (*RGR*) (Morimura *et al.,* 1999), nuclear receptor subfamily 2 group E member 3 (*NR2E3*) (Gerber *et al.,* 2000), retinaldehyde binding protein 1(*RLBP1*) (Maw *et al.,* 1997), retinitis pigmentosa 1 (RP1) (Riazuddin *et al.,* 2005) and progressive rod-cone degeneration (PRCD) (Zangerl *et al.,* 2006).

Genetic linkage studies have also identified 5 additional arRP loci at chromosomes 16p12.1-p12.3 (RP22) (Finkh *et al.,* 1998), 6cen-q15 (RP25) (Ruiz *et al.,* 1998), 2p11-p16 (RP28) (Gu *et al.,* 1999), 4q32-q34 (RP29) (Hameed *et al.,* 2001) and 1p13.3-p21.2 (RP32) (Zhang *et al.* 2005) for which the genes are yet to be identified. A description of the genes involved in recessive RP including their function, chromosomal location and involvement in other disorders is summarised in table 1.1

Table 1.1 A summary of the genes and loci involved in the pathogenesis of arRP

Gene	*Function*	*Disorder*	*Location*
1. *ABCA4*	Energy -dependent transport of a wide spectrum of substrates across membranes	STGD-1, arRP (RP19), CORD, AMD2	1p21-p13
2. *CERKL*	Key mediator of cellular apoptosis/survival	arRP (RP26)	2q31.2-q32
3. *CNGA1*	Phototransduction pathway	arRP	4p12-cen
4. *CNGB1*	Visual transduction cascade	arRP	16q13
5. *CRB1*	Cell adhesion and maintenance of cell polarity	arRP (RP12) * LCA8	1q31-q32
6. *LRAT*	Catalyses first steps in the visual cycle transforming vitamin A into 11-*cis*-retinol	arRP Early onset severe RD	4q31
7. *MERTK*	Implicated in RPE phagocytosis pathway	arRP	2q14.1
8. *NR2E3*	Ligand-dependant transcription factor	S-cone syndrome, arRP	15q23
9. *PDE6A*	Phototransduction enzyme	arRP	5q31.2-q34
10. *PDE6B*	Phototransduction enzyme	CSNB type 3, arRP	4p16.3
11. *PRCD*	Protein of unknown function	arRP	17q25.1
12. *RGR*	Retinoid metabolism	arRP, adRP	10q23
13. *RPE65*	Retinoid metabolism	arRP (RP20), LCA2	1p31.2
14. *RLBP1*	Retinoid metabolism	arRP, CORD	15q26.1
15. *RHO*	Visual transduction cascade	arRP, adRP, CSNB	3q22.1
16. *RP1*	Ciliary structure and transport	arRP, adRP	8q12.1
17. *SAG*	Visual transduction cascade	arRP, ar Oguchi disease	2q37.1
18. *TULP1*	Photoreceptor cell transcription factor	arRP (RP14), LCA	6p21.31
19. *USH2A*	Retinal development	arRP, USH2A	1q41

1.6 The Human genome

The human genome is a collective name for the different DNA molecules found in the human cells. It comprises two genomes: a complex nuclear genome and a very simple mitochondrial genome. The mitochondrial genome is defined by a circular double-stranded DNA whose complete nucleotide sequence has been established (Anderson *et al.,* 1981). Meanwhile, the nuclear genome provides the great bulk of essential genetic information, most of which specifies polypeptide synthesis on cytoplasmic ribosomes. The nuclear genome consists of 24 different human chromosomes. The total number of genes in the human genome is now thought to be 30000- 35000 which gives a rough estimate of 1400 genes per chromosome on average. However, the human genes are not evenly distributed on the chromosomes. The constitutive heterochromatin regions are devoid of genes but even within the euchromatic portion of the genome gene density can vary substantially between chromosomal regions and also between whole chromosomes (Stein, 2004).

1.6.1 The Human Genome Project

The Human Genome Project (HGP) is a 13-year project whose primary goal was to sequence the large human genome and subsequently to acquire fundamental information about our genetic make-up which would enhance our basic scientific understanding of human genetics and of the role of various genes in health and disease. An important aspect of this project was to store this information in databases, improve tools for data analysis, transfer related technologies to the private sector, and address the ethical, legal, and social issues that may arise from the project. The human genome sequence obtained by the HGP is not an exact match of any

single person's genome. Researchers used anonymous DNA samples from a number of male and female donors of different ethnic origins and because all humans share the same basic set of genes and other DNA regions, this reference sequence represents every person.

The publication of 90% of the total human genome sequence (draft sequence) in 2001 was a major achievement by the HGP (Lander *et al.,* 2001; Venter *et al.,* 2001). Subsequently, the Human Genome Sequencing Consortium concentrated on converting the draft sequence into finished sequence which was announced to be complete in April 2003 (Collins *et al.,* 2003). However, the exact number of genes encoded by the genome is still unknown and findings from The International Human Genome Sequencing Consortium in 2004 reduced the estimated number of human protein-coding genes from 35000 to only 20000 to 25000 (Stein, 2004). However, this may not represent the true number due to the fact that alternative transcripts for the same gene exist and could lead to increase in the total number of genes.

1.6.2 The DNA sequence and analysis of human chromosome 6

Following the announcement of completion of the human genome project on 14 April 2003, Mungall et al. (2003) reported mapping, sequencing and analysis of chromosome 6. Chromosome 6 is a metacentric chromosome that constitutes about 6% of the human genome and was best known for the major histocompatibility complex (MHC), a region of 3.6 megabases (Mb) on 6p21.3. After accounting for the gene-rich MHC (43 genes per Mb), chromosome 6 represents a relatively gene-poor chromosome. The length of sequence occupied by annotated genes (including introns but excluding pseudogenes) is 70,396,075 bp or 42.2%. This is comparable to

previous estimates for chromosomes 7, 14, 20 and 22 (46.5%, 43.6%, 42.4% and 51%, respectively). The chromosome sequence occupied by exons is only 2.2% with a mean exon length of 281 bp. The longest coding exon (9,114 bp) belongs to the known gene *ZNF451*; the *BPAG1* gene has the most exons (101). The longest intron is the first intron of *TCBA1* gene, spanning 479 kb. The largest gene is *PARK2* gene at 6q24, which spans almost 1.4 Mb with 12 exons. Finally the mean number of transcripts annotated per gene is 2.34 (excluding putative genes) and *FYN* oncogene has the most with 16 annotated transcripts (Mungall *et al.,* 2003). The finished sequence of chromosome 6 comprises 166,880.988 bp, representing the largest chromosome sequenced so far. With the exception of two gaps that reside in the pericentromeric and sub-telomeric regions of chromosome 6, the entire sequence has been subjected to high quality manual annotation, resulting in the evidence-supported identification of 1,557 genes and 633 pseudogenes. To date, 130 genes were reported mapping to chromosome 6 that may cause, predispose, or protect from disease (Mungall *et al.,* 2003).

1.6.3 Sequencing methods applied to the HGP

The International Human Genome Project used the hierarchical shotgun approach (HS), whereas Celera Genomics adopted the whole-genome shotgun (WGS) approach. However, both projects employed the same basic technique of shotgun sequencing developed by Sanger after the invention of DNA sequencing (Sanger *et al.,* 1982). To determine the sequence of a large DNA molecule, the method began by breaking up the DNA molecule into smaller random overlapping fragments, obtaining sequence "reads" from these fragments, and then using computer analysis to

reassemble the random reads into contigs. However, because of cloning errors the random data alone were insufficient to generate a complete and accurate sequence. Initially the technique involved sequencing the fragments from one end however in 1990 the approach was extended to sequencing the fragments from both ends, thus obtaining linking information that can be used to connect contigs separated by gaps (Edwards *et al.,* 1990). The shotgun sequencing technique can be applied to genomes with few repeat sequences but the greater challenge arises on applying this technique to complex genomes, therefore HS and WGS were used to sequence the human genome.

In HS approach, the genome was first broken into an overlapping collection of intermediate clones such as bacterial artificial chromosomes (BACs). Each BAC was then sequenced by shotgun sequencing and the sequence of the genome was obtained by merging the sequences of the BACs. By using this approach the finished genome sequence was highly accurate because of the fact that the sequence assembly was local and anchored to the genome. In WGS technique, the genome was randomly decomposed into individual random reads. That was followed by assembling the entire collection. In WGS method, each contig is an independent component that must be anchored individually to the human genome and hence the resulting sequence may be difficult to convert into finished sequence.

1.7 Identifying human disease genes

There is no single pathway to guarantee success in identifying the causative gene. However, it is the combination of the clinical data, laboratory work and computer analysis. Candidate genes may be identified without reference to their chromosomal location (position independent candidate gene approach) or more commonly through identification of candidate chromosomal region and then candidate genes are identified within these regions (positional cloning).

1.7.1 Position independent candidate gene approach

Historically, position independent candidate gene approach was of choice since no relevant mapping information existed and no techniques were available to generate it.

1.7.2 Positional cloning

In this study positional cloning was mainly employed to identify the disease gene. In positional cloning, the disease gene is identified knowing nothing except its approximate chromosomal location. The difficulty of positional cloning depends mainly on the size of the candidate region therefore the first priority was to refine the region as much as possible. Linkage disequilibrium (LD) can be a very valuable tool for fine mapping. A contig of clones must be established across the candidate region which can be downloaded from the human genome sequence database. The next step was to use the genome browser such as Ensembl (http://www.ensembl.org), the Map Viewer through the National Centre of Biotechnology Information (http://www.ncbi.nlm.nih.gov/) or the University of California Santa Cruz browser (http://www.genome.cse.ucsc.edu) to display and analyse all the genes in the

candidate region. However, genes from the candidate region must be prioritised for mutation screening. A good candidate gene should have an expression pattern and/or a function consistent with the disease phenotype. Additionally, a gene with homology to a relevant paralogous (human) or orthologous (non human) that is known to have appropriate expression or function is also considered as a good candidate.

1.7.3 Bioinformatics

Bioinformatics is the study of biological systems through the collection, sharing and analysing the data derived from DNA, RNA, protein and cellular processes. It combines the most recent work in biology, genetics, statistics and computer science to provide researchers with all aspects of genomic research in a simple and less time-consuming way.

1.7.4 Copy number variation

Understanding the genetic basis of phenotypic variations in humans is currently one of the major goals in human genetics. Single nucleotide polymorphisms (SNPs) have long been known to be associated with phenotypic variation either through direct causal effects or by serving as proxies for other causal variants with which they are highly correlated (i.e. in linkage disequilibrium) (Stranger *et al.,* 2007). Nevertheless, recently, structural variants, such as copy number variants (CNVs) have attracted much attention. A copy number variation (CNV) or a copy number polymorphism (CNP) can be defined as a segment that is 1 kilobase (Kb) or larger and present at a variable copy number in comparison to a reference genome (Feuk *et al.,* 2006). A CNV can be simple in structure, such as tandem duplication, or may involve complex

gains or losses of homologous sequences at multiple sites in the genome (Redon *et al.,* 2006).

CNVs can have dramatic phenotypic consequences by disrupting genes and altering gene dosage (McCarroll *et al.,* 2006), and can cause disease, as in microdeletion or microduplication disorders (Shaw-Smith *et al.,* 2004), or confer risk to complex disease traits such as Human Immunodeficiency Virus-1 (HIV-1) infection and glomerulonephritis (Gonzalez *et al.,* 2005; Aitman *et al.,* 2006). However, the contribution of CNVs to the common, complex diseases (e.g. diabetes, heart disease) is currently unknown. In this project we used the array-based comparative genome hybridisation (aCGH) to investigate the existence of CNVs in patients' DNA and to investigate whether it could have an impact on the phenotype of one the RP25 families.

1.8 Linkage Analysis

1.8.1 Concepts of linkage analysis

Linkage is defined as the tendency for alleles close together on the same chromosome to be transmitted together, as an intact unit through meiosis. The main value of genetic linkage in human and medical genetics is to aid in identifying, mapping and diagnosing the genes responsible for inherited diseases.

Linkage relies mainly on the concept that if two loci are located near to each other on the same chromosome they will be inherited together, unless they are separated at meiosis by a recombination event. During germ cell formation, particularly during the first meiotic cell division, the maternal and paternal homologs of each chromosome pair form a bivalent by pairing together (synapsis). At this time, each chromosome

consists of two sister chromatids joined only at their centromeres, so that the bivalent is a four-stranded structure at the metaphase plate. During prophase of meiosis I the synapsed homologs within each bivalent exchange segments in a random way. At the zygotene stage, each pair of homologs begins to form a synaptonemal complex consisting of the two chromosomes in close apposition, separated by along linear protein core. Completion of this complex marks the start of the pachytene stage, which is when recombination or crossover occurs. Crossover involves physical breakage of the double helix in one paternal and one maternal chromatid, and joining of maternal and paternal ends. Thus one crossover creates two recombinant chromatids and leaves two non-recombinant, giving 50% recombinants. The overall frequency of recombinant chromosomes in an individual or in a population is known as recombination fraction (RF) or theta (θ). If two loci on the same chromosome are close enough so that the theta value is less than 50%, the two loci are genetically linked. On the other hand, if they are far apart on the same chromosome that crossover between them produces a theta value of 50%, such loci are genetically not linked or they assort independently. RF never exceeds 50% or 0.5, however far apart the loci are. The mathematical relationship between RF and genetic map distance is described by the mapping function. Mapping function can be calculated by the following equation.

Haldane's function: w= -1/2 In (1-2theta) or theta= 1/2 [1-exp(-2w)].

Where w is the map distance, In is the logarithm to the base e, and exp means "e to the power of"

1.8.2 Genetic and physical distances

Genetic and physical distances are two different map parameters. The unit of measurement of genetic linkage is centimorgan (cM) which is the genetic length of a chromosome over which, on average one recombination event is observed per meiosis. However, physical distance is measured in base pairs (bp) or chromosomal bands. As a rough rule of thumb, 1 cM is equal to 1 Mb (one million bp) however there are recombination deserts up to 5 Mb in length and recombination jungles with >3 cM per Mb. One crossover contributes 50 cM to the overall genetic map length. By counting chiasmata under microscope and multiplying the number per cell by 50, the total map length can be estimated in cM. It has been estimated that the average male chiasma count is 50.6 per cell, giving a map length of 2530 cM (Hultén and Lindsten, 1973). However chiasmata were more frequent in female meiosis (70.3 per cell), giving a map length of 3515 cM (Tease and Hulten, 2000).

1.8.3 Genetic markers

1.8.3.1 Criteria for a useful genetic marker

Mapping human disease gene requires genetic markers. A marker is any polymorphic Mendelian character that can be used to follow a chromosomal segment through a pedigree. Useful marker should be sufficiently polymorphic that a randomly selected person has a good chance of being heterozygous. Also, it helps if the marker can be scored easily and cheaply using readily available materials.

Meiosis is not informative with a given marker if the parent is homozygous for the marker, and also in half of the cases where both parents have the same heterozygous

genotype. The informativeness of a marker is measured by its polymorphic information content (PIC). The PIC value of a marker is calculated from the number of alleles and their frequencies in the population and is related to the mean repeat length of the marker (Weber, 1990). To be of use in linkage analysis the PIC value of a genetic marker needs to be 0.7-0.8 (70-80% heterozygosity) (Botstein *et al.,* 1980).

1.8.3.2 Types of genetic markers

DNA polymorphisms are the basis of all genetic markers and it allowed human gene mapping to start in earnest.

1.8.3.2.1 Restriction fragment length polymorphisms (RFLPs)

The first generation of DNA markers were restriction fragment length polymorphisms (RFLPs) (Botstein *et al.,* 1980). Initially, RFLPs were scored by preparing Southern blots from restriction digests of the test DNA, and hybridising with radiolabelled probes which required a lot of time, money and DNA. But nowadays RFLPs can usually be typed by polymerase chain reaction (PCR) where a sequence including the restriction site is amplified and the product is incubated with the restriction enzyme and then run out on a gel to see if it has been cut. Because RFLPs have only two alleles and thus the maximum heterozygosity is 0.5, they are of limited value.

1.8.3.2.2 Minisatellites

Minisatellites or variable number tandem repeats (VNTRs) comprise a collection of moderately sized arrays of tandemly repeated DNA sequence which are dispersed over considerable portions of the nuclear genome (Nakamura *et al.,* 1987). In VNTRs

the array size is moderately long (10-60 bp) and the repeat unit is often from 9 to 65 bp long. Although these markers have many alleles and high heterozygosity they still suffer from the disadvantages of being difficult to handle by the standard PCR protocols and of not evenly spread across the genome.

1.8.3.2.2 Microsatellites

Microsatellites or short tandem repeat polymorphisms (STRPs) are small arrays of tandem repeats of a simple sequence (usually less than 10 bp) and are interspersed throughout the human genome. They may be mono, di, tri, or tetra nucleotide repeats. Array of dinucleotide repeats are the most common type, accounting for about 0.5% of the genome. CA/TG repeats are very common, accounting of 1 per 36 kb and are highly polymorphic. AT/TA (1 per 50 kb) and AG/CT (1 per 125 kb) repeats are also quite common but CG/GC repeats are very rare (1 per 10 Mb). Tri- and tetra nucleotide repeats are now replacing dinucleotide repeats as the marker of choice because they give cleaner results. Microsatellite markers can now be amplified together in a multiplex PCR reaction to give non-overlapping allele sizes and also with the florescent labelling with different colours, it is possible to score 10 markers on a sample in a single lane of an automated gel.

1.8.3.2.3 Single nucleotide polymorphisms (SNPs)

Single nucleotide polymorphisms (SNPs) are abundant polymorphic markers uniformly distributed throughout the human genome (Venter *et al.,* 2001). It has been reported that the high density of SNPs in mammalian genomes may be employed for genome wide association studies (Wang *et al.,* 1998). However, the potential of the

SNPs in genomewide linkage searches has been paid less attention. Even though, the heterozygosity of SNPs is lower than microsatellites, their global genomic distribution and adaptability to very high-throughput genotyping suggests that they will be widely amendable to genomewide linkage analyses (Matise *et al.,* 2003).

The Affymetrix 10K SNP platform is one of the several recently introduced platforms for high-throughput SNP genotyping, others include those developed by Applied Biosystems (http://www.appliedbiosystems.com/), Motorola Life Sciences (http://www.motorola.com/lifesciences/) and Illumina (http://www.illumina.com/). These platforms allow a whole-genome scan for a disease locus to be completed with greater efficiency than most laboratories can currently achieve using conventional marker sets. The GeneChip® Mapping 10k Xba Array contains 10 044 SNP markers and the final release version of the GeneChip®Mapping 10k Xba Array contains 11 555 SNP markers (Affymetrix Inc., Santa Clara, CA) with a median inter-marker distance between SNPs of only 104 kb. However, markers are not uniformly spaced through the genome and a number of regions are significantly underrepresented (telomeric and centromeric chromosomal regions). This under-representation is equivalent to the scarcity of markers in conventional microsatellite medium density ABI set of markers (applied Biosystems). It has been reported that genotyping platforms based on high density SNP markers will shortly become the dominant technology for high-throughput linkage analyses (Sellick *et al.,* 2004). In this work we have employed the GeneChip mapping 10K array to map disease loci in a number of families.

1.8.4 Requirements of linkage analysis

There are two main requirements for carrying out linkage analysis. First a family which is informative for the loci being considered secondly, the particular alignment of alleles in the parents (phase) must be known or able to be determined. Ten meioses are sufficient to give evidence of linkage if there are no recombinants, but 85 meioses would be needed to give equally strong evidence of linkage if the recombination fraction was 0.3. Thus mapping requires markers spaced at intervals no greater than 10-20 cM across the genome. However, because of imperfect informativeness of some markers a minimum of several hundred markers may be needed.

1.8.5 Linkage analysis for autosomal recessive diseases

In dealing with autosomal recessive diseases, the linkage analysis could be more difficult than in case of dominant disorders. This is due to the fact that the haplotype of unaffected offspring could be either homozygous for the normal allele or heterozygous and hence they provide less information than in dominant disease pedigrees. Therefore, to demonstrate linkage between a markers locus and an autosomal recessive disease, more individuals are required than for a dominant disease. Homozygosity mapping has been the method of choice to demonstrate linkage in case of rare recessive diseases but in a consanguineous family (Lander and Botstein, 1987). In a given consanguineous family, the affected offspring will have a high probability of being homozygous for any given allele by descent. The availability of dense maps of highly polymorphic markers allows the detection of

homozygosity by descent, by evaluating regions in which a contagious stretch of markers are homozygous.

1.8.5 Statistical analysis of linkage

Morton (1955) demonstrated that Lod scores represent the most efficient statistic method for evaluating pedigrees for linkage. Lod score (Z) is the logarithm of odds of the ratio that two loci are linked with recombination fraction ($\theta = 0$) rather than unlinked ($\theta = 0.5$). Lod score of 3 (odds= 1000:1) is the threshold for accepting linkage, with a 5% chance of error. Linkage can be rejected at Lod score of -2 or less and values of Z between -2 and 3 are inconclusive. Human linkage analysis, except in the very simplest cases, is entirely dependant on computer programs. In this thesis Cyrillic, MLINK, genehunter, ExcludeAR and ALOHOMORA programs have been used to evaluate the linkage data.

1.9 Mutation detection techniques

Mutation detection techniques are based on testing DNA samples for changes that might be anywhere within or near the relevant gene or genes. Currently, automated fluorescence sequencers are the primary means of mutation scanning since they became cheaper and easier. Sequencing generates more data than other methods and hence the requirement for analysing these data is greater. However, the quality of the sequence is critical for avoiding artefacts and reliably detecting base substitutions in heterozygotes. Alternatives to direct sequencing include denaturing high performance liquid chromatography (dHPLC), single strand confirmation polymorphism (SSCP), protein truncation test (PTT) and quantitative PCR. These tests usually use the

properties of heteroduplexes to detect differences between two sequences. Heteroduplex analysis is based on the fact that the electrophoretic mobility of heteroduplexes in non denaturing polyacrylamide gels is less than that of homoduplexes, and hence they will show abnormal mobility on the gel. Insertions, deletions and single base pair substitutions can be detected by this method if fragments of no more than 200 bp long were tested (Keen *et al.,* 1991). On the other hand SSCP technique is based on the fact that there is a tendency of the single stranded DNA to fold up and form complex structures stabilised by weak hydrogen bonds. Hence the electrophoretic mobility of such structures will not only depend on their chain length but also on their conformation (Scheffield *et al.,* 1993).

1.9.1 Identifying and confirming disease causing mutations

Searching candidate genes for sequence changes in a number of patients could reveal many variants. However, deciding whether or not a variant is pathogenic depends on the effect of this change on the gene expression and on its existence in control samples. For example a pathogenic change has to segregate with the disease phenotype within a pedigree. Additionally, it must not be present in a panel of unrelated ethnically matching control individuals. A change or mutation can introduce or abolish a restriction enzyme binding site. Hence, cosegregation of a mutation within a family can be tested by digesting the relevant DNA sequence in the presence of the enzyme. Alternatively, convenient methods such as direct sequencing analysis, SSCP, or heteroduplex analysis can be used to test the segregation. Finally, functional work will be the ultimate measure in order to prove the effect of the mutation on the expression of the gene and hence on the function of the protein.

1.10 Aim of the study

To identify the gene responsible for the phenotype of arRP in 7 Spanish families linked to the RP25 locus. Also, to explore a novel approach utilising the 10K GeneChip array for identifying the disease locus in non-consanguineous Chinese families with autosomal recessive RP. Finally, to report a novel gene, *PCDH21*, that is highly likely to be responsible for recessive RP.

CHAPTER TWO

Materials and Methods

2.1 DNA amplification by polymerase chain reaction (PCR)

2.1.1 The PCR reaction

The polymerase chain reaction or PCR is an in vitro DNA enzymatic amplification technique that has been described by Saiki *et al.* in 1985. It involves an amplification of a specific segment of DNA by as much as 10^8 folds in only a few hours. Its ability to amplify small amounts of DNA even from a single cell has revolutionised the analysis of clinical and biological material. PCR has been used in the high efficiency cloning of genomic sequences, in direct sequencing of genomic and mitochondrial DNA, and the analysis of nucleotide sequence and the rapid detection of viral pathogen.

Amplification of a specific segment of DNA is achieved by using a pair of oligonucleotide primers and repeat cycles of denaturation, primer annealing to their complementary sequences and extension of the annealed primers with the polymerase enzyme. The primers are designed to hybridise to the opposite strands of the target sequence and are oriented so that DNA synthesis by the polymerase proceeds across the region between the primers, effectively doubling the amount of that DNA segment. Since the extension product are also complementary to and capable of binding primers, successive cycles of amplification continue to double the amount of DNA synthesised in the previous cycle. This result in an enormous accumulation of the DNA segment, approximately 2n where n is the number of cycles of amplification. Meanwhile, the technological development of thermostable DNA

polymerase isolated from the bacterium *Thermus aquaticus* has markedly improved the performance of the procedure (Saiki *et al.,* 1988). Unlike the thermo labile Klenow fragment of E.coli DNA polymerase, *Taq* polymerase retains its activity after heat denaturation of the DNA and does not need to be replaced during each cycle. Moreover, the optimum high temperature of this enzyme (70-75 °C) significantly increases the specificity, yield, and length of DNA fragments that can be amplified.

2.1.2 Parameters for PCR

2.1.2.1 Standard parameters

PCR was performed in 25-µl reaction volume containing 1X buffer (10X NH4 buffer, Bioline, UK), $MgCl_2$ (1.5-3.5 mM, Bioline, UK), 0.2 mM deoxynucleoside triphosphate (dNTPs: dATP, dCTP, dGTP, dTTP, Promega, UK), 10 pmoles of each primer, 0.5 unit of *Taq* polymerase (Bioline, UK) and ~100 ng of DNA. Amplification reactions were carried out using Thermal Cycler equipped with heated lids thus eliminating the necessity to overlay the PCR reactions with mineral oil to prevent evaporation. Amplification conditions consisted of an initial denaturation step at 94 °C for 3 minutes followed by 35 cycles of denaturation at 94 °C for 30 seconds, annealing at 55 to 68 °C for 30 seconds (according to the required annealing temperature), extension at 72 °C for 30 seconds (extension time varied depending on the size of the amplicon) and a final extension step at 72 °C for 5 minutes.

2.1.2.2 Special parameters

For GC rich regions, buffer 3 (containing 22.5 mM $MgCl_2$; supplied with Boehringer Manheim GmbH-Germany) together with dimethyl sulphoxide DMSO 5% or Ready mix (AB-0795; ABgene, UK) were used.

2.1.2.3 Multiplex PCR

For multiplex PCR, an absolute QPCR mix (1x absolute QPCR buffer, 0.025 units/µl thermo start enzyme, 0.5 mM of each dNTP, and 5.5 mM $MgCl_2$ supplied by ABgene, UK) was used which required an activation step at 95 °C for 15 minutes.

2.1.3 Calculation of the annealing temperatures

The optimum annealing temperatures for the designed primers were calculated from their melting temperatures (T_m). To calculate the T_m The following formula T_m = 4(G+C) + 2(A+T) which also depends on the length of the primer and its GC content was used. An average of 2-5 °C below the estimated T_m was used as starting point for PCR optimisation.

2.1.4 Primer design

In order to design primers for PCR amplification the following parameters have to be considered: The length of the primers should be generally between 18 and 27 nucleotides (to increase the sequence specificity), random base distribution, 40-60% GC content, minimal secondary structure, low complementarity to each other especially in the 3' end to avoid the formation of primer dimer, and the difference between the T_m values of both primers should be no greater than 4 °C. In this thesis

primers were designed using Primer 3 Out put program (http://frodo.wi.mit.edu/cgi-bin/primer3/primer3_www.cgi). Primers were synthesised commercially by GenoSys (http://orders.sigma-genosys.eu.com/).

2.2 Fractionation of DNA by agarose gel electrophoresis

Agarose gel electrophoresis was used to visualise PCR products, restriction enzyme digests and to estimate DNA concentrations. The concentration of agarose used depends on the fragment size as shown in table 2.1

Agarose gel was prepared according to the following protocol: A [%(w/v)] of agarose was weighted in a clean conical flask and the corresponding volume of 1xTAE (tris acetate EDTA) was added. The mixture was mixed by gentle swirling and heated in a microwave until the agarose was dissolved. The dissolved agarose was then cooled to about 50 °C before adding the ethidium bromide to a final concentration of 0.5 µg/ml. The cooled agarose was poured into a sealed loading tray with a comb in place and allowed to set at room temperature for nearly 30 minutes to polymerise. Then the seals and the comb were removed and the gel was placed in an electrophoresis tank (Gel electrophoresis apparatus GNA-200, Pharmacia, Sweden) containing sufficient 1xTAE buffer, with the wells positioned near the cathode. Samples were prepared by adding 2 µl of orange loading dye to 5 µl of the PCR product or DNA and were loaded into the wells. An appropriate DNA size marker was also loaded, depending on the anticipated size of the PCR products (Table 2.2).

Electrophoresis was then carried out at 100 V for 45 minutes or until the required resolution has been achieved. Then gels were photographed on an UV transilluminator using a Gene Genius Camera System with an orange filter and Kodak plus-X film.

Table 2.1 Agarose gel concentrations for separating DNA fragments

Agarose [%(w/v)]	*Fragment size in Kb*
0.3	5.0-60
0.6	1.0-20
1.0	0.5-10
1.5	0.2-6.0
2.0	0.1-2.0
3.0	0.05-<0.1

Table 2.2 Size of ØX174/HaeIII and smart (1 and 10 Kb) markers in bp

ØX174/HaeIII	*Smart ladder (1Kb)*	*Smart ladder (10 Kb)*
1,358	1000	10,000
1,078	800	8,000
603	700	6,000
310	600	5,000
234	500	4,000
194	400	3,000
118	300	2,500
72	200	2,000
	100	1,500
		1,000
		800
		600
		400
		200

2.3 Purification of PCR products

PCR products were purified before carrying out the sequencing reaction in order to remove the unincorporated primers and dNTPs. The purification process was performed using one of the following methods.

2.3.1 Montage

PCR products were purified in this protocol by adding 20 µl of the PCR products to 80 µl of sterile dH_2O and then transferring the whole volume (100 µl) to the Montage plate (Millipore, UK) which was vacuumed for 10-12 minutes. 25 µl sterile dH_2O was then added to the plate which was re-vacuumed for 2-3 minutes as a washing step. Lastly, 20 µl of sterile dH_2O was added to the samples and the plate was shaken at 10,000 rpm for 10 minutes to elute the DNA. This method elutes approximately 18 µl of the PCR product which subsequently can be used for sequencing (2 µl per reaction) and the rest can be stored at -20 °C for future use.

2.3.2 ExoSAP

An aliquot of the amplification product (1 µl) was purified by adding 16.5 µl of dH_2O and 0.5 µl of Exosap [1 U shrimp alkaline phosphatase (SAP, QAmersham LifeScience, Buckinghamshire, UK) and 1 U Exonuclease I (United States Biochemicals, Ohio, USA) and incubated at 37 °C for 15 minutes then at 80 °C for another 15 minutes to deactivate the enzyme. The whole product 18 µl was then used for sequencing reaction.

2.4 Mutation detection techniques

2.4.1 Automated DNA sequencing

Automated DNA sequencing is based on a laser detection system of fluorescently tagged dideoxynucleoside triphosphates (ddNTPs) in a cycle sequencing reaction. The detected florescence is presented as a graphical image on the computer. In automated sequencing, only one primer is used which is mixed with the purified PCR products and a mix called Big Dye (applied Biosystems, Cheshire, UK) which contains dye terminators (ddNTPs), dNTPs, $MgCl_2$, Tris-HCL buffer, pH 9.0, and AmpliTaq DNA Polymerase. The ddNTPs differ from dNTPs by lacking the hydroxyl residue at the 3` position of the deoxyribose, preventing the formation of phosphodiester bond when incorporated into the elongating DNA molecule, thus leading to chain termination. AmpliTaq DNA Polymerase is a variant of the *Thermus aquaticus* DNA Polymerase which contains a point mutation in the active site, resulting in more even peak intensity due to less discrimination against ddNTPs.

After PCR amplification and purification of the products by Montage or ExoSAP methods as described in sections 2.3.1 and 2.3.2, cycle sequencing reaction was carried out in 0.2 ml microfuge tubes. In case of Montage 10 µl reaction volume was prepared containing 2 µl of the PCR product, 4.5 µl dH_2O, 2.5 µl sequencing buffer (Applied Biosystems), 0.5 µl Big Dye version 3.1, 0.5 µl (10 pmol) forward or reverse sequence specific primer. For ExoSAP the following protocol was used: the product (18 µl) was mixed with 0.5 µl Big Dye and 0.5 µl primers (10 pmol). Cycle sequencing reactions were carried out in the thermal Cycler and the temperature cycling profile consisted of initial denaturation at 96 °C for 3 minutes followed by 25 cycles of denaturation at 95 °C for 10 seconds, annealing at 50 °C for 5 seconds and

then 4 minutes at 60 °C, and finally a further extension at 4 °C for 2 minutes. After completion of the cycle sequencing reaction the DNA was precipitated by using Montage sequencing reaction cleanup kit (Millipore, UK) and then run on automated fluorescence DNA sequencer (ABI 3100, Perkin Elmer, Foster City, CA), according to manufacturers' instructions.

2.5 Gene expression analysis

Expression of four of the genes studied was assessed by PCR amplification of human cDNAs from retina, brain, kidney, liver, heart, skeletal muscle, pancreas, lung and placenta (Quick-Clone; Clontech). Four pairs of primers were designed (see section 2.1.4) for the last exon and the 3'UTR of each individual gene to create gene-specific sequence-tagged sites (STSs) (Appenidx 1, Table 1). Multiplex PCR, (see section 2.1.2.3) was performed to compare the expression level of each gene in different tissues. PCR products were visualized on a 2% agarose gel (section 2.2).

2.6 Restriction Enzyme Analysis

Restriction digests were performed on PCR products. For PCR product digests, a total volume of 20 µl containing 2 µl 10X buffer, 0.2 µl 1x Bovine Serum Albumin (BSA) to enhance the enzyme activity, 10 µl PCR product, 0.5-1.0 µl of the appropriate enzyme (5-10 units) and 7.3 µl distilled water was used. The reactions were then incubated for at least 2 hours or overnight at the specified temperature for the enzyme (usually 37 °C). After heat inactivation the product of the restriction digest were visualized by agarose gel electrophoresis (section 2.2). Enzymes were obtained from New England BioLabs or Promega, UK.

2.7 Genotyping

2.7.1 Microsatellite marker analysis

Genotyping was performed using microsatellite markers from the ABI PRISM® Linkage Mapping Sets V2.5. Additional microsatellite markers were synthesised commercially (www.thermo.com/biopolymers, Thermo, Germany) according to the information obtained from the Genome Database. The data for heterozygosity and the order of the markers used were obtained from the Marshfield Medical Research Foundation web site. Forward primers for the commercially synthesised microsatellite markers were labeled with either FAM (blue) or HEX (green) probes. Microsatellite markers were amplified from the patient genomic DNA by either standard PCR reaction (section 2.1.2.1) or by multiplex PCR (section 2.1.2.3) using 4-6 markers per reaction using QPCR mix (ABgene, UK). In multiplex PCR the selection of primers that run together was made according to the following parameters: first the distance between the primers should be at least 20 bp and secondly FAM and HEX labeled primers were mixed together since ROX ladder has been used to visualise them; meanwhile VIC and NED were mixed together since LIZ ladder was used in that case. 1- 3 µl of the PCR products was then added to 10 µl of the ladder that consisted of either ROX or LIZ with the formamide in a ratio of 50 µl to 1000 µl, respectively. Then the samples were analysed on an ABI 3100 genotyper according to manufactures instructions (Applied Biosystems).

Data collection and allele identification were performed using GeneScan and Genotyper software (Applied Biosystems). Alleles were assigned to individuals and genotypic data were used to calculate the LOD scores using the programs Cyrillic and

MLINK. The phenotype was analysed as an autosomal recessive trait with complete penetrance and with a frequency of 0.0001 for the affected allele.

2.7.2 GeneChip Mapping 10K Array

In this study, DNA samples from 17 affected individuals and 12 unaffected carriers from 7 families were genotyped by total genome-sampling analysis using the Affymetrix 10K GeneChip Mapping Array (version Xba142). The median physical distance between SNPs and their average heterozygosity were 105 kb and 0.37, respectively, predicting an average spacing of 3 fully informative markers per one Mb. Genotypes for 10,204 SNPs were called by the GeneChip DNA Analysis Software (GDAS v3.0, Affymetrix). The detailed methodology for genotyping using the GeneChip array has previously been described (Sellick *et al.* 2004).

The 10K SNP arrays were scanned with the Affymetrix GeneChip Scanner 3000 using GeneChip Operating System 1.4 (Affymetrix). Data files were generated automatically. Genotype assignments (i.e. calls) were made automatically by GeneChip Genotyping analysis Software v4.0 (GTYPE). The genetic map used in the analysis was obtained from GeneChip Mapping 10K library files: Mapping10K_Xba142. "Signal Detection Rate" is the percentage of SNPs that pass the discrimination filter. "Call Rate" is the percentage of SNPs called on the array. The genotype calls were defined as AA, AB, or BB; "no call" means the SNP does not pass the discrimination filter.

2.7.3 Analysis of the GeneChip Mapping 10K Array

2.7.3.1 Analysis of the 10K array data from consanguineous families

Regarding the consanguineous families, ExcludeAR1, 3 and 4liteCHIP2 macros were utilised to highlight significant regions of homozygosity among all affected individuals in three of the studied families (Woods *et al.,* 2004). This program seeks homozygous regions in consanguineous families and the greater the number of affected individuals who have a shared homozygous region and the greater the size of the region, the more likely it is to harbour the mutation that causes the disease.

Four versions of the ExcludeAR (AR1-4) were developed for the interpretation of data from one (AR1), two (AR2), three (AR3) and four (AR4) affected individuals. ExcludeAR first detects runs of consecutive homozygous SNP allele calls identical in all of the affected individuals analysed. It then determines if each run is of statistical significance. For example for a consanguineous cousins, a run of 12 or more homozygous SNPs in both would occur only once in 1000 analyses by chance rather than being identical by descent. Then, ExcludeAR lists the 10 largest homozygous SNP runs by genetic size. For each result the following are given: genetic size, chromosome, genetic location on chromosome, number of homozygous SNPs in run, number of "NoCalls" in the run and whether the result reaches statistical significance. Two graphs are generated: the first shows the genetic size versus number of homozygous SNPs for the statistically significant results; the second shows the size of all statistically significant results by chromosome.

2.7.3.2 Analysis of the 10K array data from non consanguineous families

A software tool called "ALOHOMORA" was utilised to analyse the 10K array data in case of non consanguineous families. ALOHOMORA is written in Perl and may be used to perform state of the art linkage scans in small and large families with any genetic model (Rüschendorf and Nürnberg, 2005).

The analysis of the data was performed using the ALOHOMRA software. Mendelian errors and the correct relationships within the families were checked for by PedCheck and graphical relationship representation (GRR) programs respectively (O'Connell and Weeks, 1998; Abecasis *et al.* 2001a). Identification and deletion of non-Mendelian errors and unlikely genotypes were performed. Uninformative SNPs were removed from the data by Merlin (Abecasis *et al.* 2001b). For parametric linkage analysis, the data were converted for Genehunter where the analysis was done in subsets of markers in a non-overlapping moving window. The haplotyping data were then used from the Genehunter file.

2.8 Comparative genome hybridisation (CGH)

Comparative genomic hybridisation is a molecular-cytogenetic method for the analysis of copy number changes (gains/losses) in the DNA content of cells. The method is based on the hybridisation of fluorescently labeled tumor DNA and normal DNA to normal human metaphase preparations. CGH detects only unbalanced chromosomal changes. However, structural chromosome aberrations such as balanced reciprocal translocations or inversions cannot be detected, as they do not change the copy number. CGH is also capable of detecting loss, gain and amplification of the copy number at the levels of chromosomes. However, it is considered that to detect a

single copy loss, the region must be at least 5-10 Mb in length. On the other hand, detection of amplification is known to be sensitive down to less than 1 Mb. Therefore, one must take into consideration that while CGH is sensitive to amplification, it is an order of magnitude less sensitive to loss.

In this work CGH was performed in Sanger centre using a Whole Genome TilePath (WGTP) array that comprises 26,574 large-insert clones representing 93.7% of the euchromatic portion of the human genome. This was carried out to study the possibility of CNVs existing within one of the recessive RP families (RP5) and its impact on the RP25 phenotype.

Dyeswap experiments were carried out for each DNA where each test sample was labeled in both Cy5 and Cy3 and co-hybridised against a male reference DNA labeled in the opposite Cy dye. The ratio of the Cy5 to Cy3 labeled DNA binding to each clone on the array is calculated. The average ratio from the two dyeswap experiments is taken and plotted clone by clone across the genome. All DNA samples were then hybridised against one male reference DNA which was the same DNA used as the reference in the array-CGH study of the HapMap collection published previously (Redon *et al.*, 2006).

2.9 Computer aided analysis

2.9.1 Computational analysis of DNA sequencing

Analysis of DNA sequence was mainly performed using Seqscape program v2.0 from Applied Biosystems and Seqman from DNA star.

2.9.2 Computational analysis of geneotyping data

Analysis of the raw data from the ABI 3100 genotyper was performed on the genotyper program v2.0 and on GeneMarker v1.1.

2.9.3 Linkage computer programs

Pedigrees were drawn on Cyrillic and the genotype information for all markers was entered for each individual sample. To obtain the LOD score, MLINK program from Cyrillic was used and the PED and DAT files were created and exported to the linkage subdirectory. Genehunter has been also used to perform multipoint linkage analysis where the DAT and PED files created by the MLINK program were scanned and uploaded in Genehunter and total statistics was obtained including the P value, parametric and non parametric Lod scores.

The data obtained from the 10K array were analysed using ExcludeAR and ALOHOMORA software for consanguineous and non consanguineous families, respectively.

2.10 Buffers and solutions

50xTAE (Tris acetate EDTA)

2 M Tris-Acetate

0.05 M EDTA

Ethidium Bromide (10 mg/ml)

1 gm ethidium bromide/100 ml distilled water

Orange Loading Dye

40% Glycerol (12 ml)

0.4% Orange G (0.12 gm)

10xTAE (6 ml of 50x)

Add up to 30 ml dH_2O

2.11 Electronic database information

Retnet (http://www.sph.uth.tmc.edu/retnet/disease.htm)

National Centre for Biotechnology Information (NCBI)

(http://www.ncbi.nlm.nih.gov/)

ENSEMBL database (http://www.ensembl.org)

Genecards (http://bioinfo1.weizmann.ac.il/genecards/index.shtml)

University of California Santa Cruz (UCSC) (http://genome.ucsc.edu/)

(http://www.fruitfly.org/seq_tools/other.html) to characterise exon-intron boundaries

EyeSAGE database (http://neibank.nei.nih.gov/EyeSAGE/index.shtml)

Database of Genome Variants (http://projects.tcag.ca/variation/)

CHAPTER 3

IDENTIFICATION OF THE CAUSATIVE GENE FOR THE RP25 LOCUS

3.1 INTRODUCTION

3.1.1 The RP25 locus

Genetic linkage to the RP25 locus was originally identified by our Spanish collaborators through targeting genes that may have functional relevance to RP. For this reason, to begin with, they investigated chromosomal regions (4p, 5q, 6q and 15q) that contain genes encoding different subunits of GABA receptors (Ruiz *et al.,* 1998). It is known that different GABA receptors are expressed in all retinal layers and the inhibition mediated by these receptors in the human retina could be related to RP (Lisman and Fain's, 1995). Homozygosity mapping led to the identification of the RP25 locus on chromosome 6p12.1-q15 between microsatellite markers D6S257 and D6S1644, a region that spans approximately 16.1 cM in 3 consanguineous (RP5, RP214 and RP167) (appendix 1 Figure 1A, B and C) and in a non-consanguineous (RP73) (appendix 1 Figure 1D) arRP Spanish families (Ruiz *et al.,* 1998). This region contains the rho1 and rho2 subunits of the GABAc receptor (Cutting *et al.,* 1991, 1992). Both subunits are expressed in the retina and form part of the GABAc receptor that is expected to mediate the lateral inhibition of the light responses in the vertebrate retina (Bormann and Feigenspan, 1995).

Subsequently, a three generation consanguineous Pakistani family with arRP was mapped to an interval 2.4 cM, between markers D6S257 and D6S1053, proximal to the same region (Khaliq *et al.,* 1999). In addition, evidence of linkage to the RP25 locus was

also reported in 3 new Spanish (RP299, RP235 and RP260) (appendix 1 Figure 1E, F, and G) (Barragan *et al.,* 2005) as well as in another 3 Chinese families (RP10, RP112 and RP116) (Abd El-Aziz *et al.,* 2007) with recessive RP (Figure 3.1). These findings support our hypothesis that RP25 gene could be a frequent cause of RP.

3.1.2 Retinal dystrophies linked to chromosome 6q

Several loci with retinal dystrophy phenotypes have been mapped to the pericentromeric region of chromosome 6 (6q14-q21) (Figure 3.2). Autosomal dominant Stargardt-like disease (STGD3) (Stone *et al.,* 1994), cone rod dystrophy (CORD7) (Kelsell *et al.,* 1998a), autosomal dominant macular dystrophy (adMD) (Griesinger *et al.,* 2000), Leber congenital amaurosis type 5 (LCA5) (Dharmaraj *et al.,* 2000) and benign concentric annular macular dystrophy (BCAMD) (van Lith-Verboeven *et al.,* 2004) are located in the overlapping region with RP25, while MCDR1 (Small *et al.,* 1992) and progressive bifocal chorioretinal atrophy (PBCRA) (Kelsell *et al.,* 1995), are in the non overlapping region. Recently, *ELOVL4* has been cloned as the gene responsible for STGD3 and adMD (Zhang *et al.,* 2001). Subsequently *RIM1* and *IMPG1* have been reported as the causative genes for CORD7 and BCAMD, respectively (Johnson *et al.,* 2003 and van Lith-Verboeven *et al.,* 2004). At the beginning of this project the gene for LCA5 was not identified hence we postulated that both LCA5 and RP25 could be due to the same genetic defect (allelic). Therefore recruiting LCA families in order to identify LCA5 subtype that genetically overlap with the RP25 locus, might be useful. Novel crossovers in linked families may have the potential of refining the genetic interval spanning the RP25 locus.

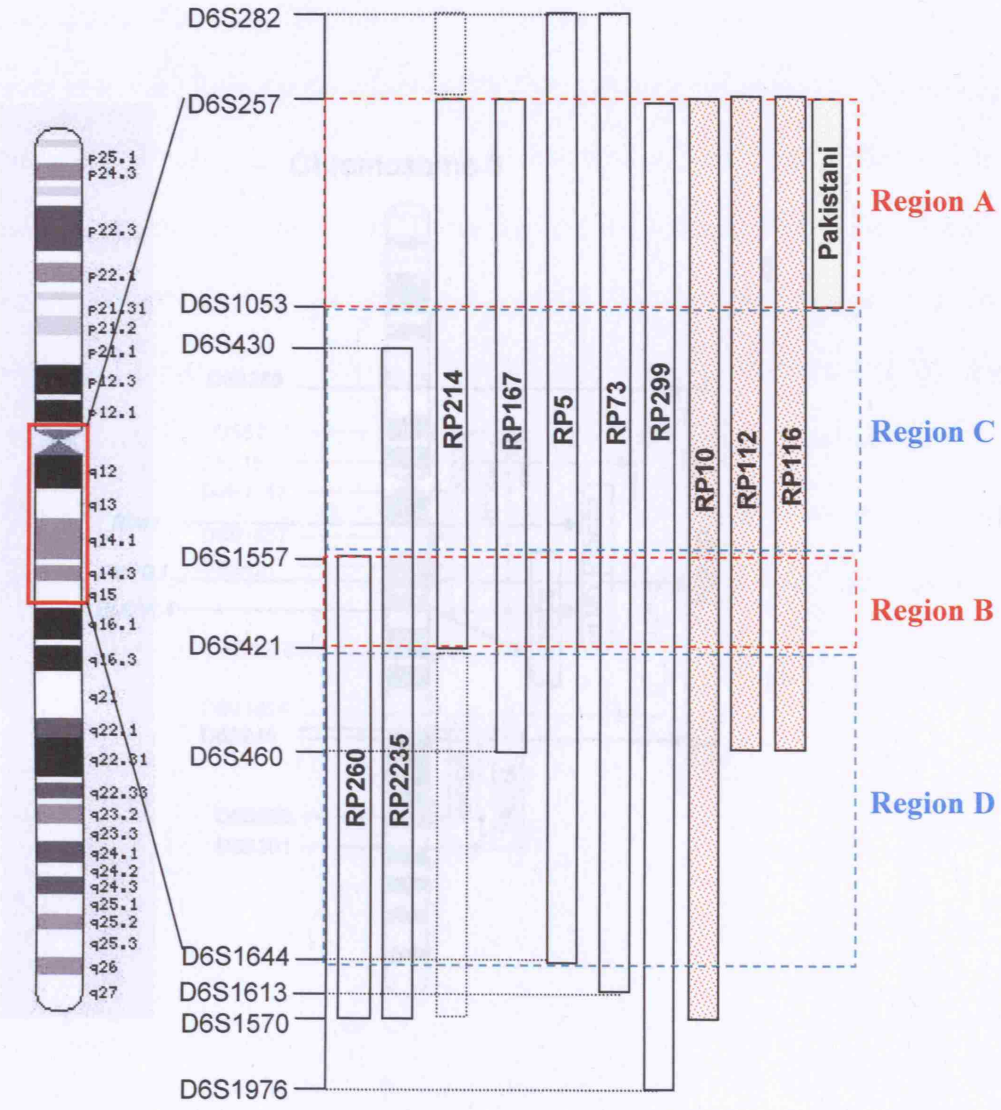

Figure 3.1 Schematic representation of chromosome 6, the RP25 locus (between microsatellite markers D6S257 and D6S1644). The genetic intervals for the Spanish (RP299, RP73, RP5, RP167, RP214, RP235 and RP260), Chinese (RP10, RP112 and RP116) and Pakistani families are represented by vertical bars. The dotted boxes in RP214 family represent the non homozygous linked intervals in this family. The interval is divided into four regions (A, B, C and D) according to the genetic data.

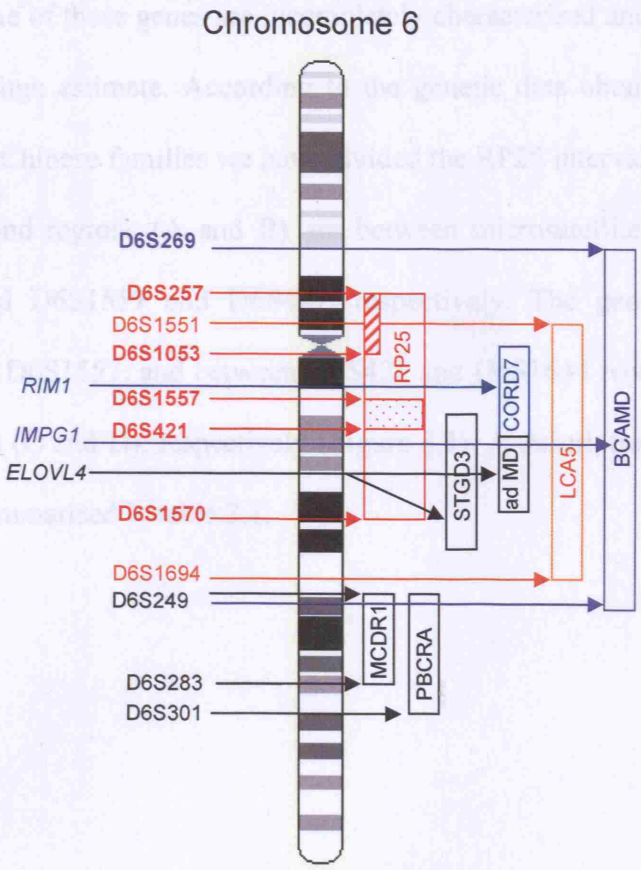

Figure 3.2 Schematic representation of chromosome 6, showing the retinal dystrophy loci in the region, as well as the localisation of *RIM1*, *ELOVL4* and *IMPG1* genes. The hatched area within the RP25 locus indicates the overlap between the Spanish and the Pakistani families and the dotted area depicts the region where all Spanish families are linked.
STGD3: ad Stargardt-like disease; adMD: ad macular degeneration; CORD7: cone-rod dystrophy; LCA5: Leber congenital amaurosis; BCAMD: benign concentric annular macular dystrophy; MCDR1: North Carolina macular dystrophy; PBCRA: progressive bifocal corioretinal atrophy.

3.1.3 RP25 genetic interval

The chromosomal interval defining the RP25 region is ~34 Mb and contains 111 genes as reported in the database for the Human Genome sequence information (Figure 3.3). However, some of these genes are incompletely characterised and therefore this number could be a rough estimate. According to the genetic data obtained from the Spanish, Pakistani and Chinese families we have divided the RP25 interval into four regions. The first and second regions (A and B) are between microsatellite markers D6S257 and D6S1053; and D6S1557 and D6S421, respectively. The genetic intervals between D6S1053 and D6S1557; and between D6S421 and D6S1644 represent the third and the fourth regions (C and D), respectively (Figure 3.1). A description of the genes in these intervals is summarised in table 3.1.

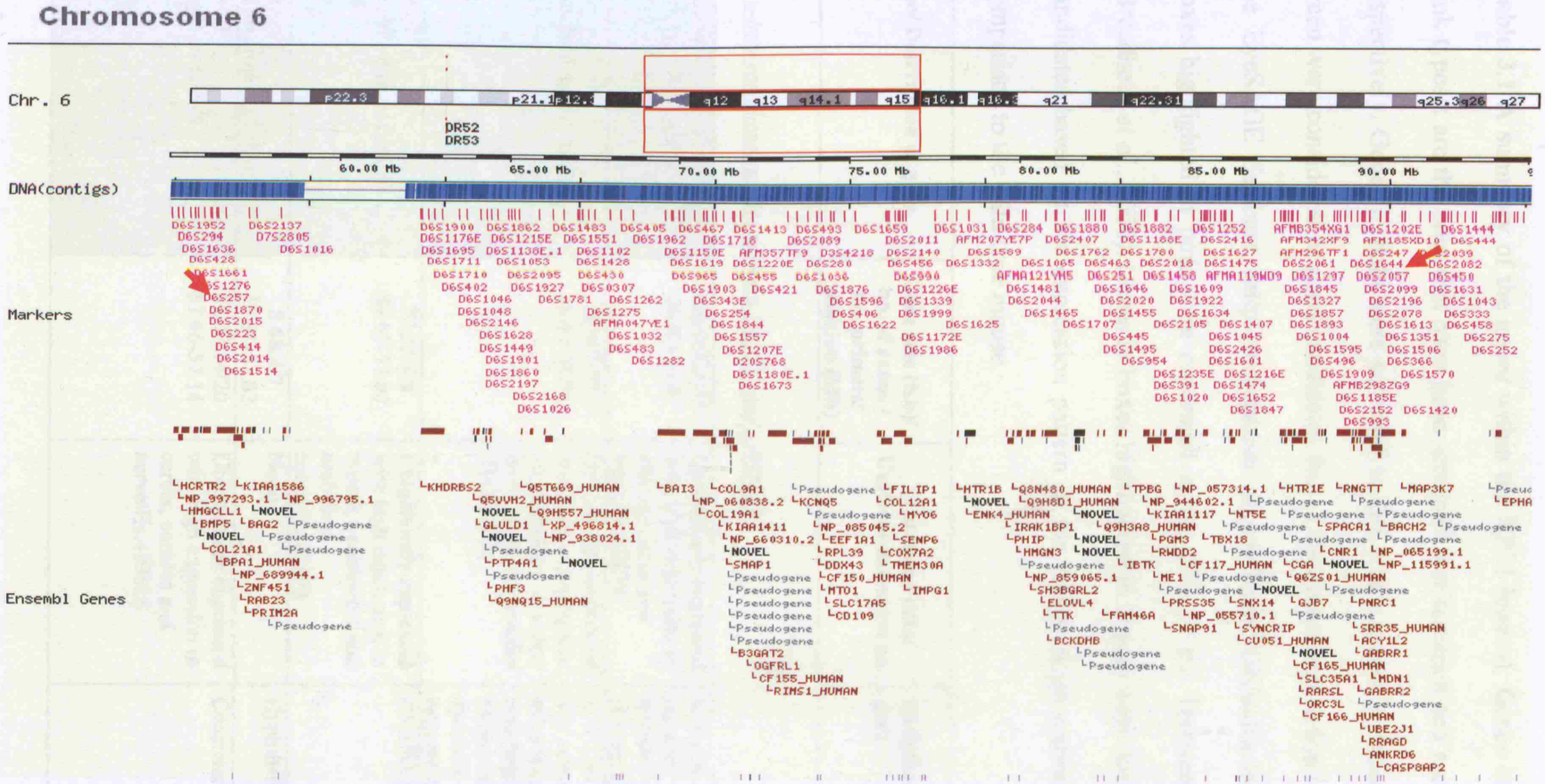

Figure 3.3 *RP25 interval (represented in Ensembl) displaying the microsatellite markers (D6S257 and D6S1644) spanning the interval (red arrows) and showing the genes within the interval.*

Table 3.1 A summary of the genes within the RP25 interval. Genes in red, black and pink typeset are the ones that have been screened, not screened and recently predicted, respectively. Genes in bold were screened in this study; genes in boxes highlighted in green were considered as good candidates due to confirmed expression in eye tissues by the EyeSAGE database (http://neibank.nei.nih.gov/EyeSAGE/index.shtml). Genes in boxes highlighted in pink were expressed in the cilia of the Trypanosome proteome (Broadhead *et al.*, 2006). Genes in boxes highlighted in orange were considered as good candidates based on the expression pattern in the retinal degeneration (rd) mouse in comparison to the wild type mouse.

Gene/ Description of gene	**Gene size (Kb)/ no. of exons / no. primers/ position (Mb)**	**Expression data/ UniGene accession no.**	**Published information about the gene**
Genes in-between microsatellite markers D6S257 and D6S1053			
1. *COL21A1*/ Collagen, type XXI, alpha 1	190.96/31/31 56.03-56.36	Ubiquitously expressed with high expression in adipose tissue and heart/Hs.47629	Is a new FACIT (fibril-associated collagen with interrupted triple helices) of the collagen family (Fitzgerald and Bateman, 2001).
2. *DST*/ Dystonin, Bullous pemphigoid antigen 1	385.67/99/ 56.43-56.92	Ubiquitously expressed with high expression in adipose tissue, bladder, bone, brain and cochlea /Hs.631992	Is a 230- to 240-kD glycoprotein that serves as an autoantigen in the blistering disease bullous pemphigoid (Stanley *et al.*, 1988). Mouse models developed severe dystonia and sensory nerve degeneration (Guo *et al.*, 1995).
3. *C6orf65*/ Chromosome 6 open reading frame 65	72.05/8/8 56.92-57.00	Ubiquitously expressed with high expression in mouth, parathyroid and umbilical cord/Hs.582993	C6orf65 protein
4. ***KIAA1586*** / KIAA1586 protein	8.68/4/7 57.01-57.02	None	Hypothetical protein
5. *ZNF451*/ Zinc finger protein 451	80.27/14/20 57.06-57.14	Ubiquitously expressed with high expression in cervix, cochlea and nerve/Hs.485628	Coactivator for steroid receptors

Gene/ Description of gene	Gene size (Kb)/ no. of exons / no. primers/ position (Mb)	Expression data/ UniGene accession no.	Published information about the gene
6. *BAG2*/ 1. BCL2-associated athanogene 2 2. BAG family molecular chaperone regulator 2	12.61/3/5/ 57.14-57.15	Ubiquitously expressed with high expression in adipose tissue, cervix, lymph node and cochlea/ HS.55220	Was reported along with BAG1 and BAG3 to interact with heat shock 70 KD protein 8 ATPase domain and inhibit its chaperone activity (Takayama *et al.*, 1999).
7. *RAB23*/ RAS associated protein RAB23	33.47/8/8/ 57.16-57.19	Ubiquitously expressed with high expression in bone and vascular tissue/ HS.555016	Open brain phenotype (opb) gene was reported to encode RAB23 (Eggenschwiler *et al.*, 2001). Mouse embryos with homozygous mutations in opb gene die during the second half of gestation with open neural tube defect (Gunther *et al.*, 1994).
8. ***PRIM2A***/ Primase, polypeptide 2A, 58kDa	329.44/14/11/ 57.28-57.62	Ubiquitously expressed with high expression in nervous tissue, ovary and oesophagus/ HS.485640	One of four subunits of the DNA polymerase-alpha/primase complex. It plays a role in both the initiation of DNA replication and the synthesis of Okazaki fragments (Shiratori *et al.*,1995).
9.*GUSBL2*/ Glucuronidase, beta-like 2 or *C6orf216*	41.64/8/6 58.35-58.39	Ubiquitously expressed with high expression in mouth and embryonic tissue/ HS.561539	Plays an important role in the degradation of dermatan and keratan sulfates.
10.***KHDRBS2***/ KH domain containing, RNA binding, signal transduction associated 2	606.27/9/9 62.44-63.05	Ubiquitously expressed with high expression in brain, eye and larynx/ HS.519794	Associated with and was methylated by protein arginine N-methyltransferase-1 (PRMT1) (Cote *et al.*, 2003).
11. *FKBP1C* /*Q5VVH2_human*/ FK506 binding protein 1C	1.58/1/1 63.996-63.98	none	Paralog to *FKBP1A* on chromosome 20p13.
12. *GLULD1*/ Glutamate-ammonia ligase domain containing 1	40.34/4/4 64.04-64.08	Expressed in few tissues but highly in eye and cranial nerve/ HS.149585	Plays a key role in the uptake and metabolism of glutamate in the retina (Barragan *et al.*, 2005).
13. ***PTP4A1*** /***PRL1***/ Protein tyrosine phosphatase type IVA, member 1 Phophatase of regenerating liver 1	11.57/6/6 64.33-64.35	Ubiquitously expressed with very high expression in cervix/ HS.227777	Over-expression of Prl1 in stably transfected cells may lead to tumorigenesis (Cates *et al.*, 1996).
14.***PHF3***/ PHD finger protein 3	79.64/16/16 64.40-64.48	Ubiquitously expressed with high expression in cochlea, pharynx and pituitary gland / HS.348921	PHF3 expression was reported to be significantly reduced in glioma (Fischer *et al.*, 2001).
15. ***Q9NQ15*** / Novel protein with EGF-like and laminin G domains – Fragment	1.2/1/3 64.488-64.489	Expressed only in brain, mammary gland, testis and thyroid / HS.25067	Has EGF-like and laminin G domains.

Gene/ Description of gene	Gene size (Kb)/ no. of exons / no. primers/ position (Mb)	Expression data/ UniGene accession no.	Published information about the gene
Genes in-between microsatellite markers D6S1053 and D6S1557			
16. *Q5T669_human*/ OTTHUMP00000016678 – Fragment	8.87/2/2 65.38-65.39	none	Has EGF-like domain.
17. *Q5T1H1* / OTTHUMP00000016679 – Fragment	9.55/3/3 65.57-65.58	Expressed in few tissues including blood, bone , brain, eye, lung and prostate/ HS.626653	Similar to Neurogenic locus Notch protein precursor.
18. *Q9H557_human* / Novel EGF-like domain containing protein (Fragment)	26.05/4/4 65.65-65.67	none	Has EGF-like domain.
19. *Q5TEL3_human* / OTTHUMP00000016683 – Fragment EGF-like-domain	0.123/1/1 65.76-65.76	none	Has EGF-like domain.
20. *Q5TEL4_human* / OTTHUMP00000016682 – Fragment EGF-like-domain	0.075/1/1 65.77-65.77	none	Has EGF-like domain.
21. *Q5VVG4_human* / OTTHUMP00000016684 – Fragment EGF-like-domain	0.111/1/1/ 65.82-65.82	none	Has EGF-like domain.
22. *Q5T3C8* / OTTHUMP00000016685 – Fragment EGF-like-domain	0.255/1/4 66.062-66.063	none	Has EGF-like domain.
23. *EGFL11* / EGF-like-domain, multiple 11	161.09/9/11 66.10-66.26	Expressed in few tissues but mainly in eye and ovary/ HS.454341	Has EGF-like domain.
24. *BAI3*/ Brain-specific angiogenesis inhibitor 3	750.22/30/31 69.40-70.15	Ubiquitously expressed with high expression in pituitary gland, brain and cochlea/ HS.13261	*BAI3* expression was reported to be absent or markedly reduced in glioblastoma cell lines suggesting that the gene may play an important role in suppression of glioblastoma (Shiratsuchi *et al.*, 1997).
25. *LMPRD1*/C6orf209/ LMBR1 domain containing 1	21.03/16/15 70.44-70.56	none	None

Gene/ Description of gene	Gene size (Kb)/ no. of exons / no. primers/ position (Mb)	Expression data/ UniGene accession no.	Published information about the gene
26. ***COL19A1***/ NM_001858/ Collagen, type XIX, alpha 1	345.71/51/41 70.63-70.97	Expressed in few tissues but mainly in blood/ HS.444842	Both *COL19A1* and *COL9A1*, were duplicated from the same ancestral gene of the FACIT family (Khaleduzzaman *et al.*, 1997).
Genes in-between microsatellite markers D6S1557 and D6S421			
27. *COL9A1*/ Collagen, type IX, alpha 1	87.03/38/39/ 70.98-71.06	Expressed in few tissues but with very high expression in cochlea/ HS.590892	A mutation in the *COL9A1* gene was reported in a family with multiple epiphyseal dysplasia (Czarny-Ratajczak *et al.*, 2001). A homozygous mutation was also reported in a recessive form of Stickler syndrome (Van Camp *et al.*, 2006).
28. ***KIAA1411*** / KIAA1411 protein	147.69/22/27 71.18-71.32	Ubiquitously expressed with high expression in larynx/ HS.211700	Excluded as causative for the RP25 locus (Abd El-Aziz *et al.*, 2006).
29. *C6orf57*/ Chromosome 6 open reading frame 57	22.65/3/5 71.33-71.35	Ubiquitously expressed/ HS.418495	C6orf57 protein.
30. *SMAP1*/ Stromal membrane-associated protein 1	194.24/11/11 71.43-71.62	Ubiquitously expressed with high expression in cochlea/ HS.485717	Excluded as causative for the RP25 locus (Barragan *et al.*, 2006).
31. *B3GAT2*/ beta-1,3-glucuronyltransferase 2	100.36/4/4 71.62-71.72	Expressed in few tissues but mainly in the eye and brain/ HS.653102	Imiya et al. 2002 reported that mouse Glcats, transfected and expressed in COS-1 cells, exhibited glucuronyltransferase activity toward glycoproteins.
32. ***OGFRL1***/ Opioid growth factor receptor-like 1	13.49/7/8 72.05-72.06	Ubiquitously expressed with high expression in cervix, kidney and larynx/ HS.368337	Excluded as causative of the RP25 locus (Abd El-Aziz *et al.*, 2006).
33. ***C6orf155***/ Chromosome 6 open reading frame 155	6.30/4/3 72.180-72.187	none	none
Genes in-between microsatellite markers D6S421 and D6S1644			
34.*RIMS1*/ Regulating synaptic membrane exocytosis 1	513.69/34/34 72.65-73.13	Expressed in few tissues but mainly in brain and cochlea/ HS.485729	Reported as the causative gene of CORD7 (Johnson *et al.*, 2003).

Gene/ Description of gene	Gene size (Kb)/ no. of exons / no. primers/ position (Mb)	Expression data/ UniGene accession no.	Published information about the gene
35. *KCNQ5*/ Potassium voltage-gated channel, KQT-like subfamily, member 5	573.12/14/16 73.38-73.96	Ubiquitously expressed but mainly in blood, bone marrow and thyroid / HS.98129	A KCNQ5 splice variant was identified in skeletal muscle displayed altered gating kinetics, notably a lack of current relaxations after hyperpolarizing voltage steps (Schroeder *et al.*, 2000).
36. *C6orf148*/ Chromosome 6 open reading frame 148	106.82/7/7 73.98-74.07	Ubiquitously expressed/ HS.433062	none
37. *DPPA5* / Developmental pluripotency associated 5	1.23/3 74.11-74.12	none	Reported to have an important role in stemness in human embryonic stem and germ cells (ESCs and EGCs) and also can be used as a marker of pluripotent stem cells (Kim *et al.*, 2005).
38. NP_001017361.1/ ES cell associated transcript 1 (ECAT1), mRNA	1.5/3/ 74.12-74.13	Expressed only in muscle and thymus/HS.128326	Embryonic stem cell associated transcript.
39. NP_001073976.1/	0.478/2/ 74.13-74.16	None	None
40. *DDX43*/ DEAD (Asp-Glu-Ala-Asp) box polypeptide 43	22.82/17/17 74.16-74.18	Expressed in few tissues but mainly in testis/ HS.125507	Known as helicase antigen (HAGE). Northern blot analysis detected expression of a 2.2-kb HAGE transcript in tumors of various histologic types at a level that was 100-fold higher than that observed in normal tissues, except for testis (Martelange *et al.*, 2000).
41. *C6orf150*/ Chromosome 6 open reading frame 150	27.41/6/6 74.17-74.21	Ubiquitously expressed/ HS.14577	C6orf150 protein
42. *MTO1*/ Mitochondrial translation optimisation 1 homolog	39.69/13 74.22-74.26	Ubiquitously expressed but with very high expression in mammary gland/ HS.347614	Reported to be involved in the process of mitochondrial RNA modification which is an important regulatory pathway in the phenotypic expression of the deafness-associated mitochondrial A1555G mutation (Bykhovskaya *et al.*, 2004).
43. *EEF1A1*/ NM_001402/ Eukaryotic translation elongation factor 1 alpha 1	4.07/7/8 74.282-74.288	Ubiquitously expressed with very high expression in all tissues/ HS.644639	Reported as an autoantibody in 66% of patients with Felty syndrome, a disorder characterised by the association of rheumatoid arthritis, splenomegaly, and peripheral destruction of neutrophils leading to neutropenia (Ditzel *et al.*, 2000).

Gene/ Description of gene	Gene size (Kb)/ no. of exons / no. primers/ position (Mb)	Expression data/ UniGene accession no.	Published information about the gene
44. *SLC17A5/* NM_012434/ Solute carrier family 17 (anion/sugar transporter), member 5	60.78/11/11 74.35-74.42	Ubiquitously expressed with high expression in parathyroid/ HS.597422	Defects in *SLC17A5* are the cause of Salla disease (SD); an ar neurodegenerative disorders that may present as a severe infantile form (ISSD) or a slowly progressive adult form. The main symptoms are hypotonia, cerebellar ataxia, and mental retardation; visceromegaly and coarse features are also present in the infantile cases. They are caused by a defect in the metabolism of sialic acid which results in increased urinary excretion of free sialic acid. Enlarged lysosomes are seen on EM studies (Verheijen *et al.*, 1999; Aula *et al.*, 2000; Martin *et al;* 2003).
45. *CD109/* CD109 molecule	128.96/33 74.46-74.59	Ubiquitously expressed with very high expression in parathyroid/ HS.399891	*CD109* is a glycosylphosphatidyl - inositol (GPI)-linked cell surface antigen expressed by CD34+ acute myeloid leukemia cell lines, T-cell lines, activated T lymphoblasts and activated platelets (Lin *et al.*, 2002). In addition, the platelet-specific antigen system, implicated in neonatal allo-immune thrombocytopenia and post-transfusion purpura, is carried by CD109 (Kelton *et al.*, 1990; Lin *et al.*, 2002).
46. *COL12A1/* Collagen, type XII, alpha 1	121.53/67 75.85-75.97	Ubiquitously expressed with high expression in bone, bone marrow, cochlea/ HS.101302	*R*eported to act as a crossbridge between fibrils and resist shear forces caused by tension. In the mouse the Col12a1 locus is tightly linked to the recessive short ear mutation, which is characterised by multiple skeletal abnormalities and defective cartilage framework (Oh *et al.*, 1992).
47. *COX7A2/* Cytochrome c oxidase subunit VIIa polypeptide 2 (liver)	6.33/4/4 76.00-76.02	Ubiquitously expressed with very high expression in pituitary gland, blood and bone marrow/ HS.70312	Reported to inhibit LH-induced StAR protein expression, and consequent testosterone production, at least in part, by increasing reactive oxygen species (ROS) activity in TM3 (established Leyding cell line) mouse Leydig cells (Chen *et al.*, 2006).

Gene/ Description of gene	Gene size (Kb)/ no. of exons / no. primers/ position (Mb)	Expression data/ UniGene accession no.	Published information about the gene
48. *TMEM30A*/ Transmembrane protein 30A	31.86/7 76.01-67.05	Ubiquitously expressed with high expression in oesophagus, parathyroid and trachea/ HS.108530	Reported that *TMEM30C* is conserved among mammals along with two other paralogs, *TMEM30A* and *TMEM30B*. However, *TMEM30C* showed specific expression in the testis of mammals, in contrast to the relatively wide expression distributions of the other paralogs (Osada *et al.*, 2007).
49. *FILIP1*/ Filamin A interacting protein 1	185.69/6 76.07-76.26	Ubiquitously expressed/ HS.526972	Reported that the C terminus of the long form of rat Filip interacted with mouse filamin A (FLNA), an actin-binding protein required for cell motility (Nagano *et al.*, 2002).
50. *SENP6* / SUMO1/sentrin specific peptidase 6	114.37/24 76.36-76.48	Ubiquitously expressed with high expression in pituitary gland and cochlea./ HS.485784	Reported to be highly expressed in reproductive organs, such as testis, ovary and prostate suggesting that it may play a role in reproduction (Kim *et al.*, 2000).
51. *MYO6*/ Myosin VI	167.28/35/34 76.51-76.68	Ubiquitously expressed with high expression in prostate and cochlea/ HS.149387	Defects in *MYO6* are the cause of both autosomal dominant nonsyndromic sensorineural deafness type 22 (DFNA22) (Melchionda *et al.*, 2001) and autosomal recessive congenital neurosensory deafness type 37 (DFNB37) (Ahmed *et al.*, 2003).
52. *IMPG1*/ Interphotoreceptor matrix proteoglycan 1	151.56/17/17 76.68-76.83	Expressed in few tissues but mainly in eye/ HS.590893	A single base-pair change (T>C) of nucleotide 1866 in exon 13, resulting in a Leu579Pro amino acid substitution was reported to be associated with benign concentric annular macular dystrophy (BCAMD) (van Lith-Verhoeven *et al.*, 2004).
53. *HTR1B*/ 5-hydroxytryptamine (serotonin) receptor 1B	1.17/1/1 78.228-78.229	Expressed only in brain and colon / HS.123016	A genetic variation (SNP; G861C) in the *HTR1B* gene was associated with attention deficit/hyperactivity disorder (ADHD) (Smoller *et al.*, 2006).
54. *IRAK1BP1*/ Interleukin-1 receptor-associated kinase 1 binding protein 1	31.13/4/4 79.63-79.66	Ubiquitously expressed with high expression in cochlea/ HS.556018	Related to activation of the inhibitor of kappa kinase.
55. *PHIP*/ Pleckstrin homology domain interacting protein	137.70/40 79.70-79.86	Ubiquitously expressed with high expression in cochlea/ HS.511817	Cloned and characterised as a novel insulin receptor substrate-1 (IRS-1) pleckstrin domain interacting protein that may link IRS-1 to the insulin receptor (Farhang-Fallah *et al.*, 2000).

Gene/ Description of gene	Gene size (Kb)/ no. of exons / no. primers/ position (Mb)	Expression data/ UniGene accession no.	Published information about the gene
56. ***HMGN3***/ High mobility group nucleosomal binding domain 3	33.49/6/6 79.96-80.00	Ubiquitously expressed with high expression in parathyroid, pharynx and pituitary gland/ HS.77558	An additional type of HMGN. Unique within the HMGN family, the HMGN3 transcript undergoes alternative splicing and generates two different variants, HMGN3a and HMGN3b. These results expand the multiplicity of the HMGN protein family (West *et al.*, 2001).
57. *Q9H8D1_human*/ CDNA FLJ13744 fis	0.534/1/1 80.076-80.077	none	None
58. *C6orf152*/ Chromosome 6 open reading frame 152	52.41/8/8 80.25-80.30	Ubiquitously expressed/ HS.21945	C6orf152 protein.
59. ***SH3BGRL2***/ SH3 domain binding glutamic acid-rich protein like 2	72.37/4/4 80.39-80.47	Ubiquitously expressed with high expression in colon, parathyroid and eye/ HS.232772	Reported as a novel human homologue of the SH3 binding glutamic acid-rich establishing a new family of highly conserved small proteins related to Thioredoxin Superfamily (Mazzocco *et al.*, 2002).
60. *ELOVL4*/ Elongation of very long chain fatty acids (FEN1/Elo2, SUR4/Elo3, yeast)-like 4	32.77/6/6 80.68-80.71	Ubiquitously expressed with very high expression in thymus/ HS.101915	A single 5-bp deletion within the protein-coding region of *ELOVL4* was reported as the genetic defect in STGD3 and adMD families (Zhang *et al.*, 2001).
61. ***TTK***/ TTK protein kinase Dual specificity protein kinase	37.88/22/18 80.77-80.80	Ubiquitously expressed with very high expression in testis and thymus/ HS.169840	Expressed primarily in tissues with a large number of rapidly proliferating cells, such as testis and thymus and has dual specificity protein kinase (tyrosine and serine/threonine residues) (Lindberg *et al.*, 1993). TTK is required for centrosome duplication and for the normal progression of mitosis (Fisk *et al.*, 2003).
62. *BCKDHB*/ Branched chain keto acid dehydrogenase E1, beta polypeptide (maple syrup urine disease)	239.60/11 80.87-81.11	Ubiquitously expressed with high expression in trachea /HS.436387	Encodes the beta subunit of alpha-keto acid decarboxylase (E1), one of the tree catalytic components. Point mutations and small deletions were reported in patients with maple syrup urine disease (Nobukuni *et al.*, 1991; Patel and Harris, 1995; Edelmann *et al.*, 2001).
63. *Q9H3A8*/	0.231/1/1 82.319-82.319.2	none	None

Gene/ Description of gene	Gene size (Kb)/ no. of exons / no. primers/ position (Mb)	Expression data/ UniGene accession no.	Published information about the gene
64. *FAM46A*/ Family with sequence similarity 46, member A	7.04/3/3 82.512-82.519	Ubiquitously expressed with high expression in pituitary gland and placenta/ HS.10784	A novel VNTR polymorphism in C6orf37 was reported in Chinese population but was not associated with colorectal cancer risk (Cui *et al.*, 2006).
65. *IBTK*/ Inhibitor of Bruton agammaglobulinemia tyrosine kinase	77.49/29/29 82.93-83.00	Ubiquitously expressed with high expression in cervix and adipose tissue /HS.306425	Required for human and mouse B cell development. Btk deficiency causes Xl agammaglobulinemia (XLA) in humans and X-linked immunodeficiency in mice (Liu *et al.*, 2001).
66. *TPBG*/ Trophoblast glycoprotein	7.2/2 83.13-83.133	Ubiquitously expressed with high expression in cochlea/ HS.82128	Recognised by monoclonal antibody 5T4 mapped to human chromosome 6q14-q15 (Boyle *et al.*, 1990). The human and mouse *TPBG* genes were determined to contain 2 exons, the second of which encodes the protein. The promoter region contains no TATA or CAAT boxes, but does have a number of potential SP1-binding sites (King *et al.*, 1999).
67. *C6orf157*/ Chromosome 6 open reading frame 157	173.36/10 83.65-83.83	Ubiquitously expressed with high expression in parathyroid/ HS.148609	C6orf157 protein
68. *DOPEY1*/ Dopey family member 1	100.74/39 83.83-83.93	Ubiquitously expressed with high expression in mammary gland/ HS.520246	None
69. *PGM3*/ Phosphoglucomutase 3	24.34/13 83.93-83.95	Ubiquitously expressed HS.646298	Reported as the 3rd phosphoglucomutase locus in man (Hopkinson and Harris, 1968). Assigned to chromosome 6q12-qter (Jahannsmann *et al.*, 1980).
70. *RWDD2*/ RWD domain containing 2	2.21/2 83.95-83.96	Ubiquitously expressed/ HS.590894	None
71. *ME1*/ Malic enzyme 1	220.68/14 83.97-84.19	Ubiquitously expressed with high expression in connective tissue, oesophagus and pituitary gland/ HS.21160	Povey et al. (1975) demonstrated that the human enzyme can be distinguished in human-mouse hybrids and that ME1 is syntenic with PGM3. It was reported that triiodothyronine (T3) appears to control ME1 transcription. However, computer analysis revealed the presence of additional putative recognition motifs suggesting that *ME1* gene is under complex regulatory control (Gonzalez-Manchon *et al.*, 1997).

Gene/ Description of gene	Gene size (Kb)/ no. of exons / no. primers/ position (Mb)	Expression data/ UniGene accession no.	Published information about the gene
72. *PRSS35*/ Protease, serine, 35	13.17/2 84.27-84.29	Ubiquitously expressed / HS.98381	Was reported to possess general features that are characteristic of serine proteases, but is unique in that the canonical Ser that defines this enzyme family is replaced by a threonine. A homologus protease PRSS23 was identified in the mouse genome database suggesting that both *PRSS35* and *PRSS23* genes have been conserved as critical ovarian proteases throughout the course of vertebrate evolution (Miyakoshi *et al.*, 2006).
73. *SNAP91*/ Synaptosomal-associated protein, 91kDa homolog	156.41/30 84.31-84.47	Ubiquitously expressed with high expression in pituitary gland / HS.368046	Cloned and designated KIAA0656. The deduced full-length protein contains 907 amino acids and shares about 83% identity with the short form of rat clathrin assembly protein Ap180. RT-PCR detected highest expression in brain, followed by testis, heart, and ovary. Little to no expression was detected in the other tissues tested (Ishikawa *et al.*, 1998).
74. *CYB5R4*/ Or *NCB5OR* Cytochrome b5 reductase 4	100.74/16 84.62-84.72	Ubiquitously expressed with high expression in blood and bladder/ HS.5741	Located in the endoplasmic reticulum (ER) and is widely expressed in organs and tissues. Targeted inactivation of the *NCB5OR* gene in mice had no impact on embryonic or fetal viability. At 7 weeks of age, these mice developed severe hyperglycemia with markedly decreased serum insulin levels and nearly normal insulin tolerance. Electron microscopy showed degranulation of beta cells and hypertrophic and hyperplastic mitochondria (Xie *et al.*, 2004).
75. Q6ZVE3/ CDNA FLJ42667 fis, clone BRAMY2020058	3/1/ 84.72-84.73	none	none
76. *C6orf117*/ Chromosome 6 open reading frame 117	57.18/4 84.80-84.85	Ubiquitously expressed/ HS.370055	none

Gene/ Description of gene	Gene size (Kb)/ no. of exons / no. primers/ position (Mb)	Expression data/ UniGene accession no.	Published information about the gene
77. *KIAA1009*/ KIAA1009 protein	103.34/26 84.89-84.99	Ubiquitously expressed with high expression in bone/ HS.485865	Cloned via screening cDNAs encoding large proteins expressed in the brain. The predicted protein was identical to the quail neuronal cell cycle withdrawal protein (Qn1) which is conserved from fugu to humans. (Nagase *et al.*, 1999). *KIAA1009* is required for normal cell division and acts as a microtubule motor (Leon *et al.*, 2006).
78. *TBX18*/ T-box 18	76.09/9/11 85.45-85.53	Ubiquitously expressed with very high expression in cochlea/ HS.251830	Cloned and shown to be highly similar to the mouse Tbx15/Tbx8, having 95% amino acid similarity and 92% identity (Yi *et al.*, 1999). Mice deficient in Tbx18 showed expansion of pedicles with transverse processes and proximal ribs, elements derived from the posterior lateral sclerotome (Bussen *et al.*, 2004). In Tbx18 -/- mice, prospective ureteral mesenchymal cells were reported be largely dislocalised to the surface of the kidneys (Airik *et al.*, 2006).
79. *NT5E*/ 5'-nucleotidase, ecto (CD73)	45.69/9/9 86.21-86.26	Ubiquitously expressed with high expression in connective tissue/ HS.153952	Catalyses the conversion at neutral pH of purine 5-prime mononucleotides to nucleosides the preferred substrate being AMP. Castrop et al. (2004) generated mice with a targeted deletion of ecto-5-prime-nucleotidase. There was no difference in blood pressure, blood and urine chemistry, and renal blood flow between null and wildtype mice; however, whereas tubuloglomerular feedback responses did not change significantly during prolonged loop of Henle perfusion in wildtype mice, a complete disappearance of the residual feedback response was noted in null mice over 10 minutes of perfusion.

Gene/ Description of gene	Gene size (Kb)/ no. of exons / no. primers/ position (Mb)	Expression data/ UniGene accession no.	Published information about the gene
80. *SNX14* / Sorting nexin 14	88.41/29 86.27-86.36	Ubiquitously expressed with high expression in testis and thyroid / HS.485871	Cloned by a gene-trap strategy which set up in embryonic stem (ES) cells aiming to trap genes expressed in restricted neuronal lineages (Carroll *et al.*, 2001).
81. *SYNCRIP*/ Synaptotagmin binding, cytoplasmic RNA interacting protein	28.56/11/ 86.37-86.40	Ubiquitously expressed/ HS.571177	A component of mRNA granule transported with inositol 1,4,5-trisphosphate receptor type 1 mRNA in neuronal dendrites and hence is suggested to be important for the stabilisation of the mRNA (Bannai *et al.*, 2004).
82. *SNHG5*/ Small nucleolar RNA host gene	1.64/4/ 86.443-86.445	Ubiquitously expressed with high expression in embryonic tissue, muscle and tonsil/ HS.292457	none
83. *Q5T5W8_human*/ OTTHUMP00000016822	0.177/1 86.501-86.502	none	none
84. *HTR1E*/ 5-hydroxytryptamine (serotonin) receptor 1E	79.13/3 87.70-87.78	Expressed only in testis/ HS.1611	Assigned to chromosme 6q14-q15 by means of in situ hybridization to human metaphase chromosomes using the cloned gene as a probe (Levy *et al.*, 1992 and 1994). HTR1E is found mainly in cerebral cortex, and the precise chromosomal assignment of the gene may help evaluate this locus as a candidate for mutations in neurologic and psychiatric diseases (Levy *et al.*, 1994).
85. *CGA*/ Chorionic gonadotrophin alpha subunit	9.63/4 87.85-87.86	Ubiquitously expressed with very high expression in pituitary gland, placenta and cochlea/ HS.119689	Assigned to chromosome 6 by Naylor et al. (1983).
86. *ZNF292*/ Zinc finger protein 292	47.78/7 87.92-88.03	Ubiquitously expressed/ HS.590890	none
87. *GJB7*/ Gap junction protein, beta 7	40.08/2 88.04-88.08	Expressed only in mouth, lung , pitutary gland and trachea / HS.146727	none
88. *C6orf162*/ Chromosome 6 open reading frame 162	18.87/3 88.08-88.10	Ubiquitously expressed with high expression in connective tissue/ HS.70769	none

Gene/ Description of gene	Gene size (Kb)/ no. of exons / no. primers/ position (Mb)	Expression data/ UniGene accession no.	Published information about the gene
89. *Q5TEEZ4_human*/ OTTHUMP00000016830	0.177/1/ 88.163-88.166	none	none
90.*C6orf165* / Chromosome 6 open reading frame 165	56.46/13 88.17-88.20	Expressed in few tissues mainly in parathyroid, testis and umbical cord/HS.82921	none
91. *SLC35A1*/ Solute carrier family 35 (CMP-sialic acid transporter), member A1	39.36/8/8 88.23-88.27	Ubiquitously expressed/ HS.423163	By 5 prime RACE, a cDNA encoding SLC35A1, the human homolog of the murine cytidine monophosphate (CMP)-sialic acid transporter was obtained (Ishida *et al.*, 1996). The International Radiation Hybrid Mapping Consortium mapped the *SLC35A1* gene to chromosome 6.
92. *RARSL*/ Arginyl-tRNA synthetase-like	75.61/22 88.28-88.35	Ubiquitously expressed/ HS.485910	none
93. *ORC3L*/ Origin recognition complex, subunit 3-like	77.32/20 88.35-88.43	Ubiquitously expressed mainly in nerve/ HS.410228	Component of the origin recognition complex (ORC) that binds origins of replication. It has a role in both chromosomal replication and mating type transcriptional silencing (Springer *et al.*, 1999).
94. *C6orf166*/ Chromosome 6 open reading frame 166	27.14/5 88.44-88.46	Ubiquitously expressed/ HS.485915	Hypothetical protein LOC 55122
95. *SPACA1*/ or *SAMP32* Sperm acrosome associated 1	19.04/7 88.81-88.83	Expressed only in brain and testis/ HS.161241	Recombinant SAMP32 reacted with serum from an infertile man, suggesting that it is isoantigenic. Antibodies against recombinant SAMP32 inhibited both the binding and the fusion of human sperm to zona-free hamster eggs (Hao *et al.*, 2002).
96. *CNR1*/ Cannabinoid receptor 1	5.5/2/5 88.90-88.93	Ubiquitously expressed but mainly in muscle/ HS.75110	A triplet repeat polymorphism was significantly associated with schizophrenia especially the hebephrenic subtype (Ujike *et al.*, 2002). A homozygous genotype within CNR1 1359A/A was associated with the vulnerability to alcohol withdrawal delirium (Schmidt *et al.*, 2002). Anorexia nervosa (AN) may be associated with different alleles of the CNR1 gene (Siegfried *et al.*, 2004).

Gene/ Description of gene	Gene size (Kb)/ no. of exons / no. primers/ position (Mb)	Expression data/ UniGene accession No.	Published information about the gene
97. *RNGTT*/ RNA guanylyltransferase and 5'-phosphatase	553.31/15 89.37-89.73	Ubiquitously expressed with high level in pituitary gland /HS.653104	Bifunctional mRNA capping enzyme exhibiting RNA 5'-triphosphatase activity in the N-terminal part and mRNA guanylyltransferase activity in the C-terminal part. Catalyses the first two steps of cap formation (Yamado-Okabe *et al.*, 1998).
98. *Q6ZNW3_human*/ CDNA FLJ27030 fis, clone SLV07741	89.730-89.733		None
99. *PNRC1*/ PROL2 Proline-rich nuclear receptor coactivator 1	4.38/2 89.84-89.85	Ubiquitously expressed/ HS.75969	Isolated from a natural killer (NK) minus T cell subtractive library which codes for a protein with high proline content (Chen *et al.*, 1995).
100. *SRR35*/ Serine-arginine repressor protein (35 kDa)	19.6/5 89.86-89.88	Highly expressed in spleen and thymus/ HS.254414	Belongs to the splicing factor (serine arginine; SR) family. *SRR35* was reported as an SR protein-like alternative splicing regulator that antagonises authentic SR proteins in the modulation of alternative 5' splice site choice (Cowper *et al.*, 2001).
101. *ACY1L2*/ Aminoacylase 1-like 2	19.52/7 89.91-89.93	Ubiquitously expressed/ HS.652106	None
102. *GABRR1*/ gamma-aminobutyric acid (GABA) receptor, rho 1	39.93/10 89.94-89.98	Expressed in few tissues including eye/ HS.437745	GABA receptor subunit rho-2 cDNA and colocalisation of the genes encoding rho-2 (GABRR2) and rho-1 (GABRR1) to human chromosome 6q14-q21 and mouse chromosome 4 was reported by Cutting et al. (1992).
103. *GABRR2*/ gamma-aminobutyric acid (GABA) receptor, rho 2	57.72/9 90.02-90.08	Expressed in few tissues including eye/ HS.99927	GABA, the major inhibitory neurotransmitter in the vertebrate brain, mediates neuronal inhibition by binding to the gaba/benzodiazepine receptor and opening an integral chloride channel. rho2 GABA receptor could play a role in retinal neurotransmission.

Gene/ Description of gene	Gene size (Kb)/ no. of exons / no. primers/ position (Mb)	Expression data/ UniGene accession no.	Published information about the gene
104. *UBE2J1*/ Ubiquitin-conjugating enzyme E2, J1	90.09-90.11	Ubiquitously expressed with very high expression in lymph node/ HS.163776	Catalyses the covalent attachment of ubiquitin to other proteins.
105. *RRAGD*/ Ras-related GTP binding D	47.63/7 90.13-90.17	Ubiquitously expressed with high expression in parathyroid, cochlea and kidney/ HS.485938	Using RRAGA as bait in a yeast 2-hybrid screen of a Burkitt lymphoma cDNA library, Sekiguchi et al. (2001) cloned RRAGD, which they called RAGD. They found that RRAGD and RRAGA interact through their C termin.
106. *ANKRD6*/ Ankyrin repeat domain 6	198.28/16 90.19-90.40	Ubiquitously expressed/ HS.651107	Cloned by sequencing clones obtained from a size-fractionated brain cDNA library (Nagase *et al.*, 1999). Ankrd6 was cloned using conductin (AXIN2) as bait in a yeast 2-hybrid screen of a mouse embryo cDNA library, cloned, which they called diversin (Schwarz-Romond *et al.*, 2002).
107. *LYRM2*/ LYR motif containing 2	2.05/3 90.403-90.405	Ubiquitously expressed/ HS.177275	Has oxidoreductase activity acting on NADH and NADPH.
108. *MDN1* Midasin homolog	176.21/100 90.40-90.58	Ubiquitously expressed/ HS.529948	Could be related to protein complex assembly and folding.
109. *CASP8AP2*/ or *FLASH* CASP8 associated protein 2 Flick associated huge protein	24.81/8 90.61-90.63	Ubiquitously expressed/ HS.558218	Cloned from a mouse T-cell lymphoma cDNA library. Through coimmunoprecipitation, Flash was reported to bind caspase-8 and Fadd. It also specifically coimmunoprecipitated with activated Fas, suggesting that Casp8ap2 is part of the death-inducing signaling complex (DISC) (Imai *et al.*, 1999).
110. *CX62*/ connexin 62	1.63/1 90.660-90.662	No information/ HS.334499	By Northern blot hybridization, *CX62* along with other *CX* genes was shown to be transcribed in different adult tissues. CX62 showed an expression in skeletal muscles and slightly in the heart which was completely different from their mouse orthologues suggesting different function (Sohl *et al.*, 2003).

Gene/ Description of gene	Gene size (Kb)/ no. of exons / no. primers/ position (Mb)	Expression data/ UniGene accession no.	Published information about the gene
111. *BACH2*/ BTB and CNC homology 1, basic leucine zipper transcription factor 2	370.21/9 90.69-91.06	Ubiquitously expressed with high expression in lymph node/ HS.269761	Mapped to chromosome 6q15 by FISH. By Southern blot was shown to be a single copy gene (Sasaki *et al.*, 2000). Bach2 -/- mice had high levels of serum IgM but diminished concentrations of IgG subclasses and IgA compared with wildtype mice. The Bach2 -/- mice also had deficient T cell-independent and T cell-dependent IgG responses concluding that BACH2 is a regulator of the antibody response (Muto *et al.*, 2004).

3.1.4 Strategies for the identification of RP25 gene

Candidate genes were selected from RP25 region on the basis of their function, tissue expression pattern and/or the genetic data.

3.1.4.1 Positional candidate gene approach

This approach was based on the genetic data obtained from families linked to the RP25 interval (Figure 3.1). It is possible that both the Pakistani family and 5 of the Spanish families have a common gene. Based on this hypothesis, all genes in the region between D6S257 and D6S1053 (Region A) were considered as good candidates for mutation screening (Figure 3.4 and Table 3.1). With the assumption that the disease gene in the Spanish families could be different from that for the Pakistani family, the genes in-between D6S1557 and D6S421 (Region B) where all Spanish families are linked were evaluated in this study (Figures 3.1 and 3.4 and Table 3.1). However, the region between D6S1053 and D6S1557 (Region C) was also considered as a high priority interval to screen since all the Spanish families apart from one family (RP260) share linkage (Figure 3.1).

A fourth possibility which cannot be ruled out is that the responsible gene could be located downstream of D6S421 (Region D) where 6 of the Spanish families overlap with the LCA5 locus (Figures 3.1, 3.2 and 3.4; Table 3.1). It is conceivable that mutations in different sites can cause different structural alterations in the predicted protein, predisposing to varying phenotypes (Rozet *et al.,* 1998). Therefore, there is a possibility that a similar situation between LCA5 and RP25 exist.

3.1.4.2 Functional candidate gene approach

An interactive tool and database for querying human retina and RPE gene expression, *EyeSAGE* (Serial Analysis of Gene Expression), has been utilised to search for good candidate genes in the RP25 interval. It compares the pattern of gene expression in the retina and RPE to that in different tissues in order to identify genes that are likely to be expressed in a single cell type such as cone/rod photoreceptor. In addition, *EyeSAGE* can be used for Genomic Convergence-combining expression data with available linkage information to generate lists of candidate genes for diseases such as RP (Rickman *et al.*, 2006). The National Eye Institute Bank (NEIBank) has listed candidate genes for 50 of the disease eye loci for which the genes are yet to be identified. RP25 locus was among these loci for which 14 genes were chosen as good candidates based on their level of expression in the retina and RPE in comparison to other tissues (Table 3.1). Interestingly five of these genes, *KHDRBS2*, *GLULD1*, *PTP4A1*, *PHF3* and *EGFL11*, were also considered as good candidates for LCA5 by the same database enforcing the possibility of a single gene defect that can lead to various disease phenotypes.

Secondly, it has been reported that successful transmission of several proteins from the cell body to the outer segment of the photoreceptor cells depends on the transport along a modified cilium and that defective passage of certain molecules results in retinal degeneration associated with RP (Marszalek and Goldstein, 2000). Recently, a number of homologus *Trypanosomal* genes mapping to retinal disease loci with a clinical spectrum suggestive of ciliary dysfunction has been reported (Broadhead *et al.*, 2006). Therefore, we considered this as a second approach to identify functional candidate genes (Table 3.2). Interestingly, one of the *Trypanosomal* proteins showed similarity in structure to the RP2 gene associated with xlRP. Additionally, within the RP25 interval

two genes, *EEF1A1* and *C6orf165_human*, were also expressed in the *Trypanosome* cilia and hence considered as attractive candidates (Table 3.2).

A third approach to identify functional candidates was to use the information available on the expression of different genes implicated in retinal degeneration (rd) mouse model. Retinal degeneration in the *rd* mouse is caused by a defect in the β subunit of rod cGMP-phosphodiesterase (Bowes *et al.*, 1990). By studying the level of expression of other genes in comparison with the defective β PDE, there was a correlation between the level of expression of β PDE and other genes for example *RHO* showed diminished expression. In that sense seven genes in our interval were considered as good candidates (Table 3.1).

3.1.4.3 Refinement of the RP25 interval

It is not uncommon for two retinal degenerations mapping to the same chromosomal region to have one responsible gene, although the mutations could be different. According to this hypothesis LCA families were tested for linkage to the RP25 locus which may lead to refinement of the genetic interval and hence restrict the number of candidate genes within the RP25 locus.

3.2 AIM OF THE STUDY

To identify the gene responsible for the RP25 phenotype in the Spanish families

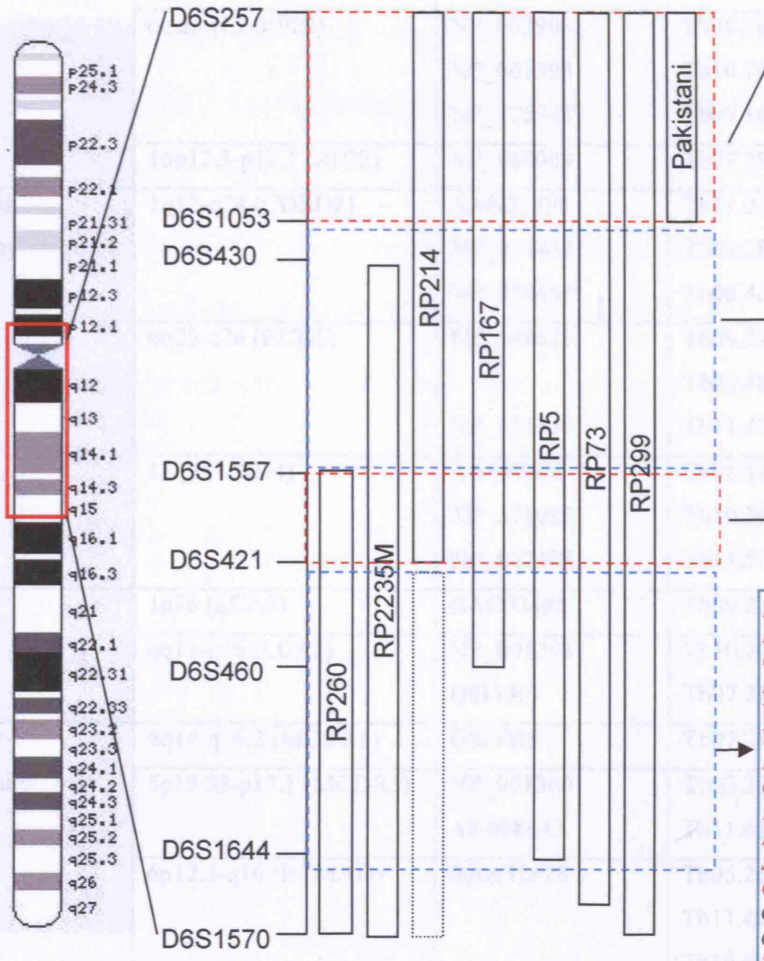

Genes	Mb
COL21A1	56.00
DST	56.40
C6orf65	56.90
KIAA1586	57.00
ZNF451	57.01
BAG2	57.14
RAB23	57.16
PRIM2A	57.29
GUSBL2	58.30
KHDRBS2	62.40
Q5VVH2	63.97
GLULD1	64.04
PTP4A1	64.34
PHF3	64.40
Q9N915	64.48
Q5T669	65.38
Q5T1H1	65.57
Q9H557	65.65
Q5TEL3	65.76
Q5TEL4	65.77
Q5VVG4	65.82
Q5T3C8	66.06
EGFL11	66.10
BAI3	69.40
C6orf209	70.44
COL19A1	70.60
COL9A1	70.90
KIAA1411	71.18
C6orf57	71.33
SMAP1	71.40
B3GAT2	71.60
OGFRL2	72.05
C6orf155	72.18
RIMS1	72.60
KCNQ5	73.38
C6orf148	73.99
DPPA5	74.12
NP_001017361.1	74.12
NP_01073976.1	74.13
DDX43	74.16
C6orf150	74.19
MTO1	74.22
EEF1A1	74.28
SLC17A5	74.35
CD109	74.46
COL12A1	75.85
COX7A2	76.00
TMEM30A	76.01
FILIP1	76.07
SENP6	76.36
MYO6	76.51
IMPG1	76.68
HTR1B	78.22
ERAK1BP1	79.63
PHIP	79.70
HMGN3	79.96
Q9H8D1	80.07
C6orf152	80.25
SH3BGRL2	80.39
ELOVL4	80.68
TTK	80.77
BCKDHB	80.87
Q9H3A8	82.31
FAM46A	82.51
IBTK	82.93
TPBG	83.13
C6orf157	83.60
KIAA1117	83.80
PGM3	83.93
RWDD2	83.96
ME1	83.97
PRSS35	84.27
SNAP91	84.31
CYB5R4	84.62
Q6ZVE3	84.72
C6orf117	84.80
KIAA1009	84.89
TBX18	85.40
NT5E	86.21
SNX14	86.27
SYNCRIP	86.37
SNHG5	86.44
Q5T5W8	86.50
HTR1E	87.70
CGA	87.85
ZNF292	87.92
GJB7	88.04
C6orf162	88.08
Q5TEEZ4	88.16
C6orf165	88.17
SLC35A1	88.23
RARSL	88.28
ORC3L	88.35
C6orf166	88.44
SPACA1	88.81
CNR1	88.91
RNGTT	89.37
Q6ZNW3	89.73
PNRC1	89.84
SRR35	89.86
ACY1L2	89.91
GABRR1	89.94
GABRR2	90.02
UBE2J1	90.09
RRAGD	90.13
ANKRD6	90.19
LYRM2	90.40
MDN1	90.58
CASP8AP2	90.61
CX62	90.66
BACH2	90.69

Figure 3.4 A diagrammatic representation of the chromosome 6 disease interval. Vertical bars represent the RP25 families. The genes within the RP25 interval are displayed on the side of the bars. Genes in red and bold are the ones that have been screened in this study. Genes in red and normal font are the ones that have been screened either before the beginning of this project or by our collaborates and finally genes in black were not screened.

Table 3.2 Trypanosome proteins mapping to retinal disease loci

Disease	Locus	Homosapiens accession No.	Trypanosome accession No.	Name of the gene/position
RP	4q32-q34 (RP29)	AAH29428	Tb08.29H22.870	*SPATA4* (177.34-177.35)
	6cen-q15 (RP25)	NP_002903	Tb08.28L1.310	*REV3L* (111.7-111.9)
		NP_001393	Tb10.70.5670	*EEF1A1* (74.282-74.288)
		NP_775943	Tb09.160.2070	*PIPL6* (109.82-109.86)
	16p12.3-p12.1 (RP22)	NP_060009	Tb07.29K4.310	*DNAH3* (20.85-21.07)
Cone/rod dystrophy	1q12-q24 (CORD8)	AAH33790	Tb11.01.8640	*C1orf92* (155.15-155.16)
		NP_037462	Tb04.2L9.1240	*NME7* (167.36-167.60)
		NP_036469	Tb08.4A8.180	*CCDC19* (158.10-158.16)
	6q25-q26 (RCD1)	NP_689623	Tb09.211.1470; Tb03.48O8.610	*PACRG* (163.06-163.65)
		NP_114130	Tb11.47.0034	*RSHL2* (159.31-159.34)
	17q (CORD4)	AAS88903	Tb08.4A8.510	*PHB* (44.83-44.84)
		XP_371082	Tb10.26.0760	*CCDC40* (75.62-75.68)
		NP_542408	Tb11.50.0007	*DYNLL2* (53.51-53.52)
LCA	1p36 (LCA9)	BAC03498	Tb09.211.2450	*C1orf201* (24.55-24.61)
	6q11-q16 (LCA5)	NP_001393	Tb10.70.5670	*EEF1A1* (74.282-74.288)
		Q8IYR0	Tb07.2F2.600	*C6orf165* (88.17-88.27)
Macular dystrophies	6q14-q16.2 (MCDR1)	Q8IYR0	Tb07.2F2.600	*C6orf165* (88.17-88.27)
	5p15.33-p13.1 (MCDR3)	NP_001360	Tb03.27F10.490	*DNAH5* (13.74-13.99)
		AK098642	Tb11.01.5260	*ROPNIL* (10.49-1051)
	6p12.3-q16 (BCMAD)	BAA91628	Tb05.26K5.190, Tb11.47.0006, Tb10.6k15.2920, Tb03.27F10.200	*EFHC1* (52.39-52.46)
Usher's syndrome	14q32 (USH1A)	AAH35256	Tb11.02.0990	*AK7* (59.92-96.02)
		NP_689540	Tb927.2.4520	-
	3p24.2-p23 (USH2B)	AAH02634	Tb10.61.2630	*SEC13L1* (10.31-10.33)
BRESEK syndrome	X	XP_373366	Tb927.1.2330	
		AAH43348	Tb10.61.2870	*RP2* (46.58-46.62)
		NP_006297	Tb09.211.2970	
Rieger syndrome	13q14	XP_370723	Tb927.1.2330	-
Joubert syndrome	9q34.3	NP_689785	Tb927.2.5660	*C9orf98* (134.59-134.72)

3.3 PATIENTS AND METHODS

3.3.1 FAMILIES

Seven Spanish families, 3 consanguineous (RP5, RP214 and RP167) and 4 non-consanguineous (RP73, RP299, RP260 and RP235) with arRP were included in this study (Figure 3.5). Additionally, 17 LCA families of which 8 are consanguineous were also included (Figures 3.6 and 3.7). An informed consent was obtained from all participants for clinical and molecular genetic studies. The study conformed to the tenets of the Declaration of Helsinki. The clinical characteristics of five of the RP25 patients are summarised in the table below (Table 3.3).

Table 3.3 Clinical characteristics of RP25 Patients

Family	Age	Age of onset	Symptoms	Visual fields	Fundus	ERG
RP5	56	15	N, VFC, VAR	CC in BE	BS & POD	NR BE
RP73	36	20	N, VFC, VAR	CC in BE	BS & POD	NR BE
RP167	57	38	N, VFC, VAR	CC in BE	BS & POD	NR BE
RP214	37	30	N, VFC	CC in BE	BS & POD	NR BE
RP299	38	15	N, VFC, VAR	CC in BE	BS & POD	NR BE

N: Nyctalopia
VFC: Visual field constriction
VAR: Visual acuity reduction
CC: Concentric constriction
BE: Both eyes
BS: Bone spicules
POD: Pale optic disc
NR: Non recordable

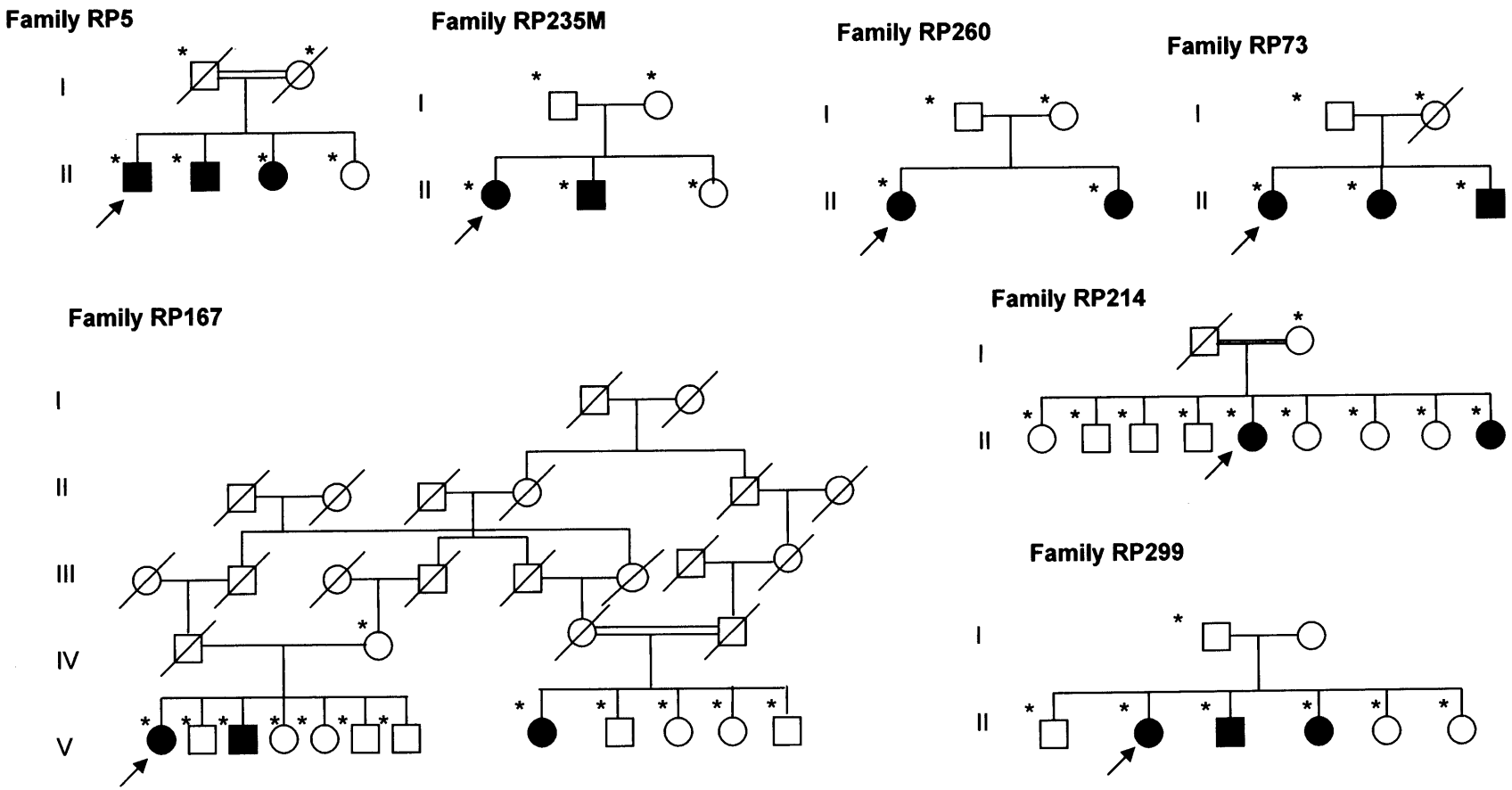

Figure 3.5 RP25 families participated in the study. Open and closed symbols denote unaffected and affected individuals, respectively. Deceased family members are denoted by diagonal slashes, asterisks indicate individuals examined both clinically and genetically and arrows indicate probands in each family.

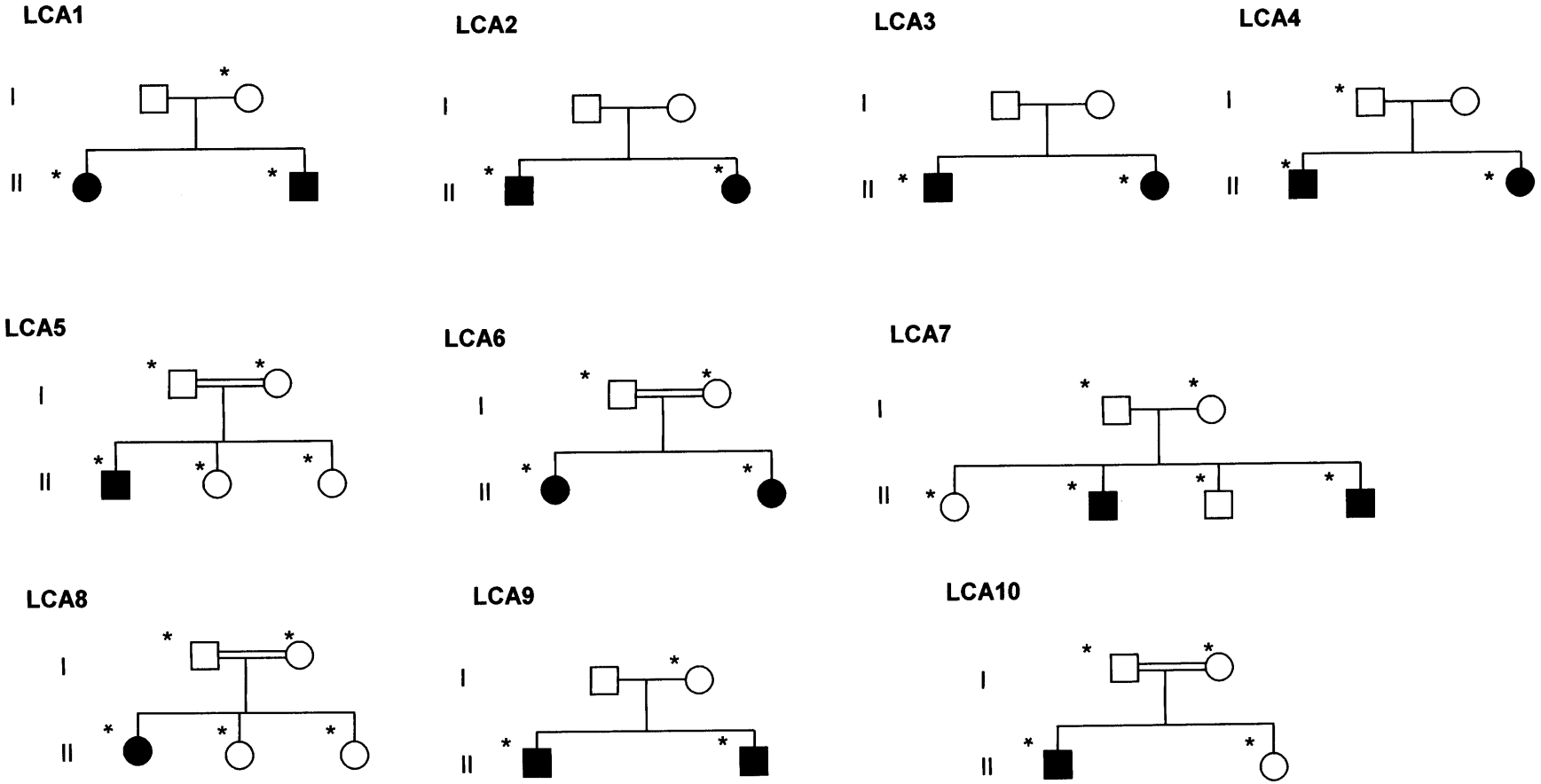

Figure 3.6 LCA families (1-10) participated in the study. Open and closed symbols denote unaffected and affected individuals, respectively. Asterisks indicate individuals examined both clinically and genetically.

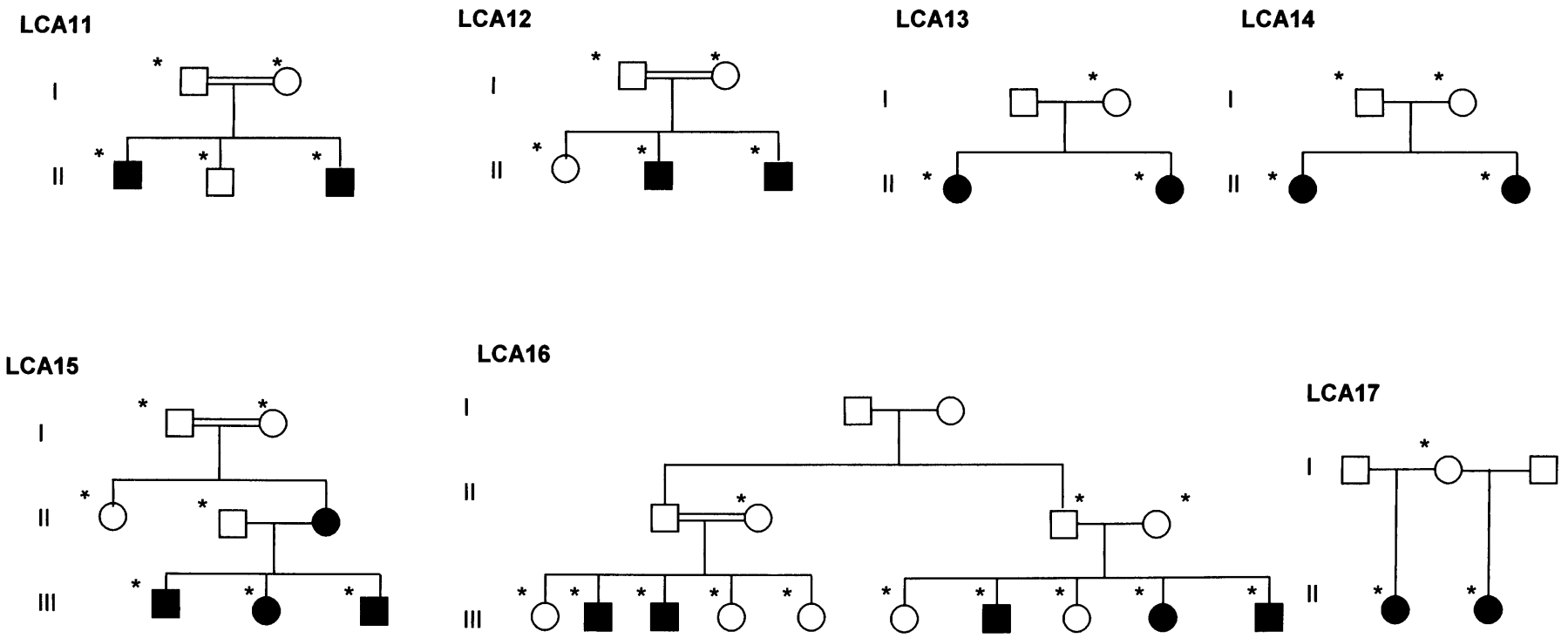

Figure 3.7 LCA families (11-17) participated in the study. Open and closed symbols denote unaffected and affected individuals, respectively. Asterisks indicate individuals examined both clinically and genetically.

3.3.2 METHODS

3.3.2.1 GeneChip mapping 10K array

A whole genome scan in 3 of the Spanish families, RP5, RP214 and RP299, was undertaken using the GeneChip 10K mapping array (see section 2.7.2) in order to confirm the original linkage observed by our Spanish collaborators (Ruiz *et al.,* 1998). DNA samples from six affected (RP5 II-1, II-2, II-3; RP214 II-5; RP299 II-2, II-3) and five unaffected (RP5 I-1, I-2, II-4; RP214 I-2; RP299 I-1) individuals from the three families were genotyped by total genome-sampling analysis using the Affymetrix 10K GeneChip Mapping Array (version Xba142) (section 2.7.2).

3.3.2.2 Analysis of the 10K Array data

The SNP data were analysed using the ExcludeAR3, AR1liteCHIP2 macros and ALOHOMORA programs for the RP5, RP214 and RP299 families, respectively (see sections 2.7.3.1 and 2.7.3.2).

ExcludeAR3 liteCHIP2 macro was utilised to analyse the three affected members in case of the RP5 family. Meanwhile, ExcludeAR1 was used in case of RP214 family since only one affected was subjected to the 10K array. However, in case of RP299 family (non consanguineous) this software was of no use since it seeks only homozygous intervals. Therefore, ALOHOMORA program was used to highlight genetic intervals of shared haplotype between the two affected members in case of the RP299 family. Additionally, we have analysed the 10K array data from this family visually on a Microsoft Excel sheet using the following formula (=IF(AND(F10205=G10205), 1, 2); where F and G represent the column IDs and 10205 represents the row number. We

have also utilised the ALOHOMORA software to analyse family RP5 to confirm the data obtained from the ExcludeAR3 macro.

RP214 family could not be analysed by the ALOHOMORA software since only one affected member was available and the least number of affected individuals that can be analysed using this software is two.

3.3.2.3 Bioinformatic analysis

Genomic sequence of the screened genes within the interval was accessed through the National Centre for Biotechnology Information (NCBI) (http://www.ncbi.nlm.nih.gov/), the ENSEMBL database (http://www.ensembl.org) and the UCSC human genome browser (http://genome.ucsc.edu/). Information on expression patterns and expressed sequence tags (ESTs) were obtained from the NCBI UniGene database. In cases where several alternatively spliced transcripts are documented in ENSEMBL, the BLAST tool (available through the NCBI) was used to compare the sequences from these transcripts and the human genome sequence databases.

3.3.2.4 Tissue expression of candidate genes

Expression analysis of four genes, *KHDRBS2, PTP4A1, KIAA1411* and *OGFRL1*, was assessed by PCR amplification of human cDNAs from retina, brain, kidney, liver, heart, skeletal muscle, pancreas, lung and placenta (Quick-Clone; Clontech) (section 2.5).

3.3.2.5 PCR amplification of candidate genes

In total 330 pairs of primers were designed using Primer 3 Output (http://frodo.wi.mit.edu/cgi-bin/primer3/primer3_www.cgi) in order to PCR amplify and screen the coding regions together with the splice sites (GT/AG), and the 5` UTRs of the selected genes (appendix 1, Table 2).

3.3.2.6 Mutation screening

Direct sequence analysis of one affected and one unaffected individual from each of the Spanish families was performed on the automated fluorescence DNA sequencer (ABI 3100, Perkin Elmer, Foster City, CA), according to manufactures instructions (section 2.4.1). The number of families included in screening the genes was dependant on the genetic data; for example in case of the genes from region A, 5 families were only included in the analysis (Figure 3.1). However, in case of region B all families were included in the process of screening genes for mutations.

3.3.2.7 Restriction enzyme analysis

To follow the segregation of a SNP within the *IMPG1* gene in our families a cosegregation study on all family members was performed using restriction enzyme digestion analysis. Exon 13 primer pairs were used to PCR-amplify the product, which was subsequently digested with 1 unit of *MsI* I enzyme (New England BioLabs, UK) and analysed on 2% agarose gel. The recognition sequence for the enzyme was 5'...CAYNN$^{\blacktriangledown}$NNRTG...3' which was present in the wild type allele (see section 2.6).

3.3.2.8 Genotyping analysis

Genotyping of the 17 LCA families was performed using 10 microsatellite markers of which 3 were from ABI PRISM® Linkage Mapping Sets V2.5 and the remaining 7 were synthesised commercially (see section 2.7.1 and Table 4, appendix 1). These markers covered the region of overlap between both RP25 and LCA5 loci. PCR amplification, genotyping analysis, data collection and allele identification were performed as described in section 2.7.1.

3.3.2.9 Comparative genome hybridisation

Comparative genome hybridisation was performed on 6 DNA samples from the RP5 family using a whole genome tiling path array (Redon *et al.*, 2006; see section 2.8).

3.4 RESULTS

3.4.1 10K GeneChip mapping array

The data obtained from ExcludeAR3 and AR1liteCHIP2 macros for families RP5 and RP214 are summarised below. In each table, the homozygous intervals across the human genome are listed in a descending order based on the number of SNPs and the genetic size of each interval. The top region that was considered as a significant locus for linkage in both families was the RP25 locus since 188 and 107 SNPs were observed to be homozygous in both RP5 and RP214 families, respectively.

Table 3.4 (A) and (B) analysis of the 10K GeneChip array data for RP5 and RP214 families, respectively

(A) RP5 Family

J	K	L	M	N	O	P	Q	R	S
Results are,			**cM**	**chrom**	**SNP's**	**significant?**	**start cM**	**finish cM**	**NoCall SNP's**
	largest		50.3	6	188	significant	73	124	6
	second		17.3	11	6	not significant	91	108	0
	third		16.6	9	7	not significant	169	185	0
	fourth		15.0	5	14	significant	187	202	1
	fifth		9.9	20	9	not significant	3	13	0
	sixth		9.7	10	9	not significant	112	122	0
	seventh		7.9	5	4	not significant	239	247	0
	eighth		7.8	2	12	significant	101	109	0
	ninth		7.4	4	5	not significant	65	72	1
	tenth		7.3	19	6	not significant	102	110	0

(B) RP214 Family

I	J	K	L	M	N	O	P	Q	R
Results are,			**cM**	**chrom**	**SNPs**	**significant?**	**start cM**	**finish cM**	**NoCall SNP's**
	largest		28.2	6	107	significant	83	112	0
	second		24.2	2	30	not significant	301	326	0
	third		17.8	1	44	not significant	193	211	0
	fourth		14.6	10	13	not significant	107	121	0
	fifth		12.9	6	11	not significant	70	83	0
	sixth		12.7	16	11	not significant	134	146	0
	seventh		12.0	17	10	not significant	73	85	1
	eighth		11.1	9	4	not significant	174	185	0
	ninth		10.8	7	9	not significant	108	119	0
	tenth		10.5	22	7	not significant	22	32	0

Additionally, the data obtained from both the visual analysis and the ALOHOMORA software for the RP299 family, were in agreement with the original genetic data and the 10K array data obtained from both RP5 and RP214 families (Table 3.5; Figure 3.8). Moreover, analysing the RP5 family using the ALOHOMORA software showed similar results to that obtained by the Exclude AR and hence confirming the results (Figure 3.8). In conclusion, the data obtained from the 10K array confirmed the initial findings of linkage to the RP25 region and showed that no other regions of shared haplotype were observed elsewhere in the human genome.

Table 3.5 Analysis of the 10K GeneChip array data for the RP299 family using the excel sheet

Order of loci	cM	Chroms	SNPs	Start cM	Finish cM	No Call SNPs
1	108.20	1	260	39.76	147.98	0
2	98.30	17	101	1.58	99.92	0
3	94.74	6	206	4.36	99.1	1
4	81.2	6	298	99.6	180.8	0
5	76.00	13	229	6.41	82.43	=
6	67.30	2	143	5.75	73.1	0
7	62.96	5	176	66.95	129.00	0
8	58.54	4	179	137.38	195.93	0
9	55.90	3	154	146.28	202.22	0
10	55.70	20	65	67.00	122.7	0

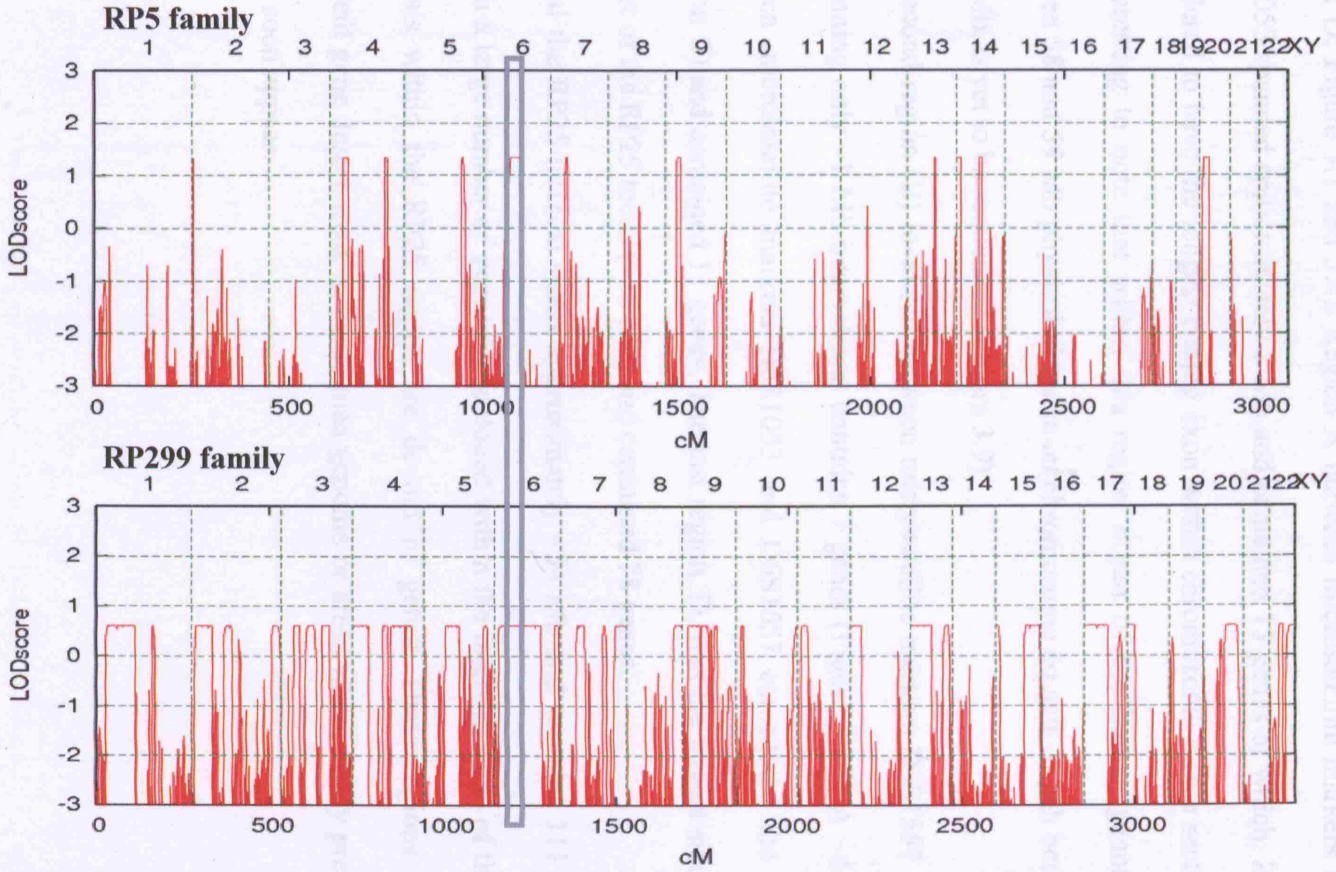

Figure 3.8 Schematic representation of the total genome analysis for families RP5 and RP299 generated by the ALOHOMORA software. The genetic interval (cM)/each chromosome (1-23) on the x axis is plotted against the LOD score on the y axis. The red peaks on each chromosome represent the LOD score for each of the single nucleotide polymorphisms (SNPs) used. The higher and the greater the width of the red peak the more likely that this representing the true locus for linkage. In families RP5 and RP299, the chromosome 6 interval, RP25, (boxed) is the most acceptable locus for linkage.

3.4.2 Bioinformatic analysis

3.4.2.1 An overview of the RP25 interval bioinformatics

According to the genetic data, we have divided the RP25 interval into four regions (A, B C and D; Figure 3.1 and 3.4). Region A between microsatellite markers D6S257 and D6S1053 spanned approximately 8 Mb and contained 15 genes of which, *ZNF451*, was considered to have the longest coding exon within chromosome 6 (see section 1.6.2). It is interesting to note that within this region a part of the human genome, ~50 Kb between 58 and 59 Mb physical distance on chromosome 6q and ~3 Mb between 59 and 61.2 Mb, is yet to be sequenced (Figure 3.9).

The second region (B) localised between microsatellite markers D6S1557 and D6S421 is spanning only ~1 Mb interval and contains 7 genes (Figure 3.10). A ~6 Mb interval between microsatellite markers D6S1053 and D6S1557 constituted the third region (Region C) and contained 11 genes. The last region, D, was the largest since it spanned the rest of the RP25 locus (~18 Mb) and contained 78 genes.

In total the RP25 interval spans approximately ~34 Mb and contains 111 genes. Even though a large number of genes are included within the interval, some of the sequenced intervals within the RP25 region are devoid of genes. These regions could either represent gene desert areas in the human genome or areas where newly predicted genes might soon appear.

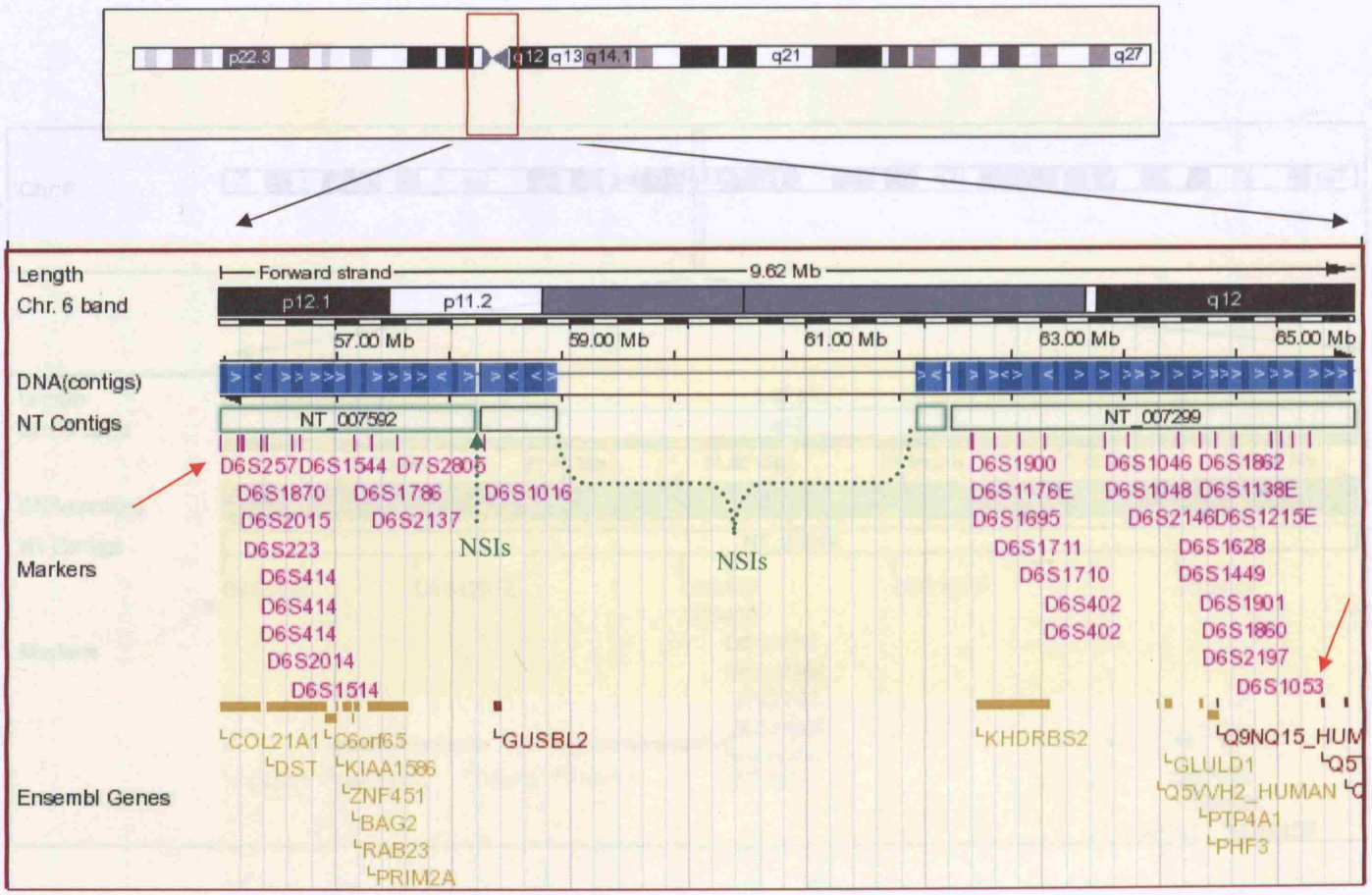

Figure 3.9 The genetic interval between microsatellite markers D6S257 and D6S1053 (red arrows). NSIs are non sequenced intervals (adapted from Ensembl).

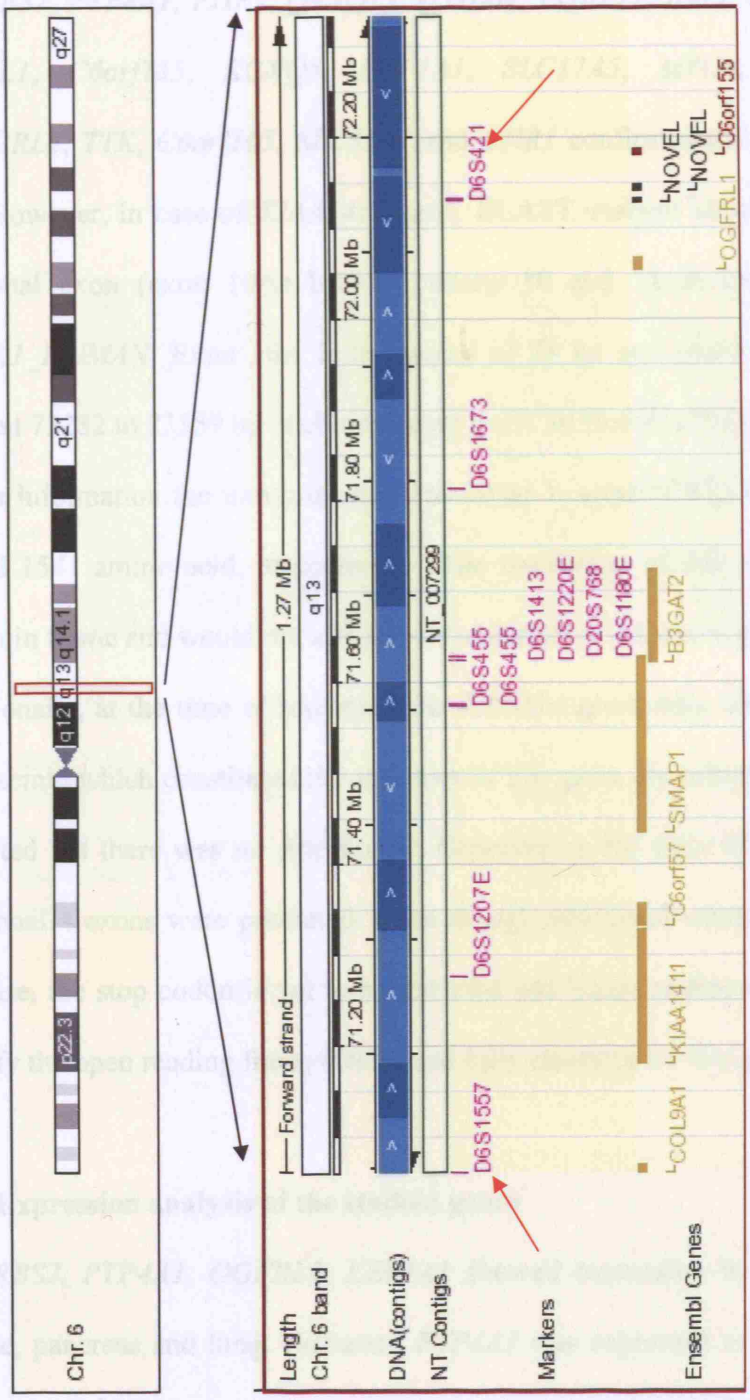

Figure 3.10 The genetic interval between microsatellite markers D6S1557 and D6S421 (red arrows). Seven genes are shown within this interval (adapted from Ensembl).

3.4.2.2 Bioinformatics of the genes within the RP25 interval

The results of bioinformatics analyses including genes' structures of *KIAA1586*, *KHDRBS2*, *PTP4A1*, *PHF3*, *Q9NQ15*, *Q5T669*, *EGFL11*, *BAI3*, *C6orf209*, *COL19A1*, *OGFRL1*, *C6orf155*, *KCNQ5*, *EEF1A1*, *SLC17A5*, *MYO6*, *IMPG1*, *HMGN3*, *SH3BGRL2*, *TTK*, *C6orf165*, *SLC35A1* and *CNR1* confirmed the previously published data. However, in case of *KIAA1411* gene, BLAST analysis showed that there was an additional exon (exon 10A) between exons 10 and 11 in the Ensembl transcript *Q5JXK1_HUMAN*. Exon 10A is composed of 78 bp and spans the genomic interval between 73282 to 73359 bp at chromosome 6 (NCBI36:6:71179310:71328195:1). Based on this information the transcript and translation lengths of KIAA1411 would be 6280 bp and 1541 amino acid, respectively. The translation of this additional exon would remain in frame and would not affect the translation of the whole protein.

Additionally, at the time of screening the *PRIM2A* gene, only 10 exons were available on Ensembl which constituted the structure of this gene, the initiation codon (ATG) was predicted but there was no stop codon. However, at the time of writing this thesis an additional 4 exons were predicted. Even though additional exons are appearing on the database, the stop codon is yet to be detected and hence additional work is required to identify the open reading frame (ORF) and fully characterise this gene.

3.4.3 Expression analysis of the studied genes

KHDRBS2, *PTP4A1*, *OGFRL1*, *EEF1A1* showed expression in retina, brain, skeletal muscle, pancreas and lung. However, *PTP4A1* was expressed at a low level in kidney and was not detected in either heart or placenta. Meanwhile, *KHDRBS2* was not expressed in either liver or heart (Figure 3.11).

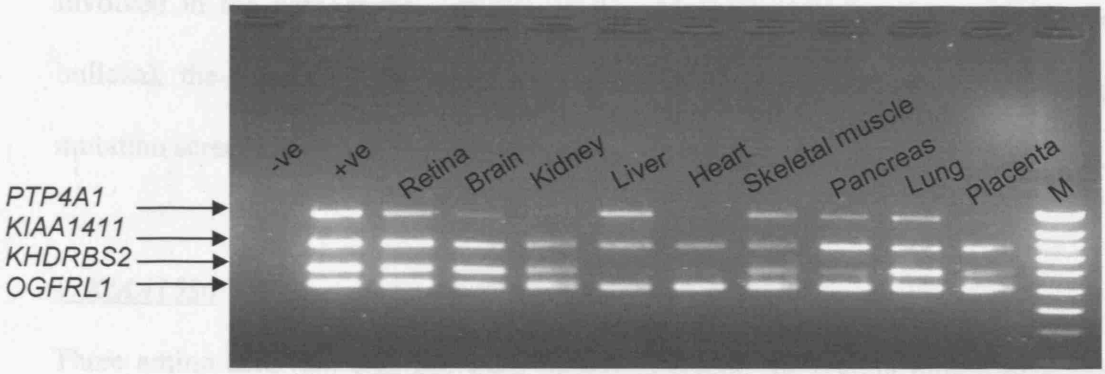

Figure 3.11 Expression pattern of *PTP4A1*, *KIAA1411*, *KHDRBS2*, and *OGFRL1* genes in human tissues as shown by multiplex PCR amplification. Lane 1: –ve control, 2: +ve genomic DNA control, lanes 3-11: cDNAs from retina, brain, kidney, liver, heart, skeletal muscle, pancreas, lung and placenta, respectively, M: 1 Kb smart ladder.

3.4.4 Mutation screening

All changes were assigned a nucleotide number starting at the first translation base of all genes studied according to the GenBank entries summarised in tables 3.6-3.10.

3.4.4.1 Mutation screening of the genes from region A

In total 15 genes were included in region A. Apart from one gene, *DST*, which was involved in the pathogenesis of one of the skin blistering conditions (epidermolysis bullosa), the remaining 14 genes were excluded as disease causing. The results of mutation screening of 6 of these genes are described below.

1. *KIAA1586*

Three amino acid (aa) changes were identified within the coding region of *KIAA1586* gene, of which one was novel. The new change led to the substitution of an amino acid isoleucine into valine and was detected in a heterozygous and homozygous conditions in the parent and the affected members of the RP5 family, respectively (Figure 3:12A and B). However, on examining the control individuals, this change was detected with an allele frequency of 12.0% denoting that it was a polymorphism (Table 3.6).

2. *PRIM2A*

Fifteen nucleotide changes were identified within *PRIM2A* gene, of which five were novel (Table 3.6). Five amino acid substitutions were detected of which four led to non synonymous changes and the only change that led to a silent aa substitution was novel (Figure 3.12 E). The remaining four novel changes were all intronic (Figure 3.12 C, D and F). Interestingly, all the changes within this gene were noted to be in a heterozygous

state in all family members. This should not be the case in both RP5 and RP214 affected individuals since it is expected that they should carry homozygous changes based on the genetic data. The results obtained showed that the heterozygous changes were not spurious since they were consistently observed. Additionally, at a specific nucleotide position a homozygous wild type allele (G/G), a homozygous mutant allele (A/A), and a heterozygous (G/A) nucleotide changes were observed in the same individual (RP5 affected), but from three independent PCR amplifications. By blast search there was no additional copy of this gene elsewhere in the human genome however by searching the database for genome variants (TCAG) we observed that CNV was reported for *PRIM2A* gene (Redon *et al.,* 2006). Therefore, the CNVs of this gene within the same chromosomal segment could explain our observation since the primers will amplify two PCR fragments of the same size and it will not be possible to identify whether one or two copies of the same nucleotide sequence was amplified unless we notice Mendelian inconsistencies such as in case of the RP5 family.

3. *KHDRBS2*

Mutation screening of *KHDRBS2* gene led to the identification of 10 genetic variants, of which 5 were novel (Table 3.6). Four out of the 10 identified changes were in the coding region of the gene, of which three were synonymous substitutions and were reported previously in the SNP database. The remaining coding change was a novel C>T transition that resulted in a missense change (P333L) (Figure 3.12 I). However, this conservative change was detected with an allele frequency of 8.0% in 100 control chromosomes.

The other 6 non-coding changes included a deletion of one bp at c.763-71delT which is a novel change, and was detected with an allele frequency of 16.0% in control population (Figure 3.12 H). The remaining five non-coding changes were A>C transversion in the 5`UTR (position -67), G>T transversion and T>C transition in the 3`UTR (positions *72 and *78 respectively), G>A transition at c.499-88 and C>A transversion at c.1231+33 (Figure 3.12 G and J). The 5`UTR change was interesting because it was heterozygous in one parent and homozygous in his affected son in a consanguineous family. Moreover, the same change was detected in a carrier state in an affected individual in another non-consanguineous family. However, it was detected with an allele frequency of 28% in 100 control chromosomes (Table 3.6).

4. *PTP4A1* No nucleotide changes were observed on sequencing this gene.

5. *PHF3* No genetic variants were observed on sequencing this gene.

6. *Q9NQ15* On sequencing this gene no changes were observed.

Table 3.6 Changes detected in *KIAA1586*, *PRIM2A* and *KHDRBS2*genes

Gene/ GenBank entry	Sequence variation	AA change	Family ID/SNP status	Allele frequency[§]	SNP ID if published / novel
***KIAA1586* / NM_020931.1**	c.21A>G	p.E7E	RP5Pand A/(-/-)	-	rs9382680
	c.241G>A	p.V81M	RP5 P and A/(-/-)	-	rs6926980
	c.2146A>G	p.I716V	RP5P/hetero RP5A/(-/-)	12.0%	Novel
***PRIM2A*/ NM_000947.2**	c.460-27G>A	-	All fam P and A/(+/-)	-	rs5011404
	c.541G>A	p.E181K	All fam P and A/(+/-)	-	rs5011403
	c.555+36T>A	-	All fam P and A/(+/-)	-	rs5011402
	c.555+99T>C	-	All fam P and A/(+/-)	-	rs5011401
	c.762-20T>A	-	All fam P and A/(+/-)	-	Novel
	c.762-38A>G	-	All fam P and A/(+/-)	-	Novel
	c.775A>G	p.S259G	All fam P and A/(+/-)	-	rs927192
	c.810G>A	p.K270K	All fam P and A/(+/-)	-	Novel
	c.834+15C>A	-	All fam P and A/(+/-)	-	rs2397502
	c.834+32G>T	-	All fam P and A/(+/-)	-	rs2397503
	c.834+38G>T	-	All fam P and A/(+/-)	-	Novel
	c.834+44G>T	-	All fam P and A/(+/-)	-	Novel
	c.A860G	p.Y287C	All fam P and A/(+/-)	-	rs9476080
	c.A866G	p.H289R	All fam P and A/(+/-)	-	rs9476081
	c.1020+78delTinsA	-	All fam P and A/(+/-)	-	rs11455120
***KHDRBS2*/ NM_152688.1**	- 67A>C	-	RP5P, RP167A/(+/-) RP5A/homo	28.0%	Novel
	c.489G>A	p.Q70Q	RP5P, RP214P/(+/-) RP167P/A,RP214A(-/-)	-	rs6921170
	c.499-88G>A	-	RP5P, RP167A/(+/-) RP5A/homo	-	rs9346001
	c.763-71delT	-	RP5P/(+/-)	16.0%	Novel
	c.1155T>C	p.Y292Y	RP167A/(+/-)	-	rs10484690
	c.1231+33C>A	-	RP5P, RP167A, RP214P/(+/-), RP5A, RP167P, RP214A/(-/-)	-	rs1555167
	c. 1277C>T	p.P333L	RP5P/(+/-)	8.0%	Novel
	c.1281G>A	p.Q334Q	RP214P, RP167A/(+/-)	-	rs1204114
	*72G>T	-	RP5P, RP167P, RP214P/(+/-)	83.0%	Novel
	*78 T>C	-	RP5P, RP167P, RP214P/(+/-)	83.0%	Novel

The asterisk denotes a change in the 3`-untranslated region, [§]: denotes allele frequency in Spanish only
All fam P and A: all families parent and affected, (+/-) heterozygous, (-/-) homozygous
E: Glutamic acid, V: Valine, M: Methionine, I: Isoleucine, K: Lysine, S: Serine, G: Glycine Y: Tyrosine, C: Cysteine, H: Histidine, R: Arginine, Q: Glutamine, P: Proline, L: Leucine

KIAA1586

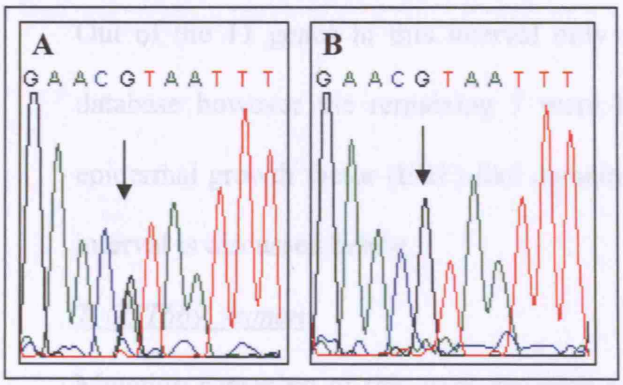

PRIM2A

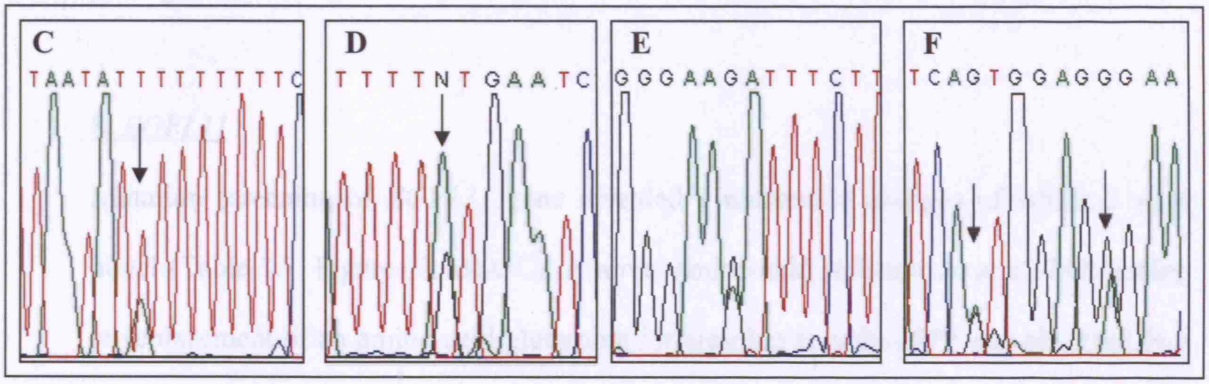

KHDRBS2

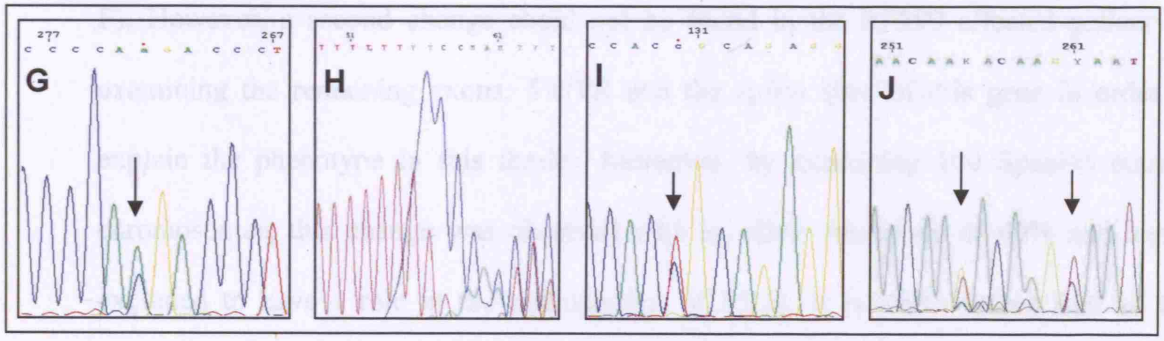

Figure 3.12: Electropherograms of the novel changes detected in ***KIAA1586*** (**A**: c.2146A>G heterozygous, **B**: c.2146A>G homozygous); ***PRIM2A*** (**C**: c.762-20T>A , **D**: c.762-38A>G , **E**: c.810G>A, **F**: c.834+38G>T , c.834+44G>T) and ***KHDRBS2*** (**G**: -67A>C, **H**: c.763--71delT , **I**: c. 1277C>T , **J**: *72G>T and *78 T>C) genes.

3.4.4.2 Mutation screening of the genes from region C

Out of the 11 genes in this interval only 4 were fully characterised by the Ensembl database however the remaining 7 were incomplete and they all shared a common epidermal growth factor (EGF)-like domain. Mutation screening of 5 genes within this interval is discussed below.

7. Q5T669_human

Mutation screening of this gene revealed no nucleotide changes either polymorphic or pathogenic.

8. EGFL11

Mutation screening of *EGFL11* gene revealed 9 nucleotide changes of which 3 were novel (Table 3.7, Figures 3.13 A-C). A novel amino acid substitution at c.1712 leading to replacement of an amino acid glutamine for arginine at codon 570 was observed in a heterozygous state in the parent and the affected son of the RP299 family (Figure 3.13 F). However, a second change could not be found in the RP299 affected patient by examining the remaining exons, 5`UTR and the splice sites of this gene in order to explain the phenotype in this family. Moreover, by examining 100 Spanish control chromosomes, this change was observed with an allele frequency of 40% and hence excluded to have a role in the pathogenesis of RP25. It is worth noting that all the changes within this gene were in agreement with the genetic data of the studied families apart from one novel change, c.863-21insT, which was heterozygous in all samples tested including both RP5 and RP214 affected members. A copy number variation for this gene has been reported in the database for genomic variants.

9. *BAI3*

Six nucleotide substitutions were detected on sequencing *BAI3* gene however they were all published in the SNP database (Table 3.7). Two were silent coding changes and the remaining 4 were intronic and hence not affecting the protein structure of the gene.

10. *C6orf209*

Mutation screening of *C6orf209* revealed three nucleotide changes (Table 3.7). One base pair deletion at c.916-48 was detected in a homozygous state in all tested patients which was not previously published (Figure 3.13 D).

11. *COL19A1*

Fifteen nucleotide changes were observed on sequencing *COL19A1* gene (Table 3.7). All the changes were documented in the SNP database apart from one novel SNP, at c.166+12A>G, which was observed in a heterozygous state in one of the RP5 parents (Figure 3.13 E).

Table 3.7 Changes detected in *EGFL11*, *BAI3*, *C6orf209* and *COL19A1* genes

Gene/ GenBank entry	Sequence variation	AA change	Family ID/SNP status	Allele frequency[§]	SNP ID if published / novel
EGFL11/ **NM_198283.1**	g.143+83T>A	-	RP73A, RP299P and A /(+/-)	-	rs13217899
	c.281C>A	p. P93P	RP73P and A/(+/-)	5.0%	Novel
	c.359C>T	p.T119M	RP5P/(+/-)	-	rs12193967
	c.862+87T>C	-	RP73A, RP299Pand A /(+/-)	-	rs4710522
	c.863-21insT	-	RP5P and A, RP73 A, RP214P and A, RP299P and A/(+/-)	20.0%	Novel
	c.1146T>C	p.N381N	RP5P and A/(-/-), RP73A, RP214P, RP299A/(+/-)	-	rs974110
	c.1300-3C>T	-	RP5P/(+/-), RP5A, RP73P and A, RP214P and A, RP299P and A(-/-)	-	rs1936439
	c.1459+103C>T	-	RP5P, RP214P, RP299P/(+/-) RP5A/(-/-)	-	rs9453265
	c.1712A>G	p.Q570R	RP299P and A/ (+/-)	40.0%	Novel
BAI3/ **NM_001704.1**	c.1998+71G>A	-	RP5P, RP167P, RP214P, RP260P and A, R299P and A/(+/-), RP73P and A/(-/-)	-	rs1336655
	c.2107+61C>T	-	RP167P and A, RP299 P and A/(+/-)	-	rs10485430
	c.2258-15A>T	-	Homozygous in all samples	-	rs618372
	c.2334-9C>G	-	RP167A, RP214A/(-/-); RP214P, RP260P and A, RP299P and A/(+/-)	-	rs2793459
	c.3522G>A	p.S1174S	RP73A/(+/-)	-	rs2296974
	c.4008 G>A	p.P1336P	RP5P and A, RP167A/ (-/-) ; RP73P, RP167P, RP214P/(+/-)	-	rs913543
C6orf209/ **NM_018368.2**	c.246+68C>T	-	RP73P, RP299A/(+/-)	-	rs2125024
	c.916-48delA	-	Homozygous in all	-	Novel
	c.1407T>A	p.D469E	RP73P, RP299P and A/(+/-)	-	rs9354880
COL19A1/ **NM_001858.4**	c.166+12A>G	-	RP5P/(+/-)	-	Novel
	c.266+53C>T	-	RP214P/(+/-), RP214A/(-/-)	-	rs9454910
	c.667-15C>T	-	RP73P/(+/-)	-	rs2345783
	c.1055 C>G	p.D352G	RP73P/(+/-) RP73A/(-/-)	-	rs2273426
	c.1134+74G>C	-	RP73A, RP214P/(+/-)	-	rs7764390

Gene/ GenBank entry	Sequence variation	AA change	Family ID/SNP status	Allele frequency[§]	SNP ID if published / novel
***COL19A1*/ NM_001858.4**	c.1171-18G>A	-	RP5P, RP73P&A, RP214P/(+/-)	-	rs7349861
	c.1224+10G>C	-	RP5P, RP73P&A, RP214P, RP299P/(+/-)	-	rs2224513
	c.1224+11C>T	-	RP5P, RP73P&A, RP214P, RP299P/(+/-)	-	rs2224514
	c.1278+9A>G	-	All fam (-/-)	-	rs7772672
	c.1573-49delTT	-	RP73P&A, RP214P/(+/-)	-	rs3831024
	c.1740+28A>G	-	RP73P&A, RP214P/(+/-), RP214A/(-/-)	-	rs9364074
	c.1771-15C>T	-	RP73A, RP214P/(+/-) RP73P, RP214A/(-/-)	-	rs7762409
	c.2286C>T	p.G762G	RP73P&A, RP214P/(+/-), RP214A/(-/-)	-	rs2229799
	c.2445+99T>G	-	RP73A, RP214P, RP299P/(+/-), RP5P&A, RP73P,RP214A/homo	-	rs802174
	c.2688 G>A	p.G896G	RP214P/(+/-), RP214A/(-/-)	-	rs2273948

§: denotes allele frequency in Spanish control chromosomes only
All fam P and A: all families parent and affected, (+/-) heterozygous, (-/-) homozygous
E: Glutamic acid, M: Methionine, S: Serine, G: Glycine, R: Arginine, Q: Glutamine, P: Proline, T: Threonine, D: Aspartic acid

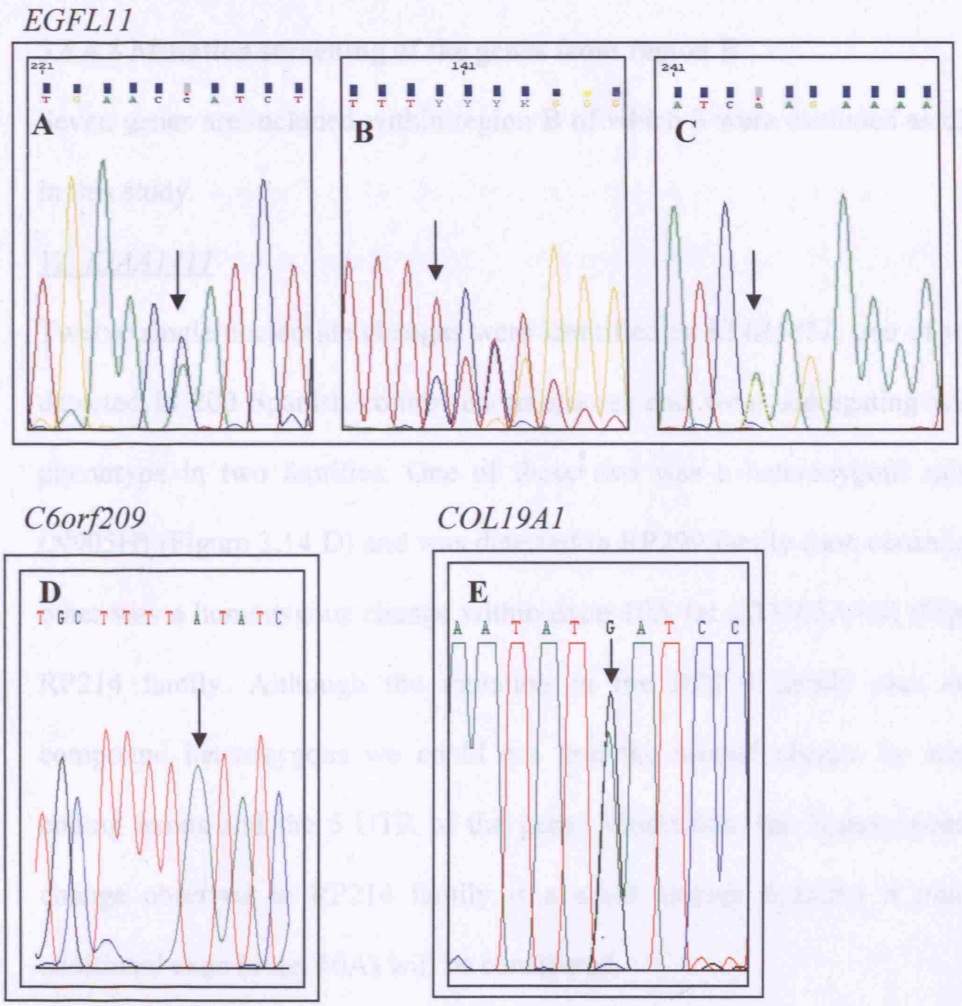

Figure 3.13: Electropherograms of the novel changes detected in ***EGFL11*** (**A**: c.281C>A , **B**: c.863-21insT , **C**: c.1712A>G); ***C6orf209*** (**D**: c.916-48delA homozygous) and ***COL19A1*** (**E**: c.166+12A>G) genes.

3.4.4.3 Mutation screening of the genes from region B

Seven genes are included within region B of which 3 were excluded as disease causing in this study.

12. *KIAA1411*

Twelve single nucleotide changes were identified in *KIAA1411*, two of which were not detected in 200 Spanish control chromosomes and were segregating with the disease phenotype in two families. One of these two was a heterozygous missense change (N905H) (Figure 3.14 D) and was detected in RP299 family (non consanguineous). The other was a homozygous change within exon 10A (at g.73305A>G) (Figure 3.14 C) in RP214 family. Although the mutation in the RP299 family was expected to be compound heterozygous we could not find the second change by screening all the coding exons and the 5`UTR of the gene. Meanwhile, the homozygous g.73305A>G change observed in RP214 family is a silent change (L282L) if translation of the additional exon (exon 10A) will be considered.

Of the remaining 10 single nucleotide changes four corresponded to previously reported changes in the SNP database (Table 3.8). Of the six novel changes, one silent substitution was detected in exon 5 and was observed in control chromosomes (Figure 3.14 B). A novel deletion (c.1030-196_201delTTTATA) was also detected in 5 families but did not co-segregate with the disease phenotype (Figure 3.14 E). The remaining 4 SNPs were C>T or G>A transitions which were located either in the intronic sequence or in the 3` UTR regions (Figure 3.14 A and F-H). Of the previously reported changes, 2 were intronic A>G transitions and the other two were a silent change and a non-conservative substitution within exons 15 and 16, respectively.

13. *OGFRL1*

Mutation screening of the *OGFRL1* gene revealed a deletion of an amino acid (lysine) from exon 7 (Figure 3.14 I). The deletion co-segregated with the disease phenotype in a non-consanguineous family (RP73). However it was detected with a minor allele frequency of 4% in 100 control chromosomes. The second change was a novel non-conservative substitution of an amino acid serine to proline at codon 46, but was detected in control chromosomes with an allele frequency of 8% (Figure 3.14 J). The other two changes were intronic polymorphisms (c.480-11A>T, c.693-3C>T) and were previously published in the SNP database (Table 3.8).

14. *C6orf155*

Mutation screening of *C6orf155* did not show either pathological or polymorphic changes.

Table 3.8 Changes detected in *KIAA1411* and *OGFRL1* genes

Gene/ GenBank entry	Sequence variation	AA change	Family ID/SNP status	Allele frequency[§]	SNP ID if published / novel
***KIAA1411*/ NM_020819**	g.366-15C>T	-	RP5P, RP299A/(+/-)	50.0%	Novel
	c.90T>A	p.I30I	RP73P, RP167P/(+/-)	-	Novel
	c.443-27A>G	-	RP5A, RP214/(-/-), RP214P, RP5P/(+/-)	-	rs2273210
	g.73305A>G	-	RP214A/(-/-), RP214P/(+/-)	0%	Novel
	c.1030-196_201delTTT ATA	-	RP73P and A(+/-), RP299P and A/hetero(+/-), RP5P(+/-), RP167A(+/-), RP260(+/-)	50.0%	Novel
	c.2713A>C	p.N905H	RP299A/(+/-)	0%	Novel
	c.3429C>T	p.N1143N	RP73P and A, RP214P/(+/-), RP214A/(-/-)	-	rs774087
	c.3725A>G	p.D1242G	RP73 P and A, RP214P/(+/-)	-	rs2747701
	c.3775+23A>G	-	RP5P/(+/-)	16.0%	Novel
	c.3868-108A>G	-	RP5P and A, RP167A/(-/-); RP73P, RP167P, RP214P/(+/-)	-	rs9283835
	c.4117+92 G>A	-	RP73P/(+/-) RP73A/(-/-)	33.0%	Novel
	*8G>A	-	RP73P and A, RP214P/(+/-)	41.0%	Novel
***OGFRL1*/ NM_024576.3**	c.139T>C	p.S46P	RP73P(+/-) RP73A/(-/-)	8.0%	Novel
	c.480-11A>T	-	RP73P and A, RP214P/(+/-)	-	rs2273889
	c.693-3C>T	-	RP73P and A, RP214P/(+/-)	-	rs16880821
	c.1186_1188delAAG	p.395delK	RP73P and A/(+/-)	4.0%	Novel

§: denotes allele frequency in Spanish control chromosomes only
All fam P and A: all families parent and affected, (+/-) heterozygous, (-/-) homozygous
S: Serine, G: Glycine, P: Proline, D: Aspartic acid, I: Isoleucine, N: Asparagine, H: Histidine, K: Lysine

KIAA1411

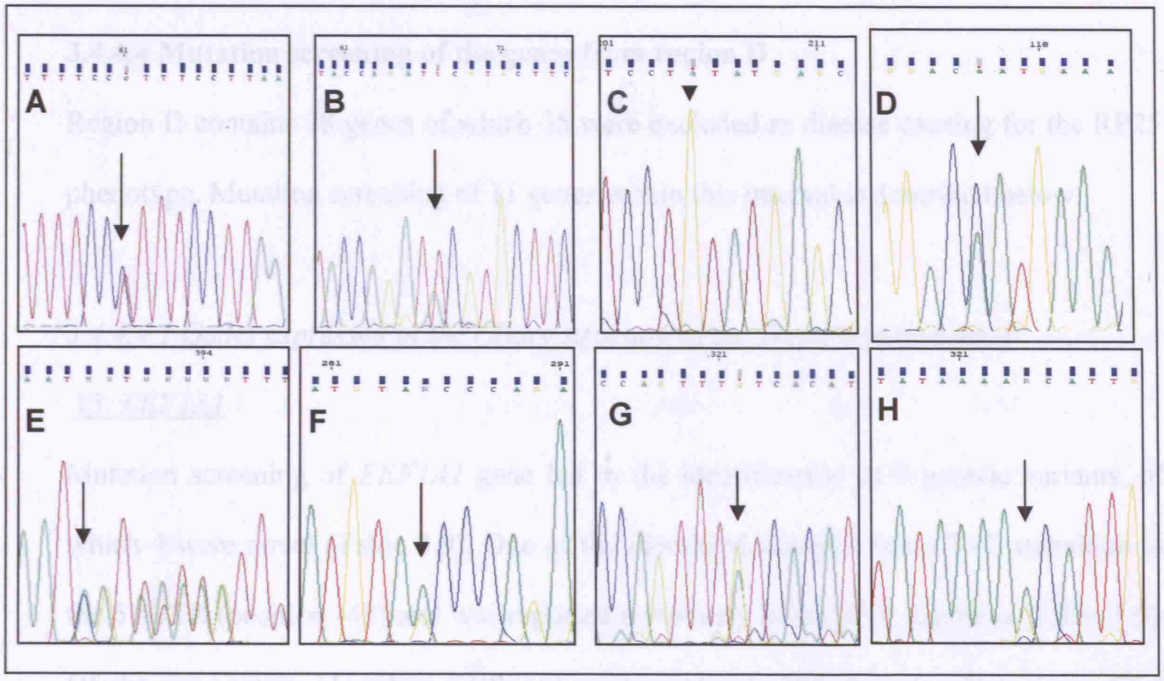

OGFRL1

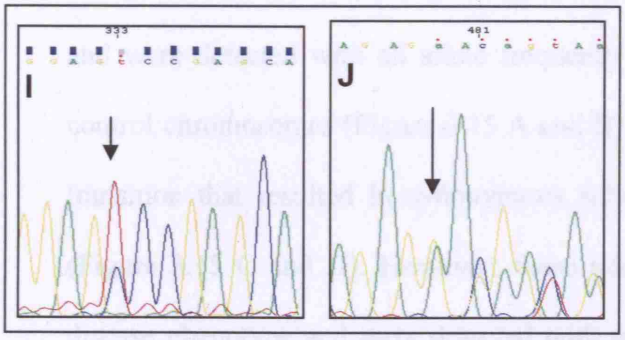

Figure 3.14 Electropherograms of the novel changes detected in ***KIAA1411*** (**A**: g.366-15C>T , **B**: c.90T>A , **C**: g.73305A>G, **D**: c.2713A>C **E**: c.1030-196_201delTTTATA , **F**: c.3775+23A>G , **G**: Ic.4117+92 G>A , **H**: ***8G>A)** and ***OGFRL1*** (**I**: c.139T>C , **J**: c.1186_1188delAAG) genes.

3.4.4.4 Mutation screening of the genes from region D

Region D contains 78 genes of which 35 were excluded as disease causing for the RP25 phenotype. Mutation screening of 11 genes within this interval is described below.

3.4.4.4.1 Genes expressed in the ciliary structure of the Trypanosoma brucei

15. *EEF1A1*

Mutation screening of *EEF1A1* gene led to the identification of 5 genetic variants, of which 4 were novel (Table 3.9). One of the identified changes was a T>C transition in the 5` UTR (position -43) and was reported previously in the SNP database (Table 3.9). Of the four newly identified SNPs, two were intronic and the other two were silent changes. The two non-coding changes included T>C transition at c.1029+28 and +71 and were detected with an allele frequency of 41.0% and 33.0%, respectively in 100 control chromosomes (Figure 3.15 A and B). The remaining coding changes were G>A transition that resulted in synonymous substitutions (K444K and Q459Q) in exon 7 (Figure 3.15 C and D). However, these silent changes were not segregating with the disease phenotype and were detected with an allele frequency of 49.0% in 100 control chromosomes.

16. *C6orf165*

Five nucleotide substitutions were identified on sequencing *C6orf165* gene of which three were novel (Table 3.9). Out of the 3 novel changes 2 were coding of which 1 led to a non synonymous amino acid replacement of aspartic acid into glycine at codon 118. This change (D118G) was detected in a heterozygous state in the parent and the affected

members of RP73 family (Figure 3.15 E). Nevertheless it was not detected in 100 control chromosomes, a second heterozygous change could not be identified to explain the role of the first change in the pathogenesis of the RP25 phenotype.

17. *SLC35A1*

Mutation screening of *SLC35A1* revealed three genetic variants of which one was novel (Table 3.9). The novel change was intronic at c.887-14T>C (Figure 3.15 H).

3.4.4.4.2 Genes with preferential expression in the retina

This group of genes contained also *RIM1* gene which has been excluded as pathogenic for the RP25 phenotype by our collaborators.

18. *MYO6*

Mutation screening of the *MYO6* gene led to the identification of 12 genetic variants of which two were novel (Table 3.6). The previously published SNPs were located in the intonic intervals of the gene apart from one SNP which was located within exon 17 leading to a silent amino acid substitution at codon 573. One of the novel genetic variants was situated in the 5`UTR of the gene at -49 (Figure 3.15 I). The second new change was located only 4 bp upstream of the donor splice site in exon 12 (Figure 3.15 J). This change was heterozygous in the parent of RP5 family however it was not detected in his affected son and therefore could not be considered as pathogenic.

19. *IMPG1*

Ten SNPs were identified in *IMPG1*, three of which were novel (Table 3.9). Of the three novel changes, one was an insertion of a single base pair (A) at c.302-212insA (Figure 3.15 K). A novel deletion of one base pair (T) at position (IVS6-9) was also detected in four of the studied families but did not co-segregate with the disease phenotype (Figure 3.15 M). The remaining unreported SNP was an intronic A>T transversion at c.562+75A>T (Figure 3.15 L). Of the previously reported changes, 2 were intronic T>C transitions, one was a deletion of one base pair at c.2044+52delA and the other four were missense changes. Two of the missense changes were nonconservative substitutions in exons 13 and 15, respectively and the other two were conservative changes in exons 15 and 16, respectively (Table 3.9).

Table 3.9 Changes detected in *EEF1A1*, *C6orf165*, *SLC35A1*, *MYO6* and *IMPG1* genes

Gene/ GenBank entry	Sequence variation	AA change	Family ID/SNP status	Allele frequency[§]	SNP ID if published / novel
EEF1A1/ **NM_001402.5**	- 43T>C	-	RP5P, RP73P/(+/-)	-	rs2073465
	c.1029+28T>C	-	RP299P, RP73P/(+/-)	41.0%	Novel
	c.1029+71T>C	-	RP5P, RP167P/(+/-)	33.0%	Novel
	c.1332G>A	p.K444K	RP214P, RP73P/(+/-)	49.0%	Novel
	c.1377G>A	p.Q459Q	RP73P, RP73P/(+/-)	49.0%	Novel
C6orf165/ **NM_001031743.1**	-70C>T	-	All fam P and A/(-/-)	-	rs7759848
	g.28-17del A	-	RP73P and A/(+/-)	-	rs11350856
	c.353A>G	p.D118G	RP73A/(+/-)	0%	Novel
	c.473-15del T	-	RP73P and A/(+/-)	-	Novel
	c.921C >T	p.T307T	RP260P and A/(+/-)	-	Novel
SLC35A1/ **NM_006416.3**	-18G>C	-	RP73P and A, RP2909A/(+/)	-	rs9450704
	c.575-121A>C	-	RP73P and A/(+/-)	-	rs6924641
	c.887-14T>C	-	RP73P and A/(+/-)	-	Novel
MYO6/ **NM_004999.3**	-49C>G	-	RP260P and A/(+/-)	-	Novel
	c.261+73 G>A	-	RP73P and A, RP299P and A, RP260P and A/(+/-)	-	rs1280052
	c.553+11T>C	-	RP5P/(+/-), RP5A/(-/-)	-	rs12210963
	c.554-65A>G	-	RP5P/(+/-), RP5A/(-/-)	-	rs12216518
	c.652-91insT	-	RP5P and RP260A/(-/-) RP73P and A, RP299P and A (+/-)	-	rs3839374
	c.1224-80T>G	-	RP5P and A, RP73P and A, RP299P and A,RP260A/(-/-), RP260P/(+/-)	-	rs3798439
	c.1224-4A>G	-	RP5P/ (+/-)	-	Novel
	c.1723C>T	p.D573D	RP260P/(+/-)	-	rs11756446
	c.2658+17C>T	-	RP5P, RP73P and A, RP299P and A/(+/-), RP260A/(+/-)	-	rs2295936
	c.3138-107T>A	-	RP73P, RP214P, RP167P and A (+/-)	-	rs720862
	c.3281-19delT	-	RP5P, RP73P and A, RP299P and A/(+/-), RP260A/(+/-)	-	rs11285982
	*12C>T		RP5P, RP73P and A/ (+/-) RP5A, RP299A/ (-/-)	-	rs12606
IMPG1/ **NM_001563.2**	c.302-212insA	-	RP5P, RP299P/(+/-)	16.0%	Novel

Gene/ GenBank entry	Sequence variation	AA change	Family ID/SNP status	Allele frequency[§]	SNP ID if published / novel
***IMPG1*/ NM_001563.2**	c.498-90T>C	-	RP73P, RP167P/(+/-)	-	rs1341568
	c.562+75A>T	-	RP299P, RP73P/(+/-)	33.0%	Novel
	c.667-9delT	-	RP260P/(+/-)	50.0%	Novel
	c.888-48C>T	-	RP73P, RP235P/(+/-)	-	rs17802616
	c.1552C>G	p.H517D	RP73P, RP167P/(+/-)	-	rs3734311
	c.2044+52delA	-	RP299P, RP73P/(+/-)	-	rs3215818
	c.2110C>T	p.R703W	RP5P, RP299P/(+/-)	-	rs10943299
	c.2132G>A	p.R710H	RP260P/(+/-)	-	rs3734313
	c.2282G>A	p.S760N	RP73P, RP235P/(+/-)	-	rs3778005

§: denotes allele frequency in Spanish control chromosomes only
All fam P and A: all families parent and affected, (+/-) heterozygous, (-/-) homozygous
K: Lysine, Q: Glutamine, D: Aspartic acid, G: Glycine, T: Threonine, H: Histidine, W: Tryptophan, S: Serine, R: Arginine, N: Asparagine

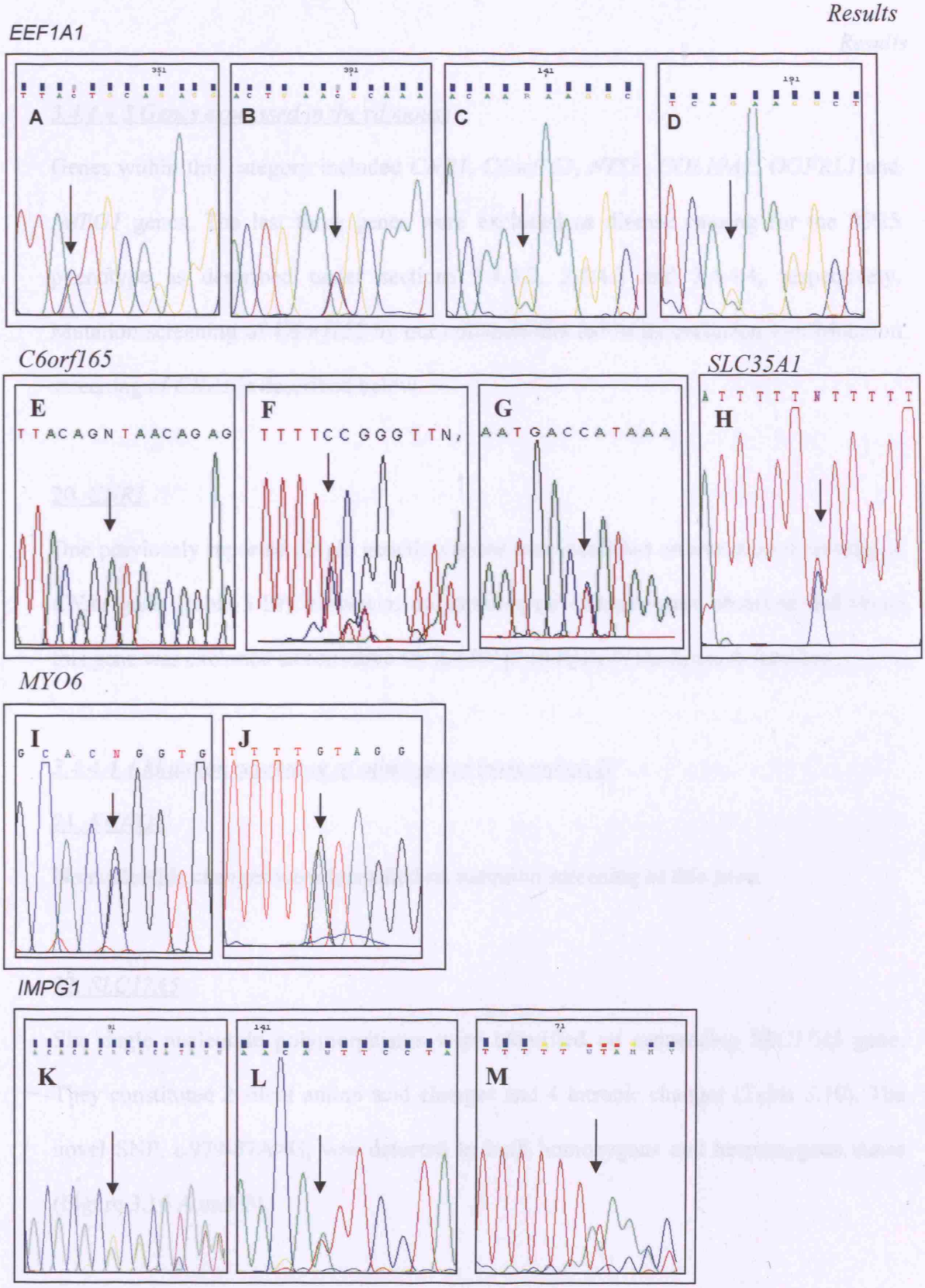

Figure 3.15 Electropherograms of the novel changes detected in ***EEF1A1*** (**A**: c.1029+28T>C , **B**: c.1029+71T>C, **C**: K444K, **D**: Q459Q); ***C6orf165*** (**E**: c.353A>G , **F**: c.473-15del T , **G**: c.921C >T); ***SLC35A1*** (**H**: c.887-14T>C) ***MYO6*** (**I**: -49C>G , **J**: c.1224-4A>G) and ***IMPG1*** (**K**: c.302-212insA , **L**: c.562+75A>T , **M**: c.667-9delT) genes.

3.4.4.4.3 Genes expressed in the rd mouse

Genes within this category included *CNR1*, *C6orf152*, *NT5E*, *COL19A1*, *OGFRL1* and *IMPG1* genes. The last three genes were excluded as disease causing for the RP25 phenotype as described under sections 3.4.4.2, 3.4.4.3 and 3.4.4.4, respectively. Mutation screening of *C6orf152* by our collaborators led to its exclusion too. Mutation screening of *CNR1* is described below.

20. *CNR1*

One previously reported single genetic variant was identified on mutation screening of *CNR1* gene (Table 3.10). However, no pathological changes were observed and hence this gene was excluded as causative for the RP phenotype in the Spanish families.

3.4.4.4.4 Mutation screening of other genes from region D

21. *KCNQ5*

No nucleotide changes were identified on mutation screening of this gene.

22. *SLC17A5*

Six single nucleotide polymorphisms were identified on sequencing *SLC17A5* gene. They constituted 2 silent amino acid changes and 4 intronic changes (Table 3.10). The novel SNP, c.979-87A>G, was detected in both homozygous and heterozygous states (Figure 3.16 A and B).

23. *HMGN3*

Mutation screening of *HMGN3* revealed 2 previously reported SNPs (Table 3.6).

24. *SH3BGRL2*

No nucleotide changes were identified on mutation screening of this gene.

25. *TTK*

Sixteen nucleotide changes were identified on mutation screening of the *TTK* gene of which 4 were novel (Table 3.10). The novel changes included a g.520C>T (Figure 3.16 C), an insertion/deletion at c.471-39 in both homozygous and heterozygous states (Figure 3.16 D and E), a G to T transversion at c.1521+25G>T (Figure 3.16 F) and finally a 6 bp deletion at c.2050-75_80 in both homozygous and heterozygous states (Figure 3.16 G and H). The novel changes could not be considered as pathogenic since they were either detected in both the parents and their affected offsprings in homozygous state or only in the parents and not in the affected siblings. This is ruling out the SNPs as disease causing since they do not segregate with the phenotype of the studied families even though still segregating with the genetic data. Out of the 12 previously published SNPs, 2 were silent coding changes and the remaining 10 were intronic (Table 3.10).

Table 3.10 Changes detected in *CNR1*, *HMGN3*, *SLC17A5* and *TTK* genes

Gene/ GenBank entry	Sequence variation	AA change	Family ID/SNP status	Allele frequency[§]	SNP ID if published / novel
CNR1/ **NM_016083.3**	c.1359G>A	p.T452T	RP73P, RP299P and A/(+/-), RP73A, RP260A 8/(-/-)	-	rs1049353
HMGN3/ **NM_138730.1**	-78T>G	-	RP5P/(+/-), RP5A/(-/-)	-	rs9361504
	c.67-16G>A	-	RP214P/(+/-), all/(-/-)	-	rs9341761
SLC17A5// **NM_012434.3**	-178delGinsC	-	RP299P and A/hetero	-	rs35519584
	c.246G>A	p.A81A	RP73P and A, RP214P and A/(+/-)	-	rs472294
	c.292-22T>C	-	RP5P/(+/-)	-	rs12206001
	c.525+36G>C	-	RP5P/(+/-)	-	rs12192476
	c.606A>G	p.S202S	RP5P/(+/-)	-	rs3757112
	c.979-87A>G	-	RP73P and A, RP214A,RP299A/ (+/-), RP214P, RP299P/(-/-)	-	Novel
TTK/ **NM_003318.3**	g.477G>T	-	RP5P and A, RP260P/ (-/ -) RP73P and A, RP299A, RP260A/ (+/-)	-	rs465483
	g.520C>T	-	RP73P, RP299P/ (+/-)	-	Novel
	c.471-39 del CATTIns TAAAGA	-	RP73A,RP299P,A,RP260A/ (+/-)	-	Novel
	c.613+59G>A	-	RP5P,A, RP73P,RP260P/ (-/-) RP73A,RP299P,A,RP260A/ (+/-)	-	rs151587
	c.613+68A>T	-	RP5P,A, RP73P,RP260P/ (-/-) RP73A,RP299P,A,RP260A/ (+/-)	-	rs239556
	c.1108+159C>T	-	RP5P and A,RP73P,RP260P/(-/-) RP73A,RP299A,RP260/ (+/-)	-	rs239567
	c.1257+52C>T	-	RP73P, RP299P/(+/-)	-	rs2273753
	c.1257+53G>A	-	RP5P,RP299A,RP260P and A/ (+/-)	-	rs17175251
	c.1521+25G>T	-	RP299A/(+/-)	-	Novel
	c.1581A>T	p.I527I	RP5P, RP299A, RP260P and A/(+/-)	-	rs17254007
	c.1614+52G>A	-	RP5A, RP73P, RP260P/ (-/-) RP5P, RP73A, RP299P,A, RP260A/ (+/-)	-	rs239584

Gene/ GenBank entry	Sequence variation	AA change	Family ID/SNP status	Allele frequency[§]	SNP ID if published / novel
TTK/ **NM_003318.3**	c.2050-75_80delAATAAT	-	RP5A,RP73P/(-/-), RP5P,RP73A, RP299P,A, RP260P,A/ (+/-)	-	Novel
	c.2131-23G>A	-	RP73P, RP299P/ (+/-)	-	rs3799493
	c.2367A>C	p.P789P	RP5P,RP299A,RP260P and A	-	rs17254438
	c.2392+96C>G	-	RP5A/ (-/-) RP5P,RP73P,A, RP260P/ (+/-)	-	rs17254438
	c.2393-33C>T	-	RP5P,A, RP73P, RP260P/ (-/-), RP73A, RP299P,A/ (+/-)	-	rs6089621

§: denotes allele frequency in Spanish control chromosomes only
All fam P and A: all families parent and affected, (+/-) heterozygous, (-/-) homozygous
T: Threonine, A: Alanine, S: Serine, I: Isoleucine, P: proline

SLC17A5

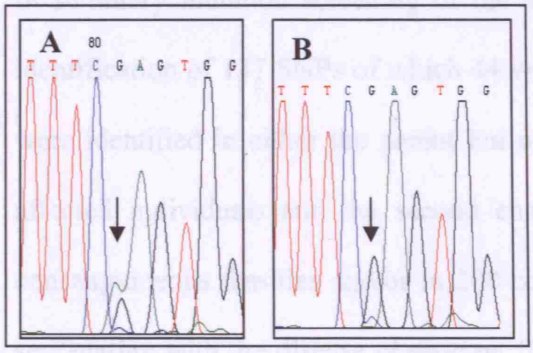

TTK

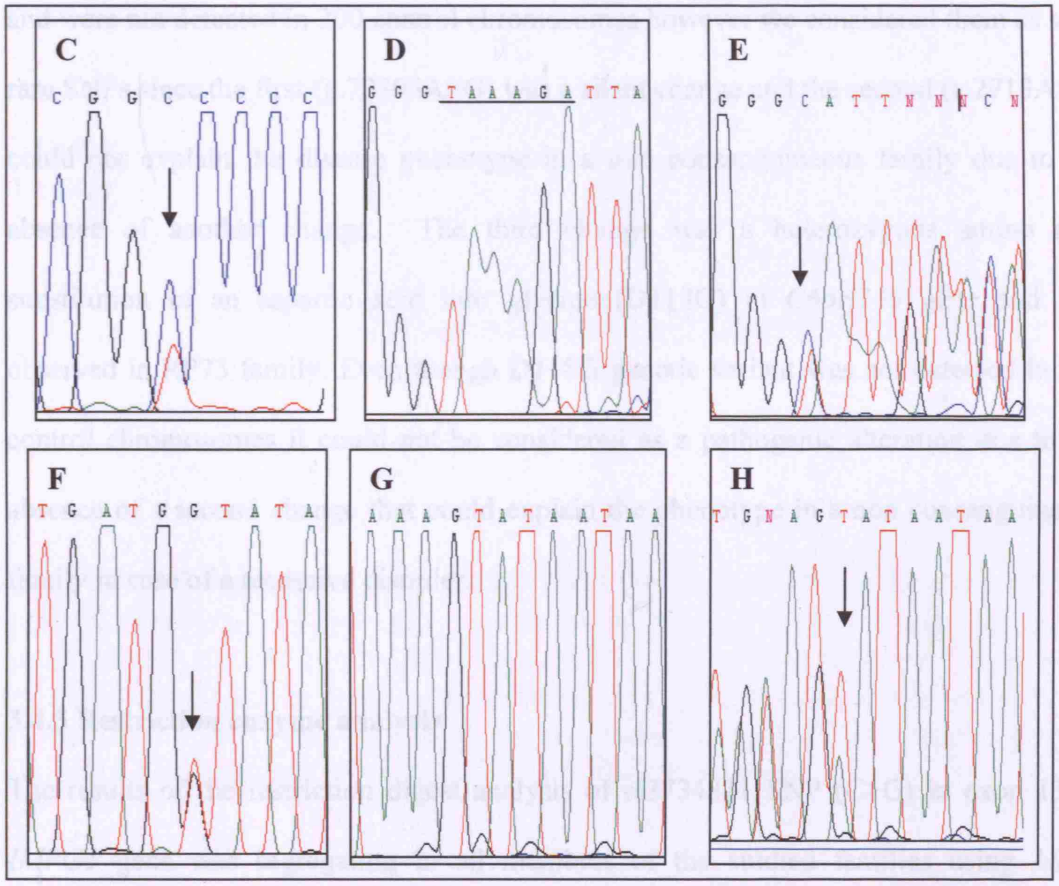

Figure 3.16 Electropherograms of the novel changes detected in ***SLC17A5*** (**A**: c.979-87A>G [heterozygous], **B**: c.979-87A>G [homozygous]) and ***TTK*** (**C**: g.520C>T, **D**: IVS4-39InsTAAAGAdelCATT [homozygous], **E**: Ic.471-39 del CATTIns TAAAGA heterozygous, **F**: c.1521+25G>T, **G**: c.2050-75_80delAATAAT [homozygous], **H**: c.2050-75_80delAATAAT [heterozygous]) genes.

In summary mutation screening of the above described twenty five genes led to the identification of 137 SNPs of which 44 were novel. Forty two out of the 44 novel SNPs were identified in either the parent but not in the affected offspring or in some of the affected individuals and the second change could not be identified in case of non consanguineous families and/or in 200 control chromosomes. Only three changes were segregating with the disease phenotype. The first two were observed in *KIAA1411* gene and were not detected in 200 control chromosomes however we considered them as very rare SNPs since the first (g.73305A>G) was a silent change and the second (c.2713A>C) could not explain the disease phenotype in a non consanguineous family due to the absence of another change. The third change was a heterozygous amino acid substitution of an aspartic acid into glycine (D118G) in *C6orf165* gene and was observed in RP73 family. Even though D118G genetic variant was not detected in 200 control chromosomes it could not be considered as a pathogenic alteration due to the absence of a second change that could explain the phenotype in a non consanguineous family in case of a recessive disorder.

3.4.5 Restriction enzyme analysis

The results of the restriction digest analysis of rs3734311 SNP (C>G) in exon 13 of *IMPG1* gene was segregating in all members of the studied families using *Msl* I restriction enzyme. The change leads to loss of the *Msl* I enzyme site therefore, on PCR amplification of the individuals with the C/C allele, a completely digested product of 385 bp was observed. On the other hand, individuals with the G/G allele remained undigested with only one band at the expected size (773bp). Parents who were heterozygous for the SNP presented with two products at 773 and 385 bp (Figure 3.17).

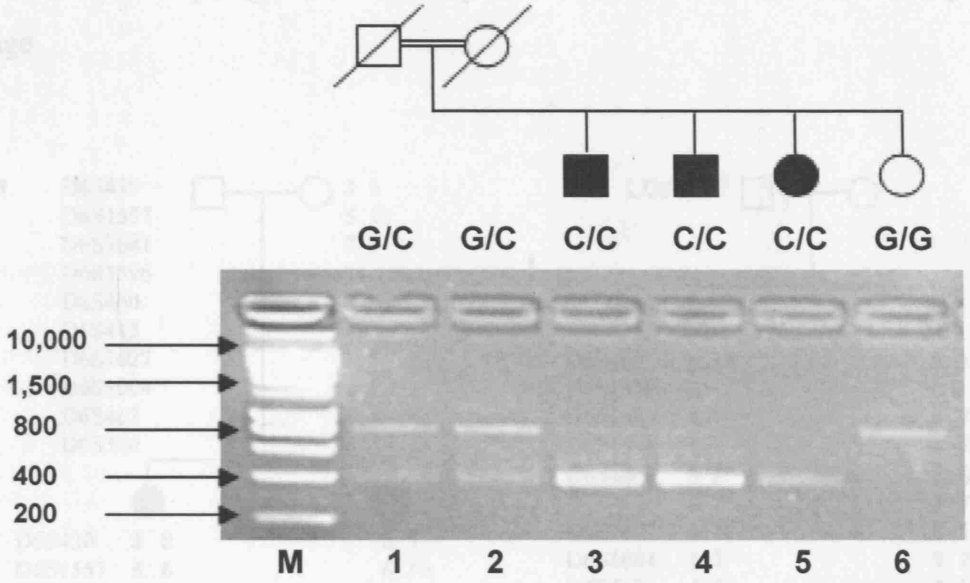

Figure 3.17 Cosegregation study of rs3734311 SNP in the RP5 family using *Msl* I restriction enzyme. Heterozygous parents (lanes 1 and 2) show partially digested products (773 and 385 bp) representing both the G/G and the C/C alleles. Lanes 3-5 (affected individuals) show a digested product (385 bp) depicting the wild type allele (C/C). Lane 6 shows a completely undigested product (773 bp) representing the mutant homozygous allele (G/G). M is a 10K smart ladder.

3.4.6 Linkage analysis of LCA families

Genotyping analysis of the 17 LCA families revealed that three of the studied families, LCA2, LCA7 and LCA14, could not be genetically excluded from the RP25 locus (Figures 3.18-3.21). Hence it is possible that these families could be LCA5 however, due to the small size of pedigrees it was not possible to achieve a LOD score compatible with linkage.

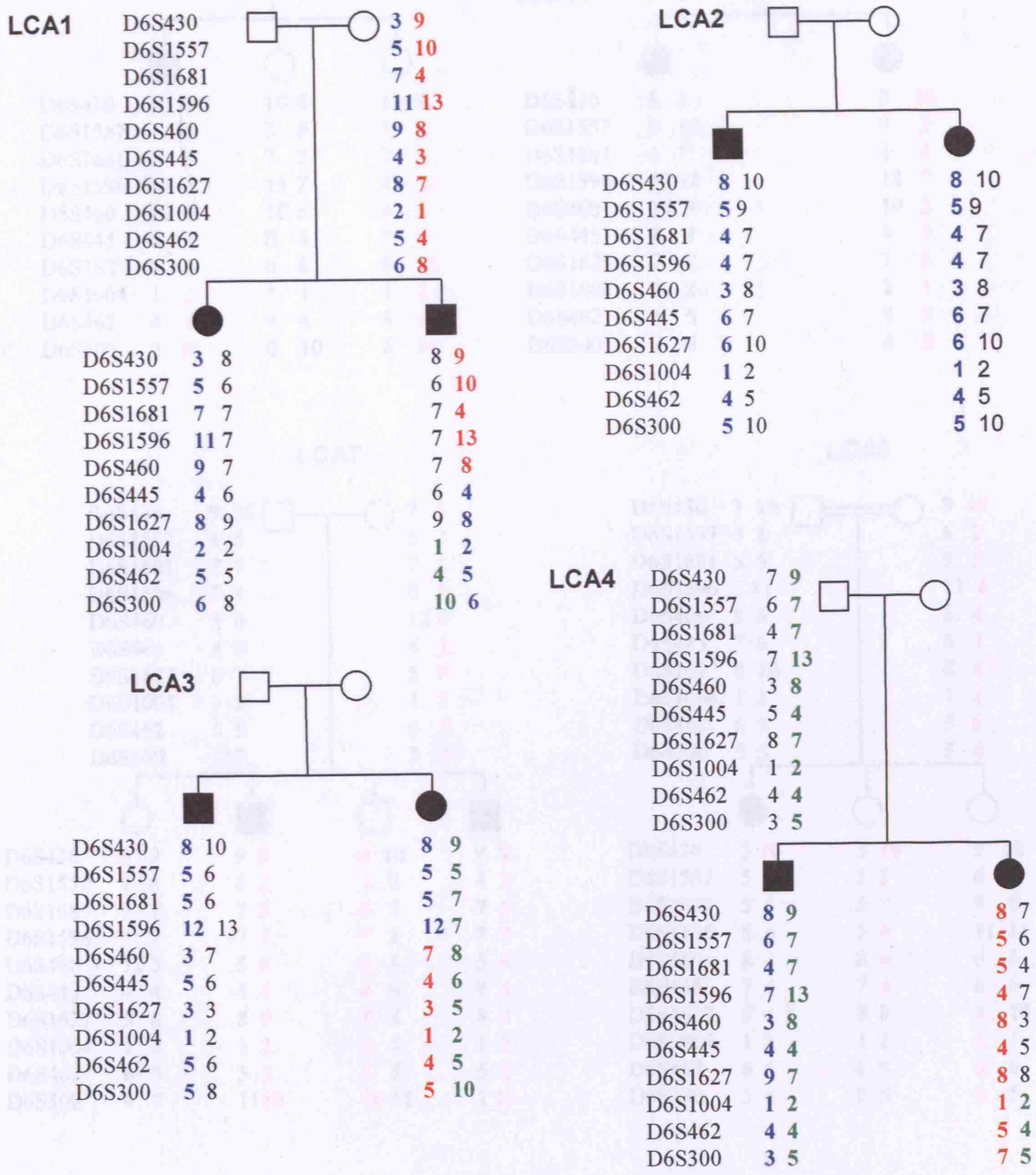

Figure 3.18 Genotyping of LCA families (1-4)

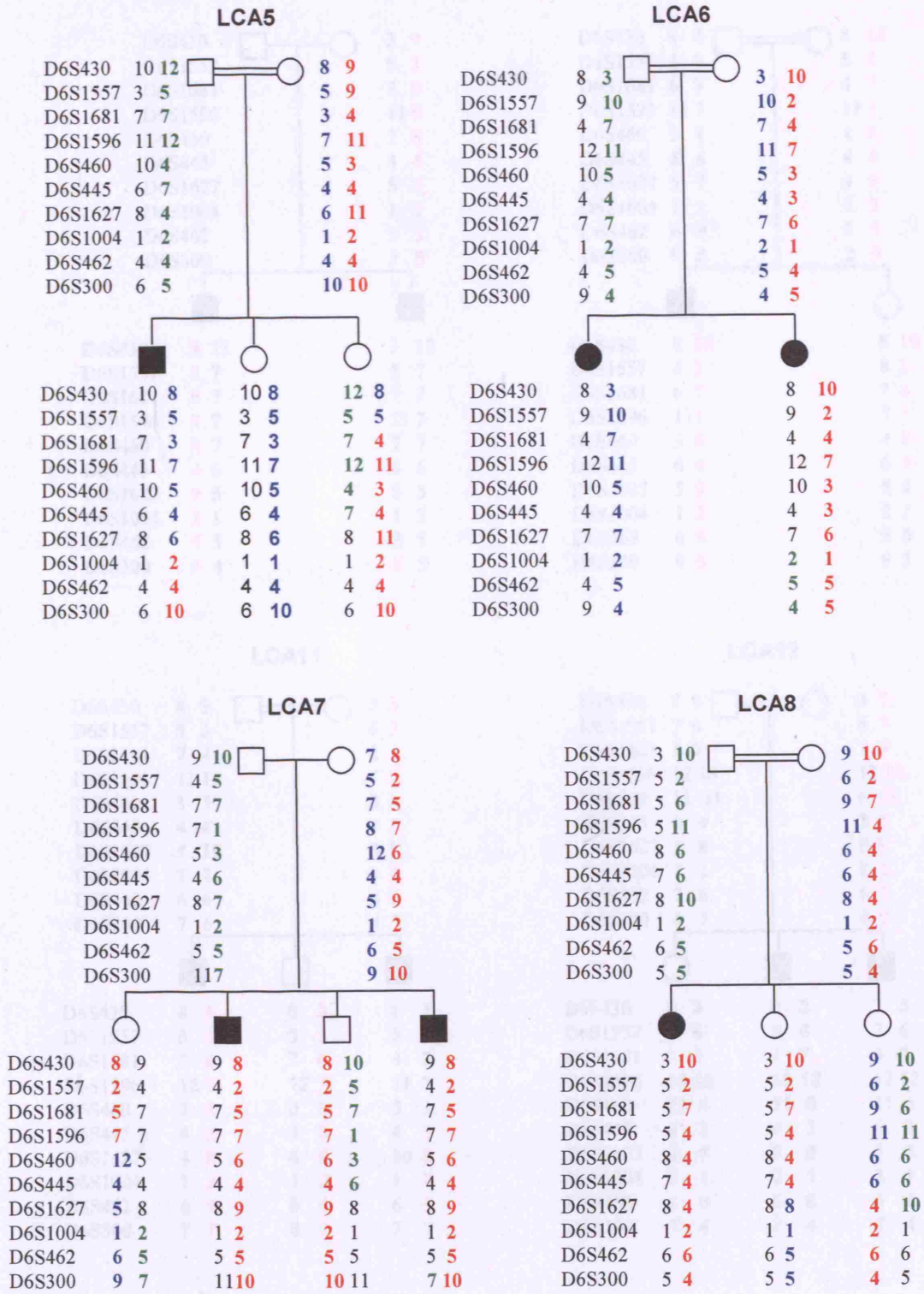

Figure 3.19 Genotyping of LCA families (5-8)

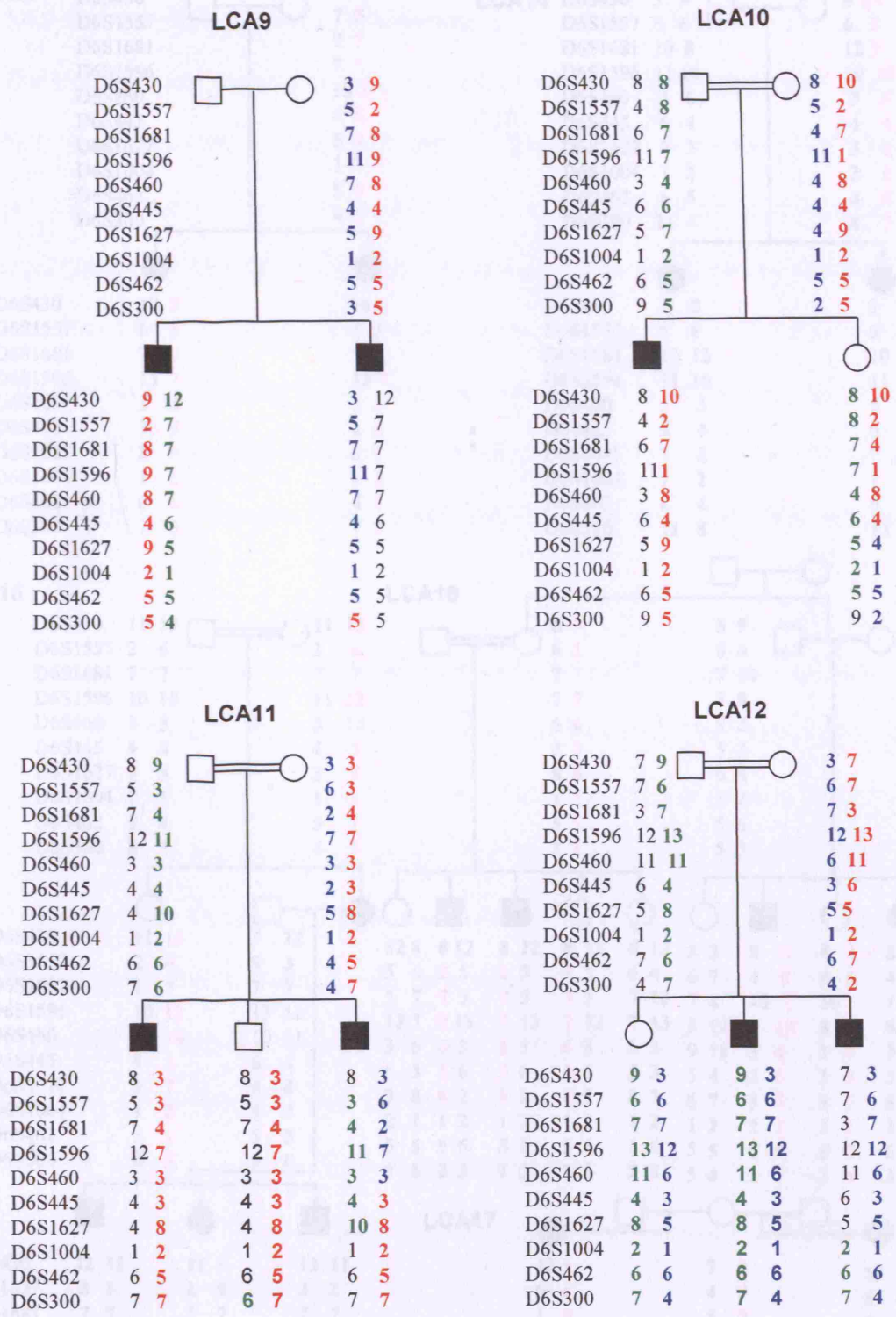

Figure 3.20 Genotyping of LCA families (9-12)

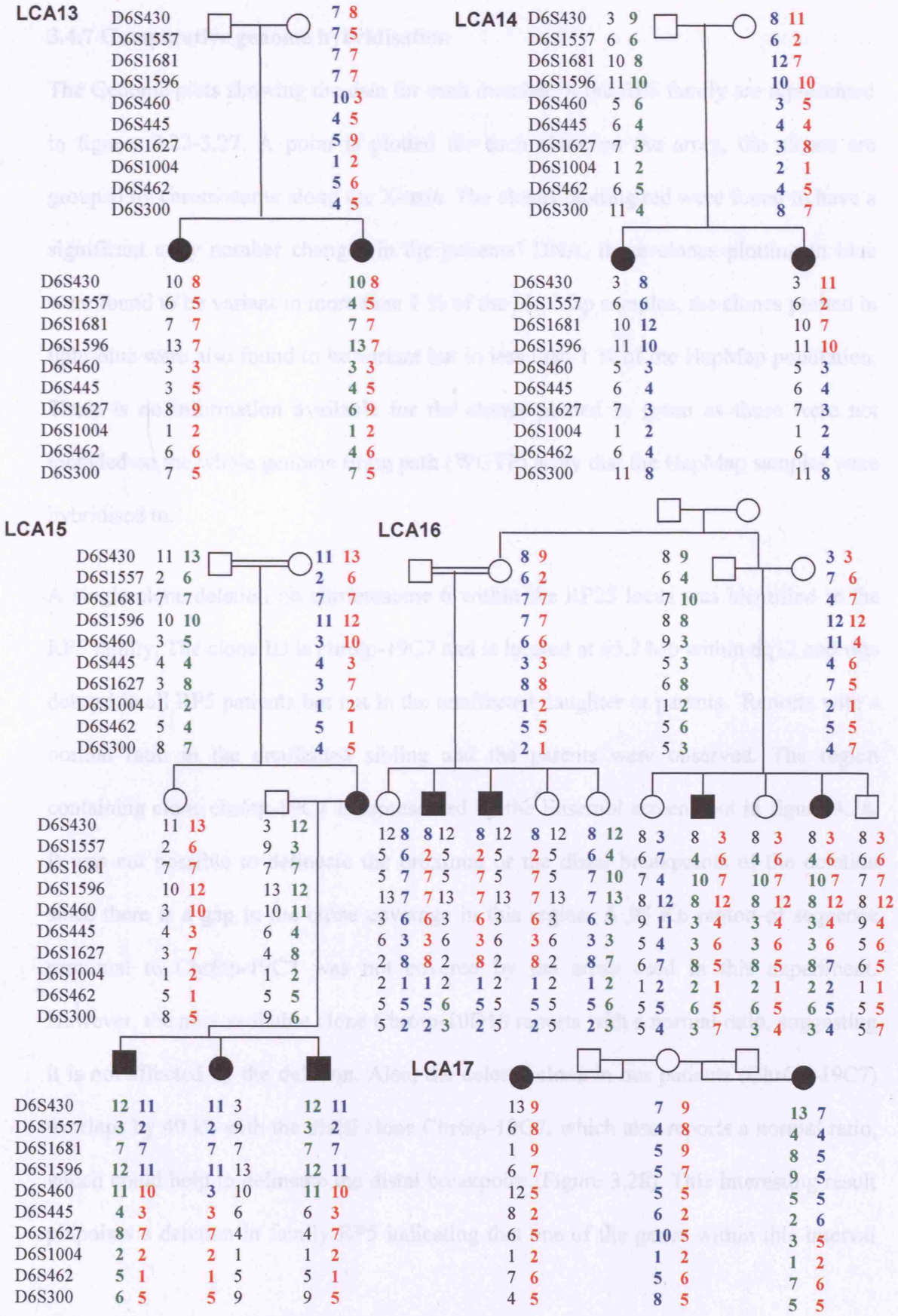

Figure 3.21 Genotyping of LCA families (13-17)

3.4.7 Comparative genome hybridisation

The Genome plots showing the data for each member of the RP5 family are represented in figures 3.22-3.27. A point is plotted for each clone on the array, the clones are grouped by chromosome along the X-axis. The clones plotting red were found to have a significant copy number changes in the patients' DNA, those clones plotting in blue were found to be variant in more than 1 % of the HapMap samples, the clones plotted in light blue were also found to be variant but in less than 1 % of the HapMap population. There is no information available for the clones plotted in green as these were not included on the whole genome tiling path (WGTP) array that the HapMap samples were hybridised to.

A single clone deletion on chromosome 6 within the RP25 locus was identified in the RP5 family. The clone ID is chr6tp-19C7 and is located at 65.7 Mb within 6q12 and was deleted in all RP5 patients but not in the unaffected daughter or parents. Reports with a normal ratio in the unaffected sibling and the parents were observed. The region containing clone chr6tp-19C7 is represented by the Ensembl screen shot in figure 3.28. It was not possible to delineate the proximal or the distal breakpoints of the deletion since there is a gap in the clone coverage in this region. A 95 Kb region of sequence proximal to Chr6tp-19C7 was not covered by the array used in this experiment. However, the next available clone Chr6tp-10D10 reports with a normal ratio, suggesting it is not affected by the deletion. Also, the deleted clone in our patients (Chr6tp-19C7) overlaps by 40 kb with the distal clone Chr6tp-10G7, which also reports a normal ratio, which could help to delineate the distal breakpoint (Figure 3.28). This interesting result pinpoints a deletion in family RP5 indicating that one of the genes within this interval

could be responsible for the RP25 phenotype. It is also possible that a nearby gene within the deleted interval is likely to be responsible for RP through a position effect. Six genes, *Q5T1H1*, *Q9H557_human*, *Q5TEL3_human*, *Q5TEL4*_human, *Q5VVG4_human* and *Q5T3C8*, are included within the deleted clone interval (Table 3.1). It is interesting to note that the above genes share a common epidermal growth factor (EGF-like) domain however they represent incomplete transcripts which is ranging between 1 to 4 exons with no defined ATG or stop codon. Additional work would therefore be required to fully characterise the above genes and to thoroughly screen them in the remaining RP25 families.

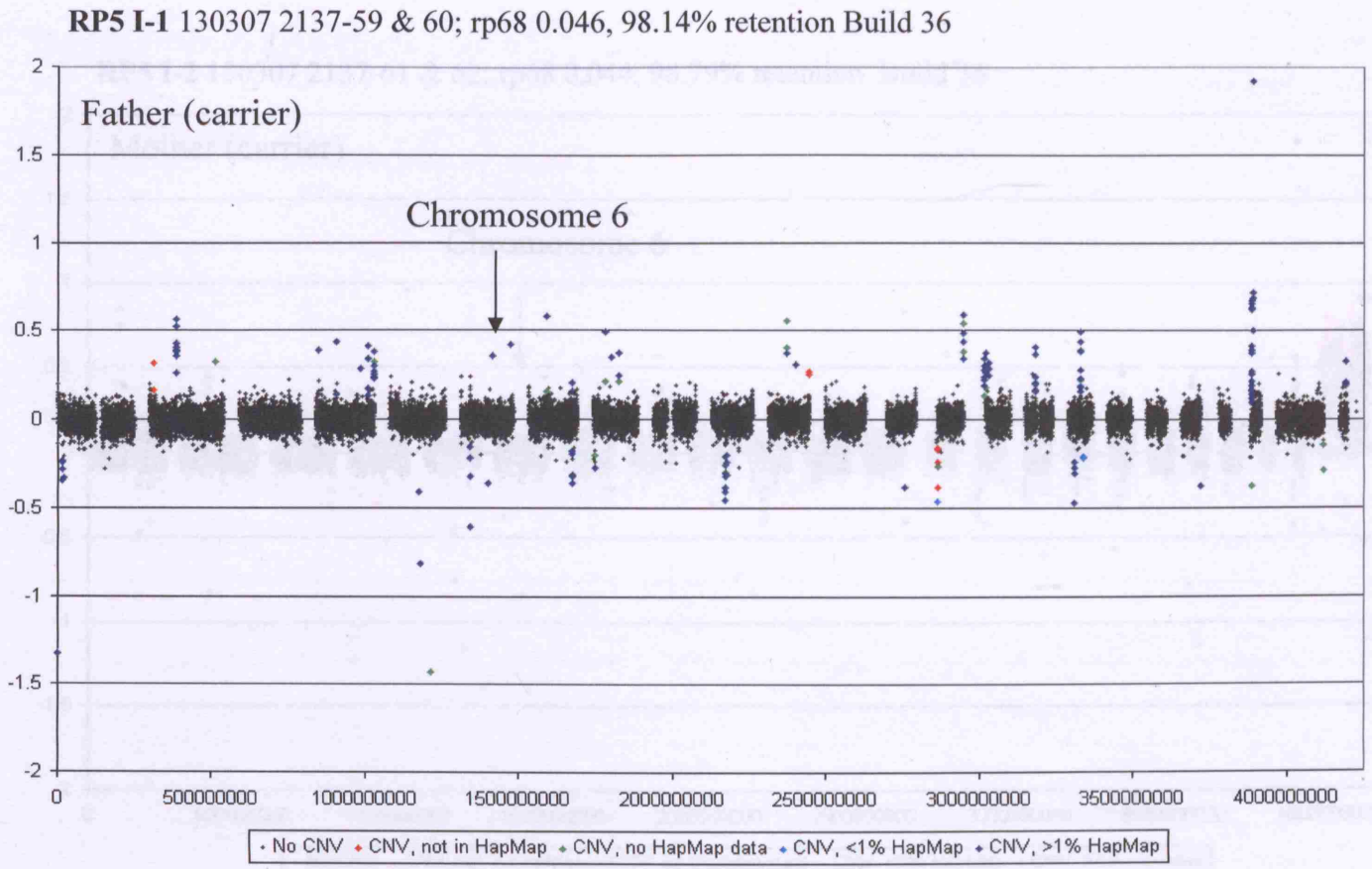

Figure 3.22 Genome plot using the CGH array on the RPI-1 member (Father) from the RP5 family. The log2 of the ratio of fluorescent intensities for each clone on the array is plotted chromosome by chromosome. The 68th percentile (rp68) of the absolute dye swap ratios for each chromosome is calculated as an estimation of the standard deviation (SD), the mean of these values gives the global rp68. The rp68 gives an indication of the quality of the array data; an experiment is rejected if the global rp68 value is greater than 0.06. A clone is called as having a copy number difference in the test compared to the reference DNA if the ratio is >6 x rp68 for an isolated clone or >4 x rp68 for consecutive clones. The clones with significant copy number difference are plotted in different colours on the genome profile. The deleted clone has a ratio of -0.201 in the father.

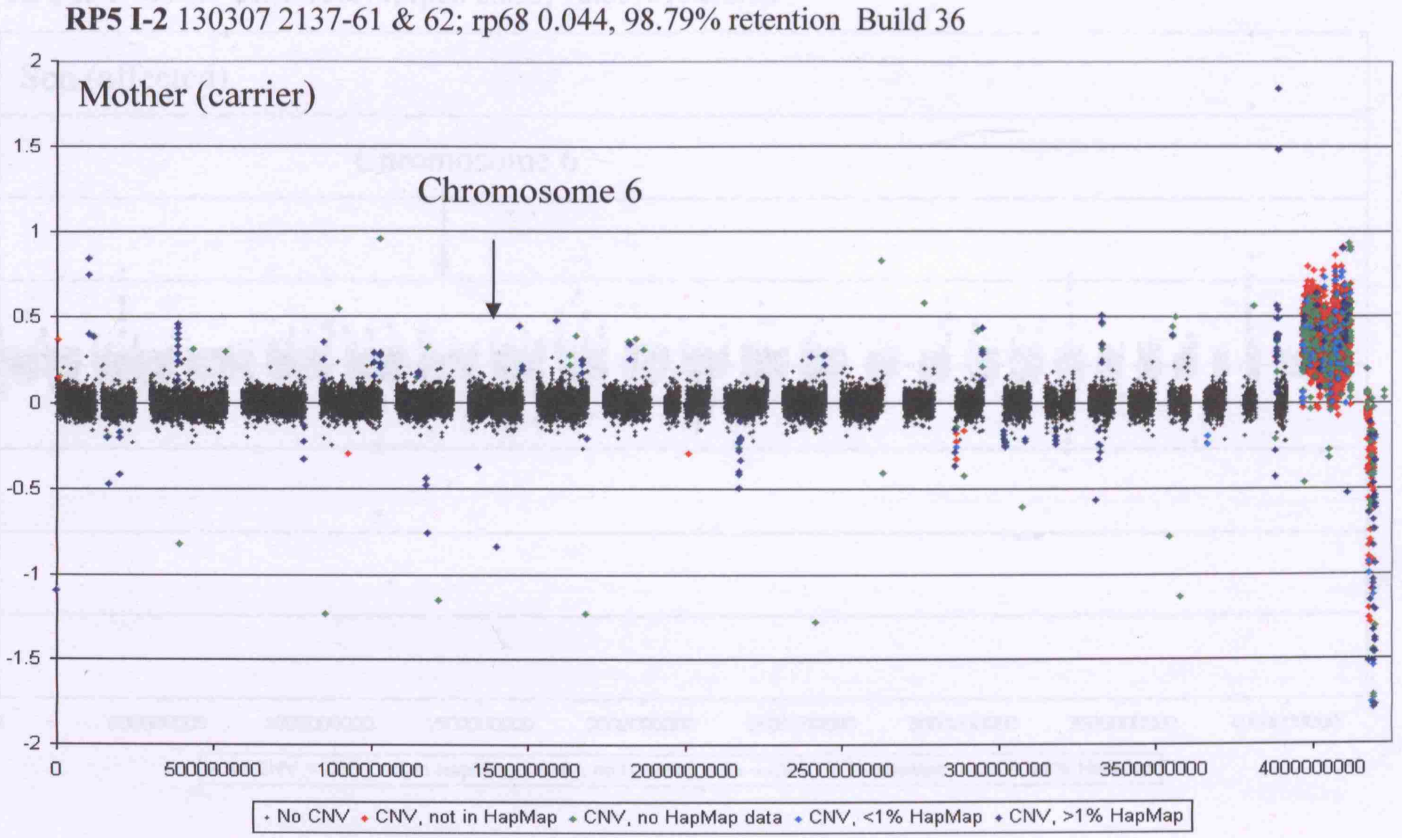

Figure 3.23 Genome plot using the CGH array on the RPII-2 member (Mother) from the RP5 family. The deleted clone has a ratio of -0.201 in the mother.

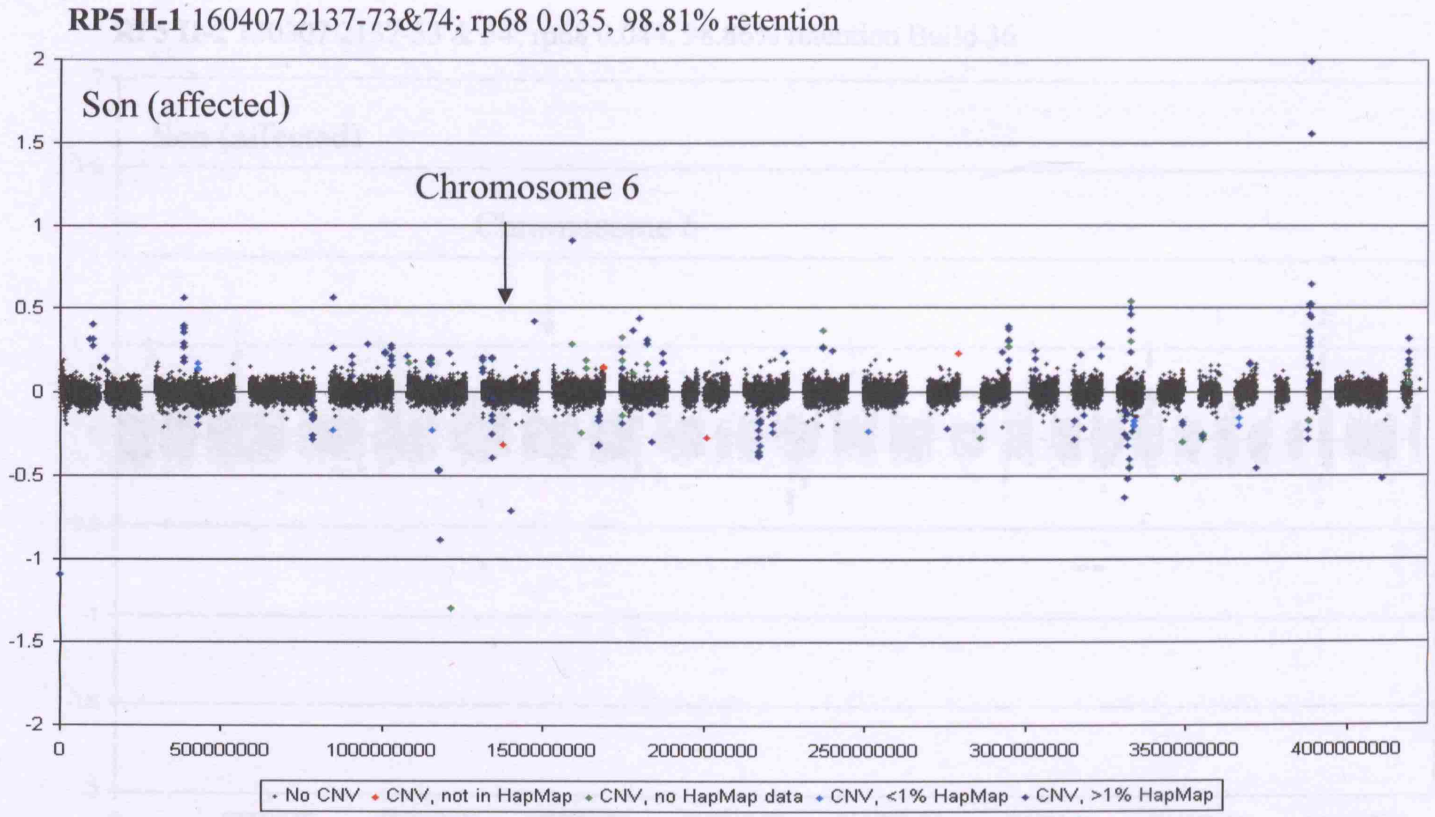

Figure 3.24 Genome plot using the CGH array on the RP5II-1 member (affected) from the RP5 family. The red dot indicates a CNV that does not exist in the HapMap. The deleted clone in chromosome 6 has a ratio of -0.307in this affected son.

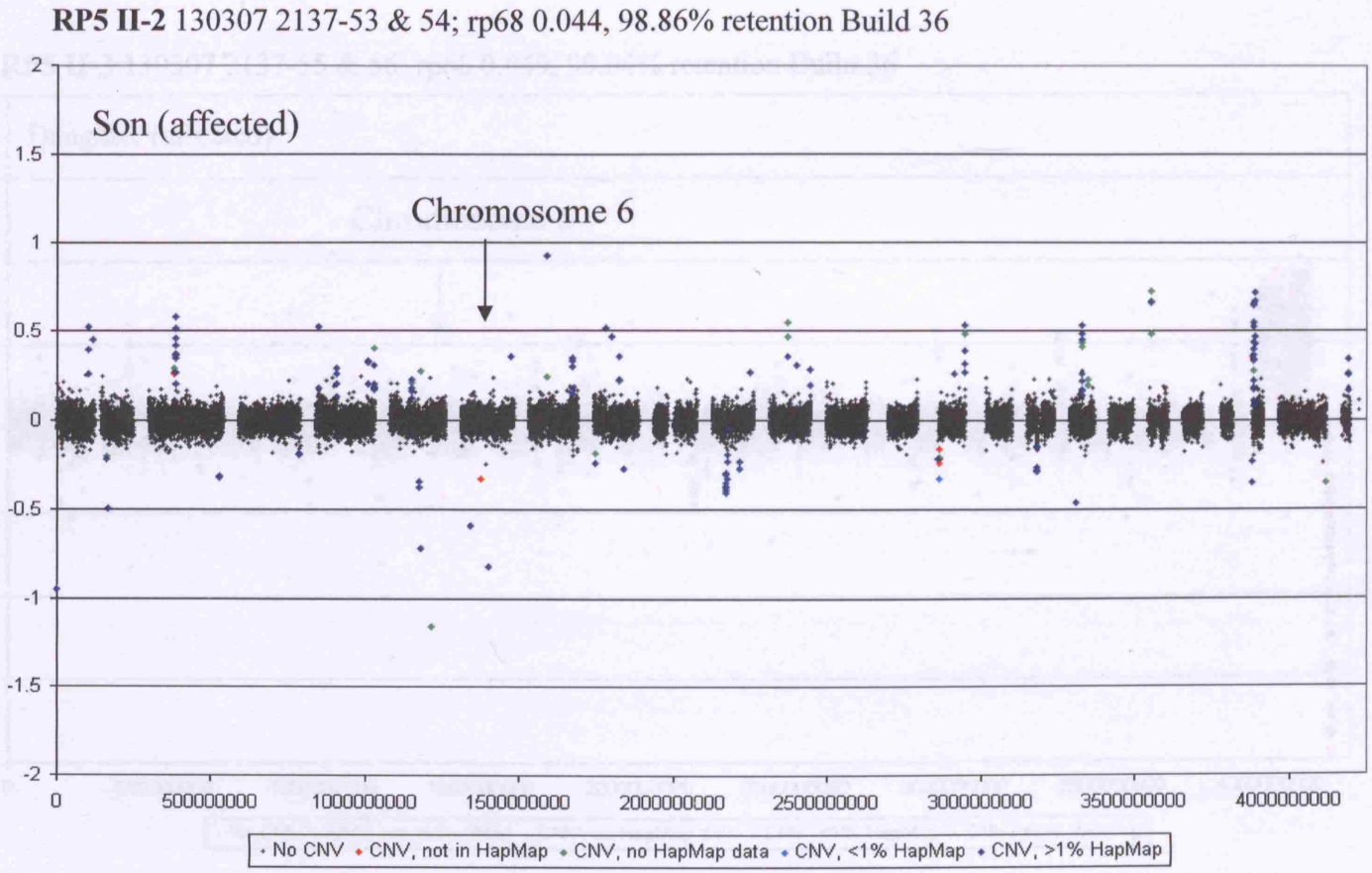

Figure 3.25 Genome plot using the CGH array on the affected RP5II-2 member of the RP5 family. The red dot indicates a CNV that does not exist in the HapMap. The deleted clone in chromosome 6 has a ratio of -0.327in this affected son.

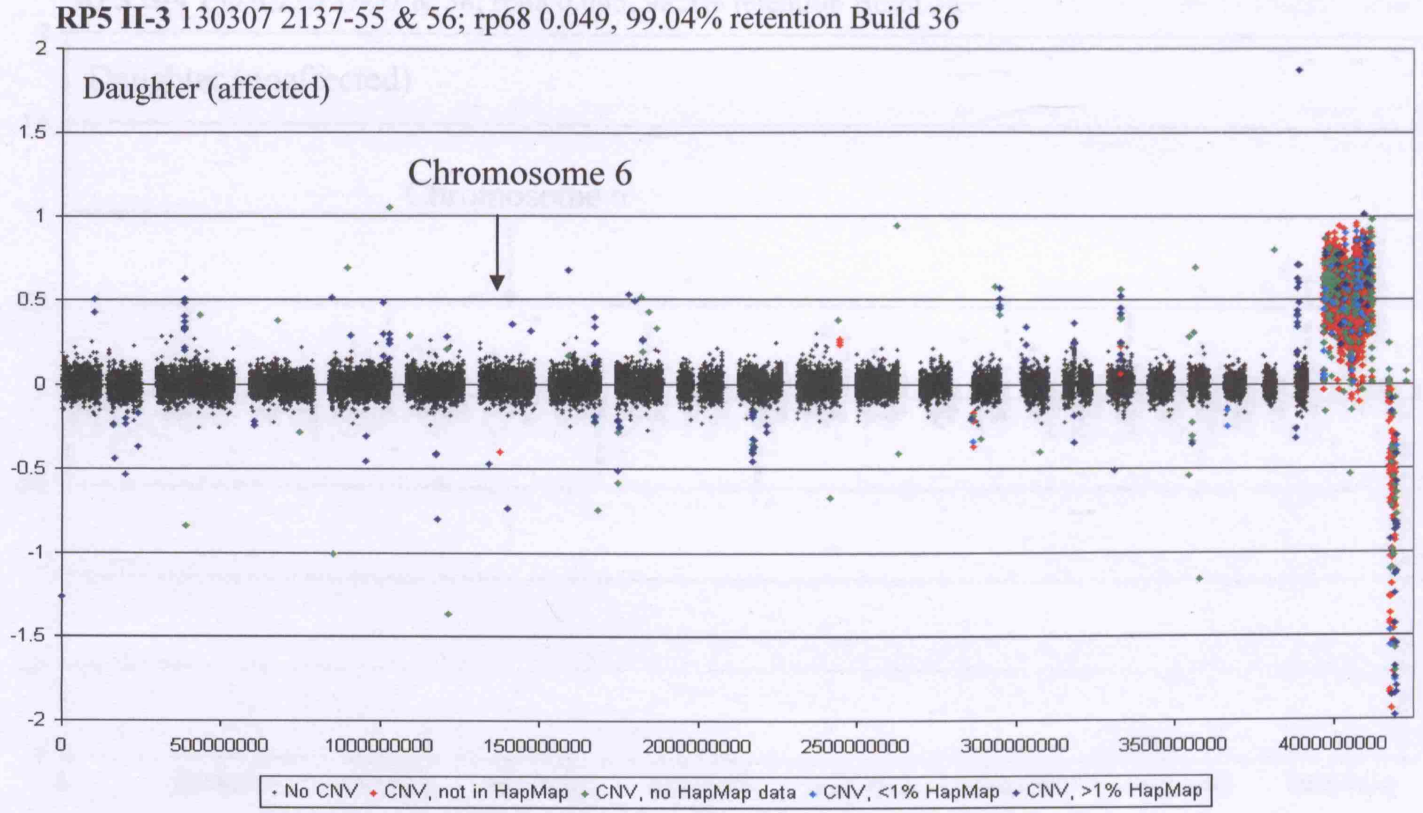

Figure 3.26 Genome plot using the CGH array on the affected RPII-3 member of the RP5 family. The red dot indicates a CNV that does not exist in the HapMap. The deleted clone in chromosome 6 has a ratio of -0.3995in this affected daughter.

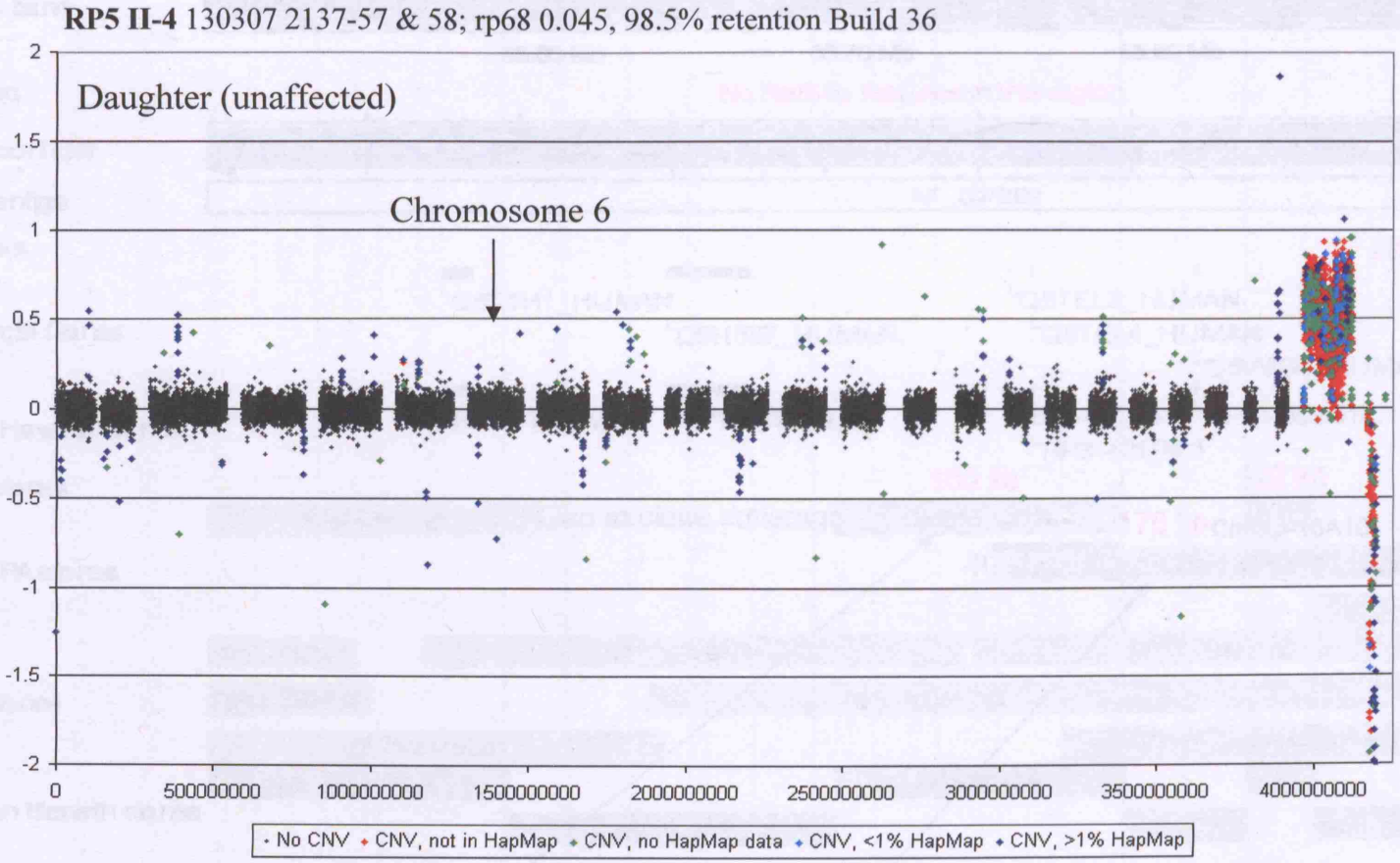

Figure 3.27 Genome plot using the CGH array on unaffected RPII-4 member of the RP5 family. The deleted clone in this daughter does not exist and it has normal ratio of 0.044.

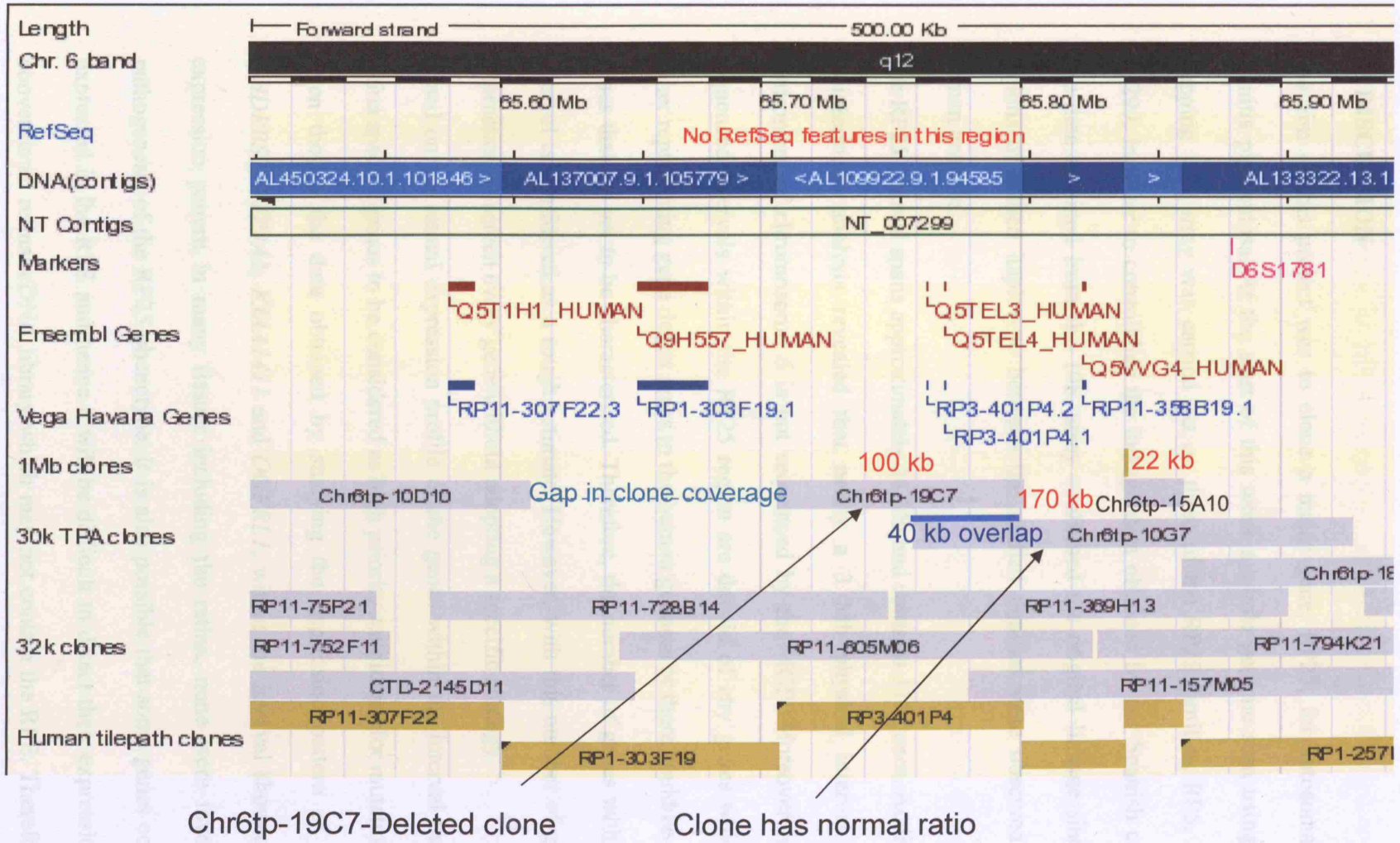

Figure 3.28 Ensembl view showing the deleted clone, the gap in the clone coverage and the overlap between the deleted clone and the distal clone (Ch6tp-10G7).

3.5 DISCUSSION

The aim of this project was to clone a major gene, RP25, for autosomal recessive retinitis pigmentosa. At the start of this work a whole genome scan using GeneChip mapping 10K array was carried out on three of the RP25 families, RP5, RP214 and RP299, in order to consolidate the linkage data obtained by our Spanish collaborates. The data obtained from the 10K array confirmed the original linkage since no other regions of shared haplotype between the studied families were observed across the human genome.

The RP25 interval spans approximately 34 Mb and contains 111 genes. Additionally, the bioinformatic analysis revealed that nearly a 3 Mb physical interval around the centromere of chromosome 6 is not sequenced by the HGP. Moreover, some of the sequenced intervals within the RP25 region are devoid of any genes which could be either representing gene desert areas in the human genome or there could be unpredicted genes that are yet to be characterised. Therefore, the number of genes within the RP25 interval is considered as a rough estimate. However, with this number of genes, it was impractical to screen every gene without adopting a specific strategy.

Based on the retinal expression profile of the genes within the interval there were no retina specific genes to be considered as high priority candidates for mutation screening. Even though the data obtained by studying the expression pattern of four genes, *KHDRBS2*, *PTP4A1*, *KIAA1411* and *OGFRL1*, within the interval showed ubiquitous expression pattern in many tissues including the retina, none were involved in the pathogenesis of the RP25 phenotype. It is also possible that some genes could be only expressed in the RPE and hence it will be difficult to detect their expression using the conventional retinal cDNA library which may not contain the RPE. Therefore studying

the expression pattern of the remaining genes within the RP25 interval was not considered while screening genes from the RP25 locus.

The positional and functional candidate gene approaches were both employed in order to clone the RP25 gene. The two strategies were overlapping each other throughout the project.

The positional approach was considered as an essential part of the strategy for selection of candidate genes. This is due to the presence of different linkage data from the Spanish families and from other families originating from different geographical regions. Based on the available genetic data (Figure 3.1) there was a possibility that either both the Pakistani family and 5 of our Spanish families had a common gene or that each population had a different RP gene linked to the RP25 interval. In view of the first hypothesis, the genes from the region between D6S257 and D6S1053 (Region A), where there is an overlap between the linkage data of both ethnic groups, were selected as good candidates (Figure 3.1).

Assuming that the disease gene in all Spanish families could be different from that for the Pakistani family and that all the Spanish families are sharing the same gene, all genes in-between D6S1557 and D6S421 markers (Region B) where all Spanish families are linked, were screened (Figure 3.1). In this case the search for the disease gene was based on the assumption that a separate and only one gene was responsible for the RP phenotype in the Spanish families. This is a possibility since all families came from the same geographical region. However, it is important to note that there is no shared haplotype between the Spanish families and therefore we expect different mutations within one gene to be responsible for the phenotype in different families.

A third possibility that cannot be ruled out is that there could be two separate genes responsible for the RP25 phenotype in the Spanish families. This is enforced by the fact that within region C (Figure 3.1) the linkage data for all the Spanish families are overlapping apart from one family (RP260). The same applies to region D downstream of microsatellite marker D6S460 where the linkage data of all families are overlapping apart from 2 families (RP214 and RP167). Therefore, it was mandatory to screen the genes between microsatellite markers D6S1053 and D6S1557 (Region C) since the linkage data for all the Spanish families except one (RP260) are overlapping together with the small number of genes within this interval in comparison to those within region D.

In the start of this project we also proposed that both RP25 and LCA5 could be allelic and that one gene could be responsible for the two phenotypes but with different types of mutations. It is likely that mutations in different sites cause different structural alterations in the predicted protein, predisposing to varying phenotypes (Rozet *et al.,* 1998). For example, *ABCR* gene has been reported as the gene responsible for both recessive Stargardt macular degeneration and arRP (Allikmets *et al.,* 1997; Martinez-Mir *et al.,* 1998). Similarly different mutations in the peripherin/RDS gene result in RP, macular dystrophy, cone rod dystrophy, pattern dystrophy, and central areolar choroidal dystrophy (Nichols *et al.,* 1993; Weleber *et al.,* 1993; Wells *et al.,* 1993; Nakazawa *et al.,*1994; Reig *et al.,* 1995; Kohl *et al.,* 1997). Moreover, LCA genes have been reported to be the cause for other retinal dystrophies. For example, *GUCY2D* mutations (LCA1) have been identified in autosomal dominant cone-rod dystrophy, (Kelsell *et al.,* 1998b) *RPE65* and *CRB1* mutations cause both arRP and LCA, (Morimura *et al.,* 1998; den Hollander *et al.,* 2001) and mutations in the *CRX* gene were reported to cause autosomal

dominant cone rod dystrophy, LCA, and late onset dominant RP (Sohocki *et al.,* 1998). Therefore, we recruited and genotyped 17 LCA families in order to identify LCA5 families which could lead to further refinement of the RP25 interval by identifying novel crossovers. However, due to the small size of the investigated families, a positive LOD score compatible with linkage could not be achieved. Interestingly, the gene for the LCA5 locus has been very recently reported (den Hollander *et al.,* 2007). It is important to note that the LCA5 gene (*Lebercillin*) has been screened for mutations in the RP25 families in the course of our project. However, a previously reported SNP but no pathogenic changes were observed within this gene and hence excluding it as responsible for the RP25 phenotype.

Functional candidate gene approach was also utilised to select genes for mutation screening in the Spanish families. This is based on the fact that a gene could demonstrate a functional relationship with the underlying defect (RP) or there could be human homologs of genes responsible for similar disease phenotype in other species. Alternatively, some genes might have been identified as members of a gene family of which other members have been implicated in a related disorder.

Two genes, *EEF1A1* and *C6orf165* were considered as the human orthologs for the protein that was shown to be expressed in the cilia of the *Trypanosome* proteome which made these genes excellent candidates (Broadhead *et al.,* 2006). It has been previously reported that successful transmission of several proteins from the cell body to the outer segment of the photoreceptor cells depends on transport along a modified cilium and that defective passage of certain molecules results in retinal degeneration associated with RP (Marszalek and Goldstein, 2000). For example, the BBS5 gene has been identified by comparative genomics based on the fact that the gene responsible for BBS should

encode proteins involved in basal body/flagellar assembly (Li *et al.,* 2004). Similarly, we screened *EEF1A1* and *C6orf165* genes based on the assumption that they both have a role in the maintenance of an integral cilia in the flagellated *Trypanosome*.

An excellent candidate gene for chromosome 6q linked retinopathies, *IMPG1*, has also been screened based on its chromosomal localisation and the potential role of IPM molecules in retinal adhesion and in the maintenance of photoreceptor polarisation, orientation, turnover and viability (Hageman *et al.,* 1991; Gehrig *et al.,* 1998). Screening *IMPG1* for mutations in STGD3, MCDR1, PBCRA, CORD7 and LCA5 revealed no sequence alterations (Gehrig *et al.,* 1998; Kelsell *et al.,* 1998a; Dharmaraj *et al.,* 2000). However, mutation screening of *IMPG1* in BCAMD patients revealed L579P amino acid substitution, which may play a causal role (van Lith-Verboeven *et al.,* 2004). Thus, to understand the role of IPM in the normal and diseased human retina it was crucial to screen *IMPG1* in the RP25 families. However, the data obtained ruled out involvement of this gene in the pathogenesis of the RP25 phenotype.

Additionally, we have utilised highly efficient genetic databases in order to identify functional candidates. For example the data obtained from the *EyeSAGE* website revealed that 14 genes within the RP25 locus are considered as good candidates according to their level of expression in the retina and RPE in comparison to other tissues (Figure 3.1). Even though these genes were part of the high priority group of genes to be screened according to the genetic data, considering their functional role made them excellent candidate. Additionally, 7 genes, *COL19A1*, *OGFRL1*, *IMPG1*, *CF152*, *ELOVL4*, *NT5E* and *CNR*, were also considered as good candidates according to their level of expression in the *rd* mouse. Therefore, screening the genes within the

RP25 interval was dependant on combining both the genetic and functional information about the genes in the interval.

Since this project was carried out in collaboration with our colleagues from Seville, Spain, mutation screening of the genes within the interval was shared between the two groups. At the time of writing up this thesis 61 out of 111 genes were screened for mutations and excluded as disease causing by direct sequencing analysis of at least a DNA sample from one affected member from each of the Spanish families. This is corresponding to 55 % of the genes from the interval. Throughout screening the genes, a large number of SNPs of which a significant proportion was novel were identified.

Herein, 25 genes have been screened in which 137 SNPs were identified, of which 44 were novel. Out of the 44 SNPs only 3 were considered as significant changes in terms of segregation with the disease phenotype. Even though these changes were not observed in 200 control chromosomes, they were not considered as pathogenic. This is because they have been observed either in non-consanguineous families where a second change is necessary to explain their role as disease causing genes or in a consanguineous family but the change did not affect the structure of the protein.

In any of the studied genes all the identified SNPs were segregating with the genetic data apart from one gene, *PRIM2A*, where heterozygous SNPs were observed within a stretch of homozygosity in the affected members of two families (RP5 and RP214; consanguineous). Even though this is in controversy to the linkage data it is only acceptable in this case since a second copy of the gene was discovered to be existing within that interval. Therefore it is possible that the primers amplified the nucleotide sequence of the two copies of the gene at the same time. Additionally it is possible that in one of the copies at a specific nucleotide position a sequence of TT exist however, in

the second copy at the same position the nucleotide sequence could be AA. Therefore by amplifying the two fragments the outcome will be observing the two strands of the DNA on top of each other due to the double amplification which could explain the heterozygsity of some of the SNPs in the affected members of consanguineous families. The observation of such changes had stimulated us to investigate the possibility of CNVs existing in our families which could have an impact on the phenotype of the RP25 families. It has been postulated that CNVs could have a direct effect on transcription regulation which in turn may be a cause for disease susceptibility and phenotypic variation (Redon *et al.,* 2006). Hence, in collaboration with Sanger Centre, six samples belonging to one of the consanguineous families (RP5) were subjected to the CGH array. The data obtained reveled that a clone within the RP25 locus was deleted in all the affected members of this family. However, it was completely normal in the unaffected daughter and reduced in case of the parents. The data obtained from CGH denoted that further investigation is required to identify the boundaries of the deleted clone and to prove or decline its association with the disease phenotype in this family.

In summary our 10K array data revealed that the studied families are linked to the RP25 locus since no other loci with shared haplotype were observed elsewhere in the human genome. The assumption of one gene responsible for both RP25 and LCA5 phenotypes is now ruled out since the gene for LCA5 has been identified. The strategies used for mutation screening of the genes within the interval were in a systematic way. To date ~ 55 % of the genes in the interval are excluded as causative for the pathogenesis of the RP25 phenotype. Whenever, a SNP was observed, a thorough investigation of its association with the disease was carried out. The data obtained from the CGH array are

exciting and future work will involve identifying the boundaries of the deleted clone in the RP5 family which may represent part of a gene within the interval. Hence, this deletion could have a deleterious effect on the protein structure encoding the gene. Full characterisation of six genes, *Q5T1H1*, *Q9H557_human*, *Q5TEL3_human*, *Q5TEL4*_human, *Q5VVG4_human* and Q5T3C8, within this refined interval will be performed. Additionally, mutation screening of the above genes will be carried out for the remaining RP25 families.

3.6 FUTURE WORK

Future work on the RP25 locus will involve thorough mutation screening of the 6 genes (see section 3.4.7) located within the genetic interval refined by the deleted clone identified in the RP5 family. If this proves involvement of any of those genes in the pathogenesis of the RP25 families, additional work would be required to fully characterise the causative gene. This will be followed by further identification of other pathogenic changes in the remaining RP25 and Chinese families. Also, mutation screening of an extensive panel of recessive RP patients will be performed in order to determine the frequency and types of mutations causing the disease.

Functional analysis of the protein will be the next step, which will involve identification of biologically important conserved domains by comparison of complete cDNA and genomic sequences in other species (e.g. mouse, bovine and chicken). Homologous genes elsewhere in the human genome will also be searched for by Southern blotting using low stringency probings, which may lead to the cloning of genes from other loci that may serve as candidates for future RP research.

Tissue specific expression pattern of the identified gene will also be undertaken by both Northern blot analysis and tissue in-situ hybridisation. Studies of the wild-type and mutant protein products will be conducted in-vitro to understand their biochemical role as appropriate.

A detailed and comprehensive biochemical analysis will be instigated. Such a study is necessary to address the query about the underlying genetic mechanisms associated with many retinal degenerations: is it the lack of the enzymatic activity/protein function that leads to degeneration or is it the loss of protein structure which elicits the degenerative

response? To address these possibilities we will express the identified gene as a recombinant protein using an appropriate expression system.

If an expressed protein is an enzyme, it will be subjected to thorough kinetic investigation such that, values for kcat and km will be ascertained over a wide pH range. A similar profile will be obtained for the mutated protein which will identify any effect that the mutation could have on its activity. With regards to the effect of the mutation on the structure of the protein, we initially plan to analyse the "wild type" and mutant protein by circular dichroism (CD) spectroscopy. This technique has the potential to identify not only gross changes in the secondary structure of the protein by studying of the far UV-CD but can also detect more subtle environmental changes in the aromatic side chains of the Phe, Tyr and Trp by a study of the near UV-CD (Siligardi and Drake, 1995). Other physical properties of the protein including its thermal stability and susceptibility to proteolysis will be also investigated. As a part of our long-term goal the protein will be used in crystallisation trials in order to ascertain the exact molecular effect of the mutation.

We could also make use of the in-vitro expression systems to express the normal and the mutant proteins to understand their biological function and interrelation with each other and with other proteins similar to what has been carried out for rhodopsin mutations (Sung *et al.,* 1993, 1994). Once we know the function of the disease gene we could formulate a hypothesis as to how the mutations in the gene can lead to the disease.

Since RP25 is of recessive inheritance, the disease phenotype is probably due to a 'Null allele'. Therefore in the long term 'knock out' animal models may be generated using gene targeting in mouse embryonic stem cells and mutations will be introduced at the actual gene locus by homologous recombination (for example Kim *et al.,* 1998). 'Null

allele' or haplo-insufficiency phenotypes could also be created by gene targeting (Humphries *et al.,* 1997). Retinal development and physiology could then be studied in detail in these animals to determine the primary defect in each case. Such animal models would also provide ideal tool for testing potential drug or environmental therapies and could be used in experiments on gene therapy based on antisense RNA or over expression of the normal product (for review see Gibson and Shillitoe, 1997; Pepose and Leib, 1994).

CHAPTER FOUR

A NOVEL GENETIC STUDY OF CHINESE FAMILIES WITH ARRP

4.1 Introduction

4.1.1 Loci identified for autosomal recessive retinitis pigmentosa

To date, 24 loci have been implicated in the pathogenesis of arRP (http://www.sph.uth.tmc.edu/retnet/). The genes for five of these loci (RP22, RP25, RP28, RP29 and RP32), still remain to be identified (Finckh *et al.,* 1998; Ruiz *et al.,* 1998; Gu *et al.,* 1999; Hameed *et al.* 2001; Zhang *et al.,* 2005). Due to this large number of loci it is challenging to identify the gene mutation responsible for arRP in newly ascertained patients. Moreover, it is anticipated that many genes are yet to be identified since known loci cannot explain all cases of recessive RP. Based on the observed prevalence of 1-5% for each of the arRP loci found so far (Tuson *et al.,* 2004), searching for a novel gene that may account for a significant proportion of recessive families will be a major achievement in retinal degeneration genetics.

4.1.2 Homozygosity mapping

Traditionally, homozygosity mapping has been the basis for genetic mapping of recessive traits using either a set of 300-400 microsatellite markers or the high-density SNPs (Botstein and Risch, 2003; Daly *et al.,* 2001) and more recently the 10K GeneChip Array (Affymetrix, Inc., Santa Clara, CA). This method proved to be effective in cases of consanguineous families where the regions adjacent to the disease loci are likely to be homozygous by descent (Lander and Botstein, 1987; Sheffield *et al.,* 1998). However, this is not the ideal approach in targeting the mutant gene in non-consanguineous

families since the possibility of having compound heterozygosity exists (Kondo *et al.*, 2004). Additionally, mutation screening of the previously identified genes in such families particularly in genetically heterogeneous disorders is time consuming and costly.

Therefore, in this study a systematic method for identifying the disease locus in small non-consanguineous arRP families has been implemented (Figure 4.1). Initially, direct mutation screening or SNPs/microsatellite marker analyses approach have been used for linkage testing of the known recessive RP genes/loci. This was followed by a whole genome scan in all families using the 10K GeneChip Mapping Array in order to identify common regions of shared haplotype on both chromosomes. Whenever more than one region of shared haplotype was observed in all families, we undertook detailed microsatellite marker analysis and pooled the data. Pooling of the linkage data was built on the fact that all families were anticipated to be genetically homogenous. This was followed by an evaluation of suitable candidate genes within the regions of shared haplotype. For example, visual system homeobox 1 homolog (*VSX1*) gene was located in the vicinity of an interval that showed evidence of linkage in our families and is known to be expressed in the bipolar cells of the retinal inner nuclear layer (Hayashi *et al.*, 2000). Hence, it was mandatory to screen this gene for mutations in the families studied.

This proposed approach could be a useful tool for genetic mapping in cases of rare and genetically heterogeneous recessive traits. Subsequently, this will help in revealing the underlying genetic defect of such disorders.

4.2 AIM OF THE STUDY

To identify the disease locus in small non-consanguineous Chinese families with arRP

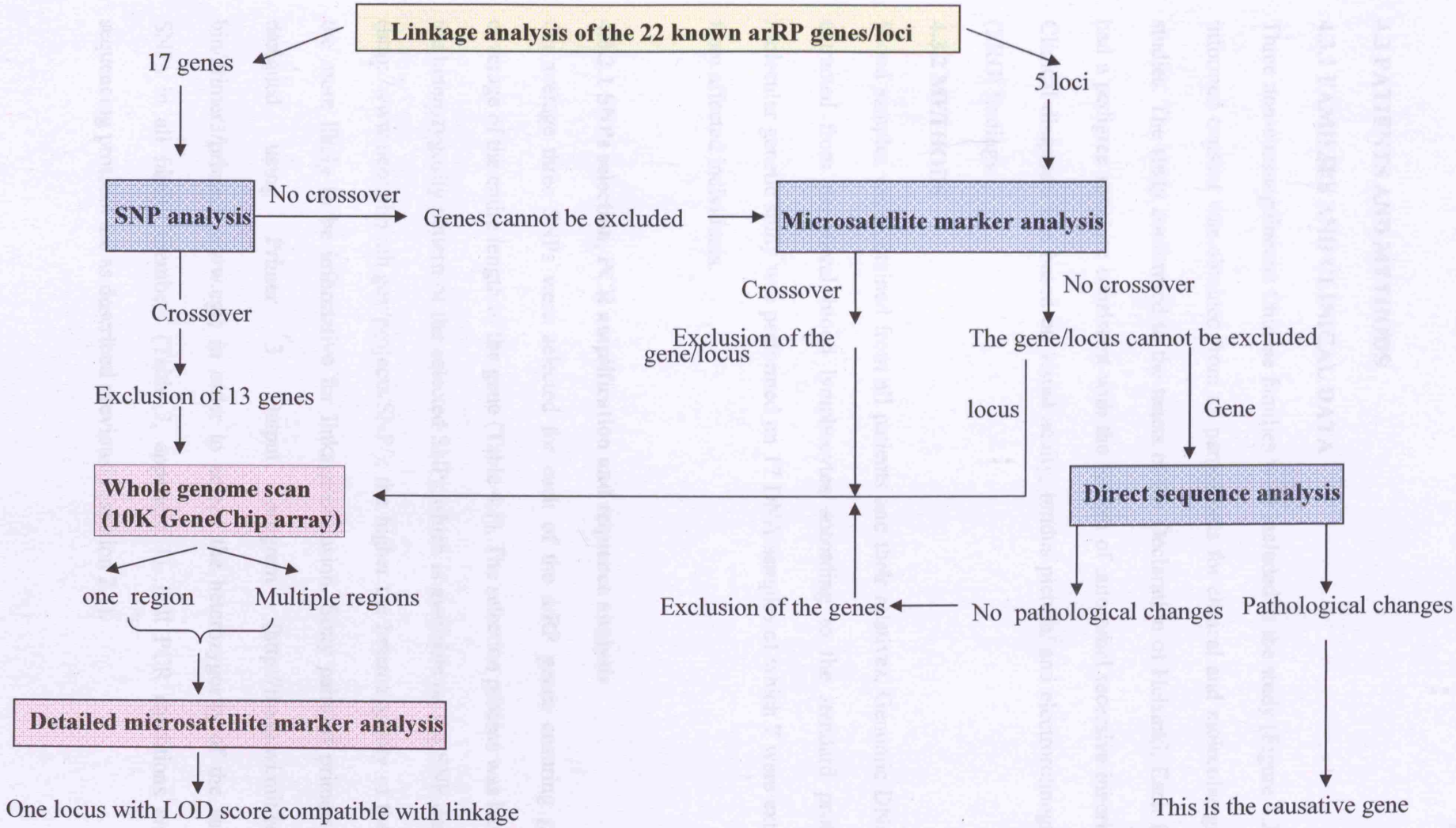

Figure 4.1: A flow chart describing our strategy for identifying the disease locus in autosomal recessive nuclear non consanguineous families

4.3 PATIENTS AND METHODS

4.3.1 FAMILIES AND CLINICAL DATA

Three non-consanguineous Chinese families were included in the study (Figure 4.2). An informed consent was obtained from all participants for clinical and molecular genetic studies. The study conformed to the tenets of the Declaration of Helsinki. Each family had a pedigree structure consistent with the pattern of autosomal recessive inheritance. Clinical diagnosis was based on visual acuity, fundus picture, and electroretinographic (ERG) findings.

4.3.2 METHODS

Blood samples were obtained from all patients and their relatives. Genomic DNA was extracted from peripheral blood lymphocytes according to the standard protocols. Molecular genetic study was performed on 17 DNA samples of which 7 were extracted from affected individuals.

4.3.2.1 SNPs selection, PCR amplification and sequence analysis

On average three SNPs were selected for each of the arRP genes ensuring genetic coverage of the entire length of the gene (Table 4.1). The selection process was based on the heterozygosity pattern of the selected SNPs which is available on the SNP database (http://www.ncbi.nlm.nih.gov/projects/SNP/); the higher the heterozygosity of the SNP the more likely to be informative for linkage/exclusion. Sixty pairs of primers were designed using Primer 3 Output program (http://frodo.wi.mit.edu/cgi bin/primer3/primer3_www.cgi) in order to screen the heterozygosity of the selected SNPs in all family members (Table 3, appendix 1). Full PCR conditions and the sequencing protocol are as described previously (section 2.4).

Family 10

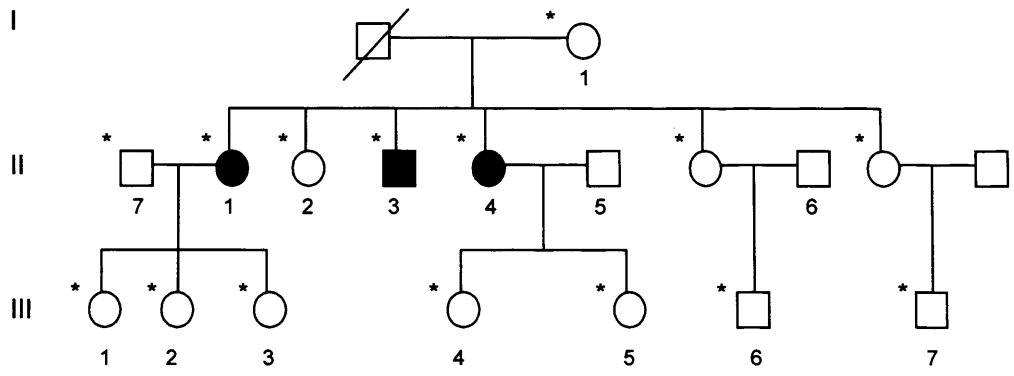

Family 112

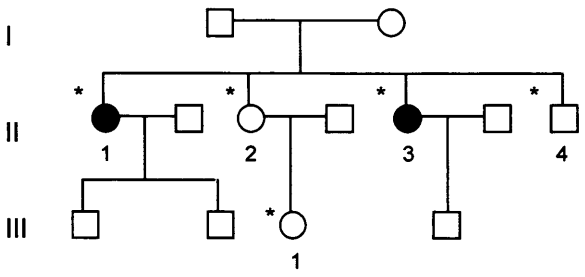

Family 116

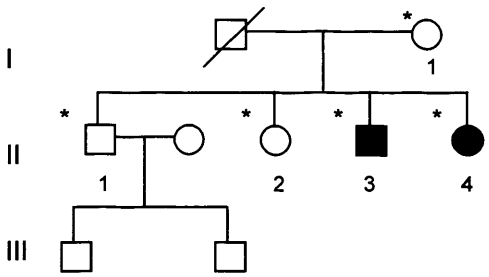

Figure 4.2 Pedigrees of the families participating in the study. Open and closed symbols denote unaffected and affected individuals, respectively. Deceased family members are denoted by diagonal slashes. Individuals examined both clinically and genetically are marked by asterisks.

Table 4.1 SNPs/microsatellite markers (msm_s) used for studying the known arRP loci in families 10 (I-1 and II-1 to II-6), 112 (II-1 to II-4) and 116 (I-1 and II-1 to II-4). Affected members in each family are underlined and in bold. Boxes marked with diagonal slashes denote the genes and the corresponding families that could not be excluded by this method. Alleles that are different across the affected individuals are underlined

Gene name	Gene size (Kb) /no. of exons /position (Mb)	SNPs/ msm_s	SNPs/ msm_s Position (Mb)	I-1 /10	**II-1** /10	II-2 /10	**II-3** /10	**II-4** /10	II-5 /10	II-6 /10	**II-1** /112	II-2 /112	**II-3** /112	II-4 /112	I-1 /116	II-1 /116	II-2 /116	**II-3** /116	**II-4** /116
1. *ABCA4*	128.30/50 /94.23-94.35	D1S2868	93.10	4/4	3/4	4/4	4/4	3/4	3/4	3/4	3/4	3/4	4/4	3/4	2/2	2/3	2/2	2/2	2/3
		D1S2849	93.30	2/4	4/4	2/2	2/4	2/4	2/4	2/4	2/4	2/2	2/2	2/4	1/2	2/3	1/2	1/2	1/3
		rs3945204	94.20	1/1	1/1	1/1	1/1	1/1	1/1	1/1	1/1	1/2	1/1	1/1	1/1	1/1	1/1	1/1	1/1
		rs1191231	94.28	1/1	1/1	1/1	1/1	1/1	1/1	1/1	1/1	1/1	1/1	1/1	1/1	1/1	1/1	1/1	1/1
		rs2151848	94.31	1/2	1/1	1/2	1/1	1/2	1/1	1/2	1/2	1/1	1/2	1/1	1/2	1/1	2/2	2/2	1/2
		D1S2819	95.30	2/3	2/3	2/4	2/3	2/2	3/3	2/2	2/2	2/2	1/2	2/2	1/2	1/1	2/2	2/2	2/2
2. *CRB1*	210.18/12 /195.5-195.7	D1S2816	194.9	1/3	1/1	1/3	1/3	1/1	1/3	1/3	1/4	2/4	2/4	1/4	1/3	1/3	1/4	1/3	1/4
		rs3790380	195.5	1/1	1/1	1/1	1/1	1/1	1/1	1/1	1/1	1/1	1/1	1/1	1/2	1/2	1/2	1/1	1/2
		rs949571	195.6	1/2	1/1	1/1	2/2	1/1	1/1	1/1	1/1	1/1	1/2	1/2	1/1	1/1	1/1	1/1	1/1
		rs1345529	195.7	1/1	1/1	1/1	1/1	1/1	1/1	1/1	1/2	1/2	1/2	1/2	1/1	1/2	1/2	1/2	1/2
		D1S413	196.9	1/2	1/1	1/4	1/2	1/1	1/4	1/4	1/3	1/3	2/2	2/2	1/5	1/5	4/5	1/5	¼
3. *CNGA1*	16.28/8 /47.63-47.67	rs1012844	47.64	1/2	1/2	1/1	1/2	1/1	1/1	1/2	1/1	1/1	1/1	1/1	1/1	1/1	1/1	1/1	1/1
		rs1440224	47.65	1/1	1/1	1/1	1/1	1/1	1/1	1/1	1/1	1/1	1/2	1/1	1/1	1/1	1/1	1/1	1/1
		rs1371729	47.65	1/1	1/1	1/1	1/1	1/1	1/1	1/1	1/1	1/1	1/1	1/1	1/2	1/1	1/2	1/2	1/1
		rs1371732	47.66	1/1	1/1	1/1	1/1	1/1	1/1	1/1	1/1	1/1	1/1	1/1	1/2	1/1	1/2	1/2	2/2
		rs4695318	47.67	1/1	1/2	1/2	1/2	1/1	1/2	1/1	1/1	1/1	1/2	1/1	1/1	1/1	1/2	1/1	1/1
		D4S3002	48.3	2/4	2/3	2/4	2/3	2/2	2/2	2/3	2/2	2/2	2/3	2/2	1/3	1/1	1/1	1/3	1/1
4. *CERKL*	118.82/13 /182.1-182.23	D2S2310	181.87	3/4	3/3	3/3	3/3	3/4	3/4	3/4	1/2	1/2	1/2	1/2	2/2	2/3	2/3	2/3	2/3
		rs1047307	182.11	1/1	1/2	1/2	1/2	1/2	1/2	1/2	1/2	1/2	1/2	1/1	1/2	1/2	1/2	1/1	1/1
		rs763860	182.13	1/1	1/1	1/1	1/1	1/2	1/2	1/1	1/2	1/2	1/2	1/2	1/1	1/2	1/1	1/2	1/2
		rs6433926	182.18	1/1	1/1	1/1	1/1	1/1	1/1	1/1	1/1	1/1	1/1	1/1	1/1	1/1	1/2	1/2	1/2
		rs1372119	182.20	1/1	1/1	1/1	1/1	1/1	1/1	1/1	1/1	1/1	1/1	1/1	1/2	1/1	1/2	1/2	1/2
		rs1473295	182.22	1/1	1/1	1/1	1/1	1/1	1/1	1/1	1/2	1/2	1/2	2/2	2/2	1/2	1/2	1/2	1/2
		D2S364	182.74	1/4	1/2	1/2	1/2	1/4	4/4	1/2	2/4	4/5	2/4	2/2	2/2	1/2	2/4	2/4	2/4

Table 4.1 (continued).

Gene name	Gene size (Kb) /no. of exons /position (Mb)	SNPs/ msm_s	SNPs/ msm_s Position (Mb)	I-1 /10	**II-1** /10	II-2 /10	**II-3** /10	**II-4** /10	II-5 /10	II-6 /10	**II-1** /112	II-2 /112	**II-3** /112	II-4 /112	I-1 /116	II-1 /116	II-2 /116	**II-3** /116	**II-4** /116
5. *CNGB1*	87.49 /33 /56.47-56.56	D16S3140	54.80	2/4	2/3	2/2	2/3	2/2	2/3	2/3	1/2	1/2	1/2	1/2	1/2	1/2	1/2	1/2	1/2
		D16S3057	56.08	3/3	3/3	2/3	3/3	3/3	2/3	3/3	1/2	1/2	1/2	1/2	1/2	1/2	1/2	1/2	1/2
		rs2033249	56.47	1/2	1/2	1/2	1/2	1/2	1/2	1/1	1/1	1/1	1/1	1/1	1/1	1/1	1/1	1/1	1/1
		rs376270	56.50	1/2	1/2	1/2	1/2	1/2	1/2	1/1	1/1	1/1	1/1	1/1	1/1	1/1	1/1	1/1	1/1
		rs691897	56.51	1/2	1/1	1/1	1/1	1/1	1/1	1/2	1/2	1/1	1/1	1/2	1/1	1/1	1/1	1/1	1/2
		rs2241771	56.57	1/1	1/1	1/1	1/1	1/1	1/1	1/1	1/2	1/1	1/1	1/2	1/2	2/2	1/1	1/2	1/1
		rs8055820	56.58	1/2	1/2	1/1	1/2	1/2	1/1	2/2	1/1	1/1	1/1	1/1	1/1	1/1	1/1	1/1	1/1
		D16S3038	56.97	2/3	2/3	2/3	2/3	3/3	2/3	2/3	1/2	1/2	1/2	1/2	1/2	1/2	1/2	1/2	½
6. *LRAT*	10.2/3 /155.88-155.89	D4S3049	154.99	5/9	5/9	5/9	5/5	3/5	3/9	5/9	3/3	3/8	3/3	3/8	4/6	4/5	4/5	3/6	3/6
		D4S3021	155.15	3/4	3/4	3/4	3/4	3/3	3/3	3/4	1/1	1/4	1/1	1/4	1/2	1/2	1/2	1/2	1/2
		D4S2883	155.71	1/2	1/2	1/1	1/2	1/2	1/2	1/2	1/2	1/2	1/2	1/2	1/2	1/2	1/2	1/2	1/2
		D4S1285	155.78	1/2	1/2	1/2	1/2	1/2	1/2	1/2	1/2	1/2	1/2	1/2	1/2	1/2	1/2	1/2	1/2
		rs1061100	155.884	1/1	1/1	1/1	1/1	1/1	1/1	1/1	1/1	1/1	1/1	1/1	1/1	1/1	1/1	1/1	1/1
		rs201825	155.886	1/1	1/1	1/1	1/1	1/1	1/1	1/1	1/1	1/1	1/1	1/1	1/1	1/2	1/2	1/2	1/2
		rs201823	155.888	1/1	1/1	1/1	1/1	1/1	1/1	1/1	1/1	1/1	1/1	1/1	1/1	1/1	1/1	1/1	1/1
		rs201822	155.889	1/1	1/1	1/1	1/1	1/1	1/1	1/1	1/1	1/1	1/1	1/1	1/2	1/2	2/2	2/2	2/2
		rs12507608	155.891	1/1	1/1	1/1	1/1	1/1	1/1	1/1	1/1	1/1	1/1	1/1	1/2	1/1	1/2	1/2	1/2
		D4S2976	156.01	5/6	5/6	5/6	5/5	5/6	5/6	5/6	4/5	3/5	4/5	3/5	4/5	4/4	4/5	4/4	4/4
7. *MERTK*	130.69/19 /112.37-112.50	rs1400323	112.38	1/1	1/1	1/1	1/1	1/1	1/1	1/1	1/2	1/2	1/2	1/2	1/1	1/2	1/1	1/1	1/1
		D2S1896	112.40	7/7	7/8	7/7	7/8	7/8	7/7	7/7	2/7	2/2	2/2	2/2	1/6	4/6	6/7	1/7	6/7
		rs1113418	112.42	1/2	1/2	1/2	1/2	1/2	1/2	1/2	1/2	1/2	1/2	1/2	1/1	1/2	1/1	1/1	1/1
		rs1554215	112.46	1/1	1/1	1/1	1/1	1/1	1/1	1/1	1/2	1/2	1/2	1/2	1/1	1/2	1/1	1/1	1/1
		rs6710591	112.48	1/2	1/2	1/2	1/2	1/2	1/2	1/2	1/2	1/2	1/1	1/2	1/2	1/2	1/2	1/2	1/2
		D2S2269	112.67	2/3	2/3	2/5	2/3	2/3	3/5	2/5	1/2	1/2	1/2	1/2	1/2	1/2	1/2	1/2	1/2
		D2S160	112.71	2/3	2/3	2/5	2/3	2/3	3/5	2/5	5/5	5/5	5/5	3/5	3/4	3/3	3/3	3/4	3/3
8. *NR2E3*	7.7 /9 /69.88-69.89	D15S131	68.97	2/3	2/4	2/2	2/3	2/4	2/2	2/2	1/3	1/1	1/1	1/1	1/6	1/3	1/1	3/6	1/1
		rs2723343	69.895	1/2	1/1	1/1	1/1	1/1	1/1	1/1	1/1	1/1	1/1	1/1	1/2	1/2	1/2	1/2	1/2
		D15S204	70.08	2/6	2/5	2/2	2/2	2/5	2/6	2/6	1/4	1/4	2/4	2/4	2/6	2/3	2/3	2/3	2/5

Table 4.1 (continued).

Gene name	Gene size (Kb) /no. of exons /position (Mb)	SNPs/ msm_s	SNPs/ msm_s Position (Mb)	I-1 /10	**II-1** /10	II-2 /10	**II-3** /10	**II-4** /10	II-5 /10	II-6 /10	**II-1** /112	II-2 /112	**II-3** /112	II-4 /112	I-1 /116	II-1 /116	II-2 /116	**II-3** /116	**II-4** /116
9. *PDE6A*	84.13/22 /149.22-149.30	rs10515637	149.22	1/2	1/2	1/1	1/1	1/2	1/1	1/2	2/2	1/2	1/2	2/2	1/1	1/1	1/1	1/1	1/1
		rs10515637	14922	1/1	1/1	1/1	1/1	1/1	1/1	1/1	1/1	1/1	1/1	1/1	1/2	1/1	1/1	1/2	1/1
		rs251346	149.26	1/2	1/2	1/2	1/2	1/1	1/2	1/2	1/1	1/1	2/2	1/1	1/1	1/1	1/1	1/1	1/1
		rs152951	149.26	1/1	1/1	1/1	1/1	1/1	1/1	1/1	1/1	1/1	1/1	1/1	1/2	1/1	1/2	1/1	1/2
		rs30826	149.27	1/1	1/1	1/1	1/1	1/1	1/1	1/1	1/1	1/1	1/1	1/1	1/1	1/1	1/1	1/1	1/1
		rs2277926	149.30	1/2	1/2	1/1	1/1	1/2	1/1	1/2	1/2	1/1	1/1	1/2	1/2	1/1	1/2	1/1	1/1
10. *PDE6B*	44.52/22 /0.609-0.653	D4S3360	0.105	3/3	3/4	3/3	3/4	3/4	3/4	3/3	3/3	3/3	3/3	3/5	3/3	3/5	3/5	3/3	3/5
		D4S3038	0.108	4/5	1/4	2/4	1/4	1/5	1/4	2/4	1/2	1/2	1/4	1/2	2/2	1/2	1/2	2/3	1/2
		D4S412	0.335	1/2	1/2	1/2	1/2	1/2	1/2	1/2	1/3	1/2	1/2	1/3	1/2	1/2	1/2	1/2	1/2
		rs1135375	0.637	1/1	1/1	1/1	1/1	1/1	1/1	1/1	1/1	1/1	1/1	1/1	1/1	1/1	1/1	1/1	1/1
		D4S2936	0.682	2/5	2/6	2/2	2/6	2/6	2/6	2/2	3/3	3/3	3/5	3/3	3/3	2/3	2/3	2/3	3/3
11. *RGR*	14.09/7 /85.99-86.00	D10S1686	85.55	2/4	2/4	2/4	2/2	2/2	2/4	2/4	2/2	2/2	1/2	2/2	2/3	1/3	1/3	1/3	2/3
		rs738786	86.00	1/2	1/2	1/2	1/2	1/2	1/2	1/2	1/1	1/1	1/1	1/1	1/2	1/2	1/1	1/1	1/1
		D10S573	86.29	4/4	4/4	2/4	4/4	2/4	2/4	2/4	4/5	4/5	2/5	4/5	2/2	2/5	2/5	2/5	2/2
12. *RHO*	6.71/5/ 130.73-130.73	rs7984	130.730	1/1	1/1	1/2	1/2	1/2	1/2	1/2	1/1	1/2	1/2	1/1	1/1	1/1	1/2	1/2	1/1
13. *RLBP1*	11.82/9 /87.554-87.565	D15S979	86.63	2/2	2/4	2/6	2/6	2/4	2/4	2/6	4/4	2/4	2/4	2/4	3/6	3/5	3/5	5/6	5/6
		D15S1045	87.39	3/5	3/3	4/5	4/5	3/3	3/3	4/5	3/4	2/4	2/4	3/4	2/2	2/2	2/2	2/2	2/3
		rs2070780	87.56	1/2	1/2	1/2	1/2	1/2	1/2	1/2	1/1	1/1	1/1	1/1	1/2	1/2	1/2	1/2	1/2
		D15S202	87.80	1/2	1/2	1/2	1/2	1/2	1/2	1/2	1/2	1/2	1/2	1/2	1/2	1/2	1/2	1/2	1/2
14. *RPE65*	21.2 /14 /68.667-68.688	D1S198	66.78	5/7	7/8	5/7	5/5	7/8	7/8	7/8	3/4	1/4	1/3	4/4	4/5	4/4	5/5	4/5	4/4
		D1S410	67.91	1/8	1/7	8/8	7/8	1/7	1/7	1/7	1/7	7/7	1/7	7/7	1/7	1/6	1/6	6/7	7/8
		rs3125898	68.67	1/2	1/2	1/2	1/2	1/2	1/2	1/2	1/1	1/1	1/1	1/1	1/2	1/2	1/2	1/2	1/2
		D1S219	69.61	3/4	3/4	4/4	3/4	3/4	3/4	3/4	3/4	4/4	4/4	3/4	1/4	3/4	1/3	3/4	3/4

Table 4.1 (continued).

Gene name	Gene size (Kb) /no. of exons /position (Mb)	SNPs/ msm_s	SNPs/ msm_s Position (Mb)	I-1 /10	**II-1** /10	II-2 /10	**II-3** /10	**II-4** /10	II-5 /10	II-6 /10	**II-1** /112	II-2 /112	**II-3** /112	II-4 /112	I-1 /116	II-1 /116	II-2 /116	**II-3** /116	**II-4** /116
15. *SAG*	39.07/15 /233.881-233.920	D2S2344	233.152	1/5	1/4	1/4	1/4	1/5	4/5	1/5	2/2	2/3	2/2	3/3	2/3	2/3	3/3	2/3	2/3
		D2S206	233.416	3/4	3/3	3/3	3/3	3/4	4/4	3/4	4/4	1/3	4/4	1/4	3/4	3/5	4/5	4/5	3/5
		rs1978921	233.881	1/1	1/1	1/1	1/1	1/1	1/1	1/1	1/1	1/1	1/1	1/1	1/1	1/1	1/1	1/1	1/1
		rs12623795	233.888	1/2	1/2	1/2	1/2	1/2	1/2	1/2	1/1	1/1	1/1	1/1	1/1	1/1	1/1	1/1	1/1
		rs2304777	233.892	1/2	1/1	1/1	1/1	1/2	1/1	1/1	1/1	1/2	1/1	1/2	1/1	1/2	1/2	1/1	1/2
		rs11891546	233.897	1/2	1/1	1/1	1/1	2/2	1/1	1/2	1/1	1/1	1/1	1/2	1/1	1/2	1/2	1/2	1/2
		rs3792100	233.899	1/1	1/1	1/1	1/1	1/1	1/1	1/1	1/1	1/1	1/1	1/2	1/2	1/2	1/2	1/2	1/1
		rs3792097	233.903	1/2	1/2	1/2	1/2	1/1	1/2	1/2	1/1	1/2	1/1	1/2	1/2	1/2	1/2	1/2	1/2
		rs1000141	233.907	1/2	1/2	1/2	1/2	1/2	1/2	1/2	1/1	1/2	1/1	1/2	1/2	1/2	1/2	1/1	1/1
		rs1046974	233.920	1/1	1/1	1/1	1/1	1/1	1/1	1/1	1/1	1/1	1/1	1/2	1/2	1/2	1/2	2/2	2/2
16. *TULP1*	15.00/15 /35.57-35.58	D6S1611	35.48	1/2	1/2	1/2	1/2	2/2	1/2	1/2	1/2	1/2	2/2	1/2	1/3	3/3	3/4	3/4	3/3
		rs2273000	35.58	1/2	1/2	1/2	1/2	1/2	1/2	1/2	1/1	1/1	1/1	1/1	1/1	1/1	1/1	1/1	1/1
		D6S291	36.37	1/3	3/3	3/3	3/3	3/3	2/3	3/3	1/2	1/3	2/2	2/3	1/2	2/2	2/2	1/2	2/2
17. *USH2A*	249.44/21 /213.86-214.66	D1S2703	211.15	5/11	5/5	5/9	5/5	5/5	5/9	5/1	8/9	8/8	8/8	8/8	1/5	5/7	5/7	4/5	4/5
		D1S2827	214.20	3/5	3/3	2/3	3/5	3/3	2/3	3/5	2/5	3/4	3/4	3/5	3/5	2/5	2/5	2/5	3/5
		rs1324330	214.45	1/1	1/2	1/1	1/2	1/2	1/1	1/2	1/1	1/1	1/1	1/1	1/2	1/2	1/2	1/2	1/2
		D1S227	215.36	2/2	2/2	2/2	2/2	2/2	2/2	2/2	2/2	2/2	2/4	2/2	3/3	2/3	2/3	2/3	2/3
18. RP22	3.77 /19.17-22.94	D16S3041	19.30	6/2	2/3	6/3	6/4	2/4	2/3	6/4	4/6	4/6	4/4	4/6	2/3	3/3	2/3	2/3	3/3
		D16S3046	20.79	1/5	1/5	1/5	2/5	1/5	1/5	2/5	2/3	3/4	2/5	3/4	2/4	1/4	2/4	1/4	2/4
		D16S403	22.94	5/5	5/9	5/7	5/9	5/9	5/7	5/9	2/3	4/7	2/3	4/7	1/6	2/6	1/3	2/6	1/3
		D16S3068	25.47	1/2	1/3	1/2	2/3	1/3	1/1	2/3	1/2	2/2	1/2	2/2	1/2	1/1	2/3	1/1	2/3
		D16S3100	26.48	2/3	2/3	2/3	3/3	2/3	2/2	3/3	2/2	1/3	2/2	1/3	1/2	2/2	1/1	2/2	1/1
19. RP28	3.39 /62.67-66.06	D2S147	64.02	4/4	3/4	4/5	3/4	4/5	4/5	4/5	2/9	2/9	9/9	2/9	2/4	4/7	4/7	3/4	2/3
		D2S380	65.50	5/7	7/7	3/5	7/7	5/7	3/5	3/5	1/3	1/3	3/3	1/3	7/7	7/7	7/7	7/7	5/7
		D2S2293	65.80	3/4	4/5	1/3	4/5	3/5	1/3	1/3	4/4	3/4	3/4	4/4	1/3	3/4	3/4	3/4	1/4

Table 4.1 (continued).

Gene name	Gene size (Kb) /no. of exons /position (Mb)	SNPs/ msm_s	SNPs/ msm_s Position (Mb)	I-1 /10	II-1 /10	II-2 /10	II-3 /10	II-4 /10	II-5 /10	II-6 /10	II-1 /112	II-2 /112	II-3 /112	II-4 /112	I-1 /116	II-1 /116	II-2 /116	II-3 /116	II-4 /116
20. RP29	7.1 /173.31-180.41	D4S1597	170.20	3/3	3/3	3/3	3/3	3/3	3/3	3/3	3/3	3/3	3/3	3/3	3/8	3/8	3/3	3/3	3/3
		D4S1595	174.55	5/7	7/7	5/7	5/7	6/7	6/7	5/7	6/7	6/7	5/7	6/7	5/6	5/6	5/5	5/5	5/7
		D4S1539	175.92	3/4	3/3	3/4	3/4	3/3	3/3	3/4	3/3	3/3	3/3	3/3	2/3	3/3	3/3	3/3	3/4
		D4S415	178.94	7/7	7/8	2/7	7/8	2/7	2/7	7/8	2/8	2/8	2/2	2/8	2/3	2/2	2/3	2/3	2/3
		D4S2920	184.70	3/5	3/4	3/5	4/5	3/5	4/5	3/4	2/5	4/4	2/4	4/5	3/5	2/5	4/5	4/5	2/5
21. RP32	8.94 /101.74-110.68	D1S206	101.46	1/3	3/6	3/3	1/3	3/6	1/6	3/6	4/8	4/9	4/9	4/8	2/2	2/6	2/2	2/2	2/6
		D1S495	102.33	4/4	3/4	4/4	4/4	3/4	3/4	3/4	7/8	7/10	7/10	7/8	3/7	3/7	3/7	3/7	3/3
		D1S2726	110.80	6/8	7/8	6/6	6/8	6/7	7/8	6/7	3/4	3/4	3/3	4/4	3/4	3/4	3/4	3/4	3/4

4.3.2.2 Microsatellite markers and genotyping

In total 89 microsatellite markers have been used, of which 45 were from the ABI PRISM® Linkage Mapping Sets V2.5. The remaining 44 markers were synthesised commercially according to the sequence information obtained from the Genome Database (Table 4, appendix 1). The data for heterozygosity and the order of the markers used were obtained from the Marshfield Medical Research Foundation web site.

Multiplex microsatellite genotyping was performed using 4-6 markers per reaction utilising QPCR mix (ABgene, UK) (see section 2.1.2.3). Data collection and allele identification were performed using GeneScan and Genotyper software (Applied Biosystems). Alleles were assigned to individuals and genotypic data were used to calculate the LOD scores using Cyrillic and MLINK programs. The phenotype was analysed as an autosomal recessive trait with complete penetrance with a frequency of 0.0001 for the affected allele (section 2.9).

4.3.2.3 Mutation screening

Fifty pairs of primers were designed for four genes, *CERKL*, *LRAT*, *SAG* and *MERTK*, in order to search for mutations in the families where both SNPs and microsatellite markers were unable to exclude them by linkage as disease causing genes (Table 5, appendix 1). The primers were used to PCR amplify the genes and perform direct genomic sequencing as previously described (section 2.4).

4.3.2.4 GeneChip Mapping 10K Array

DNA samples from seven affected and three unaffected individuals were genotyped by total genome-sampling analysis using the Affymetrix 10K GeneChip Mapping Array (version Xba142). The median physical distance between SNPs and their average heterozygosity were 105 kb and 0.37, respectively, predicting an average spacing of 3 fully informative markers per megabase. Genotypes for 10,204 SNPs were called by the GeneChip DNA Analysis Software (GDAS v3.0, Affymetrix). The detailed methodology for genotyping using the GeneChip array has been previously described (see section 2.7.2).

4.3.2.5 Analysis of the GeneChip Mapping 10K Array

The analysis of the data was performed using the ALOHOMORA software (Rüschendorf and Nürnberg, 2005). Mendelian errors and the correct relationships within the families were checked for by PedCheck and GRR programs, respectively (O'Connell and Weeks, 1998; Abecasis *et al.* 2001a) (Section 2.7.3.2).

The software was utilised to search for regions of shared haplotype between the affected members in each family and then the data from the three families were combined in order to identify regions of shared haplotype. Further investigations of these regions were based on two criteria: 1. Identifying 10 or more consecutive SNPs that is shared between all families ensuring that the parents are heterozygous. 2. The shared region spanned at least a 3 Mb interval.

4.3.6 Mutation screening of the *VSX1* gene

Five pairs of primers were designed in order to screen the coding regions together with the splice sites (GT/AG) and the 5`UTR of the *VSX1* gene (Table 4.2). The primers were used to PCR amplify and sequence the target gene as previously described (Section 2.4).

Table 4.2 Primers designed for amplification of *VSX1* gene

Exon no.	Sequence (5`.....3`)	Product size (bp)	$MgCl_2$	Temp.
Exon 1 F	GCGGAGTCACTGTCCCTTAC	940	0795 AB mix	58.5°C
Exon 1 R	GGGATTTAGGATGCAGCAAG			
Exon 2 F	AATAGCAGCAGCCATTTTGG	399	1.5 mM	57°C
Exon 2 R	CCGGGCCATAAATTCTCAG			
Exon 3 F	CATTCAGAGGTGGGGTGTTC	422	1.5 mM	57°C
Exon 3 R	AGCTCTTGTGGTGCCTTCAG			
Exon 4 F	CCTCGGGAGCTATTTCCTTC	432	1.5 mM	57°C
Exon 4 R	ACTGACGTTGCTTTGCTTTG			
Exon 5 F	CCAATGCCAATCACTGTGTC	696	1.5 mM	57°C
Exon 5 R	CCCTAGGTCACTCATCTGTCC			

4.4 RESULTS

4.4.1 Clinical data

All affected subjects had clinical manifestations of RP including variable grades of low visual acuity, waxy pallor of the optic disc, attenuation of the retinal blood vessels, bone spicule pigmentation and flat or absent ERG. The clinical data of the patients are described in the table below.

Table 4.3 Clinical data of the patients participated in the study

Family no	Patient no.	Sex	Age	Age of Onset	VA OD unaided	VA OS unaided	Visual field	RP changes	Optic disc	N
10	II-1	F	49	42	$20/30^{-2}$	$20/30^{-1}$	Constricted	Diffuse	Mild pallor	+
10	II-3	M	45	36	20/50	20/40	Constricted	Diffuse	Mild pallor	+
10	II-4	F	35	20	$20/30^{-3}$	$20/30^{-3}$	Constricted	Diffuse	Mild pallor	+
112	II-1	F	52	10	$20/50^{-2}$	20/30	Constricted	Sectorial	-	+
112	II-3	F	46	11	20/30	20/30	Constricted	Sectorial	-	+
116	II-3	M	34	22	0.3+	0.3+	Constricted	Diffuse	-	+
116	II-4	F	41	19	20/100	20/100	Constricted	Diffuse	-	+

VA OD: visual acuity right eye

VA OS: visual acuity left eye

N: Nyctalopia

4.4.2 SNP/microsatellite marker analyses and mutation screening of the 17 known arRP genes

Intergenic SNP analysis has enabled the exclusion of 13 out of 17 known genes, since non segregation of the haplotypes within affected family members in a given gene rules out its involvement in the pathogenesis of the disease (Table 4.1). However, the remaining four genes, (*CERKL* and *LRAT* in families 112 and 114, *SAG* in family 112 and *MERTK* in family 10), were not excluded by this approach because all SNPs screened were segregating with the disease phenotype. Consequently, microsatellite markers spanning the above four genes were used for linkage testing. Although the markers were highly informative, the above four genes could not be excluded since the observed alleles did not result in recombination to be inferred between the markers and the disease locus. Thus, it was mandatory to screen these genes for mutations in their corresponding families by direct sequence analysis. Mutation screening of the coding regions, splice sites and the 5`UTR of the four genes revealed no pathological sequence alterations. Hence, they were consequently excluded as disease causing for RP in our families. However, it is important to take into account that the methodology used in this study cannot detect large heterozygous deletions or intronic mutations.

4.4.3 Microsatellite marker analysis of the remaining 5 known arRP loci

Microsatellite marker analysis has excluded four of the remaining 5 arRP loci (RP22, RP25, RP28, RP29 and RP30) by achieving LOD scores of minus infinity for the analysed markers. Only the RP25 locus could not be excluded in the studied families where LOD scores suggestive of linkage were obtained (Figure 4.3).

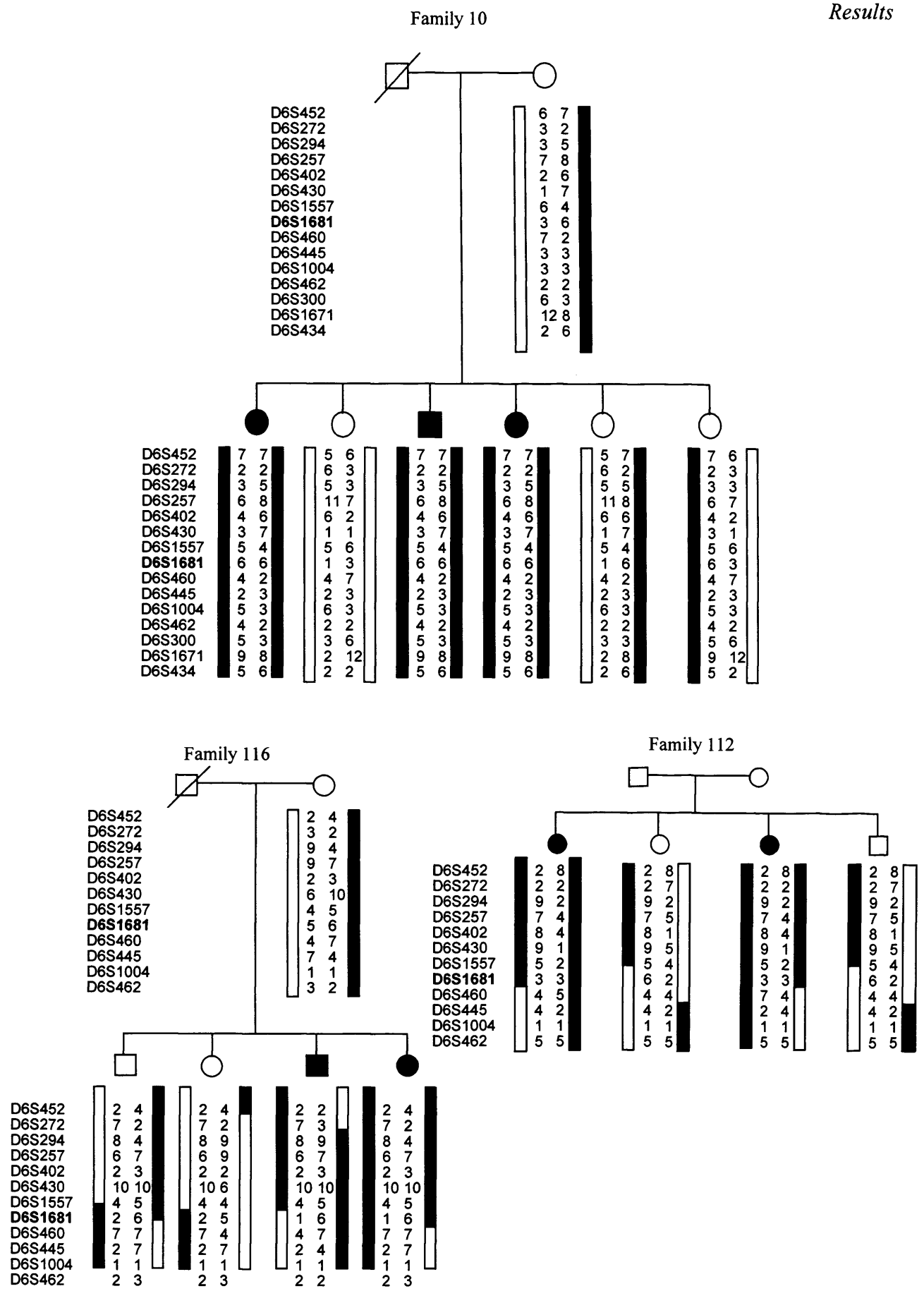

Figure 4.3 Haplotype analysis of families 10, 112 and 116 using microsatellite markers on 6p12.1-q12. Recombination events between markers D6S294 and D6S460 are shown in families 112 and 116. The maximum LOD score was obtained by marker D6S1681 shown in bold (see table 4.5).

4.4.4 GeneChip Mapping 10K Array and further analysis

The GeneChip mapping data showed that affected members from each family had multiple regions of shared haplotype. However, by combining the data from the three families, three regions of tentative linkage were identified (Table 4.4). The largest region of shared haplotype was on the 6p12.1-q12 (RP25) followed by the regions on 20p11.21-q12 and 6q24.3-q25.3 corresponding to 16.1, 15.2 and 9.7 Mb intervals, respectively. Further investigation of these regions by using highly informative microsatellite markers confirmed linkage to the RP25 locus, a well defined locus for recessive RP. The density of markers in this interval was increased in order to achieve the maximum LOD score for each of the families under study and to identify new crossovers. All the tested markers in the vicinity of RP25 generated positive LOD scores. We pooled the linkage data from all families as previously stated. A maximum LOD score of 3.27 for the marker D6S1681 at $\theta = 0$ was generated (Table 4.5). Recombination events defined a critical interval spanning ~10 cM interval on chromosome 6 between markers D6S294 and D6S460 (Figure 4.3) which was similar to the previous report in the Spanish families with arRP (Ruiz *et al.,* 1998) and hence the disease interval could not be further refined. However, in case of 6q24.3-q25.3 and 20p11.21-q12 loci, additional work has excluded linkage from the region 6q24 and narrowed the interval in 20p11 region to 8 Mb with a maximum LOD score for all families of 1.48 at $\theta = 0$ for the marker D20S484 (Figure 4.4). It is interesting to note that there was no common allele between the examined families in the regions suggestive of linkage. Ultimately, this has excluded the possibility that the mutation in the causative gene might be due to a common founder effect.

Table 4.4 Common regions of shared haplotype in each family and in all families using the 10K GeneChip array

Regions	Family 10	Family 112	Family 116	MI with all FC
6p12.1-q12 (RP25)				
Interval in cM	68	24.9	5.9	5.9
Interval in Mb	87.5	31.8	16.1	16.1
No. of SNPs	332	116	41	41
6q24.3-q25				
Interval in cM	33.8	26.4	16.9	16.9
Interval in Mb	19.2	15.9	9.7	9.7
No. of SNPs	102	85	50	50
20p11.21-q12				
Interval in cM	43.1	8.6	27.7	8.6
Interval in Mb	33.6	15.2	26.6	15.2
No. of SNPs	120	29	77	29

cM: centiMorgan (genetic distance), Mb: megabase (physical distance), No. of SNPs: number of SNPs in each region, MI: minimum interval, FC: families combined

Table 4.5 LOD score for families 10, 112 and 116 in the RP25 interval. The maximum Lod score at the D6S1681 marker is shown in bold

Theta (θ)	**0.00**	**0.01**	**0.05**	**0.10**	**0.2**	**0.3**	**0.4**
Markers/F							
D6S452 (10)	1.57	1.54	1.4	1.2	0.83	0.44	0.12
(112)	-0.03	-0.013	-0.012	-0.010	-0.006	-0.002	-0.0007
(116)	-∞	-1.1	-0.54	-0.299	-0.11	-0.003	-0.008
D6S272 (10)	1.57	1.54	1.4	1.2	0.83	0.44	0.12
(112)	0.63	0.61	0.54	0.45	0.29	0.14	0.03
(116)	-∞	-1.3	-0.65	-0.17	-0.06	-0.06	-0.013
D6S294 (10)	0.97	0.93	0.78	0.59	0.26	0.05	0.00
(112)	-0.013	-0.013	-0.012	-0.010	-0.006	-0.002	-0.0007
(116)	-∞	-1.53	-0.82	-0.59	-0.22	-0.08	-0.02
D6S257 (10)	1.57	1.54	1.4	1.2	0.83	0.44	0.12
(112)	0.65	0.63	0.56	0.48	0.31	0.15	0.04
(116)	0.15	0.15	0.15	0.14	0.10	0.05	0.014
D6S402 (10)	1.57	1.54	1.4	1.2	0.83	0.44	0.12
(112)	0.65	0.63	0.56	0.48	0.31	0.15	0.04
(116)	0.24	0.24	0.2	0.15	0.08	0.03	0.007
D6S430 (10)	1.57	1.54	1.4	1.2	0.83	0.44	0.12
(112)	0.65	0.63	0.56	0.48	0.31	0.15	0.04
(116)	0.15	0.15	0.15	0.14	0.1	0.05	0.014
D6S1557 (10)	0.64	0.64	0.59	0.53	0.38	0.21	0.06
(112)	0.65	0.63	0.56	0.48	0.3	0.15	0.04
(116)	0.24	0.24	0.2	0.15	0.08	0.03	0.007
D6S1681 (10)	**1.57**	**1.54**	**1.4**	**1.2**	**0.83**	**0.44**	**0.12**
(112)	**0.85**	**0.83**	**0.74**	**0.63**	**0.40**	**0.20**	**0.05**
(116)	**0.85**	**0.83**	**0.74**	**0.62**	**0.4**	**0.20**	**0.05**
D6S460 (10)	0.64	0.64	0.002	0.53	0.38	0.21	0.06
(112)	-∞	-2.6	-1.3	-0.81	-0.34	-0.13	-0.03
(116)	-∞	-1.4	-0.74	-0.4	-0.19	-0.07	-0.017
D6S445 (10)	0.002	0.002	0.6	0.002	0.001	0.0006	0.0001
(112)	0.013	-0.013	-0.012	-0.01	-0.006	-0.002	-0.0007
(116)	-∞	-1.5	-0.82	-0.51	-0.22	-0.08	-0.02
D6S1004 (10)	0.67	0.66	0.6	0.53	0.37	0.22	0.06
(112)	0.00	0.00	0.00	0.00	0.00	0.00	0.00
(116)	0.00	0.00	0.00	0.00	0.00	0.00	0.00
D6S462 (10)	0.67	0.66	1.4	0.53	0.37	0.22	0.06
(112)	0.00	0.00	0.00	0.00	0.00	0.00	0.00
(116)	-∞	-1.18	-0.5	-0.2	-0.10	-0.03	-0.008
D6S300 (10)	1.57	1.54	1.4	1.2	0.83	0.44	0.12
D6S1671 (10)	1.57	1.54	1.4	1.2	0.83	0.44	0.12
D6S434 (10)	1.57	1.54	1.4	1.2	0.83	0.44	0.12

(F) Families (10, 112 and 116)

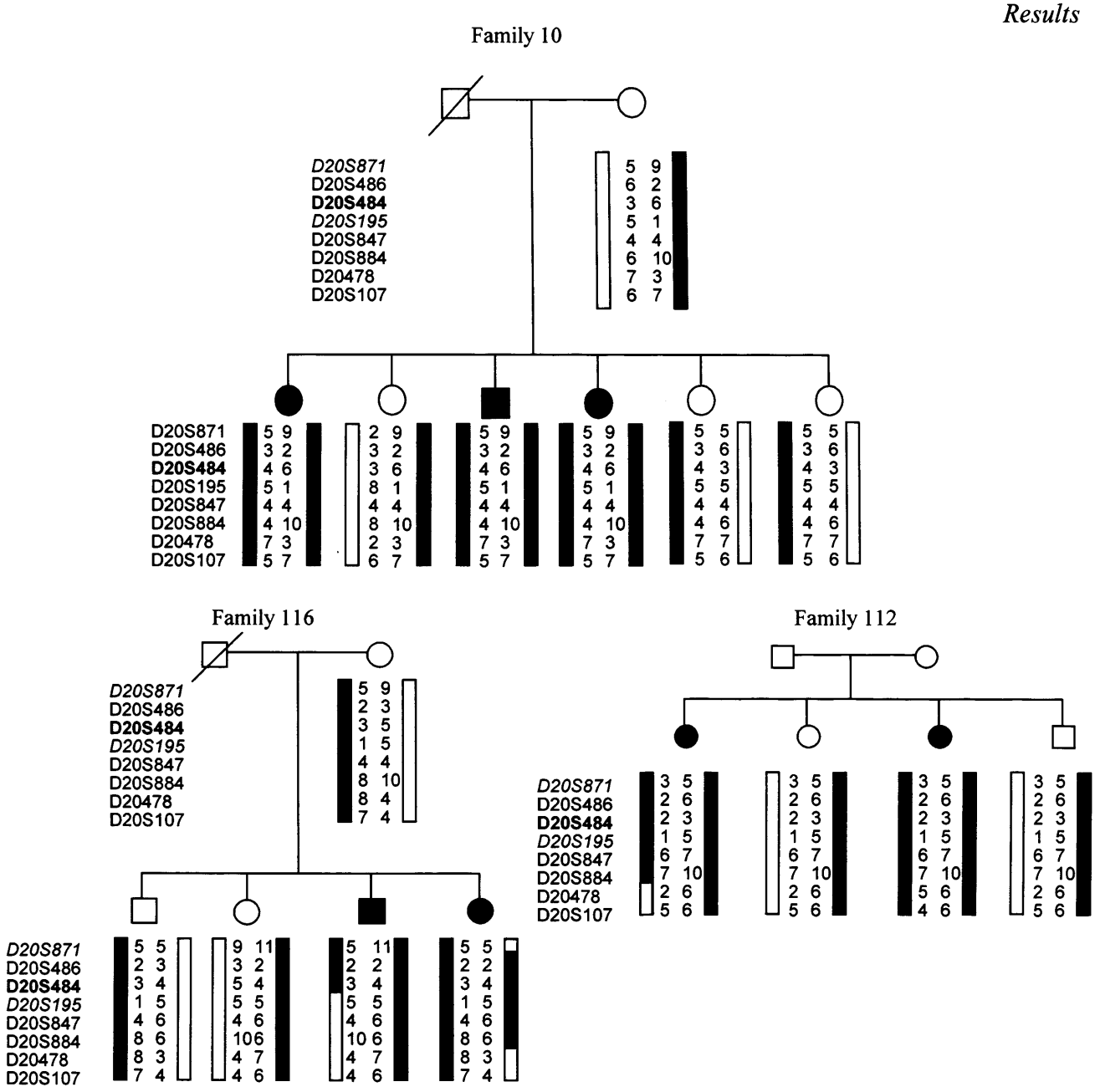

Figure 4.4 Microsatellite marker analysis of chromosome 20 in families 10, 112 and 116. D20S871 and D20S195 in italic defining the minimal critical interval in family 116. D20S484 is shown in bold where the maximum LOD score was achieved in all families.

4.4.5 Bioinformatic analysis of the regions with positive LOD scores

The work described up to this point has identified two regions of interest, one on chromosome 6p12.1-q12 (RP25) and the other on 20p11.21-q12 (Figures 4.3 and 4.4, respectively) for detailed computational analysis. The eight Mb interval in 20p11.21-q12 contained approximately 100 genes. By studying the function of these genes, there were no good candidates for RP apart from the *VSX1* gene that was previously reported to be expressed in the inner nuclear layer of the adult retina. Regarding the RP25 locus, a full description of the interval involving the genes and the current work was described in the previous chapter.

4.4.6 Mutation screening of the *VSX1* gene

Mutation screening of the *VSX1* gene revealed no pathological changes in all families. However, three SNPs were identified of which two were novel. The novel SNPs were heterozygous transition of C to T at position -14 and heterozygous transition of G to A at c.665 depicting a change of amino acid from arginine to glutamine at codon 222. All changes were assigned a nucleotide number starting at the first translation base of *VSX1* gene according to the Genbank entry NM_014588.4.

The identified SNPs were segregating with the disease phenotype and were detected with an allele frequency of 4.7 and 8.3 % in 100 control chromosomes, respectively.

4.5 DISCUSSION

Herein we report the linkage of three non-consanguineous Chinese families with arRP to the RP25 locus on chromosome 6p12.1-q12. In addition, we propose a systematic method for identifying the disease locus in small non-consanguineous recessive families (Figure 4.1). In the beginning, the SNP analysis approach was undertaken to identify whether any of the 17 known arRP genes showed linkage in the families studied. It is generally accepted that one crossover in 100 meioses relates to approximately a genetic distance of one cM and on average this equates to a physical distance of one Mb. For this reason, our choice of selecting three or more SNPs per gene should be sufficient to exclude the gene if a crossover is observed, since the physical size of the recessive RP genes ranged between 4 and 250 kb. The SNP approach proved to be effective in excluding the genes particularly if more than two affected individuals were evaluated per family. Microsatellite markers were adopted in two occasions: 1) whenever the SNPs showed segregation of the haplotypes with the disease in any of the 17 genes; 2) in studying the 5 loci where the genetic interval was large. However, in this study neither the SNPs nor the microsatellite markers were able to exclude four of the studied genes where the haplotype within the families segregated with the disease phenotype. Hence, direct sequence analysis of these genes in their corresponding families was the outcome measure in order to search for mutations or to exclude these genes as disease causative. This was both cost and time effective in comparison to sequencing known recessive genes in each family. Subsequently, all families studied were subjected to a whole genome scan using the 10K GeneChip to search for regions of common haplotype between the families investigated.

To the best of our knowledge, this is the first application of the 10K array in case of non-consanguineous autosomal recessive RP families. It has been reported that the 10K SNP-chip has a >99% chance in detecting heterozygosity compared to a 70% in case of microsatellite markers and consequently in exclusion of linkage (Woods *et al.,* 2004). Thus, the 10K GeneChip also has a potential role in homozygosity mapping. However, it is a different scenario in case of non-consanguineous families where the mutation probably has to be compound heterozygous and then no regions of homozygosity are expected. Thus, in our study we used the 10K GeneChip in order to detect regions of shared haplotype between affected members in each family, which was followed by combining the data from different families.

The data obtained from the GeneChip mapping 10K array showed that there are three regions of shared haplotype, 6p12.1-q12, 20p11.21-q12 and 6q24.3-q25.3, between all families across the whole genome. Further genetic analysis of the three loci with highly informative markers has excluded the region of linkage at the telomeric end of chromosome 6 and reduced the interval on chromosome 20 to 8 Mb where a good candidate gene; *VSX1* resides. Even though this gene has been implicated in the pathogenesis of posterior polymorphous dystrophy and keratoconus, its expression is mainly in the retina and not in the cornea or the lens (Heon *et al.,* 2002). However, our data showed no pathological changes in this gene and therefore it was excluded as disease causing in our families. As a result, combining the data obtained from both microsatellite markers and the 10K GeneChip suggests that our families are probably linked to the RP25 locus.

The linkage data reported here is similar to what has been previously reported in the Spanish and Pakistani families with arRP (Ruiz *et al.,* 1998; Khaliq *et al.,* 1999),

signifying that we might be investigating a major locus for recessive RP. However, the answer to this question will eventually be clarified upon cloning the RP25 gene and detecting additional mutations in a larger collection of arRP families and sporadic cases. In summary, this is the first comprehensive genetic study in the Chinese population with arRP. We proposed an effective strategy for mapping the disease loci in nuclear non-consanguineous recessive families. The three Chinese families reported here are likely to be linked to the RP25 locus. Future work will involve applying the genetic mapping strategy on other nuclear non-consanguineous recessive families to further investigate its applicability.

CHAPTER 5

PROTOCADHERIN-21 (*PCDH21*), A NOVEL GENE FOR JUVENILE-ONSET RECESSIVE RETINITIS PIGMENTOSA

5.1 INTRODUCTION

5.1.1 Juvenile-onset recessive RP

Onset of symptoms in early adulthood is typical of RP, however a number of forms present at an earlier age and the spectrum of the disease may overlap with infantile onset retinal dystrophies (RDs) and LCA. Clinically, nyctalopia, mid peripheral visual field constriction and pigmentary retinal changes are common features for all cases of RP. Patients with juvenile RP are known to have a good central vision during the first decade of life, while in LCA severe visual impairment have been recorded from birth to the first year of life (Lorenz *et al.,* 2000; Morimura *et al.,* 1998).

To date 24 loci have been implicated in the pathogenesis of recessive RP in addition to 9 LCA genes (http://www.sph.uth.tmc.edu/Retnet/); however these loci cannot explain the whole spectrum of the disease. Therefore, identifying new RP genes is still a precedence in the field of retinal genetics, since genetic screening is not only used as a new modality to confirm diagnosis in such hereditary disorders but is also crucial for better understanding of the molecular basis of the disease.

5.1.2 Cadherins

Cadherins are a group of integral membrane proteins that mediate calcium-dependent cell-cell adhesion (Angst *et al.,* 2001). To date, more than 80 cadherins have been characterised in humans. Common to all cadherins are multiple tandemly repeated, (5 to

34) cadherin domains (extracellular domains, EC). ECs contain the evolutionarily highly conserved Ca^{2+}-binding motifs that mediate homophilic association of cadherin molecules. Mutations in the genes encoding cadherin-23 and protocadherin-15 (*CDH23* and *PCDH15*), account for two subgroups of autosomal recessive USH1, USH1D (Bolz *et al.,* 2001; Bork *et al.,* 2001) and USH1F (Ahmed *et al.,* 2001; Alagramam *et al.,* 2001), respectively. Additionally, alterations in *CDH3* underlie hypotrichosis with juvenile macular dystrophy (Sprecher *et al.,* 2001).

5.1.3 Protocadherin-21

Protocadherin-21 (PCDH21) amino acid sequence consists of a signal peptide, six ECs, a putative transmembrane domain, and a cytoplasmic domain of ~150 amino acids (Figure 5.1). Even though the number and arrangement of the domains within PCDH21 conform to that of other cadherins there was no homology to any known cadherin suggesting interacting partners different from those of other cadherins. *PCDH21* expression is limited to the base of the outer segment at the junction between the photoreceptor inner and outer segments (Rattner *et al.,* 2001). It has been reported that targeted disruption of the *PCDH21* gene in the mouse results in disorganisation of photoreceptor outer segments and a progressive loss of photoreceptor cells, indicating that *PCDH21* is essential for outer segment architecture and photoreceptor survival (Rattner *et al.,* 2001). *PCDH21* is therefore a good candidate for human inherited retinal diseases, such as RP and LCA.

5.2 AIM OF THE STUDY

The objective here was to identify the disease causing gene in a consanguineous Jordanian family with juvenile onset arRP

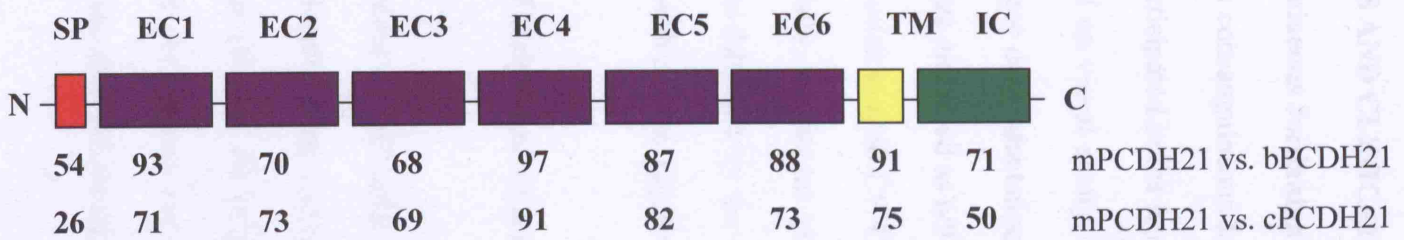

Figure 5.1 Domain structure and percent amino acid identity between individual domains of bovine, mouse and chicken PCDH21. Abbreviations are as follows: SP: signal peptide, EC: extracellular domain, TM: transmembrane domain, IC: intracellular domain, m: murine, b: bovine, c: chicken (adapted from Rattner *et al.,* 2001)

5.3 PATIENTS AND METHODS

5.3.1 PATIENTS AND CLINICAL DATA

5.3.1.1 Consanguineous Jordanian recessive RP pedigree

A two generation consanguineous Jordanian family with an autosomal recessive pattern of inheritance participated in the study (Figure 5.2, family A). Clinical diagnosis of this family was based on visual acuity, fundus picture and ERG findings. History of night blindness with poor dark adaptation starting at the age of 18-25 was recorded and the visual acuities were measured as 6/9 (Snellen) at the age of 35, however by the age of 42 the vision deteriorated to 6/60-CF. Colour vision and visual field defects progressed at a similar rate. Initially, the fundus picture showed minimal RPE changes with granular mottling. This was followed by the appearance of bone spicule like pigmentation in the peripheral retina with circular patches and atrophy of the RPE (Figure 5.3).

5.3.1.2 Cohort of early onset retinal dystrophy (EORD), LCA and juvenile recessive RP

Additionally, a panel of 192 arRP and EORD, in addition to 96 LCA patients from Moorfields Eye Hospital were also included in this study. The family structure of one of the sporadic cases (Family B) is presented in figure 5.2. An informed consent was obtained from all participants for clinical and molecular genetic studies. The study conformed to the tenets of the Declaration of Helsinki.

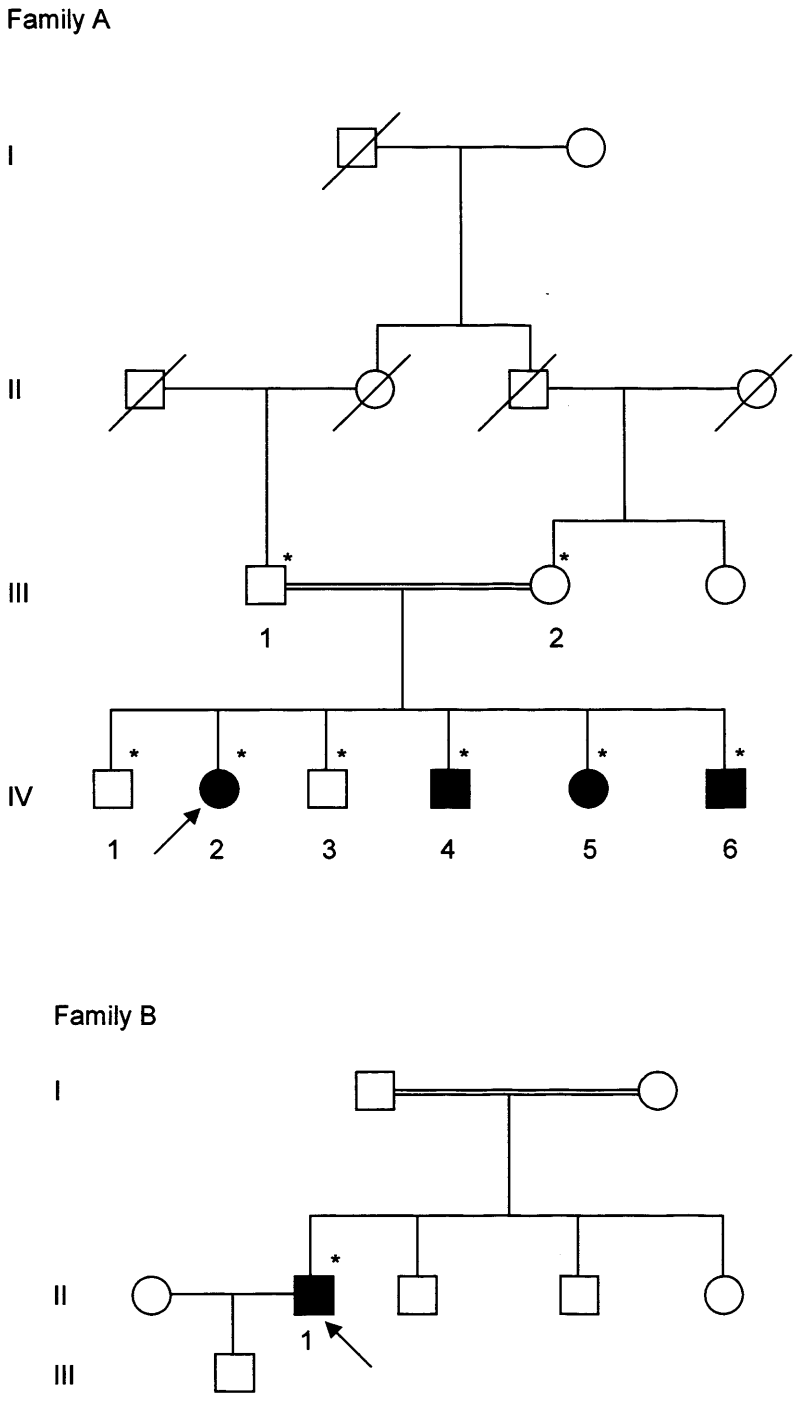

Figure 5.2 Pedigrees of the families participated in the study. Family A: Jordanian, Family B: showing the sporadic patient. Open and closed symbols denote unaffected and affected individuals, respectively. Deceased family members are denoted by diagonal slashes, arrows indicate the probands in each family and asterisks indicate individuals examined both clinically and genetically.

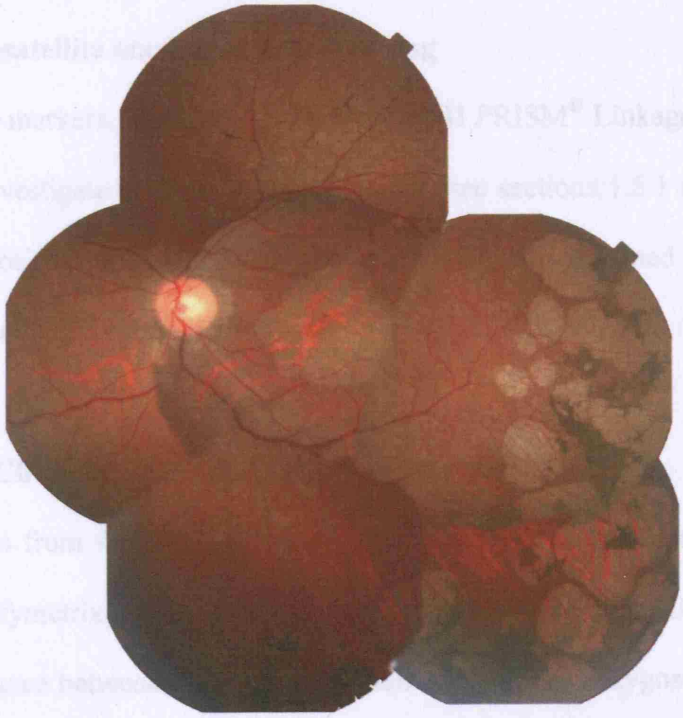

Figure 5.3 Fundus photograph of the proband from family A showing attenuated retinal arteries, bone corpuscle pigmentation and peripheral areas of RPE atrophy.

5.3.2 METHODS

Blood samples from all family members were collected and DNA was isolated according to standard protocols.

5.3.2.1 Microsatellite markers and genotyping

Microsatellite markers were selected from the ABI PRISM® Linkage Mapping Set V2.5 in order to investigate the known loci for arRP (see sections 1.5.1 and 4.3.4). The data for heterozygosity and the order of the markers used were obtained from the Marshfiled Medical Research Foundation web site.

5.3.2.2 GeneChip Mapping 10K Array

DNA samples from family A members, 4 affected and 4 unaffected, were genotyped using the Affymetrix 10K GeneChip Mapping Array (version Xba142). The median physical distance between the SNPs and their average heterozygosity were 105 kb and 0.37, respectively, predicting an average spacing of 3 fully informative markers per megabase. Genotypes for 10,204 SNPs were ascertained by the GeneChip DNA Analysis Software (GDAS v3.0, Affymetrix). The detailed methodology for genotyping using the GeneChip array is as previously described (see section 2.7.2).

5.3.2.3 Analysis of the GeneChip Mapping 10K Array

The ALOHOMORA software was utilised to highlight regions of significant LOD score in family A (Rüschendorf and Nürnberg, 2005) (section 2.7.3.2).

5.3.2.4 Bioinformatic analysis

Computational analysis of the 10q23.1-23.3 interval was performed in order to prioritise genes for genetic analysis. Genomic sequence of the selected genes within the interval was accessed through the NCBI and the ENSEMBL databases.

5.3.2.5 PCR amplification of candidate genes

Twelve pairs of primers were designed using the Primer 3 Output program (http://frodo.wi.mit.edu/cgi-bin/primer3/primer3_www.cgi) in order to screen the coding regions together with the splice sites (GT/AG), and the 5` UTR of both *RGR* and *LRRC21* genes (Table 6, appendix 1). The primers used for mutation screening of the *PCDH21* gene together with the primers for the CA-dinucleotide repeat within intron 9 of the *PCDH21* were as previously published (Bolz *et al.,* 2005).

5.3.2.6 Mutation screening

Direct sequence analysis of one affected member from family A was performed for mutation screening of the above three genes. This was performed on the automated fluorescence DNA sequencer (ABI 3100, Perkin Elmer, Foster City, CA), according to manufacture's instruction (section 2.4.1). Subsequently, 56 patients with EOCD/LCA/arRP were included in the mutation screening of *PCDH21* gene.

5.3.2.7 Restriction enzyme analysis

To confirm the segregation pattern of the change identified within exon 4 of *PCDH21* gene in family A, a restriction enzyme digest analysis using *Hae*III enzyme (Promega, UK) was carried out as previously described (see section 2.6).

5.3.2.8 Genotyping analysis

A cohort of 192 patients with EOCD/LCA/arRP were genotyped using a CA-dinucleotide repeat within intron 9 of the *PCDH21* gene in order to study the role of *PCDH21* gene in other types of retinal degenerations. Searching for a homozygous pattern of the CA repeat within the above cohort was undertaken. This is based on the assumption that patients harbouring a mutation within *PCDH21* gene may belong to consanguineous families. Genotyping was performed on the ABI PRISM 3100 genetic analyser (Applied Biosystems). Data collection and allele identification were performed using GeneScan and Genotyper software version 3.7 (Applied Biosystems) (section 2.7.1).

5.3.2.9 Haplotyping analysis

Haplotyping analysis of the parents, one unaffected and one affected members of family A together with two sporadic patients was performed using 11 SNPs and 6 microsatellite markers within and spanning the *PCDH21* gene, respectively (Table 5.1). The data for heterozygosity and the optimisation conditions for the microsatellite markers are shown in table 7, appendix 1.

5.4 RESULTS

5.4.1 10K GeneChip mapping array for family A

A region of homozygosity starting from 84021870 to 94744240 Mb spanning an interval of 10 cM on chromosome 10q23.1-23.3 was identified using the ALOHOMORA software (Figure 5.4). This represented the most significant region of homozygosity across the human genome in the family studied based on its length, the number of contiguous SNPs within the interval (47) and on their heterozygosity which was deduced from the parents and the unaffected individuals' alleles. Other regions of homozygosity were also observed on chromosomes 7 and 12. However, they were not significant based on the number of contiguous SNPs and or their heterozygosity. A LOD score of more than 2, suggestive of linkage, on 10q23.1-23.3 was generated by Genehunter (Figure 5.5).

Figure 5.4 Lod score of family A generated by the ALOHOMORA software

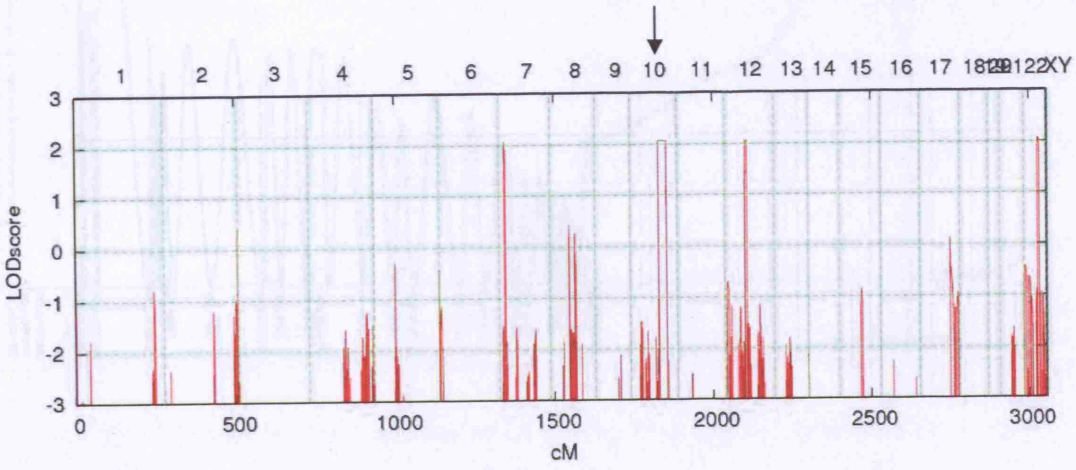

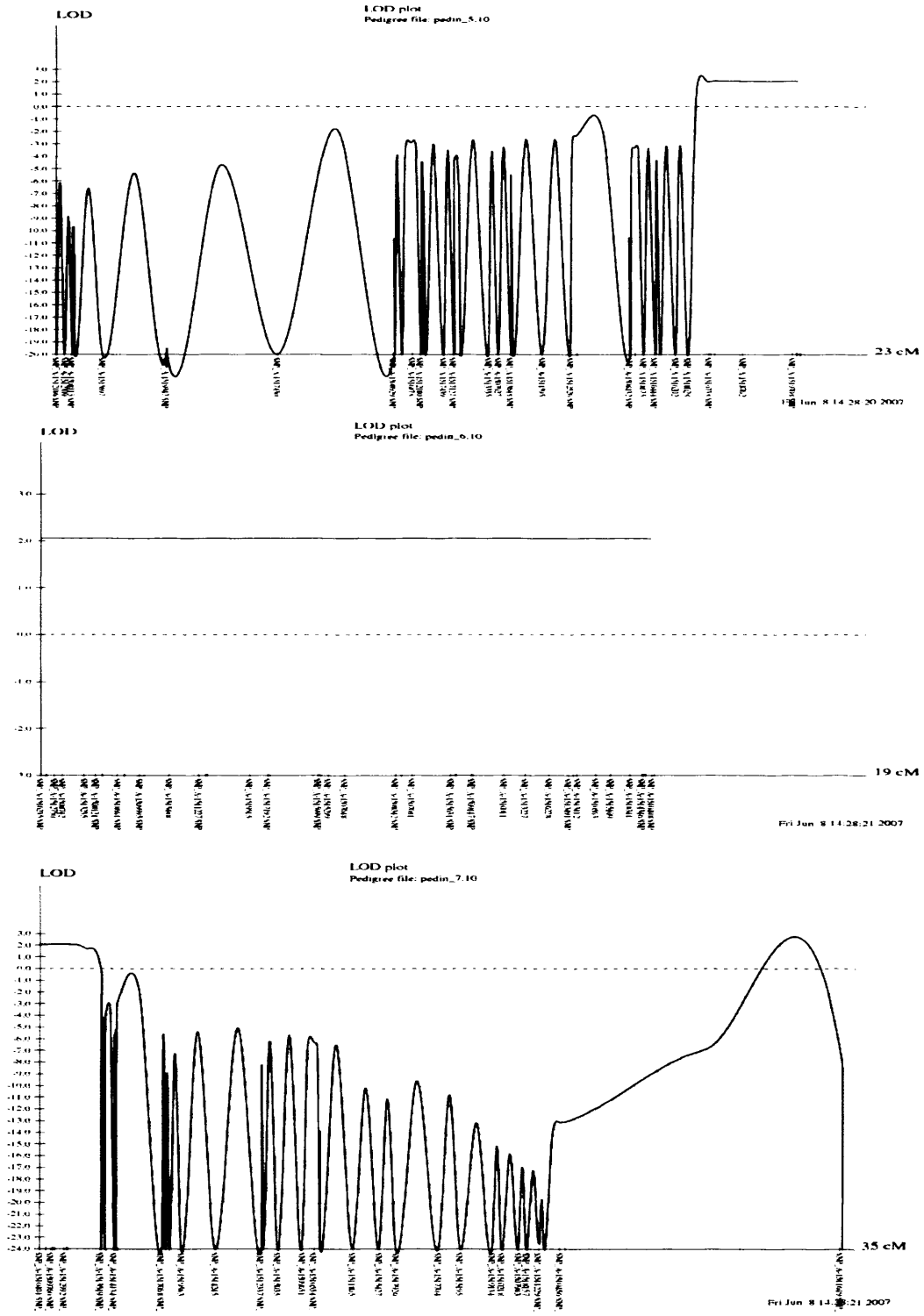

Figure 5.5 LOD plots generated by Genehunter on chromosome 10q23.1-23.3

5.4.2 Bioinformatic analysis

Computational analysis revealed that the 10q23.1-23.3 interval contains approximately 45 genes of which 4, *PCDH21*; *LRRC21* (Leucine-rich repeat-containing protein 21 precursor Retina-specific protein PAL); *RGR* (RPE-retinal G protein-coupled receptor) and *OPN4* (Melanopsin), were considered as good candidates for the retinal dystrophy phenotype in the Jordanian family.

5.4.2.1 *PCDH21*

PCDH21 (MIM609502) known as *prCAD* was initially reported to be specifically expressed in the olfactory bulb of the rat brain (Yagi and Takeichi 2000; Nakajima *et al.*, 2001). Subsequently, hybridisation of mouse and bovine *prCAD* cDNA probe to total RNA from various rat and bovine tissues revealed a 4.5 kb transcript present exclusively in the retina. In situ hybridisation to mouse and bovine retina has further defined the distribution of *prCAD* mRNA to the photoreceptors. Furthermore, rabbit polyclonal antibodies were raised to localise the prCAD protein within photoreceptor cells revealing that it is confined to the base of the photoreceptor outer segment in both rods and cones. Furthermore, in the pcdh21 knockout mice, progressive loss of photoreceptor cells with a 50% reduction in nuclei number by the age of 6 months has been reported making this gene an ideal candidate for retinal dystrophies (Rattner *et al.*, 2001).

5.4.2.2 *LRRC21*

The second interesting gene within the refined interval was *LRRC21* that encodes a putative type I transmembrane protein containing five leucine-rich repeats (LRRs), a single C2 type immunoglobulin (Ig)-like domain and a single fibronectin type III domain. *LRRC21* showed specific expression in the rat retina but only on day 14

postnatally (P14) and was considered to be a new member of the LRR and Ig superfamily and hence named Pal (photoreceptor-associated LRR superfamily). Additionally, it has been reported that Pal might take part in the phototransduction pathway because of the correlation between its expression and the photoreceptor cells response to light (Gomi *et al.,* 2000).

5.4.2.3 *RGR*

RGR (MIM 600342) is a rhodopsin homologue that has been reported to be preferentially expressed in the RPE and Müller cells of the neural retina (Jiang *et al.,* 1993). Later, Morimura et al. (1999) reported a homozygous missense mutation in one index patient with recessive RP together with a heterozygous one base pair insertion near the 3` end of the coding region in a patient diagnosed with choroidal sclerosis.

5.4.2.4 *OPN4*

Melanopsin (*OPN4*-MIM 606665), the last candidate gene within the interval was originally reported to be expressed only in the eye. Then, via in situ hybridisation histochemistry *OPN4* expression was shown to be restricted to a few cells within the ganglion and the amacrine cell layers of the primate and murine retinas. Based on the unique inner retinal localisation of *OPN4* it was concluded that it may mediate non visual photoreceptor tasks, such as circadian rhythms regulation and acute suppression of pineal melatonin (Provencio *et al.,* 2000). Recently, generation of melanopsin knockout mice showed that these mice entrained to a light/dark cycle, phase shifted after a light response and increased circadian period when light intensity increased (Ruby *et al.,* 2002).

5.4.3 Mutation screening

5.4.3.1 Mutation screening of *RGR* and *LRRC21* genes

Initially, mutation screening of both *RGR* and *LRRC21* genes in family A was carried out. The data obtained revealed no pathological sequence alterations within the coding regions or the splice sites of the two genes and hence ruled them out as causative for the RD phenotype in this family.

5.4.3.2 Mutation screening of *PCDH21* gene

Molecular genetic analysis of the full coding regions and the splice sites (GT/AG) of the cDNA sequence of *PCDH21* (GenBank accession number NM_033100.1) revealed a single base-pair deletion within exon 4 (c.338delG p.113fs) in the proband of the Jordanian family. The deletion was homozygous in the proband and heterozygous in her unaffected father, leading to a frameshift and a termination codon 3-bp downstream of the change (Figure 5.6 A-C).

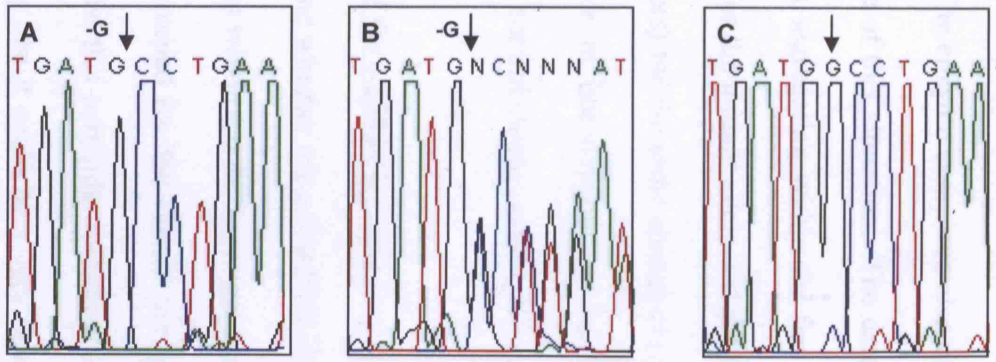

Figure 5.6 Electropherograms of a change detected in *PCDH21*. (**A**) The proband of Family A (IV-2) showing a homozygous c.338delG; (**B**) Unaffected parent of family A (III-1) displaying the c.338delG as heterozygote; (**C**) Control individual showing the wild type allele at c.338G/G.

5.4.4 Restriction enzyme analysis

5.4.4.1 Cosegregation analysis of family A

To study the segregation pattern of the change identified in family A, a restriction enzyme digest analysis was carried out as previously described (see section 2.6). The mutation leads to loss of the *Hae*III enzyme site with the recognition sequence 5`...GG$^{\nabla}$CC...3`. The enzyme assay was also used to test the control population for the presence or absence of this alteration. The data obtained from this assay revealed that the frame shift was segregating within the family members since all affected siblings were homozygous for the mutant allele and the parents and the unaffected siblings were heterozygous (carriers) for the same change (Figure 5.7). Also, the same change has not been detected either in homozygous or heterozygous state in 292 Caucasian and ethnically matching control chromosomes, reinforcing its pathogenic nature.

5.4.4.2 Frequency of the c.338delG change

In order to determine whether the c.338delG could be considered as a recurrent change or a mutation hotspot within the *PCDH21* gene, a panel of 192 arRP/EOCD and 96 LCA patients has been screened for that change using the restriction enzyme assay. The data obtained revealed that this particular mutation was not detected in any of the examined patients highlighting that it could be a very rare mutation confined to a specific ethnic group.

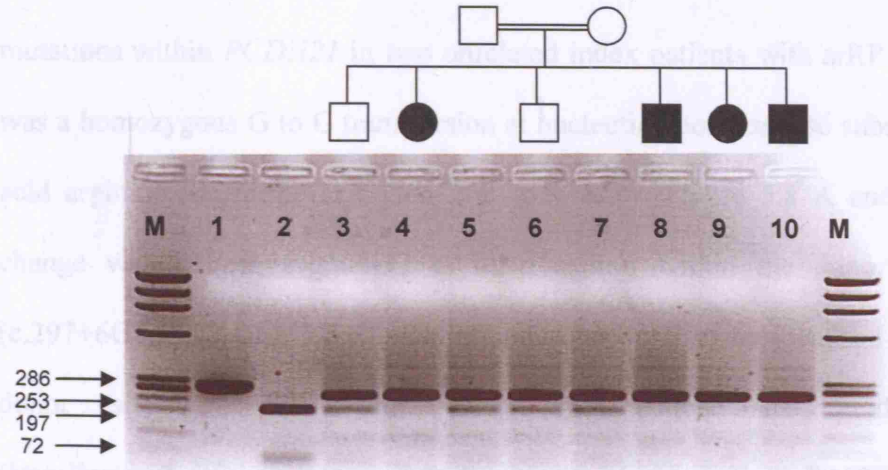

Figure 5.7 Cosegregation study of Family A members using *Hae*III restriction enzyme. Lane 1 is an undigested PCR product (286 bp). Lane 2 is a completely digested PCR product representing the wild type allele (two products 197 and 56 bp). Affected individuals (lanes 4, 8, 9 and 10) showed the homozygous mutant allele (one product 253 bp). Unaffected individuals, carriers (lanes 3, 5, 6 and 7) display the mutant allele in a heterozygous state (two products 253 and 197 bp). M is the ϕX174RF DNA *Hae*III marker.

5.4.5 Genotyping analysis

Fifty six out of 192 patients were found homozygous for the CA repeat denoting that it could be in close LD with the disease phenotype. Therefore, these patients were considered as good candidates for *PCDH21* mutation screening. PCR amplification and direct sequence analyses of the full length *PCDH21* gene was carried out for the above patients. The data obtained from the analysis revealed two additional homozygous mutations within *PCDH21* in two unrelated index patients with arRP. The first change was a homozygous G to C transversion at nucleotide position 486 substituting an amino acid arginine for serine at codon 162 (p.R162S) (Figure 5.8 A and B). The second change was a homozygous G to A transition within the donor site of exon 3 (c.297+6G>A) (Figure 5.8 C and D) and was found to be localised within the splice donor site of the gene using the splice site prediction software (http://www.fruitfly.org/seq_tools/splice.html). Moreover the p.R162S was predicted to be in a highly conserved region of the protein as determined by multiple sequence alignment, CLUSTAL W (1.82) program, across different species (Figure 5.9). Since the two changes, p.R162S and c.297+6G>A, did not create or abolish a restriction enzyme site, a rapid enzyme digest assay could not be established to test their frequency in control population. Hence direct sequencing was used which confirmed that the two changes were not detected in 292 control chromosomes.

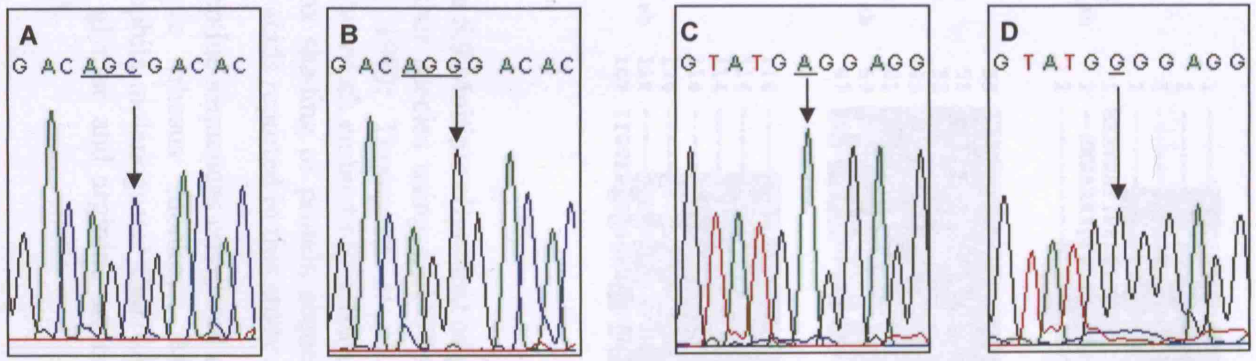

Figure 5.8 Electropherograms of the changes detected in *PCDH21*. (**A**) sporadic patient 1 (S1) and (**B**) control individual are depicting the p.R162S change (G>C) and its wild type allele, respectively; (**C**) sporadic patient 2 (S2) and (**D**) control subject are displaying the splice site change (G>A) and its wild type allele, respectively.

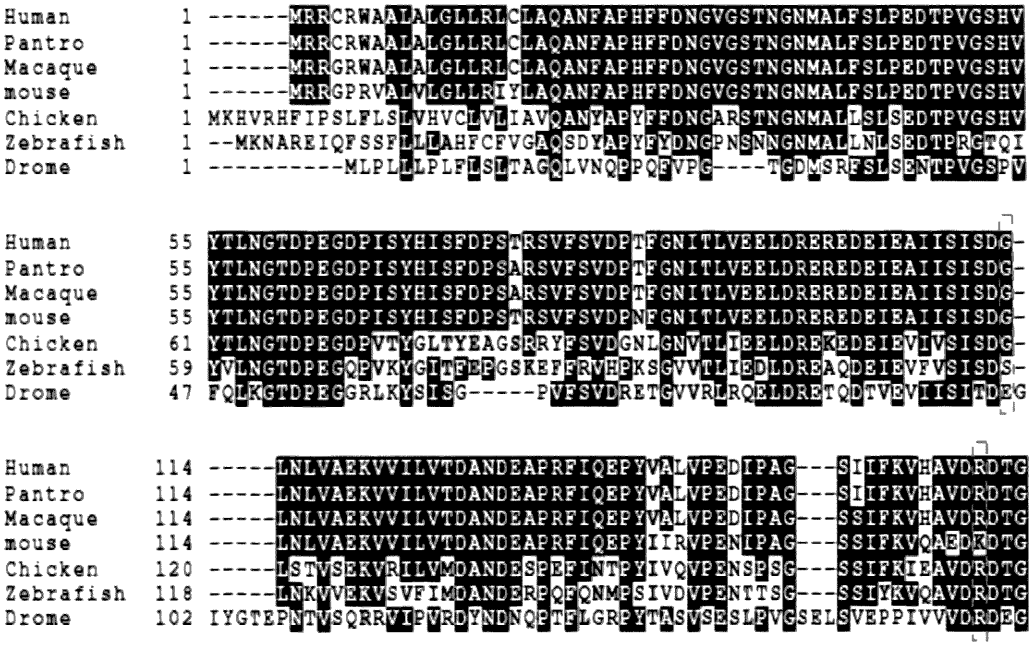

Figure 5.9 Multiple alignment of part of PCDH21 peptide sequence in human and other species using CLUSTAL W program version 1.82 (Higgins and Sharp, 1989; Thompson *et al.*,1994). The WWW-BOX-SHADE–server (http://www.ch.embnet.org/software/BOX_form.html) was used for aligning and box shading of protein sequences. The positions of two of the mutated amino acids reported in this study are boxed.

The peptide sequences compared are PCDH21 Human, Pantro (Chimpanzee), Macaque (rhesus monkey), Mouse, Chicken, Zebrafish and Drome (Drosophila melanogaster Cad74A). Both c.338delG and p.R162S are boxed where glycine and arginine amino acids are highly conserved among other species.

5.4.6 Haplotyping analysis

The data obtained from this analysis revealed that all the affected subjects were homozygous for the tested SNPs or microsatellite markers but with different crossover positions (Table 5.1). Hence, this is confirming that the second sporadic patient is a product of a consanguineous family since the possibility of having a homozygous change within a patient originating from non consanguineous marriage is rare.

Table 5.1 Haplotype analysis of parents (A-III-1 and A/III-2), an unaffected (A/IV-2) and an affected (A/IV-2) members of family A, in addition to two sporadic patients (B/S1) and (S2) using SNPs and msm_s within and flanking the *PCDH21* gene, respectively.

Family ID/patient No.			A/III-1	A/III-2	A/IV-1	A/IV-2	B/S1	S2	SNP/ msm_s /mutation
SNP/msm_s	SNP/msm_s Position (Mb)	AA change	Haplotype of the identified SNPs, msm and mutations						
D10S580	77.728	-	5/6	6/9	6/9	6/6	5/6	3/8	msm
D10S1730	78.601	-	4/5	4/8	4/8	4/4	1/1	4/6	msm
D10S1686	85.555	-	4/5	5/11	5/11	5/5	8/8	5/8	msm
c.151+95C>T	85.945	-	C/T	C/C	C/C	C/C	C/C	C/C	rs11592361
c.159C>A	85.946	H53H	C/A	C/C	C/C	C/C	C/C	C/C	rs12781048
c.240C>T	85.946	V80V	C/T	C/C	C/C	C/C	C/C	C/C	rs11593005
c.297+6G>A	85.946	-	G/G	G/G	G/G	G/G	G/G	***A/A***	Mutation
c.338delG	85.946	p.113fs	***G/-***	***G/-***	***G/-***	***-/-***	G/G	G/G	Mutation
c.349-62T>C	85.948	-	T/T	T/T	T/T	T/T	T/T	T/T	rs17103205
c.349-49T>C	85.948	-	T/T	T/T	T/T	T/T	C/C	T/T	rs11200917
c.439-83A/C	85.950	-	A/A	A/C	A/C	A/A	A/A	A/A	rs11200920
c.439-61C/T	85.950	-	C/T	C/C	C/C	C/C	T/T	C/C	rs10788334
c.477A>G	85.950	A159A	A/G	A/A	A/A	A/A	G/G	A/A	rs4933975
c.486G>C	85.950	R163S	G/G	G/G	G/G	G/G	***C/C***	G/G	Mutation
c.728C>T	85.952	A243V	C/C	C/C	C/C	C/C	C/C	T/T	rs7086200
c.863-282$(CA)_{15}$	85.955	-	3/5	3/8	3/8	3/3	6/6	2/2	rs33968278
c.863-9C/T	85.955	-	C/C	C/C	C/C	C/C	T/T	T/T	rs4933977
c.1662A>G	85.962	E554E	A/G	A/A	A/A	A/A	A/A	G/G	rs10749482
D10S1774	86.000	-	3/4	3/7	3/7	3/3	6/6	2/2	msm
D10S573	86.291	-	3/5	3/5	3/5	3/3	7/7	6/6	msm
D10S1765	89.591	-	4/5	4/5	4/5	4/4	5/5	1/7	msm

SNP: single nucleotide polymorphisms, msm_s: microsatellite markers, S1: sporadic number 1, S2: sporadic number 2, AA: amino acid

5.5 DISCUSSION

Herein a genomewide linkage search in a consanguineous Jordanian pedigree with arRP phenotype has been performed using the 10K GeneChip Mapping Array. The data obtained revealed linkage to a 10-cM interval on chromosome 10q23.1-23.3 where a good candidate gene that has been associated with progressive photoreceptor degeneration in the prCAD$^{-/-}$ mice, *PCDH21*, resides. Mutation screening of this gene revealed a homozygous one base pair deletion, c.338delG, leading to a frameshift and premature stop codon which was segregating with the disease phenotype in the family and was not detected in 292 ethnically matching control chromosomes.

Also, we have utilised a highly polymorphic CA repeat, IVS9-CA (c.863-282(CA)$_{15}$), within the gene to investigate if this repeat was in close LD with the disease phenotype via genotyping a cohort of LCA/EORD/juvenile RP patients. Fifty six out of 192 patients of the cohort exhibited homozygosity of the CA repeat. In these 56 patients, *PCDH21* was screened for mutations where two novel homozygous point mutations, c.297+6G>A and p.R162S, were identified in two arRP index cases (Figure 5.10). These changes were located in the splice donor site and/or at highly conserved regions of the protein among other species suggesting that *PCDH21* is highly likely a novel gene for arRP (Figure 5.9). It is important to note that two of the identified mutations, c.338delG and c.297+6G>A, are located within the EC1 domain of the PCDH21. Additionally, the p.R162S mutation is positioned within the second EC domain. The three mutations could therefore be affecting the Ca^{2+} binding motif which is necessary for the function of the protein.

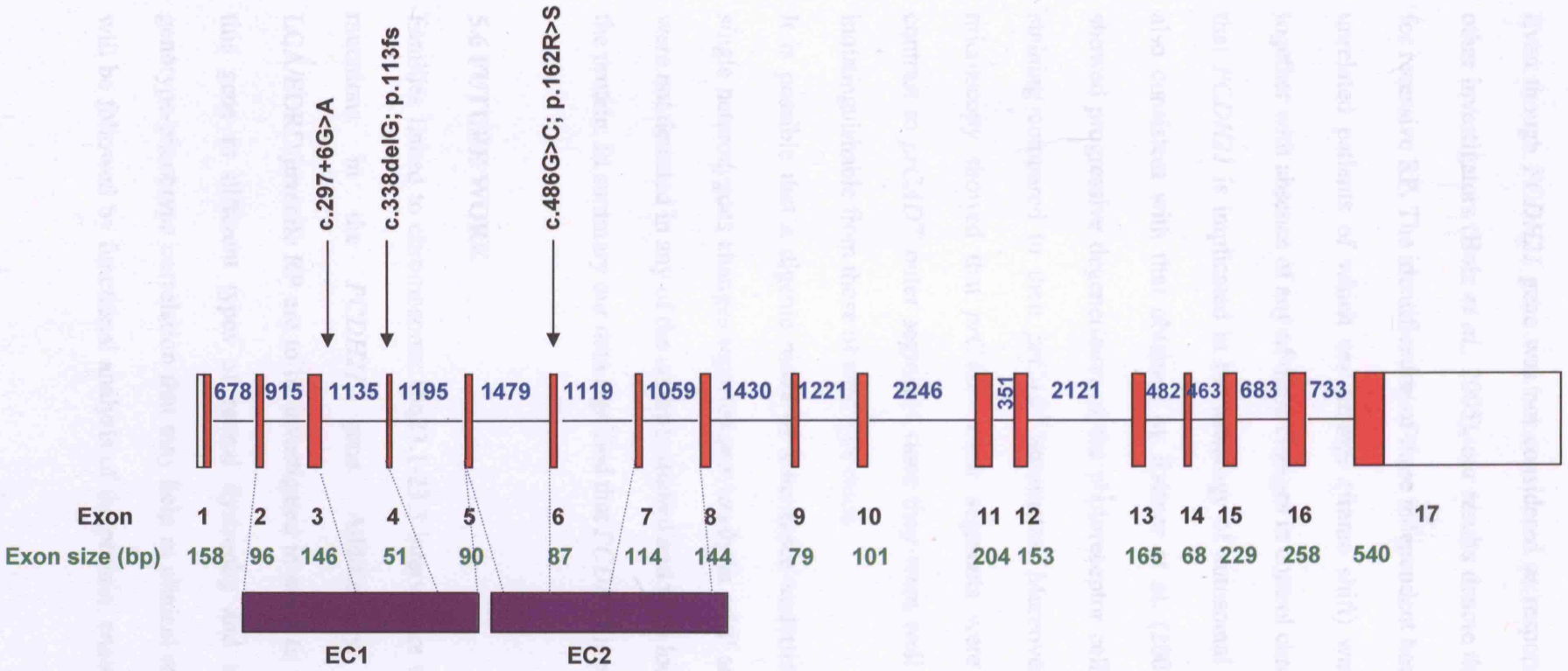

Figure 5.10 Genomic structure of the human *PCDH21* gene. Intron and exon sizes are given in blue and green typeset, respectively. The positions of the mutations identified in relation to the domain structure are depicted (adapted from Bolz *et al.*, 2005)

Even though *PCDH21* gene was not considered as responsible for retinal diseases by other investigators (Bolz *et al.*, 2005), our results denote that *PCDH21* is a novel gene for recessive RP. The identification of three independent homozygous mutations in three unrelated patients of which one change (frame shift) was segregating in the family together with absence of any of these changes in control chromosomes strongly indicates that *PCDH21* is implicated in the aetiology of autosomal recessive RP. This data are also consistent with that obtained by Rattner et al. (2001) since the *prCAD*$^{-/-}$ mice showed progressive degeneration of the photoreceptor cells as determined by TUNEL staining compared to their *prCAD*$^{+/-}$littermates. Moreover, the transmission electron microscopy showed that *prCAD*$^{-/-}$ outer segments were shorter and misaligned in contrast to *prCAD*$^{+/-}$ outer segments since they were well aligned and appeared to be indistinguishable from those of wild type mice.

It is possible that a digenic mode of inheritance underlines the pathogenecity of the single heterozygous changes reported previously in arRP and USH1 patients since they were not detected in any of the controls studied and were located in conserved regions of the protein. In summary our data signified that *PCDH21* is a novel gene for arRP.

5.6 FUTURE WORK

Families linked to chromosome 10q23.1-23.3 interval are to be screened for additional mutations in the *PCDH21* gene. Additionally, sporadic patients with LCA/EORD/juvenile RP are to be investigated in order to better understand the role of this gene in different types of retinal dystrophy and to establish prevalence and genotype-phenotype correlation that may help in clinical management of patients. This will be followed by functional analysis of the protein, encoded by the gene, which may

elucidate the biological basis of the disease. Ultimately the knowledge about the pathobiology of mutations in different RP patients will effectively allow genetic approaches for therapy to be explored.

CHAPTER 6

GENERAL DISCUSSION

6.1 Overview of the work presented

The molecular genetics of autosomal recessive retinitis pigmentosa described herein highlights the marked genetic heterogeneity of retinal dystrophies. Linkage studies have revealed the value of identifying more genes for such debilitating disorder since it will lead to further understanding of the normal visual processes and of pathogenetic mechanisms that lead to retinal degeneration.

This work focused mainly on cloning a major gene, RP25, for recessive RP. RP25 has been mapped to chromosome 6p12.1-q15 between genetic markers D6S257 and D6S1644, a region that spans approximately 16.1 cM in seven Spanish families (Ruiz *et al.,* 1998). Later, a family of Pakistani origin was mapped to an interval 2.4 cM proximal to the same region on chromosome 6 (Khaliq *et al.,* 1999). Recently we have identified 3 Chinese families that also showed linkage to the same interval (Abd El-Aziz *et al.,* 2007). Taking these findings together, strongly supports our hypothesis that RP25 gene could be a frequent cause of retinitis pigmentosa.

At the start of this work confirmation of the original linkage of RP25 (Ruiz *et al.,* 1998) using the 10K array analysis was undertaken. This was followed by implementation of different strategies in order to identify the disease gene. To date, with the combined effort of the two groups (London-Seville) ~55 % of the genes in the interval were excluded as responsible for the pathogenesis of the RP25 phenotype. Additionally, the data obtained from the CGH array revealed a deleted clone within the RP25 interval in all affected members of a consanguineous family indicating that one of the genes within

this interval could be responsible for the RP25 phenotype.

A novel strategy for mapping disease loci in nuclear non-consanguineous recessive RP families has also been presented in this work. Initially, linkage analysis using SNPs/microsatellite markers or mutation screening of the known arRP genes excluded all loci/genes with the exception of the RP25 locus in the 3 Chinese families. Subsequently, a whole genome scan for the three families using the 10K GeneChip Mapping Array was performed in order to identify the possible disease locus. To the best of our knowledge, this is the first report on the utilisation of the 10K GeneChip to study linkage in non-consanguineous Chinese arRP. This analysis indicated that the studied families were probably linked to the RP25 locus and hence enforcing the speculation that RP25 represents a major locus for recessive RP.

Finally, a genomewide linkage search in a consanguineous Jordanian pedigree with arRP phenotype has been performed using the 10K GeneChip Mapping Array. The data obtained revealed linkage to a 10-cM interval on chromosome 10q23.1-23.3 where *PCDH21* gene, a good candidate that has been associated with progressive photoreceptor degeneration in the prCAD$^{-/-}$ mice, resides. Mutation screening of *PCDH21* revealed a homozygous one base pair deletion, c.338delG, leading to a frameshift and premature stop codon which was segregating with the disease phenotype in the family studied and was not detected in 292 ethnically matching control chromosomes. Furthermore, two homozygous point mutations, c.297+6G>A and p.R162S, were also identified in two arRP index cases and were located in the splice donor site and/or at highly conserved regions of the protein among other species suggesting that *PCDH21* is highly likely to be a novel gene for arRP.

The work presented here is not only a contribution to ophthalmic genetics but also a step forward in the study of the pathogenesis of recessive RP. It is anticipated that future development of novel therapies in clinical medicine will incorporate informed pharmacogenomics and gene based therapies. Therefore it is essential that as many of the remaining RP causing genes are identified rapidly to develop a comprehensive understanding of the pathogenetic mechanisms involved in RP.

6.2 Molecular genetics and its therapeutic role

The heterogeneous nature of retinal dystrophies complicates the application of any potential therapy, since treatment may need to be targeted for defects in a range of genes. However, cloning of each gene leads to further understanding of the normal visual processes and of the mechanisms leading to retinal degeneration. Before any therapy for a retinal dystrophy can be formulated, we need to completely understand the molecular basis of the disease. Once we understand how the disease process is mediated and how the mutated gene triggers the response, only then can a rational therapy be designed.

By studying the genes and mutations involved in retinal degeneration we hope to learn more about how these genes function and interact normally and how they malfunction to cause progressive blindness. Also by sorting out all the different forms of eye diseases that share the common symptom of retinal degeneration and pigmentation, we can alongside our clinical colleagues; establish a genotype/phenotype correlation and offer genetic counselling for families with RP.

Identifying DNA mutation(s) responsible for RP can form the basis of new, DNA-based diagnostic tests. Such tests may allow better care of patients, where individuals at risk of

the disease can be identified at the earliest stages of the disease and will have the opportunity to benefit from informed genetic counselling. Carriers of mutant genes can also be identified, making it possible to precisely diagnose cases before the development of clinically recognisable symptoms. Therefore, it will be possible to offer prenatal and postnatal diagnosis of pre-symptomatic individuals which will enable possible therapeutic interventions to be made at an early stage.

The next step will be to develop new methods of treatment based on the specific molecular patho-physiology that has been discovered as a result of characterising the abnormal gene and resultant gene products. Once the gene is identified, it will be possible to develop cell culture methods and to generate animal models to study the functions of the relevant gene. Ultimately, the characterisation of the gene will be a first step toward gene or gene based therapy which theoretically can involve the specific replacement, correction, or augmentation of a dysfunctional gene.

In addition to understanding the pathogenesis of retinal degenerations, identification of disease genes may offer the possibility of treatment at a molecular level by direct transfer of therapeutic genes into the relevant tissue. Such genes may be transferred by a variety of viral or non-viral vectors. It has been reported that gene transfer was able to correct the complex ultrastructural photoreceptor cell defect in the retinal degeneration slow (rds) mouse (Ali *et al.,* 2000). This approach is potentially much easier in recessive diseases where the transfer of a single copy of the gene may be sufficient to correct the loss of function that is causing the disease phenotype. Ultimately, through the research outlined in this thesis we hope to contribute to the development of an effective therapy for the recessive forms of RP.

6.3 Animal models

Understanding the pathway from the occurrence of a gene mutation to the development of a specific phenotype in patients is critical before rationally designing a therapy. Animal models are crucial to understanding this process and to develop a treatment. Some naturally occurring animal models are known. However, over the past few years, transgenic engineering has allowed the generation of a rapidly growing number of animal models (Fauser *et al.*, 2002).

It has been reported that apoptosis is the mechanism of photoreceptor cell death in different models with various underlying genetic defects (Portera-Cailliau *et al.*, 1994) postulating that blocking this common pathway may be the ultimate cure. Even though blocking apoptosis proved its inefficiency in preventing retinal degeneration (Joseph and Li, 1996), the combination of two apoptosis inhibitor genes delayed retinal degeneration in a genetic model by a synergistic effect (Eversole-Cire *et al.*, 2000).

Potential therapeutic agents, such as vitamin A (Li *et al.*, 1998) or somatic gene therapy (Acland *et al*, 2001; Ali *et al.*, 2000) have been tested using animal models. Additionally, studying environmental effects such as diet or light on the process of degeneration have been also studied. For example light was reported to accelerate the retinal degeneration in various animal models (Hafezi *et al.*, 1997; LaVail *et al.*, 1999).

6.4 Future perspectives for therapy

The outcome of ophthalmic genetics is the early detection and treatment of eye diseases. The retina is an attractive target for gene therapy because of its accessibility and immune privilege. Research studies are working towards retinal therapy and advances will ultimately allow therapy for a larger range of ocular disorders.

In dealing with recessive disorders it is anticipated that gene therapy will be the ideal treatment since the transfer of a single copy of a gene may be sufficient to correct the loss of function that is causing the disease phenotype.

It has been reported that gene replacement therapy in RPE65-deficient dogs via subretinal injection of the defective gene was successful (Acland *et al.,* 2005). This was proved by the fact that electrophysiological analysis demonstrated restoration of rod and cone photoreceptor function which started as early as 15 days post-injection, reaching its peak function at 3 months post-injection, and remaining stable thereafter in all animals treated at 8-11 months of age. This was assessed by the ability of these animals to avoid obstacles in both dim and normal light; functional vision was restored in the treated eye, whereas the untreated contralateral eye served as an internal control. However, the dog treated at a later age (30 months) did not recover retinal function or vision, suggesting that there might be a therapeutic window for the successful treatment of RPE65-/- dogs by such a technique (Le Meur *et al.,* 2007). Subsequently, the same technique has been used for the first time in a patient with LCA who had a mutation in the same gene, RPE65, however, the results are yet to be reported. I strongly believe that the knowledge gained from this study and others may contribute enormously in the refinement of molecular pathophysiology of retinitis pigmentosa and could lead to new methods of prevention, diagnosis and treatment.

REFERENCES

Abd El-Aziz, M.M., El-Ashry, M.F., Chan, W.M., Chong, K.L., Barragan, I., Antinolo, G., Pang, C.P. and Bhattacharya, S.S. (2007) A novel genetic study of Chinese families with autosomal recessive retinitis pigmentosa. *Ann. Hum. Genet.* **71**(3): 281-294.

Abd El-Aziz, M.M., Patel, R.J., El-Ashry, M.F., Barragan, I., Marcos, I., Borrego, S., Antinolo, G. and Bhattacharya S.S. (2006) Exclusion of four candidate genes, KHDRBS2, PTP4A1, KIAA1411 and OGFRL1, as causative of autosomal recessive retinitis pigmentosa. *Ophthalmic. Res.* **38**(1): 19-23.

Abd El-Aziz, M.M., Patel, R.J., El-Ashry, M.F., Barragan, I., Marcos, I., Borrego, S., Antinolo, G. and Bhattacharya S.S. (2005) Molecular Genetic Analysis of Two Functional Candidate Genes in the Autosomal Recessive Retinitis Pigmentosa, RP25, Locus. *Curr. Eye Res.* **30**(12): 1081-1087.

Abecasis, G.R., Cherny, S.S., Cookson, W.O. and Cardon, L.R. (2001a) GRR: graphical representation of relationship errors. *Bioinformatics* **17**(8): 742-743.

Abecasis G.R., Cherny S.S., Cookson W.O. and Cardon L.R. (2001b) Merlin-rapid analysis of dense genetic maps using sparse gene flow trees. *Nat. Genet.* **30**(1): 97-101.

Acland, G.M., Aguirre, G.D., Bennett, J., Aleman, T.S., Cideciyan, A.V., Bennicelli, J., Dejneka, N.S., Pearce-Kelling, S.E., Maguire, A.M., Palczewski, K., Hauswirth, W.W., Jacobson and S.G. (2005) Long-term restoration of rod and cone vision by single dose rAAV-mediated gene transfer to the retina in a canine model of childhood blindness. *Mol.Ther.* **12**(6): 1072-1082.

Acland, G.M., Aguirre, G.D., Ray, J., Zhang, Q., Aleman, T.S., Cideciyan, A.V., Pearce-Kelling, S.E., Anand, V., Zeng, Y., Maguire, A.M., Jacobson, S.G., Hauswirth, W.W. and Bennett, J. (2001) Gene therapy restores vision in a canine model of childhood blindness. *Nat. Genet.* **28**(1): 92-95.

Ahmed, Z.M., Morell, R.J., Riazuddin, S., Gropman, A., Shaukat, S., Ahmad, M.M., Mohiddin, S.A., Fananapazir, L., Caruso, R.C., Husnain, T., Khan, S.N., Riazuddin, S., Griffith, A.J., Friedman, T.B. and Wilcox, E.R. (2003) Mutations of *MYO6* are associated with recessive deafness, DFNB37. *Am. J. Hum. Genet.* **72**(5): 1315-1322.

Ahmed, Z.M., Riazuddin, S., Bernstein, S.L., Ahmed, Z., Khan, S., Griffith, A.J., Morell, R.J., Friedman, T.B., Riazuddin, S. and Wilcox, E.R. (2001) Mutations of the protocadherin gene PCDH15 cause Usher syndrome type 1F. *Am. J. Hum. Genet.* **69**(1): 25-34.

Airik, R., Bussen, M., Singh, M.K., Petry, M. and Kispert, A. (2006) Tbx18 regulates the development of the ureteral mesenchyme. *J. Clin. Invest.* **116**(3): 663-674.

Aitman, T.J., Dong, R., Vyse, T.J., Norsworthy, P.J., Johnson, M.D., Smith, J., Manglon, J., Roberton-Lowe, C., Marshall, A.J., Petretto, E. Hodges, MD, Bhangal, G, Patel, SG, Sheehan-Rooney, K., Duda, M., Cook, P.R., Evans, D.J., Domin, J., Flint, J., Boyle, J.J., Pusey, C.D. and Cook, H.T. (2006) Copy number polymorphism in *Fcgr3* predisposes to glomerulonephritis in rats and humans. *Nature* **439**(7078): 851–855.

Alagramam, K.N., Yuan, H., Kuehn, M.H., Murcia, C.L., Wayne, S., Srisailpathy, C.R., Lowry, R.B., Knaus, R., Van Laer, L., Bernier, F.P., Schwartz, S., Lee, C., Morton, C.C., Mullins, R.F., Ramesh, A., Van Camp, G., Hageman, G.S., Woychik, R.P. and Smith, R.J. (2001) Mutations in the novel protocadherin PCDH15 cause Usher syndrome type 1F. *Hum. Mol. Genet.* **10**(16): 1709-1718.

Ali, R.R., Sarra, G.M., Stephens, C., Alwis, M.D., Bainbridge, J.W., Munro, P.M., Fauser, S., Reichel, M.B., Kinnon, C., Hunt, D.M., Bhattacharya, S.S. and Thrasher, A.J. (2000) Restoration of photoreceptor ultrastructure and function in retinal degeneration slow mice by gene therapy. *Nat Genet.* **25**(3): 306-10.

Al-Khayer, K., Hagstrom, S., Pauer, G., Zegarra, H., Sears, J. and Traboulsi, E. I. (2004) Thirty-year follow-up of a patient with Leber congenital amaurosis and novel RPE65 mutations. *Am. J. Ophthalmol.* **137**(2): 375-377.

Allen, L.E., Zito, I., Bradshaw, K., Patel, R.J., Bird, A.C., Fitzke, F., Yates, J.R., Trump, D., Hardcastle, A.J. and Moore, A.T. (2003) Genotype-phenotype correlation in British families with X linked congenital stationary night blindness.*Br. J. Ophthalmol.* **87**(11): 1413-1420.

Allikmets, R., Singh, N., Sun, H., Shroyer, N.F., Hutchinson, A., Chidambaram, A., Gerrard, B., Baird, L., Stauffer, D., Peiffer, A., Rattner, A., Smallwood, P., Li, Y., Anderson, K.L., Lewis, R.A., Nathans, J., Leppert, M., Dean, M. and Lupski, J.R. (1997) A photoreceptor cell–specific ATP-binding transporter gene (*ABCR*) is mutated in recessive Stargardt macular dystrophy. *Nat. Genet.* **15**(3): 236–246.

Anderson, S., Bankier, A.T., Barrell, B.G., de Bruijn, M.H., Coulson, A.R., Drouin, J., Eperon, I.C., Nierlich, D.P., Roe, B.A., Sanger, F., Schreier, P.H., Smith, A.J., Staden, R. and Young, I.G. (1981) Sequence and organization of the human mitochondrial genome. *Nature* **290**(5806): 457-465.

Angst, B.D., Marcozzi, C. and Magee, A.I. (2001) The cadherin superfamily. *J. Cell Sci.* **114**(4): 625-626.

Aula, N., Salomaki, P., Timonen, R., Verheijen, F., Mancini, G., Mansson, J.E., Aula, P. and Peltonen, L. (2000) The spectrum of *SLC17A5*-gene mutations resulting in free

sialic acid-storage diseases indicates some genotype-phenotype correlation. *Am. J. Hum. Genet.* **67**(4): 832-840.

Ayoub, G.S. and Matthews, G. (1992), Substance P modulates calcium current in retinal bipolar neurons. *Vis. Neurosci.* **8**(6): 539.

Ayuso, C., Garcia-Sandoval, B., Najera, C., Valverde, D., Carballo, M. and Antinolo, G. (1995) Retinitis pigmentosa in Spain. The Spanish multicentric and multidisciplinary group for research into retinitis pigmentosa. *Clin. Genet.* **48**(3): 120-122.

Baala, L., Romano, S., Khaddour, R., Saunier, S., Smith, U.M., Audollent, S., Ozilou, C., Faivre, L., Laurent, N., Foliguet, B., Munnich, A., Lyonnet, S., Salomon, R., Encha-Razavi, F., Gubler, M.C., Boddaert, N., de Lonlay, P., Johnson, C.A., Vekemans, M., Antignac, C., Attie-Bitach, T. (2007) The Mekel-Gurber syndrome gene, MKS3, is mutated in Joubert syndrome. *Am J. Hum.Genet.* **80**: 186-194.

Bannai H., Fukatsu K., Mizutani A., Natsume T., Iemura S., Ikegami T., Inoue T. and Mikoshiba K. (2004) An RNA-interacting protein, SYNCRIP (heterogeneous nuclear ribonuclear protein Q1/NSAP1) is a component of mRNA granule transported with inositol 1,4,5-trisphosphate receptor type 1 mRNA in neuronal dendrites. *J. Biol. Chem.* **279**(51): 53427-34.

Bareil C., Hamel C.P., Delague V., Arnaud B., Demaille J. and Claustres M. (2001) Segregation of a mutation in CNGB1 encoding the beta-subunit of the rod cGMP-gated channel in a family with autosomal recessive retinitis pigmentosa. *Hum. Genet.* **108**(4): 328-334.

Barragan I., Marcos I., Borrego S. and Antiñolo G. (2005) Mutation screening of three candidate genes, *ELOVL5*, *SMAP1* and *GLULD1* in autosomal recessive retinitis pigmentosa. *Int. J. Mol. Med.* **16**(6): 1163-1167.

Barragan I., Marcos I., Borrego S. and Antiñolo G. (2005) Molecular analysis of RIMI in autosomal recessive retinitis pigmentosa. *Ophthalmic Res.* **37**(2): 89-93.

Baylor, D.A. (1987) Photoreceptor signals and vision. Proctor lecture. *Invest. Ophthalmol. Vis. Sci.* **28**(1): 34-49.

Bech-Hansen, N.T., Naylor, M.J., Maybaum, T.A., Pearce, W.G., Koop, B., Fishman, G.A., Mets, M., Musarella, M.A. and Boycott, K.M. (1998) Loss-of-function mutations in a calcium-channel alpha-1-subunit gene in Xp11.23 cause incomplete X-linked congenital stationary night blindness. *Nat. Genet.* **19**(3): 264-267.

Bessant, D.A.R., Kaushal, S. and Bhattashaya, S.S. (2003) Genetics and biology of the inherited retinal disorders In Adler's physiology of the eye (Paul L. Kaufman, and Albert Alm) 10th ed .

Bessant, D.A., Ali, R.R. and Bhattacharya, S.S. (2001) Molecular genetics and prospects for therapy of the inherited retinal dystrophies. *Curr. Opin. Genet. Dev.* **11**(3): 307-316.

Bird, A.C. (1995) Retinal photoreceptor dystrophies LI. Edward Jackson Memorial Lecture. *Am. J. Ophthalmol.* **119**(5): 543-562.

Bolz, H. and Ebermann, I. and Gal, A. (2005) Protocadherin-21 (PCDH21), a candidate gene for human retinal dystrophies.*Mol. Vis.* **11**: 929-933.

Bolz, H., von Brederlow, B., Ramírez, A., Bryda, E.C., Kutsche, K., Nothwang, H.G., Seeliger, M., del C-Salcedó, Cabrera, M., Vila, M.C., Molina, O.P., Gal, A. and Kubisch, C. (2001) Mutation of CDH23, encoding a new member of the cadherin gene family, causes Usher syndrome type 1D. *Nat. Genet.* **27**(1): 108-112.

Bork, J.M., Peters, L.M., Riazuddin, S., Bernstein, S.L., Ahmed, Z.M., Ness, S.L., Polomeno, R., Ramesh, A., Schloss, M., Srisailpathy, C.R., Wayne, S., Bellman, S., Desmukh, D., Ahmed, Z., Khan, S.N., Kaloustian, V.M., Li, X.C., Lalwani, A., Riazuddin, S., Bitner-Glindzicz, M., Nance, W.E., Liu, X.Z., Wistow, G., Smith, R.J., Griffith, A.J., Wilcox, E.R., Friedman, T.B. and Morell, R.J. (2001) Usher syndrome 1D and nonsyndromic autosomal recessive deafness DFNB12 are caused by allelic mutations of the novel cadherin-like gene CDH23. *Am. J. Hum. Genet.* **68**(1): 26-37.

Bormann, J. and Feigenspan, A. (1995) GABAc receptors. *Trends Neurosci.* **18**(12): 515–519.

Botstein, D. and Risch N. (2003) Discovering genotypes underlying human phenotypes: Past successes for mendelian disease, future approaches for complex disease. *Nat. Genet.* **33**: 228-37.

Botstein, D., White R.L., Skolnick M. and Davis R.W. (1980) Construction of a genetic linkage map in man using restriction fragment length polymorphisms. *Am. J. Hum. Genet.* **32**(3): 314-331.

Bowes, C. Li, T., Danciger, M., Baxter, L.C., Applebury, M.L. and Farber, D.B. (1990) Retinal degeneration in the rd mouse is caused by a defect in the beta subunit of rod cGMP-phosphodiesterase. *Nature.* **347**(6294): 677-680.

Boyle J.M., Grzeschik K.H., Heath P.R., Morten J.E. and Stern P.L. (1990) Trophoblast glycoprotein recognised by monoclonal antibody 5T4 maps to human chromosome 6q14-q15. *Hum. Genet.* **84**(5): 455-458.

Broadhead, R., Dawe, H.R., Farr, H., Griffiths, S., Hart, S.R., Portman, N., Shaw, M.K., Ginger, M.L., Gaskell, S.J., McKean, P.G. and Gull, K. (2006) Flagellar motility is required for the viability of the bloodstream trypanosome. *Nature* **440**(7081): 224-227.

Bron, A.J., Tripathi, R.C. and Tripathi, B.J. (2003) The retina, in Wolff's Anatomy of the Eye and Orbit, 8th edition pp. 460-464.

Burghes, A.H.M., Vaessin, H.E.F. and de la Chapelle, A. (2001) The land between mendelian and multifactorial inheritance. *Science* **293**(5538): 2213-2214.

Bussen, M., Petry, M., Schuster-Gossler, K., Leitges, M., Gossler, A. and Kispert, A. (2004) The T-box transcription factor Tbx18 maintains the separation of anterior and posterior somite compartments. *Genes Dev.* **18**(10): 1209-1221.

Bykhovskaya, Y., Mengesha, E., Wang, D., Yang, H., Estivill, X., Shohat, M. and Fischel-Ghodsian, N. (2004) Phenotype of non-syndromic deafness associated with the mitochondrial A1555G mutation is modulated by mitochondrial RNA modifying enzymes MTO1 and GTPBP3. *Mol. Genet. Metab.* **83**(3):199-206.

Callanan D. Chapter 19: Toxic retinopathies. Text Atlas of the Retina. Eds. Hamilton, Gregson, and Fish. Martin Dunitz Ltd.: London, 1998.

Camuzat, A., Dollfus, H., Rozet, J.-M., Gerber, S., Bonneau, D., Bonnemaison, M., Briard, M.-L., Dufier, J.-L., Ghazi, I., Leowski, C., Weissenbach, J., Frezal, J., Munnich, A. and Kaplan, J. (1995) A gene for Leber's congenital amaurosis maps to chromosome 17p. *Hum. Molec. Genet.* **4**(8): 1447-1452.

Cao, H., Williams, C., Carter, M. and Hegele, R.A. (2004) CKN1 (MIM 216400): mutations in Cockayne syndrome type A and a new common polymorphism. *J. Hum. Genet.* **49**(1): 61-63.

Carroll, P., Renoncourt, Y., Gayet, O., De Bovis, B. and Alonso, S. (2001) Sorting nexin-14, a gene expressed in motoneurons trapped by an in vitro preselection method. *Dev. Dyn.* **221**(4): 431-42.

Castrop, H., Huang, Y., Hashimoto, S., Mizel, D., Hansen, P., Theilig, F., Bachmann, S., Deng, C., Briggs, J. and Schnermann, J. (2004) Impairment of tubuloglomerular feedback regulation of GFR in ecto-5-prime-nucleotidase/CD73-deficient mice. *J. Clin. Invest.* **114**(5): 634-642.

Cates, C.A., Michael, R.L., Stayrook, K.R., Harvey, K.A., Burke, Y.D., Randall, S.K., Crowell, P.L. and Crowell, D.N. (1996) Prenylation of oncogenic human PTP(CAAX) protein tyrosine phosphatases. *Cancer Lett.* **110**(1-2): 49-55.

Chen, J., Liu, L. and Pohajdak, B. (1995) Cloning a cDNA from human NK/T cells which codes for a protein with high proline content. *Biochim. Biophys. Acta.* **1264**(1): 19-22.

Chen, L., Xin, Z.C., Li, X., Tian, L., Yuan, Y.M., Liu, G., Jiang, X.J. and Guo, Y.L. (2006) Cox7a2 mediates steroidogenesis in TM3 mouse Leydig cells. *Asian J. Androl.* **8**(5): 589-594.

Cohen, A.I. (1992) The Retina. In MJ Hart Jr (ed), *Adler's Physiology of the Eye 9th ed.* St. Louis: Mosby-Year Book, p. 579.

Collin, G.B., Marshall, J.D., Ikeda, A., So, W.V., Russell-Eggitt, I., Maffei, P., Beck, S., Boerkoel, C.F., Sicolo, N., Martin, M., Nishina, P.M. and Naggert, J.K. (2002) Mutations in *ALMS1* cause obesity, type 2 diabetes and neurosensory degeneration in Alstrom syndrome. *Nat. Genet.* **31**(1): 74-78.

Collins, L.J., Poole, A.M. and Penny, D. (2003) Using ancestral sequences to uncover potential gene homologues. *Appl. Bioinformatics.* **2**(3 suppl):S85-95.

Cook, C.S., Ozanics, V. and Jakobiec, F.A. (1994) Prenatal development of the eye and its adnexa. In W Tasman, EA Jaeger [eds], Duanes Foundations of clinical ophthalmology [Vol 1]. Philadelphia: Lippincott, p. 49.

Cote, J., Boisvert, F.M., Boulanger, M.C., Bedford, M.T. and Richard, S. (2003) Sam68 RNA binding protein is an in vivo substrate for protein arginine N-methyltransferase 1. *Molec. Biol. Cell.* **14**(1): 274-287.

Cowper, A.E., Cáceres, J.F., Mayeda, A. and Screaton, G.R. Serine-arginine (SR) protein-like factors that antagonize authentic SR proteins and regulate alternative splicing. *J. Biol. Chem.* **276**(52): 48908-14.

Cui, J., Wang, W., Lai, M.D., Xu, E.P., Lv, B.J., Lin, J., Ruan, W.J., Ma, Y. and Yao, C. (2006) Identification of a novel VNTR polymorphism in C6orf37 and its association with colorectal cancer risk in Chinese population. *Clin. Chim. Acta.* **368**(1-2): 155-9.

Cutting, G.R., Curristin, S., Zoghbi, H., O'Hara, B., Seldin, M.F. and Uhl, G.R. (1992) Identification of a γ-aminobutyric acid (GABA) receptor subunit rho_2 cDNA and colocalization of the genes encoding rho_2 (GABRR2) and rho1 (GABRR1) to human chromosome 6q14-q21 and mouse chromosome 4. *Genomics* **12**(4): 801--806.

Cutting, G.R., Lu, L., O'Hara, B.F., Kasch, L.M., Montrose-Rafizadeh, C., Donovan, D.M., Shimada, S., Antonarakis, S.E., Guggino, W.B., Uhl, G.R. and Kazazian JR, H.H. (1991) Cloning of the γ-aminobutyric acid (GABA) ρ1 cDNA: a GABA receptor subunit highly expressed in the retina. *Proc. Natl. Acad. Sci. USA* **88**(7): 2673–2677.

Czarny-Ratajczak, M., Lohiniva, J., Rogala, P., Kozlowski, K., Perala, M., Carter, L., Spector, T.D., Kolodziej, L., Seppanen, U., Glazar, R., Krolewski, J., Latos-Bielenska, A. and Ala-Kokko, L. (2001) A mutation in COL9A1 causes multiple epiphyseal dysplasia: further evidence for locus heterogeneity. *Am. J. Hum. Genet.* **69**(5): 969-980.

Daly, M.J., Rioux, J.D., Schaffner, S.F., Hudson, T.J. and Lander, E. (2001) High-resolution haplotype structure in the human genome. *Nat. Genet.* **29**(2): 229–232.

den Hollander, A.I., Heckenlively, J.R., van den Born, L.I., de Kok, Y.J., van der Velde-Visser, S.D., Kellner, U., Jurklies, B., van Schooneveld, M.J., Blankenagel, A., Rohrschneider, K., Wissinger, B., Cruysberg, J.R., Deutman, A.F., Brunner, H.G., Apfelstedt-Sylla, E., Hoyng, C.B. and Cremers, F.P. (2001) Leber congenital amaurosis and retinitis pigmentosa with Coats-like exudative vasculopathy are associated with mutations in the crumbs homologue 1 (CRB1) gene. *Am. J. Hum. Genet.* **69**(1): 198-203.

den Hollander, A.I., Koenekoop, R.K., Mohamed, M.D., Arts, H.H., Boldt, K., Towns, K.V., Sedmak, T., Beer, M., Nagel-Wolfrum, K., McKibbin, M., Dharmaraj, S., Lopez, I., Ivings, L., Williams, G.A., Springell, K., Woods, C.G., Jafri, H., Rashid, Y., Strom, T.M., van der Zwaag, B., Gosens, I., Kersten, F.F., van Wijk, E., Veltman, J.A., Zonneveld, M.N., van Beersum, S.E., Maumenee, I.H., Wolfrum, U., Cheetham, M.E., Ueffing, M., Cremers, F.P., Inglehearn, C.F. and Roepman, R. (2007) Mutations in LCA5, encoding the ciliary protein lebercilin, cause Leber congenital amaurosis. *Nat. Genet.* **39**(7): 889-895.

den Hollander, A.I., ten Brink, J.B., de Kok, Y.J., van Soest, S., van den Born, L.I., van Driel, M.A., van de Pol, D.J., Payne, A.M., Bhattacharya, S.S., Kellner, U., Hoyng, C.B., Westerveld, A., Brunner, H.G., Bleeker-Wagemakers, E.M., Deutman, A.F., Heckenlively, J.R., Cremers, F.P. and Bergen, A.A. (1999) Mutations in a human homologue of Drosophila crumbs cause retinitis pigmentosa (RP12). *Nat. Genet.* **23**(2): 217-221.

Dharmaraj, S., Li, Y., Robitaille, J. M., Silva, E., Zhu, D., Mitchell, T.N., Maltby, L.P., Baffoe-Bonnie, A.B. and Maumenee, I.H. (2000) A novel locus for Leber congenital amaurosis maps to chromosome 6q. *Am J Hum Genet.* **66**(1):319-326.

Diamond, R.H., Cressman, D.E., Laz, T.M., Abrams, C.S. and Taub, R. (1994) PRL-1, a unique nuclear protein tyrosine phosphatase, affects cell growth. Cell Biol. **14**(6): 3752-3762.

Ditzel, H.J., Masaki, Y., Nielsen, H., Farnaes, L. and Burton, D.R. (2000) Cloning and expression of a novel human antibody--antigen pair associated with Felty's syndrome. *Proc. Nat. Acad. Sci.* **97**(16): 9234-9239.

Dowling, J.E. (1987) The retina: an approachable part of the brain, Cambridge, The Belknap Press of Harvard University Press.

Dryja, T.P., Finn, J.T., Peng, Y.W., McGee, T.L., Berson, E.L. and Yau, K.W. (1995) Mutations in the gene encoding the alpha subunit of the rod cGMP-gated channel in autosomal recessive retinitis pigmentosa. *Proc. Nat. Acad. Sci.* **92**(22): 10177-10181.

Dryja, T.P., Hahn, L.B., Cowley, G.S., McGee, T.L. and Berson, E.L. (1991) Mutation spectrum of the rhodopsin gene among patients with autosomal dominant retinitis pigmentosa. *Proc. Nat. Acad. Sci.* **88**(20): 9370-9374.

Dryja, T.P., McGee, T.L., Hahn, L.B., Cowley, G.S., Olsson, J.E., Reichel, E., Sandberg, M.A. and Berson, E.L. (1990) Mutations within the rhodopsin gene in patients with autosomal dominant retinitis pigmentosa. *New Eng. J. Med.* **323**(19): 1302-1307

Dryja, T.P., McGee, T.L., Berson, E.L., Fishman, G.A., Sandberg, M.A., Alexander, K.R., Derlacki, D.J. and Rajagopalan, A.S. (2005) Night blindness and abnormal cone electroretinogram ON responses in patients with mutations in the *GRM6* gene encoding mGluR6. *Proc. Nat. Acad. Sci.* **102**(13): 4884-4889.

Eckmiller, M.S. (1990) Distal invaginations and the renewal of cone outer segments in anuran and monkey retinas. *Cell Tissue Res.* **260**(1): 19-28.

Edelmann, L., Wasserstein, M.P., Kornreich, R., Sansaricq, C., Snyderman, S.E. and Diaz, G.A. (2001) Maple syrup urine disease: identification and carrier-frequency determination of a novel founder mutation in the Ashkenazi Jewish population. *Am. J. Hum. Genet.* **69** (4): 863-868.

Edwards, A., Voss, H., Rice, P., Civitello, A., Stegemann, J., Schwager, C., Zimmermann, J., Erfle, H., Caskey, C.T. and Ansorge, W. (1990) Automated DNA sequencing of the human HPRT locus. *Genomics* **6**(4): 593-608.

Eggenschwiler, J.T., Espinoza, E. and Anderson, K.V. (2001) Rab23 is an essential negative regulator of the mouse Sonic hedgehog signalling pathway. *Nature* **412**(6843): 194-198.

Euler, T. and Wassle, H. (1995) Immunocytochemical identification of cone bipolar cells in the rat retina. *J. Comp. Neurol.* **361**(3): 461-478.

Eversole-Cire, P., Concepcion, F.A., Simon, M.I., Takayama, S., Reed, J.C. and Chen, J. (2000) Synergistic effect of Bcl-2 and BAG-1 on the prevention of photoreceptor cell death. *Invest. Ophthalmol. Vis. Sci.* **41**(7): 1953-1961.

Farhang-Fallah, J., Yin, X., Trentin, G., Cheng, A.M. and Rozakis-Adcock, M. (2000) Cloning and characterization of PHIP, a novel insulin receptor substrate-1 pleckstrin homology domain interacting protein. *J. Biol. Chem.* **275**(51): 40492-40497.

Farrar, G.J., Kenna, P.F. and Humphries P. (2002) On the genetics of retinitis pigmentosa and on mutation-independent approaches to therapeutic intervention. *EMBO* **21**(5): 857-864.

Farrar, G.J., Kenna, P., Jordan, S.A., Kumar-Singh, R., Humphries, M.M., Sharp, E.M., Sheils, D.M. and Humphries, P. (1991) A three-base-pair deletion in the peripherin-RDS gene in one form of retinitis pigmentosa. *Nature* **354**(6353): 478-80.

Farrar, G.J., McWilliam, P., Bradley, D.G., Kenna, P., Lawler, M., Sharp, E.M. Humphries, M.M., Eiberg, H., Conneally, P.M., Trofatter, J.A. and Humphries, P. (1990) Autosomal dominant retinitis pigmentosa: linkage to rhodopsin and evidence for genetic heterogeneity. *Genomics* **8**(1): 35-40.

Fauser, S., Luberichs, J. and Schuttauf, F. (2002) Genetic animal models for retinal degeneration. *Surv. Ophthalmol.* **47**(4): 357-67.

Ferland, R.J., Eyaid, W., Collura, R.V., Tully, L.D., Hill, R.S., Al-Nouri, D., Al-Rumayyan, A., Topcu, M., Gascon, G., Bodell, A., Shugart, Y.Y., Ruvolo, M., Walsh, C.A. (2004) Abnormal cerebellar development and axonal decussation due to mutations in AHI1 in Joubert syndrome. *Nat. Genet.* **36**(10): 1008-113.

Feuk, L., Marshall, C.R., Wintle, R.F. and Scherer, S.W. (2006) Structural variants: changing the landscape of chromosomes and design of disease studies. *Hum. Mol. Genet.* **15**: R57-66.

Finckh, U., Xu, S., Kumaramanickavel, G., Schurmann, M., Mukkadan, J.K., Fernandez, S.T., John, S., Weber, J.L., Denton, M.J. and Gal, A. (1998) Homozygosity mapping of autosomal recessive retinitis pigmentosa locus (RP22) on chromosome 16p12.1-p12.3. *Genomics* **48**(3): 341-345.

Fischer, U., Struss, A.K., Hemmer, D., Michel, A., Henn, W., Steudel, W.I. and Meese, E. (2001) PHF3 expression is frequently reduced in glioma. *Cytogenet. Cell Genet.* **94**(3-4): 131-136.

Fisk, H.A., Mattison, C.P. and Winey, M. (2003) Human Mps1 protein kinase is required for centrosome duplication and normal mitotic progression. *Proc. Nat. Acad. Sci.* **100**(25): 14875-14880.

Fitzgerald, J. and Bateman, J.F. (2001) A new FACIT of the collagen family: COL21A1. *FEBS* **505**(2): 275-280.

Francois, J. (1968) Leber's congenital tapetoretinal degeneration. *Int. Ophthalmol. Clin.* Winter **8**(4): 929-47.

Freund, C.L., Wang, Q.L., Chen, S., Muskat, B.L., Wiles, C.D., Sheffield, V.C., Jacobson, S.G., McInnes, R.R., Zack, D.J. and Stone, E.M. (1998) De novo mutations in the CRX homeobox gene associated with Leber congenital amaurosis. *Nat. Genet.* **18**(4): 311-312.

Friedman, J.S., Chang, B., Kannabiran, C., Chakarova, C., Singh, H.P., Jalali, S., Hawes, N.L., Branham, K., Othman, M., Filippova, E., Thompson, D.A., Webster, A.R., Andreasson, S., Jacobson, S.G., Bhattacharya, S.S., Heckenlively, J.R. and Swaroop, A. (2006) Premature truncation of a novel protein, RD3, exhibiting subnuclear localization is associated with retinal degeneration. *Am. J. Hum. Genet.* **79**(6): 1059-1070.

Fuchs, S., Nakazawa, M., Maw, M., Tamai, M., Oguchi, Y. and Gal, A. (1995) A homozygous 1-base pair deletion in the arrestin gene is a frequent cause of Oguchi disease in Japanese. *Nat. Genet.* **10**(3): 360-362.

Gal, A., Li, Y., Thompson, D.A., Weir, J., Orth, U., Jacobson, S.G., Apfelstedt-Sylla, E. and Vollrath, D. (2000) Mutations in MERTK, the human orthologue of the RCS rat retinal dystrophy gene, cause retinitis pigmentosa. *Nat. Genet.* **26**(3): 270-271.

Gal, A., Orth, U., Baehr, W., Schwinger, E. and Rosenberg, T. (1994) Heterozygous missense mutation in the rod cGMP phosphodiesterase beta-subunit gene in autosomal dominant stationary night blindness. *Nat. Genet.* **7**(4): 64-68.

Gehrig, A., Felbor, U., Kelsell, R.E., Hunt, D.M., Maumenee, I.H. and Weber, B.H. (1998) Assessment of the interphotoreceptor matrix proteoglycan-1 (IMPG1) gene localised to 6q13-q15 in autosomal dominant Stargardt-like disease (ADSTGD), progressive bifocal chorioretinal atrophy (PBCRA), and North Carolina macular dystrophy (MCDR1). *J. Med. Genet.* **35**(8): 641-645.

Gerber, S., Rozet, J.M., Takezawa, S.I., dos Santos, L.C., Lopes, L., Gribouval, O., Penet, C., Perrault, I., Ducroq, D., Souied, E., Jeanpierre, M., Romana, S., Frézal, J., Ferraz, F., Yu-Umesono, R., Munnich, A. and Kaplan, J. (2000) The photoreceptor cell-specific nuclear receptor gene (PNR) accounts for retinitis pigmentosa in the Crypto-Jews from Portugal (Marranos), survivors from the Spanish Inquisition. *Hum. Genet.* **107**(3): 276-284.

Gibson, S.A. and Shillitoe, E.J. (1997) Ribozymes. Their functions and strategies for their use. *Mol. Biotechnol.* **7**(2): 125-137.

Goldstein, O., Zangerl, B., Pearce-Kelling, S., Sidjanin, D.J., Kijas, J.W., Felix, J., Acland, G.M. and Aguirre, G.D. (2006) Linkage disequilibrium mapping in domestic dog breeds narrows the progressive rod-cone degeneration interval and identifies ancestral disease-transmitting chromosome. *Genomics* **88**(5): 541-550.

Gomi, F., Imaizumi, K., Yoneda, T.., Taniguchi, M., Mori, Y., Miyoshi, K., Hitomi, J., Fujikado, T., Tano, Y. and Tohyama, M. (2000) Molecular Cloning of a Novel Membrane Glycoprotein, Pal, Specifically Expressed in Photoreceptor Cells of the Retina and Containing Leucine-Rich Repeat. *J. Neurosci.* **20**(9): 3206-3213.

Gonzalez, E., Kulkarni, H., Bolivar, H., Mangano, A., Sanchez, R., Catano, G., Nibbs, R.J., Freedman, B.J., Quinones, M.P., Bamshed, M.J. Murthy, K.K., Rovin, B.H.,

Bradley, W., Clark, R.A., Anderson, S.A., O'connell, R.J., Agan, B.K., Ahuja, S.S., Bologna, R., Sen, L., Dolan, M.J. and Ahuja, S.K. (2005) The influence of *CCL3L1* gene—containing segmental duplications on HIV-1/AIDS susceptibility. *Science* **307**(5714): 1434–1440.

Gonzalez-Fernandez, F., Kurz, D., Bao, Y., Newman, S., Conway, B.P., Young, J.E., Han, D.P. and Khani, S.C. (1999) 11-cis Retinal dehydrogenase mutations as a major cause of the congenital night-blindness disorder known as fundus albipunctatus. *Molec. Vis.* **5**: 41.

Gonzalez-Manchon, C., Butta, N., Ferrer, M., Ayuso, M.S. and Parrilla, R. (1997) Molecular cloning and functional characterization of the human cytosolic malic enzyme promoter: thyroid hormone responsiveness. *DNA Cell Biol.* **16**(5): 533-544.

Griesinger, I.B., Sieving, P.A. and Ayyagari, R. (2000) Autosomal dominant macular atrophy at 6q14 excludes CORD7 and MCDR1/PBCRA loci. *Invest. Ophthalmol. Vis. Sci.* **41**(1): 248-255.

Gu, S., Kumaramanickavel, G., Srikumari, C.R., Denton, M.J. and Gal, A. (1999) Autosomal recessive retinitis pigmentosa locus RP28 maps between D2S1337 and D2S286 on chromosome 2p11-p15 in an Indian family. *J. Med. Genet.* **36**(9): 705-707.

Gunther, T., Struwe, M., Aguzzi, A. and Schughart, K. (1994) open brain, a new mouse mutant with severe neural tube defects, shows altered gene expression patterns in the developing spinal cord. *Development* **120**(11): 3119-3130.

Guo, L., Degenstein, L., Dowling, J., Yu, Q.C., Wollmann, R., Perman, B. and Fuchs, E. (1995) Gene targeting of BPAG1: abnormalities in mechanical strength and cell migration in stratified epithelia and neurologic degeneration. *Cell* **81**(2): 233-243.

Hafezi, F., Steinbach, J.P., Marti, A., Munz, K., Wang, Z.Q., Wagner, E.F., Aguzzi, A. and Reme, C.E. (1997) The absence of c-fos prevents light-induced apoptotic cell death of photoreceptors in retinal degeneration in vivo. *Nat. Med.* **3**(3): 346-349.

Hageman, G.S., Kirchoff-Rempe, M.A., Lewis, G.P., Fisher, S.K. and Anderson, D.H. (1991) Sequestration of basic fibroblast growth factor in the primate retinal interphotoreceptor matrix. *Proc. Natl. Acad. Sci.* U S A. **88**(15): 6706-10.

Hageman, G.S. and Kuehn, M.H., (1998) The pigmented retinal epithelium: Current aspects of function and disease. In: Marmor, M., Wolfensberger, T. (Eds.), Biology of the Retina-IPM-RPE Interface. Oxford University Press, New York, pp 417-454.

Hageman, G.S., Marmor, M.F., Yao, X.Y. and Johnson, L.V. (1995) The interphotoreceptor matrix mediates primate retinal adhesion. *Arch. Ophthalmol.* **113**(5): 655-660.

Hagstrom, S.A., North, M.A., Nishina, P.M., Berson, E.L. and Dryja, T.P. (1998) Recessive mutations in the gene encoding the tubby-like protein TULP1 in patients with retinitis pigmentosa. *Nat. Genet.* **18**(2): 174-176.

Hameed, A., Khaliq, S., Ismail, M., Anwar, K., Ebenezer, N.D., Jordan, T., Mehdi, S.Q., Payne, A.M. and Bhattacharya S.S. (2000) A novel locus for Leber congenital amaurosis (LCA4) with anterior keratoconus mapping to chromosome 17p13. *Invest. Ophthalmol. Vis. Sci.* **41**(3): 629-633.

Hameed, A., Khaliq, S., Ismail, M., Anwar, K., Mehdi, S.Q., Bessant, D., Payne, A.M. and Bhattacharya, S.S. (2001) A new locus for autosomal recessive RP (RP29) mapping to chromosome 4q32-q34 in a Pakistani family. *Invest. Ophthalmol. Vis. Sci.***42**(7): 1436–1438.

Hao, Z., Wolkowicz, M.J., Shetty, J., Klotz, K., Bolling, L., Sen, B., Westbrook, V.A., Coonrod, S., Flickinger, C.J. and Herr, J.C. (2002) SAMP32, a testis-specific, isoantigenic sperm acrosomal membrane-associated protein. *Biol. Reprod.* **66**(3): 735-44.

Hayashi, T., Huang, J. and Deeb, S.S. (2000) RINX (VSX1), a novel homeobox gene expressed in the inner nuclear layer of the adult retina. *Genomics* **67**(2): 128-139.

Hardcastle, A.J., Thiselton, D.L., Van Maldergem, L., Saha, B.K., Jay, M., Plant, C., Taylor, R., Bird, A.C. and Bhattacharya, S. (1999) Mutations in the RP2 gene cause disease in 10% of families with X-linked retinitis pigmentosa assessed in this study. *Am. J. Hum. Genet.* **64**(4): 1210-1215.

Hearn, T., Renforth, G.L., Spalluto, C., Hanley, N.A., Piper, K., Brickwood, S., White, C., Connolly, V., Taylor, J.F.N.; Russell-Eggitt, I.; Bonneau, D.; Walker, M. and Wilson, D. I. (2002) Mutation of *ALMS1*, a large gene with a tandem repeat encoding 47 amino acids, causes Alstrom syndrome. *Nat. Genet.* **31**(1): 79-83.

Henning, K.A., Li, L., Iyer, N., McDaniel, L.D., Reagan, M.S., Legerski, R., Schultz, R.A., Stefanini, M., Lehmann, A.R., Mayne, L.V. and Friedberg, E.C. (1995) The Cockayne syndrome group A gene encodes a WD repeat protein that interacts with CSB protein and a subunit of RNA polymerase II TFIIH. *Cell* **82**(4): 555-564.

Heon, E., Greenberg, A., Kopp, K.K., Rootman, D., Vincent, A.L., Billingsley, G., Priston, M., Dorval, K.M., Chow, R.L., McInnes, R.R., Heathcote, G., Westall, C., Sutphin, J.E., Semina, E., Bremner, R. and Stone, E.M. (2002) VSX1: a gene for posterior polymorphous dystrophy and keratoconus. *Hum. Mol. Genet.* **11**(9): 1029-1036.

Higgins, D.G. and Sharp, P.M. (1989) Fast and sensitive multiple sequence alignments on a microcomputer. *Comput. Appl. Biosci.* **5**(2): 151-3.

Hims, M.M., Diager, S.P. and Inglehearn, C.F. (2003) Retinitis pigmentosa: genes, proteins, and prospects. *Dev. Ophthalmol.* **37**: 109-125.

Hollyfield, J.G., Varner, H.H., Rayborn, M.E. and Osterfeld, A.M. (1989) Retinal attachment to the pigment epithelium. Linkage through an extracellular sheath surrounding cone photoreceptors. *Retina* **9**(1): 59-68.

Holt, I.J., Harding, A.E., Petty, R.K.H. and Morgan-Hughes, J.A. (1990) A new mitochondrial disease associated with mitochondrial DNA heteroplasmy. *Am. J. Hum. Genet.* **46**(3): 428-433.

Hopkinson, D.A. and Harris, H. (1968) A third phosphoglucomutase locus in man. *Ann. Hum. Genet.* **31**(4): 359-368.

Hu D.N. (1987) Prevalence and mode of inheritance of major genetic diseases in China. *J. Med Genet.* **24**(10): 584-588.

Huang, S.H., Pittler, S.J., Huang, X., Oliveira, L., Berson, E.L. and Dryja, T.P. (1995) Autosomal recessive retinitis pigmentosa caused by mutations in the alpha subunit of rod cGMP phosphodiesterase. *Nat. Genet.* **11**(4): 468-471.

Hulten, M. and Lindsten, J. (1973) Cytogenetic aspects of human male meiosis. *Adv. Hum. Genet.* **4**: 327-87.

Humphries, M.M., Rancourt, D., Farrar, G.J., Kenna, P., Hazel, M., Bush, R.A., Sieving, P.A., Sheils, D.M., McNally, N., Creighton, P., Erven, A., Boros, A., Gulya, K., Capecchi, M.R. and Humphries, P. (1997) Retinopathy induced in mice by targeted disruption of the rhodopsin gene. *Nat. . Genet.* **15**(2): 216-219.

Imai, Y., Kimura, T., Murakami, A., Yajima, N., Sakamaki, K. and Yonehara, S. (1999) The CED-4-homologous protein FLASH is involved in Fas-mediated activation of caspase-8 during apoptosis. *Nature* **398**(6730): 777-785.

Imiya, K., Ishizaki, T., Seiki, T., Saito, F., Inazawa, J., Oka, S. and Kawasaki, T. (2002) cDNA cloning, genomic structure and chromosomal mapping of the mouse glucuronyltransferase-S involved in the biosynthesis of the HNK-1 carbohydrate epitope. *Gene* **296**(1-2): 29-36.

Ishida, N., Miura, N., Yoshioka, S. and Kawakita, M. (1996) Molecular cloning and characterization of a novel isoform of the human UDP-galactose transporter, and of related complementary DNAs belonging to the nucleotide-sugar transporter gene family. *J. Biochem.* **120**(6): 1074-1078.

Ishikawa, K., Nagase, T., Suyama, M., Miyajima, N., Tanaka, A., Kotani, H., Nomura, N. and Ohara, O. (1998) Prediction of the coding sequences of unidentified human genes. X. The complete sequences of 100 new cDNA clones from brain which can code for large proteins in vitro. *DNA Res.* **5**(3): 169-176.

Jahannsmann, R., Schwinger, E. and Grzeschik, K.H. (1980) Assignment of the gene locus for human phosphoglucomutase 3 to chromosome 6q12-qter. *Ann. Genet.* **23**(1): 12-14.

Janecke, A. R., Thompson, D. A., Utermann, G., Becker, C., Hubner, C. A., Schmid, E., McHenry, C. L., Nair, A. R., Ruschendorf, F., Heckenlively, J., Wissinger, B., Nurnberg, P. and Gal, A. (2004) Mutations in RDH12 encoding a photoreceptor cell retinol dehydrogenase cause childhood-onset severe retinal dystrophy. *Nat. Genet.* **36**(8): 850-854.

Jiang, M., Pandey, S., Fong, HK. (1993) An opsin homologue in the retina and pigment epithelium. *Invest. Ophthalmol. Vis. Sci.* **34**(13): 3669-3678.

Johnson, S., Halford, S., Morris, A.G., Patel, R.J., Wilkie, S.E., Hardcastle, A.J., Moore, A.T., Zhang, K. and Hunt, D.M. (2003) Genomic organisation and alternative splicing of human RIM1, a gene implicated in autosomal dominant cone-rod dystrophy (CORD7). *Genomics* **81**(3): 304-314.

Joseph, R.M. and Li, T. (1996) Overexpression of Bcl-2 or Bcl-XL transgenes and photoreceptor degeneration. *Invest. Ophthalmol. Vis. Sci.* **37**(12): 2434-2446

Kajiwara, K., Hahn, L.B., Mukai, S., Travis, G.H., Berson, E.L. and Dryja, T.P. (1991) Mutations in the human retinal degeneration slow gene in autosomal dominant retinitis pigmentosa. *Nature* **354**(6353): 480-483.

Kajiwara, K., Berson, E.L. and Dryja, T.P. (1994) Digenic retinitis pigmentosa due to mutations at the unlinked peripherin/RDS and ROM1 loci. *Science* **264**(5165): 1604-1608.

Katsanis, N., Ansley, S.J., Badano, J.L., Eichers, E.R., Lewis, R.A., Hoskins, B.E., Scambler, P.J., Davidson, W.S., Beales, P.L. and Lupski, J.R. (2001) Triallelic inheritance in Bardet-Biedl syndrome, a mendelian recessive disorder. *Science* **293** (5538): 2256-2259.

Keen, T.J., Mohamed, M.D., McKibbin, M., Rashid, Y., Jafri, H., Maumenee, I.H. and Inglehearn, C.F. (2003) Identification of a locus (LCA9) for Leber's congenital amaurosis on chromosome 1p36. *Europ. J. Hum. Genet.* **11**(5): 420-423.

Keen, J., Lester, D., Inglehearn, C., Curtis, A. and Bhattacharay, S.S. (1991) Rapid detection of single base mismatches as heteroduplexes on hydrolink gels. *Trends Genet.* 7(1): 5.

Kelsell, R.E., Godley, B.F., Evans, K., Tiffin, P.A.C., Gregory, C.Y., Plant, C., Moore, A.T., Bird, A.C. and Hunt, D.M. (1995) Localization of the gene for progressive bifocal chorioretinal atrophy (PBCRA) to chromosome 6q. *Hum. Mol. Genet.* **4**(9): 1653-1656.

Kelsell, R.E., Gregory-Evans, K., Gregory-Evans, C.Y., Holder, G.E., Jay, M.R., Weber, B.H.F., Moore, A.T., Bird, A.C. and Hunt, D.M. (1998a) Localization of a gene (CORD7) for a dominant cone-rod dystrophy to chromosome 6q. *Am. J. Hum. Genet.* **63** (1): 274-279.

Kelsell, R.E., Gregory-Evans, K., Payne, A.M., Perrault, I., Kaplan, J., Yang, R.B., Garbers, D.L., Bird, A.C., Moore, A.T. and Hunt, D.M. (1998b) Mutations in the retinal guanylate cyclase (RETGC-1) gene in dominant cone-rod dystrophy. *Hum. Mol. Genet.* 7(7): 1179-1184.

Kelton, J.G., Smith, J.W., Horsewood, P., Humbert, J.R., Hayward, C.P.M. and Warkentin, T.E. (1990) Gov(a/b) alloantigen system on human platelets. *Blood* **75**(11): 2172-2176.

Khaleduzzaman, M., Sumiyoshi, H., Ueki, Y., Inoguchi, K., Ninomiya, Y. and Yoshioka, H. (1997) Structure of the human type XIX collagen (COL19A1) gene, which suggests it has arisen from an ancestor gene of the FACIT family. *Genomics* **45**(2): 304-312.

Khaliq, S., Abid, A., Ismail, M., Hameed, A., Mohyuddin, A., Lall, P., Aziz, A., Anwar, K. and Mehdi, S.Q. (2005) Novel association of *RP1* gene mutations with autosomal recessive retinitis pigmentosa. *J. Med. Genet.* **42** (5): 436-438.

Khaliq, S., Hameed, A., Ismail, M., Mehdi, S.Q., Bessant, D.A., Payne, A.M. and Bhattacharya, S.S. (1999) Refinement of the locus for autosomal recessive Retinitis pigmentosa (RP25) linked to chromosome 6q in a family of Pakistani origin. *Am. J. Hum. Genet.* **65**(2):571-574.

Kim, E., Ambroziak, P., Veniant, M.M., Hamilton R.L. and Young S.G. (1998) A gene-targeted mouse model for familial hypobetalipoproteinemia. Low levels of apolipoprotein B mRNA in association with a nonsense mutation in exon 26 of the apolipoprotein B gene. *J. Biol. Chem.* **273**(51): 33977-33984.

Kim, K.I., Baek, S.H., Jeon, Y.J., Nishimori, S., Suzuki, T., Uchida, S., Shimbara, N., Saitoh, H., Tanaka, K. and Chung, C.H. (2000) A new SUMO-1-specific protease, SUSP1, that is highly expressed in reproductive organs. *J. Biol. Chem.* **275**(19): 14102-14106.

Kim, S.K., Suh, M.R., Yoon, H.S., Lee, J.B., Oh, S.K., Moon, S.Y., Moon,. S.H., Lee, J.Y., Hwang, J.H., Cho, W.J. and Kim, K.S. (2005) Identification of developmental pluripotency associated 5 expression in human pluripotent stem cells. *Stem Cells* **23**(4): 458-462.

Kimberling, W.J., Weston, M.D., Moller, C., van Aarem, A., Cremers, C.W.R.J., Sumegi, J., Ing, P.S., Connolly, C., Martini, A., Milani, M., Tamayo, M.L., Bernal, J., Greenberg, J. and Ayuso, C. (1995) Gene mapping of Usher syndrome type IIa: localization of the gene to a 2.1-cM segment on chromosome 1q41. *Am. J. Hum. Genet.* **56**(1): 216-223.

King, K.W., Sheppard, F.C., Westwater, C., Stern, P.L. and Myers, K.A. (1999) Organisation of the mouse and human 5T4 oncofoetal leucine-rich glycoprotein genes and expression in foetal and adult murine tissues. *Biochim. Biophys. Acta* **1445**(3): 257-270.

Kita, M., and Marmor, M.F. (1992) Effects on retinal adhesive force in vivo of metabolically active agents in the subretinal space. *Invest. Ophthalmol. Vis. Sci.***33**(6): 1883-1887.

Knudsen, S.M., Frydenberg, J., Clark, B.F. and Leffers, H. (1993) Tissue-dependent variation in the expression of elongation factor-1 alpha isoforms: isolation and characterisation of a cDNA encoding a novel variant of human elongation-factor 1 alpha. *Eur. J. Biochem.* **215**(3): 549-554.

Kohl, S., Christ-Adler, M., Apfelstedt-Sylla, E., Kellner, U., Eckstein, A., Zrenner, E. and Wissinger, B. (1997) RDS/peripherin gene mutations are frequent causes of central retinal dystrophies. *J. Med. Genet.* **34**(8): 620–626.

Kolb, H., Linberg, K.A. and Fisher, S.K. (1992) Neurons of the human retina: a Golgi study. *J. Comp. Neurol.* **318**(2): 147-187.

Kolb, H., Zhang, L. and Dekorver, L. (1993) Differential staining of neurons in the human retina with antibodies to protein kinase C with isoenzymes. *Vis. Neurosci.* **10**(2): 341-351.

Kolehmainen, J., Black, G.C.M., Saarinen, A., Chandler, K., Clayton-Smith, J., Traskelin, A.-L., Perveen, R., Kivitie-Kallio, S., Norio, R., Warburg, M., Fryns, J.-P., de la Chapelle, A. and Lehesjoki, A.-E. (2003) Cohen syndrome is caused by mutations in a novel gene, COH1, encoding a transmembrane protein with a presumed role in vesicle-mediated sorting and intracellular protein transport. *Am. J. Hum. Genet.* **72**(6): 1359-1369.

Kondo, H., Qin, M., Mizota, A., Kondo, M., Hayashi, H., Hayashi, K., Oshima, K., Tahira, T. and Hayashi, K. (2004) A homozygosity-based search for mutations in patients with autosomal recessive retinitis pigmentosa using microsatellite markers. *Invest. Ophthalmol. Vis. Sci.* **45**(12): 4433-4439.

Krause, W.J. and Cutts, J.H. (1981) *Concise Text of Histology.* Baltimore: Williams and Wilkins, p. 180.

Lander, E.S. and Botestein, D. (1987) Homozygosity mapping: a way to map human recessive traits with the DNA of inbred children. *Science* **236**(4808): 1567-1570.

Lander, E.S., Linton, L.M., Birren, B., Nusbaum, C., Zody, M.C., Baldwin, J., Devon, K., Dewar, K., Doyle, M., FitzHugh, W., Funke, R., Gage, D., Harris, K., Heaford, A., Howland, J., Kann, L., Lehoczky, J., LeVine, R., McEwan, P., McKernan, K., Meldrim, J., Mesirov, J.P., Miranda, C., Morris, W., Naylor, J., Raymond, C., Rosetti, M., Santos, R., Sheridan, A., Sougnez, C., Stange-Thomann, N., Stojanovic, N., Subramanian, A., Wyman, D., Rogers, J., Sulston, J., Ainscough, R., Beck, S., Bentley, D., Burton, J., Clee, C., Carter, N., Coulson, A., Deadman, R., Deloukas, P., Dunham, A., Dunham, I., Durbin, R., French, L., Grafham, D., Gregory, S., Hubbard, T., Humphray, S., Hunt, A., Jones, M., Lloyd, C., McMurray, A., Matthews, L., Mercer, S., Milne, S., Mullikin, J.C., Mungall, A., Plumb, R., Ross, M., Shownkeen, R., Sims, S., Waterston, R.H., Wilson, R.K., Hillier, L.W., McPherson, J.D., Marra, M.A., Mardis, E.R., Fulton, L.A., Chinwalla, A.T., Pepin, K.H., Gish, W.R., Chissoe, S.L., Wendl, M.C., Delehaunty, K.D., Miner, T.L., Delehaunty, A., Kramer, J.B., Cook, L.L., Fulton, R.S., Johnson, D.L., Minx, P.J., Clifton, S.W., Hawkins, T., Branscomb, E., Predki, P., Richardson, P., Wenning, S., Slezak, T., Doggett, N., Cheng, J.F., Olsen, A., Lucas, S., Elkin, C., Uberbacher, E., Frazier, M., Gibbs, R.A., Muzny, D.M., Scherer, S.E., Bouck, J.B., Sodergren, E.J., Worley, K.C., Rives, C.M., Gorrell, J.H., Metzker, M.L., Naylor, S.L., Kucherlapati, R.S., Nelson, D.L., Weinstock, G.M., Sakaki, Y., Fujiyama, A., Hattori, M., Yada, T., Toyoda, A., Itoh, T., Kawagoe, C., Watanabe, H., Totoki, Y., Taylor, T., Weissenbach, J., Heilig, R., Saurin, W., Artiguenave, F., Brottier, P., Bruls, T., Pelletier, E., Robert, C., Wincker, P., Smith, D.R., Doucette-Stamm, L., Rubenfield, M., Weinstock, K., Lee, H.M., Dubois, J., Rosenthal, A., Platzer, M., Nyakatura, G., Taudien, S., Rump, A., Yang, H., Yu, J., Wang, J., Huang, G., Gu, J., Hood, L., Rowen, L., Madan, A., Qin, S., Davis, R.W., Federspiel, N.A., Abola, A.P., Proctor, M.J., Myers, R.M., Schmutz, J., Dickson, M., Grimwood, J., Cox, D.R., Olson, M.V., Kaul, R., Raymond, C., Shimizu, N., Kawasaki, K., Minoshima, S., Evans, G.A., Athanasiou, M., Schultz, R., Roe, B.A., Chen, F., Pan, H., Ramser, J., Lehrach, H., Reinhardt, R., McCombie, W.R., de la Bastide, M., Dedhia, N., Blocker, H., Hornischer, K., Nordsiek, G., Agarwala, R., Aravind, L., Bailey, J.A., Bateman, A., Batzoglou, S., Birney, E., Bork, P., Brown, D.G., Burge, C.B., Cerutti, L., Chen, H.C., Church, D., Clamp, M., Copley, R.R., Doerks, T., Eddy, S.R., Eichler, E.E., Furey, T.S., Galagan, J., Gilbert, J.G., Harmon, C., Hayashizaki, Y., Haussler, D., Hermjakob, H., Hokamp, K., Jang, W., Johnson, L.S., Jones, T.A., Kasif, S., Kaspryzk, A., Kennedy, S., Kent, W.J., Kitts, P., Koonin, E.V., Korf, I., Kulp, D., Lancet, D., Lowe, T.M., McLysaght, A., Mikkelsen, T., Moran, J.V., Mulder, N., Pollara, V.J., Ponting, C.P., Schuler, G., Schultz, J., Slater, G., Smit, A.F., Stupka, E., Szustakowski, J., Thierry-Mieg, D., Thierry-Mieg, J., Wagner, L., Wallis, J., Wheeler, R., Williams, A., Wolf, Y.I., Wolfe, K.H., Yang, S.P., Yeh, R.F., Collins, F., Guyer, M.S., Peterson, J., Felsenfeld, A., Wetterstrand, K.A., Patrinos, A., Morgan, M.J., de Jong, P., Catanese, J.J., Osoegawa, K., Shizuya, H., Choi, S. and Chen, Y.J. (2001) International Human Genome Sequencing Consortium. Initial sequencing and analysis of the human genome *Nature* **409**(6822): 860-921.

LaVail, M.M., Gorrin, G.M., Yasumura, D. and Matthes, M.T. (1999) Increased susceptibility to constant light in nr and pcd mice with inherited retinal degenerations. *Invest. Ophthalmol. Vis. Sci.* **40**(5): 1020-1024.

Lee, J.S. and Burr, J.G. (1999) Salpα and Salpβ, growth-arresting homologs of Sam68. *Gene* **240**(1): 133-147.

Lee, S., Stollar, E. and Wang, E. (1993) Localization of S1 and elongation factor-1 alpha mRNA in rat brain and liver by non-radioactive in situ hybridization. *J. Histochem. Cytochem.* **41**(7): 1093-1098.

Leeson, C.R. and Leeson, S.T. (1976) Histology. Philadelphia: Saunders;556.

Le Meur, G., Stieger, K., Smith, A.J., Weber, M., Deschamps, J.Y., Nivard, D., Mendes-Madeira, A., Provost, N., Pereon, Y., Cherel, Y., Ali, R.R., Hamel, C., Moullier, P. and Rolling, F. (2007) Restoration of vision in RPE65-deficient Briard dogs using an AAV serotype 4 vector that specifically targets the retinal pigmented epithelium. *Gene Ther.* **14**(4): 292-303.

Leon, A., Omri, B., Gely, A., Klein, C. and Crisanti, P. (2006) QN1/KIAA1009: a new essential protein for chromosome segregation and mitotic spindle assembly. *Oncogene* **25**(13): 1887-1895.

Levy, F.O., Gudermann, T., Birnbaumer, M., Kaumann, A.J. and Birnbaumer, L. (1992) Molecular cloning of a human gene (S31) encoding a novel serotonin receptor mediating inhibition of adenylyl cyclase. *FEBS Lett.* **296**(2): 201-206.

Levy, F.O., Holtgreve-Grez, H., Tasken, K., Solberg, R., Ried, T. and Gudermann, T. (1994) Assignment of the gene encoding the 5-HT-1E serotonin receptor (S31) (locus HTR1E) to human chromosome 6q14-q15. *Genomics* **22**(3): 637-640.

Li, J.B., Gerdes, J.M., Haycraft, C.J., Fan, Y., Teslovich, T.M., May-Simera, H., Li, H., Blacque, O.E., Li, L., Leitch, C.C., Lewis, R.A., Green, J.S., Parfrey,, P.S., Leroux, M.R., Davidson, W.S., Beales, P.L., Guay-Woodford, L.M., Yoder, B.K., Stormo, G.D., Katsanis, N. and Dutcher, SK. (2004) Comparative genomics identifies a flagellar and basal body proteome that includes the BBS5 human disease gene. *Cell* **117**(4): 541-552.

Li, T., Sandberg, M.A., Pawlyk, B.S., Rosner, B., Hayes, K.C., Dryja, T.P. and Berson, E.L. (1998) Effect of vitamin A supplementation on rhodopsin mutants threonine-17 --> methionine and proline-347 --> serine in transgenic mice and in cell cultures. *Proc. Natl. Acad. Sci. U S A.* **95**(20): 11933-8.

Li, Y., Marcos, I., Borrego, S., Yu, Z., Zhang, K. and Antinolo, G. (2001) Evaluation of the ELOVL4 gene in families with retinitis pigmentosa linked to the RP25 locus. *J. Med. Genet.* **38**(7): 478-480.

Lin, M., Sutherland, D. R., Horsfall, W., Totty, N., Yeo, E., Nayar, R., Wu, X.F. and Schuh, A.C. (2002) Cell surface antigen CD109 is a novel member of the alpha-2 macroglobulin/C3, C4, C5 family of thioester-containing proteins. *Blood* **99**(5): 1683-1691.

Lindberg, R.A., Fischer, W.H. and Hunter, T. (1993) Characterization of a human protein threonine kinase isolated by screening an expression library with antibodies to phosphotyrosine. *Oncogene* **8**(2): 351-359.

Lisman, J., Fain, G. (1995) Support for the equivalent light hypothesis for RP. *Nat. Med.* **1**(12): 1254-1255.

Liu, W., Quinto, I., Chen, X., Palmieri, C., Rabin, R.L., Schwartz, O.M., Nelson, D.L. and Scala, G. (2001) Direct inhibition of Bruton's tyrosine kinase by IBtk, a Btk-binding protein. *Nature Immun.* **2**(10): 939-946.

Lorenz, B., Gyurus, P., Preising, M., Bremser, D., Gu, S., Andrassi, M., Gerth, C. and Gal, A. (2000) Early-onset severe rod-cone dystrophy in young children with RPE65 mutations. *Invest. Ophthalmol. Vis. Sci.* **41**(9): 2735-42.

Maita, H., Kitaura, H., Keen, T.J., Inglehearn, C.F., Ariga, H. and Iguchi-Ariga, S.M.M. (2004) PAP1, the mutated gene underlying the RP9 form of dominant retinitis pigmentosa, is a splicing factor. *Exp. Cell Res.* **300**(2): 283-296.

Mansergh, F.C., Millington-Ward, S., Kennan, A., Kiang, A.S., Humphries, P., Farrar, G.J., Humphries, P. and Kenna, P.F. (1999) Retinitis pigmentosa and progressive sensorineural hearing loss caused by a C12258A mutation in the mitochondrial *MTTS2* gene. *Am. J. Hum. Genet.* **64**(4): 971-85.

Marcos, I., Borrego, S. and Antinolo, G. (2003) Molecular cloning and characterization of human RAB23, a member of the group of Rab GTPases. *Int. J. Mol. Med.* **12**(6): 983-987.

Marcos, I., Galan, J.J., Borrego, S. and Antinolo, G. (2002) Cloning, characterization, and chromosome mapping of the human GlcAT-S gene. *J. Hum. Genet.* **47**(12): 677-680.

Marcos, I., Ruiz, A., Blaschak, C.J., Borrego, S., Cutting, G.R. and Antinolo, G. (2000) Mutation analysis of GABRR1 and GABRR2 in autosomal recessive retinitis pigmentosa. *J. Med. Genet.* **37**(6): E5.

Marlhens, F., Bareil, C., Griffoin, J.M., Zrenner, E., Amalric, P., Eliaou, C., Liu, S.Y., Harris, E., Redmond, T.M., Arnaud, B., Claustres, M. and Hamel, C.P. (1997) Mutations in RPE65 cause Leber's congenital amaurosis. *Nat. Genet.* **17**(2): 139-141.

Marmor, MF. (1977) Fundus albipunctatus: a clinical study of the fundus lesions, the physiologic deficit, and the vitamin A metabolism. *Doc. Ophthalmol.* **43**(2): 277-302.

Marszalek, J.R. and Goldstein, L.S. (2000) Understanding the functions of kinesin-II. *Biochim. Biophys. Acta.* **1496**(1): 142-150.

Martelange, V., De Smet, C., De Plaen, E., Lurquin, C. and Boon, T. (2000) Identification on a human sarcoma of two new genes with tumor-specific expression. *Cancer Res.* **60**(14): 3848-3855.

Martin, R.A., Slaugh, R., Natowicz, M., Pearlman, K., Orvisky, E., Krasnewich, D., Kleta, R., Huizing, M. and Gahl, W.A. (2003) Sialic acid storage disease of the Salla phenotype in American monozygous twin female sibs. *Am. J. Med. Genet.* **120**(1): 23-27.

Martinez-Mir, A., Paloma, E., Allikmets, R., Ayuso, C., del Rio, T., Dean, M., Vilageliu, L., Gonzàlez-Duarte, R. and Balcells, S. (1998) Retinitis pigmentosa caused by a homozygous mutation in the Stargardt disease gene *ABCR. Nat. Genet.* **18**(1): 11-12.

Matise, T.C., Sachidanandam, R., Clark, A.G., Kruglyak, L., Wijsman, E., Kakol, J., Buyske, S., Chui, B., Cohen, P., de Toma, C., Ehm, M., Glanowski, S., He, C., Heil. J., Markianos, K., McMullen, I., Pericak-Vance, M.A., Silbergleit, A., Stein, L., Wagner, M., Wilson, A.F., Winick, J.D., Winn-Deen, E.S., Yamashiro, C.T., Cann, H.M., Lai, E. and Holden, A.L. (2003) A 3.9-centimorgan-resolution human single-nucleotide polymorphism linkage map and screening set. *Am. J. Hum. Genet.* **73**(2): 271-284.

Maw, M.A., John, S., Jablonka, S., Muller, B., Kumaramanickavel, G., Oehlmann, R., Denton, M.J. and Gal, A. (1995) Oguchi disease: suggestion of linkage to markers on chromosome 2q. *J. Med. Genet.* **32**(5): 396-398.

Maw, M.A., Kennedy, B., Knight, A., Bridges, R., Roth, K.E., Mani, E.J., Mukkadan, J.K., Nancarrow, D., Crabb, J.W. and Denton, M.J. (1997) Mutation of the gene encoding cellular retinaldehyde-binding protein in autosomal recessive retinitis pigmentosa. *Nat. Genet.* **17**(2): 198-200.

Mazzocco, M., Maffei, M., Egeo, A., Vergano, A., Arrigo, P., Di Lisi, R., Ghiotto, F. and Scartezzini, P. (2002) The identification of a novel human homologue of the SH3 binding glutamic acid-rich (SH3BGR) gene establishes a new family of highly conserved small proteins related to Thioredoxin Superfamily.*Gene* **29**(1-2): 233-239.

McCarroll, S.A., Hadnott, T.N., Perry, G.H., Sabeti, P., Zodi, M.C., Barrett, J., Dallaire, S., Gabriel, S.B., Lee, C., Daly, M.J. and Altshuler, DM. (2006) Common deletion variants in the human genome. *Nat. Genet.* **38**(1): 86–92.

McLaughlin, M.E., Sandberg, M.A., Berson, E.L. and Dryja, T.P. (1993) Recessive mutations in the gene encoding the beta-subunit of rod phosphodiesterase in patients with retinitis pigmentosa. *Nat. Genet.* **4**(2): 130-134.

Melchionda, S., Ahituv, N., Bisceglia, L., Sobe, T., Glaser, F., Rabionet, R., Arbones, M. L., Notarangelo, A., Di Iorio, E., Carella, M., Zelante, L., Estivill, X., Avraham, K.B. and Gasparini, P. (2001) MYO6, the human homologue of the gene responsible for deafness in Snell's Waltzer mice, is mutated in autosomal dominant nonsyndromic hearing loss. *A. J. Hum. Genet.* **69**(3): 635-640.

Mieziewska, K.E., van Veen, T., Murray, J.M. and Aguirre, G.D. (1991) Rod and cone specific domains in the interphotoreceptor matrix. *J. Comp. Neurol.* **308**(3): 371-380.

Misteli, T. (1999) RNA splicing: What has phosphorylation got to do with it? *Curr Biol.* **9**(6): R198-R200.

Miyakoshi, K., Murphy, M.J., Yeoman, R.R., Mitra, S., Dubay, C.J. and Hennebold, J.D. (2006) The identification of novel ovarian proteases through the use of genomic and bioinformatic methodologies. *Biol. Reprod.* **75**(6): 823-835.

Mohamed, M.D., Topping, N.C., Jafri, H., Raashed, Y., McKibbin, M.A. and Inglehearn, C.F. (2003) Progression of phenotype in Leber's congenital amaurosis with a mutation at the LCA5 locus. *Br. J. Ophthalmol.* **87**(4): 473–475.

Morimura, H., Fishman, G.A., Grover, S.A., Fulton, A.B., Berson, E.L. and Dryja, T.P. (1998) Mutations in the RPE65 gene in patients with autosomal recessive retinitis pigmentosa or leber congenital amaurosis. *Proc. Natl. Acad. Sci.* **95**(6): 3088-3093.

Morimura, H., Saindelle-Ribeaudeau, F., Berson, E.L. and Dryja, T.P. (1999) Mutations in RGR, encoding a light-sensitive opsin homologue, in patients with retinitis pigmentosa. *Nat. Genet.* **23**(4): 393-394.

Morton, N.E. (1955) Sequential tests for the detection of linkage. *Am. J. Hum Genet.* **7**(3): 277-318.

Moslemi, A.R., Darin, N., Tulinius, M., Oldfors, A. and Holme, E. (2005) Two new mutations in the *MTATP6* gene associated with Leigh syndrome. *Neuropediatric* **36**(5): 314-318.

Mungall, A.J., Palmer, S.A., Sims, S.K., Edwards, C.A., Ashurst, J.L., Wilming, L., Jones, M.C., Horton, R., Hunt, S.E., Scott, C.E., Gilbert, J.G., Clamp, M.E., Bethel, G., Milne, S., Ainscough, R., Almeida, J.P., Ambrose, K.D., Andrews, T.D., Ashwell, R.I., Babbage, A.K., Bagguley, C.L., Bailey, J., Banerjee, R., Barker, D.J., Barlow, K.F., Bates, K., Beare, D.M., Beasley, H., Beasley, O., Bird, C.P., Blakey, S., Bray-Allen, S., Brook, J., Brown, A.J., Brown, J.Y., Burford, D.C., Burrill, W., Burton, J., Carder, C.,

Carter, N.P., Chapman, J.C., Clark, S.Y., Clark, G., Clee, C.M., Clegg, S., Cobley, V., Collier, R.E., Collins, J.E., Colman, L.K., Corby, N.R., Coville, G.J., Culley, K.M., Dhami, P., Davies, J., Dunn, M., Earthrowl, M.E., Ellington, A.E., Evans, K.A., Faulkner, L., Francis, M.D., Frankish, A., Frankland, J., French, L., Garner, P., Garnett, J., Ghori, M.J., Gilby, L.M., Gillson, C.J., Glithero, R.J., Grafham, D.V., Grant, M., Gribble, S., Griffiths, C., Griffiths, M., Hall, R., Halls, K.S., Hammond, S., Harley, J.L., Hart, E.A., Heath, P.D., Heathcott, R., Holmes, S.J., Howden, P.J., Howe, K.L., Howell, G.R., Huckle, E., Humphray, S.J., Humphries, M.D., Hunt, A.R., Johnson, C.M., Joy, A.A., Kay, M., Keenan, S.J., Kimberley, A.M., King, A., Laird, G.K., Langford, C., Lawlor, S., Leongamornlert, D.A., Leversha, M., Lloyd, C.R., Lloyd, D.M., Loveland, J.E., Lovell, J., Martin, S., Mashreghi-Mohammadi, M., Maslen, G.L., Matthews, L., McCann, O.T., McLaren, S.J., McLay, K., McMurray, A., Moore, M.J., Mullikin, J.C., Niblett, D., Nickerson, T., Novik, K.L., Oliver, K., Overton-Larty, E.K., Parker, A., Patel, R., Pearce, A.V., Peck, A.I., Phillimore, B., Phillips, S., Plumb, R.W., Porter, K.M., Ramsey, Y., Ranby, S.A., Rice, C.M., Ross, M.T., Searle, S.M., Sehra, H.K., Sheridan, E., Skuce, C.D., Smith, S., Smith, M., Spraggon, L., Squares, S.L., Steward, C.A., Sycamore, N., Tamlyn-Hall, G., Tester, J., Theaker, A.J., Thomas, D.W., Thorpe, A., Tracey, A., Tromans, A., Tubby, B., Wall, M., Wallis, J.M., West, A.P., White, S.S., Whitehead, S.L., Whittaker, H., Wild, A., Willey, D.J., Wilmer, T.E., Wood, J.M., Wray, P.W., Wyatt, J.C., Young, L., Younger, R.M., Bentley, D.R., Coulson, A., Durbin, R., Hubbard, T., Sulston, J.E., Dunham, I., Rogers, J. and Beck, S. (2003) The DNA sequence and analysis of human chromosome 6. *Nature* **425**(6960): 805-811.

Muto, A., Tashiro, S., Nakajima, O., Hoshino, H., Takahashi, S., Sakoda, E., Ikebe, D., Yamamoto, M. and Igarashi, K. (2004) The transcriptional programme of antibody class switching involves the repressor Bach2. *Nature* **429**(6991): 566-571.

Nagano, T., Yoneda, T., Hatanaka, Y., Kubota, C., Murakami, F. and Sato, M. (2002) Filamin A-interacting protein (FILIP) regulates cortical cell migration out of the ventricular zone. *Nature Cell Biol.* **4**(7): 495-501.

Nagase, T., Ishikawa, K., Suyama, M., Kikuno, R., Hirosawa, M., Miyajima, N., Tanaka, A., Kotani, H., Nomura, N. and Ohara, O. (1999) Prediction of the coding sequences of unidentified human genes. XIII. The complete sequences of 100 new cDNA clones from brain which code for large proteins in vitro. *DNA Res.* **6**(1): 63-70.

Nakajima, D., Nakayama, M., Kikuno, R., Hirosawa, M., Nagase, T. and Ohara, O. (2001) Identification of three novel non-classical cadherin genes through comprehensive analysis of large cDNAs. *Mol. Brain Res.* **94**(1-2): 85-95.

Nakamura, Y., Leppert, M., O'Connell, P., Wolff, R. Holm, T., Culver, M., Martin, C., Fujimoto, E., Hoff, M., Kumlin, E. and White, R. (1987) Vraiable number of tandem repeat (VNTR) markers for human genome mapping. *Science* **235**(4796): 1616-1622.

Nakamura, M., Ito, S. and Miyake, Y. (2002) Novel de novo mutation in CRX gene in a Japanese patient with Leber Congenital Amaurosis. *Am. J. Ophthal.* **134**(3): 465-467.

Nakazawa, M., Kikawa, E., Chida, Y. and Tamai, M. (1994) Asn244His mutation of the peripherin/*RDS* gene causing autosomal dominant cone-rod degeneration. *Hum. Mol. Genet.* **3**(7): 1195–1196.

Nakazawa, M., Wada, Y. and Tamai, M. (1998) Arrestin gene mutations in autosomal recessive retinitis pigmentosa. *Arch. Ophthalmol.***116**(4): 498-501.

Naylor, S.L., Chin, W.W., Goodman, H.M., Lalley, P.A., Grzeschik, K.H., Sakaguchi, A. Y. (1983) Chromosome assignment of the genes encoding the alpha and beta subunits of the glycoprotein hormones in man and mouse. *Somat. Cell Genet.* **9**(6): 757-770.

Nichols, B.E., Sheffield, V.C., Vandenburgh, K., Drack, A.V., Kimura, A.E. and Stone, E.M. (1993) Butterfly-shaped pigment dystrophy of the fovea caused by a point mutation in codon 167 of the RDS gene. *Nat. Genet.* **3**(3): 202–207.

Nobukuni, Y., Mitsubuchi, H., Akaboshi, I., Indo, Y., Endo, F., Yoshioka, A. and Matsuda, I. (1991) Maple syrup urine disease: complete defect of the E1-beta subunit of the branched chain alpha-ketoacid dehydrogenase complex due to a deletion of an 11-bp repeat sequence which encodes a mitochondrial targeting leader peptide in a family with the disease. *J. Clin. Invest.* **87**(5): 1862-1866.

Norio, R., Raitta, C. and Lindahl, E. (1984) Further delineation of the Cohen syndrome; report on chorioretinal dystrophy, leukopenia and consanguinity. *Clin. Genet.* **25**(1): 1-14.

O'Connell, J.R. and Weeks D.E. (1998) PedCheck: a program for identification of genotype incompatibilities in linkage analysis. *Am. J. Hum. Genet.* **63**(1): 259-266.

Oh, S.P., Taylor, R.W., Gerecke, D.R., Rochelle, J.M., Seldin, M.F. and Olsen, B.R. (1992) The mouse alpha 1(XII) and human alpha 1(XII)-like collagen genes are localized on mouse chromosome 9 and human chromosome 6. *Genomics* **14**(2): 225-231.

Osada, N., Hashimoto, K., Hirai, M. and Kusuda, J. (2007) Aberrant termination of reproduction-related TMEM30C transcripts in the hominoids. *Gene* **392**(1-2): 151-156.

Parisi, M.A., Bennett, C.L., Eckert, M.L., Dobyns, W.B., Gleeson, J.G., Shaw, D.W., McDonald, R., Eddy, A., Chance, P.F., Glass, I.A. (2004) *NPHP1* gene deletion associated with juvenile nephronophthisis is present in a subset of individuals with Joubert syndrome. *Am.J.Hum. Genet.* **75**(1): 82-91.

Patel, M.S. and Harris, R.A. (1995) Mammalian alpha-keto acid dehydrogenase complexes: gene regulation and genetic defects. *FASEB J.* **9**(12): 1164-1172.

Peng, Y., Genin, A., Spinner, N.B., Diamond, R.H. and Taub, R. (1998) The gene encoding human nuclear protein tyrosine phosphatase, PRL-1: cloning, chromosomal localization, and identification of an intron enhancer. *J. Biol. Chem.* **273**(27): 17286-17295.

Pepose, J.S. and Leib, D.A. (1994) Herpes simplex viral vectors for therapeutic gene delivery to ocular tissues. Recent breakthroughs in the molecular genetics of ocular diseases. *Invest. Ophthalmol. Vis. Sci.* **35**(6): 2662-2666.

Perrault, I., Hanein, S., Gerber, S., Barbet, F., Ducroq, D., Dollfus, H., Hamel, C., Dufier, J.L., Munnich, A., Kaplan, J. and Rozet, J.M. (2004) Retinal dehydrogenase 12 (RDH12) mutations in Leber congenital amaurosis. *Am. J. Hum. Genet.* **75**(4): 639-646.

Perrault, I., Rozet, J. M., Calvas, P., Gerber, S., Camuzat, A., Dollfus, H., Chatelin, S., Souied, E., Ghazi, I., Leowski, C., Bonnemaison, M., Le Paslier, D., Frezal, J., Dufier, J.-L., Pittler, S., Munnich, A. and Kaplan, J. (1996) Retinal-specific guanylate cyclase gene mutations in Leber's congenital amaurosis. *Nat. Genet.* **14**(4): 461-464.

Portera-Cailliau, C., Sung, C.H., Nathans, J. and Adler, R. (1994) Apoptotic photoreceptor cell death in mouse models of retinitis pigmentosa. *Proc. Natl. Acad. Sci.* USA. **91**(3): 974-978.

Povey, S., Wilson, D.E., Harris, H., Gormley, I.P., Perry, P. and Buckton, K.E. (1975) Sub-unit structure of soluble and mitochondrial malic enzyme: demonstration of human mitochondrial enzyme in human-mouse hybrids. *Ann. Hum. Genet.* **39**(2): 203-212.

Provencio, I., Rodriguez, I.R., Jiang, G., Hayes, W.P., Moreira, E.F. and Rollag, M.D. (2000) A novel human opsin in the inner retina. *J. Neurosci.* **20**(2): 600-605.

Purves, D., Augustine, G.J., Fitzpatrick, D., Katz, L.C., LaMantia, A.S., McNamara, J.O. and Williams, S.M. (2001) Neuroscience - a novelty for the nervous. *NeuroScience*, Sunderland, MA: Sinauer Associates. 562 pp.

Rattner, A., Smallwood, P.M., Williams, J., Cooke, C., Savchenko, A., Lyubarsky, A., Pugh, E.N. and Nathans, J. (2001) A photoreceptor-specific cadherin is essential for the structural integrity of the outer segment and for photoreceptor survival. *Neuron* **32**(5): 775-786.

Rattner, A., Chen, J. and Nathans, J. (2004) Proteolytic shedding of the extracellular domain of photoreceptor cadherin: Implications for outer segment assembly. *J. Biol. Chem.* **279**(40): 42202-42210.

Redon, R., Ishikawa, S., Fitch, K.R., Feuk, L., Perry, G.H., Andrews, T.D., Fiegler, H., Shapero, M.H., Carson, A.R., Chen, W., Cho, E.K., Dallaire, S., Freeman, J.L., Gonzalez, J.R., Gratacos, M., Huang, J., Kalaitzopoulos, D., Komura, D., MacDonald,

J.R., Marshall, C.R., Mei, R., Montgomery, L., Nishimura, K., Okamura, K., Shen, F., Somerville, M.J., Tchinda, J., Valsesia, A., Woodwark, C., Yang, F., Zhang, J., Zerjal, T., Zhang, J., Armengol, L., Conrad, D.F., Estivill, X., Tyler-Smith, C., Carter, N.P., Aburatani, H., Lee, C., Jones, K.W., Scherer, S.W. and Hurles, M.E. (2006) Global variation in copy number in the human genome. *Nature* **444**(7118): 444-454.

Reig, C., Alicia, S., Gean, E., Vidal, M., Arumi, J., De la Calzada, M.D., Antich, J. and Carballo, M. (1995) A point mutation in the RDS-peripherin gene in a Spanish family with central areolar choroidal dystrophy. *Ophthalmic Genet.* **16**(2): 39–44.

Reiners, J., Nagel-Wolfrum, K., Jurgens, K., Marker, T. and Wolfrum, U. (2006) Molecular basis of human Usher syndrome: deciphering the meshes of the Usher protein network provides insights into the pathomechanisms of the Usher disease. *Exp. Eye Res.* **83**(1): 97-119.

Riazuddin, S.A., Zulfiqar, F., Zhang, Q., Sergeev, Y.V., Qazi, Z.A., Husnain, T., Caruso, R., Riazuddin, S., Sieving, P.A. and Hejtmancik, J.F. (2005) Autosomal recessive retinitis pigmentosa is associated with mutations in *RP1* in three consanguineous Pakistani families. *Invest. Ophthalmol. Vis. Sci.* **46**(7): 2264-2670.

Rickman, C.B., Ebright, J.N., Z\ avodni, Z.J., Yu, L., Wang, T., Daiger, S.P., Wistow, G., Boon, K. and Hauser, M.A. (2006) Defining the Human Macula Transcriptome and Candidate Retinal Disease Genes Using EyeSAGE. *Invest. Ophthalmol. Vis. Sci.***47**(6): 2305-2316.

Rivolta, C., Sweklo, E.A., Berson, E.L. and Dryja, T.P. (2000) Missense mutation in the USH2A gene: association with recessive retinitis pigmentosa without hearing loss. *Am. J. Hum. Genet.* **66**(6): 1975-1978.

Rodiek, R.W. (1998) The first steps in seeing, Sunderland, Mass, *Sinauer Associates.*

Rosenfeld, P.J., Cowley, G.S., Hahn, L.B., Sandberg, M.A., Berson, E.L. and Dryja, T.P. (1992) A null mutation within the rhodopsin gene in a family with autosomal recessive retinitis pigmentosa. *Invest. Ophthalmol. Vis. Sci.* **1**(3): 209-213.

Rozet, J.M., Gerber, S., Souied, E., Perrault, I., Chatelin, S., Ghazi, I., Leowski, C., Dufier, J.L., Munnich, A. and Kaplan, J. (1998) Spectrum of ABCR gene mutations in autosomal recessive macular dystrophies. *Eur. J. Hum. Genet.* **6**(3): 291-295.

Ruby, N.F., Brennan, T.J., Xie, X., Cao, V., Franken, P., Heller, H.C. and O'Hara, B.F. (2002) Role of melanopsin in circadian responses to light. *Science* **298**(5601): 2211-2213.

Ruiz, A., Borrego, S., Marcos, I. and Antinolo, G. (1998) A major locus for autosomal recessive retinitis pigmentosa on 6q, determined by homozygosity mapping of

chromosomal regions that contain gamma-aminobutyric acid-receptor clusters. *Am. J. Hum. Genet.* **62**(6): 1452-1459.

Rüschendorf, F. and Nürnberg, P. (2005) ALOHOMORA: a tool for linkage analysis using 10K SNP array data. *Bioinformatics* **21**(9): 2123-2125.

Ryan, S.J. In basic science and inherited retinal disease: Ogden, T.E., Hinton, D.R., Schachat, A.P., and Hengst T.C. (eds) third edition 2001.

Saiki, P.K., Schorf, S., Faloona, F., Mullis, K.B., Horn, G.T., Ehrlich, H.A. and Arnheim, N. (1985) Enzymatic amplification of beta globin sequences and restriction site analysis for diagnosis of sickle cell anaemia. *Science* **230**(4732): 1350-1354.

Saiki, R.K., Gefland, D.H., Stoffel, S., Scharf, S., Higuchi, R., Horn, G.T., Mullis, K.B. and Ehrlich, H.A. (1988) Primer directed enzymatic amplification of DNA with thermostable DNA polymerase. *Science* **239**(4839): 487-491.

Sanger, F., Coulson, A.R., Hong, G.F., Hill, D.F. and Petersen, G.B. (1982) Nucleotide sequence of bacteriophage lambda DNA. *J. Mol. Biol.* **162**(4): 729-773.

Sasaki, S., Ito, E., Toki, T., Maekawa, T., Kanezaki, R., Umenai, T., Muto, A., Nagai, H., Kinoshita, T., Yamamoto, M., Inazawa, J., Taketo, M.M., Nakahata, T., Igarashi, K. and Yokoyama, M. (2000) Cloning and expression of human B cell-specific transcription factor BACH2 mapped to chromosome 6q15. *Oncogene* **19**(33): 3739-3749.

Sayer, J.A., Otto, E.A., O'Toole, J.F., Nurnberg, G., Kennedy, M.A., Becker, C., Hennies, H.C., Helou, J., Attanasio, M., Fausett, B.V., Utsch, B., Khanna, H., Liu, Y., Drummond, I., Kawakami, I., Kusakabe, T., Tsuda, M., Ma, L., Lee, H., Larson, R.G., Allen, S.J., Wilkinson, C.J., Nigg, E.A., Shou, C., Lillo, C., Williams, D.S., Hoppe, B., Kemper, M.J., Neuhaus, T., Parisi, M.A., Glass, I.A., Petry, M., Kispert, A., Gloy, J., Ganner, A., Walz, G., Zhu, X., Goldman, D., Nurnberg, P., Swaroop, A., Leroux, M.R. and Hildebrandt, F. (2006) The centrosomal protein nephrocystin-6 is mutated in Joubert syndrome and activates transcription factor ATF4. *Nat. Genet.* **38**(6): 674-681.

Sheffield, V.C., Beck, J.S., Kwitek, A.E., Sandstrom, D.W. and Stone, E.M. (1993) The sensitivity of single-strand conformation polymorphism analysis for the detection of single base substitutions. *Genomics.* **16**(2): 325-32.

Schmidt, L.G., Samochowiec, J., Finckh, U., Fiszer-Piosik, E., Horodnicki, J., Wendel, B., Rommelspacher, H. and Hoehe, M.R. (2002) Association of a CB1 cannabinoid receptor gene (CNR1) polymorphism with severe alcohol dependence. *Drug Alcohol Depend.* **65**(3): 221-224.

Schroeder, B.C., Hechenberger, M., Weinreich, F., Kubisch, C. and Jentsch, T. J. (2000) KCNQ5, a novel potassium channel broadly expressed in brain, mediates M-type currents. *J. Biol. Chem.* **275** (31): 24089-24095.

Schwahn, U., Lenzner, S., Dong, J., Feil, S., Hinzmann, B., van Duijnhoven, G., Kirschner, R., Hemberger, M., Bergen, A.A.B., Rosenberg, T., Pinckers, A.J.L.G., Fundele, R., Rosenthal, A., Cremers, F.P.M., Ropers, H.H. and Berger, W. (1998) Positional cloning of the gene for X-linked retinitis pigmentosa 2. *Nat. Genet.* **19**(4): 327-332.

Schwarz-Romond, T., Asbrand, C., Bakkers, J., Kuhl, M., Schaeffer, H.J., Huelsken, J., Behrens, J., Hammerschmidt, M. and Birchmeier, W. (2002) The ankyrin repeat protein diversin recruits casein kinase I-epsilon to the beta-catenin degradation complex and acts in both canonical Wnt and Wnt/JNK signaling. *Genes Dev.* **16**(16): 2073-2084.

Sellick, G.S., Longman, C., Tolmie, J., Newbury-Ecob, R., Geenhalgh, L., Hughes, S., Shaw-Smith, C., Redon, R., Rickman, L., Rio, M., Willatt, L., Fiegler, H., Firth, H., Sanlaville, D., Winter, R., Colleaux, L., Bobrow, M. and Carter, N.P. (2004) Microarray based comparative genomic hybridisation (array-CGH) detects submicroscopic chromosomal deletions and duplications in patients with learning disability/mental retardation and dysmorphic features. *J. Med. Genet.* **41**(4): 241-248.

Sellick, G.S., Longman, C., Tolmie, J., Newbury-Ecob, R., Geenhalgh, L., Hughes, S., Whiteford, M., Garrett, C. and Houlston, R.S. (2004) Genomewide linkage searches for Mendelian disease loci can be efficiently conducted using high-density SNP genotyping arrays. *Nucleic Acids Res.* **23**(20): e164.

Sekiguchi, T., Hirose, E., Nakashima, N., Ii, M. and Nishimoto, T. (2001) Novel G proteins, Rag C and Rag D, interact with GTP-binding proteins, Rag A and Rag B. *J. Biol. Chem.* **276**(10): 7246-7257.

Shaw-Smith, C., Redon, R., Rickman, L., Rio, M., Willatt, L., Fiegler, H., Firth, H., Sanlaville, D., Winter, R., Colleaux, L., Bobrow, M. and Carter, N.P. (2004) Microarray based comparative genomic hybridisation (array-CGH) detects submicroscopic chromosomal deletions and duplications in patients with learning disability/mental retardation and dysmorphic features. *J. Med. Genet.* **41**(4): 241-248.

Sheffield, V.C., Stone, E.M. and Carmi, R. (1998) Use of isolated inbred human populations for identification of disease genes. *Trends Genet.* **14**(10): 391-396.

Shiratori, A., Okumura, K., Nogami, M., Taguchi, H., Onozaki, T., Inoue, T., Ando, T., Shibata, T., Izumi, M., Miyazawa, H., Hanaoka, F., Murakami, Y. and Eki, T. (1995) Assignment of the 49-kDa (PRIM1) and 58-kDa (PRIM2A and PRIM2B) subunit genes of the human DNA primase to chromosome bands 1q44 and 6p11.1-p12. *Genomics* **28**(2): 350-353.

Shiratsuchi, T., Nishimori, H., Ichise, H., Nakamura, Y. and Tokino, T. (1997) Cloning and characterization of BAI2 and BAI3, novel genes homologous to brain-specific angiogenesis inhibitor 1 (BAI1). *Cytogenet Cell Genet.* **79**(1-2): 103-108.

Siegfried, Z., Kanyas, K., Latzer, Y., Karni, O., Bloch, M., Lerer, B. and Berry, E.M. (2004) Association study of cannabinoid receptor gene (CNR1) alleles and anorexia nervosa: differences between restricting and binging/purging subtypes. *Am. J. Med. Genet B Neuropsychiatr Genet.* **125**(1): 126-130.

Sieving, P.A., Richards, J.E., Naarendorp, F., Bingham, E.L., Scott, K. and Alpern, M. (1995) Dark-light: model for nightblindness from the human rhodopsin gly90-to-asp mutation. *Proc. Nat. Acad. Sci.* **92**(3): 880-884.

Sigelman, J. and Ozanics, V. (1982) Retina, *in Ocular Anatomy, embryology, and Teratology* (ed. F. Jakobiec), Harper and Row, Philadelphia, p. 441.

Siligardi, G. and Drake, A.F. (1995) The importance of extended conformations and, in particular, the PII conformation for the molecular recognition of peptides. *Biopolymers* **37**(4): 281-292.

Small, K.W., Weber, J.L., Roses, A., Lennon, F., Vance, J.M. and Pericak-Vance, M.A. (1992) North Carolina macular dystrophy is assigned to chromosome 6. *Genomics* **13**(3): 681-685.

Smoller, J.W., Biederman, J., Arbeitman, L., Doyle, A.E., Fagerness, J., Perlis, R.H., Sklar, P. and Faraone, S.V. (2006) Association between the 5HT1B receptor gene (HTR1B) and the inattentive subtype of ADHD. *Biol. Psychiat.* **59**(5): 460-467.

Sohl, G., Nielsen, P.A., Eiberger, J. and Willecke, K. (2003) Expression profiles of the novel human connexin genes hCx30.2, hCx40.1, and hCx62 differ from their putative mouse orthologues. *Cell Commun. Adhes.* **10**(1): 27-36.

Sohocki, M.M., Bowne, S.J., Sullivan, L.S., Blackshaw, S., Cepko, C.L., Payne, A.M., Bhattacharya, S. S., Khaliq, S., Mehdi, S.Q., Birch, D.G., Harrison, W.R., Elder, F.F. B., Heckenlively, J.R. and Daiger, S.P. (2000) Mutations in a new photoreceptor-pineal gene on 17p cause Leber congenital amaurosis. *Nat. Genet.* **24**(1): 79-83.

Sohocki, M.M., Sullivan, L.S., Mintz-Hittner, H.A., Birch, D., Heckenlively, J.R., Freund, C.L., McInnes, R.R. and Daiger, S.P. (1998) A range of clinical phenotypes associated with mutations in CRX, a photoreceptor transcription-factor gene. *Am. J. Hum. Genet.* **63**(5): 1307-1315.

Sprecher, E., Bergman, R., Richard, G., Lurie, R., Shalev, S., Petronius, D., Shalata, A., Anbinder, Y., Leibu, R., Perlman, I., Cohen, N. and Szargel, R. (2001) Hypotrichosis with juvenile macular dystrophy is caused by a mutation in CDH3, encoding P-cadherin. *Nat. Genet.* **29**(2): 134-136.

Springer, J., Nanda, I., Hoehn, K., Schmid, M. and Grummt, F. (1999) Identification and chromosomal localization of murine ORC3, a new member of the mouse origin recognition complex. *Cytogenet. Cell Genet.* **87**(3-4): 245-51.

Stanley, J.R., Tanaka, T., Mueller, S., Klaus-Kovtun, V. and Roop, D. (1988) Isolation of complementary DNA for bullous pemphigoid antigen by use of patients' autoantibodies. *J. Clin. Invest.* **82**(6): 1864-1870.

Stein, L.D. (2004) Human genome: end of the beginning. *Nature* **431**(7011): 915-916.

Stockton, D.W., Lewis, R.A., Abboud, E.B., Al-Rajhi, A., Jabak, M., Anderson, K.L. and Lupski, J.R. (1998) A novel locus for Leber congenital amaurosis on chromosome 14q24. *Hum. Genet.* **103**(3): 328-333.

Stone, E.M., Nichols, B.E., Kimura, A.E., Weingeist T.A., Drack, A. and Sheffield V.C. (1994) Clinical features of a Stargardt-like dominant progressive macular dystrophy with genetic linkage to chromosome 6q. *Arch. Ophthalmol.* **112**(6): 765-772.

Stranger, B.E., Forrest, M.S., Dunning, M., Ingle, C.E., Beazley, C., Thorne, N., Redon, R., Bird C.P., de Grassi, A., Lee, C., Tyler-Smith, C., Carter, N., Scherer, S.W., Tavare, S., Deloukas, P., Hurles, M.E. and Dermitzakis ET. (2007) Relative impact of nucleotide and copy number variation on gene expression phenotypes. *Science* **315**(5813): 848-853.

Sung, C.H., Davenport, C.M. and Nathans, J. (1993) Rhodopsin mutations responsible for autosomal dominant retinitis pigmentosa. Clustering of functional classes along the polypeptide chain. *J. Biol. Chem.* **268**(35): 26645-26649.

Sung, C-H., Mackino, C., Baylor, D. Nathans, J. (1994) A rhodopsin gene mutation responsible for autosomal dominant retinitis pigmentosa results in a protein that is defective in localization to the photoreceptor outer segment. *J. Neurosci.* **14**(10): 5818-5833.

Swain, P.K., Chen, S., Wang, Q.L., Affatigato, L.M., Coats, C.L., Brady, K.D., Fishman, G.A., Jacobson, S.G., Swaroop, A., Stone, E., Sieving, P.A. and Zack, D.J. (1997) Mutations in the cone-rod homeobox gene are associated with the cone-rod dystrophy photoreceptor degeneration. *Neuron* **19**(6): 1329-1336.

Swaroop, A., Wang, Q.-L., Wu, W., Cook, J., Coats, C., Xu, S., Chen, S., Zack, D. J. and Sieving, P. A. (1999) Leber congenital amaurosis caused by a homozygous mutation (R90W) in the homeodomain of the retinal transcription factor CRX: direct evidence for the involvement of CRX in the development of photoreceptor function. *Hum. Molec. Genet.* **8**(2): 299-305.

Takayama, S., Xie, Z. and Reed, J.C. (1999) An evolutionarily conserved family of Hsp70/Hsc70 molecular chaperone regulators. *J. Biol. Chem.* **274**(2): 781-786.

Tease, C. and Hulten, M.A. (2004) Inter-sex variation in synaptonemal complex lengths largely determine the different recombination rates in male and female germ cells. *Cytogenet. Genome. Res.* **107**(3-4): 208-215.

Thompson, D.A., Li, Y., McHenry, C.L., Carlson, T.J., Ding, X., Sieving, P.A., Apfelstedt-Sylla, E. and Gal, A. (2001) Mutations in the gene encoding lecithin retinol acyltransferase are associated with early-onset severe retinal dystrophy. *Nat. Genet.* **28**(2): 123-124.

Thompson, J.D., Higgins, D.G. and Gibson, T.J. (1994) CLUSTAL W: improving the sensitivity of progressive multiple sequence alignment through sequence weighting, position-specific gap penalties and weight matrix choice. *Nucleic Acids Res.* **22**(22) 4673-80.

Tuson, M., Marfany, G. and Gonzalez-Duarte, R. (2004) Mutations of *CERKL*, a novel human ceramide kinase gene, causes autosomal recessive retinitis pigmentosa (RP26) *Am. J. Hum. Genet.***74**(1): 128-138.

Usui, T., Ichibe, M., Ueki, S., Takagi, M., Hasegawa, S., Abe, H., Sekiya, K. and Nakazawa, M. (2000) Mizuo phenomenon observed by scanning laser ophthalmoscopy in a patient with Oguchi disease. *Am. J. Ophthalmol.* **130**(3): 359-361.

Ujike, H., Takaki, M., Nakata, K., Tanaka, Y., Takeda, T., Kodama, M., Fujiwara, Y., Sakai, A. and Kuroda, S. (2002) CNR1, central cannabinoid receptor gene, associated with susceptibility to hebephrenic schizophrenia. *Mol. Psychiatry* 7(5): 515-518.

Valente, E.M., Silhavy, J.L., Brancati, F., Barrano, G., Krishnaswami, S.R., Castori, M., Lancaster, M.A., Boltshauser, E., Boccone, L., Al-Gazali, L., Fazzi, E., Signorini, S., Louie, C.M. and Bellacchio, E. (2006) International Joubert Syndrome Related Disorders Study Group; Bertini E, Dallapiccola B, Gleeson JG. Mutations in *CEP290*, which encodes a centrosomal protein, cause pleiotropic forms of Joubert syndrome. *Nat. Genet.* **38**(6): 623-625.

Van Camp, G., Snoeckx, R.L., Hilgert, N., van den Ende, J., Fukuoka, H., Wagatsuma, M., Suzuki, H., Smets, R.M.E., Vanhoenacker, F., Declau, F., Van De Heyning, P. and Usami, S. (2006) A new autosomal recessive form of Stickler syndrome is caused by a mutation in the COL9A1 gene. *Am. J. Hum. Genet.* **79**(3): 449-457.

van Lith-Verboeven, J.J.C., Hoyng, C.B., van den Helm, B., Deutman, A.F., Brink, H.M.A., Kemperman, M.H., de Jong, W.H.M., Kremer, H. and Cremers, F.P.M. (2004) The benign concentric annular macular dystrophy locus maps to 6p12.3-q16. *Invest. Ophthalmol. Vis. Sci.* **45**(1): 30-35.

Venter, J.C., Adams, M.D., Myers, E.W., Li, P.W., Mural, R.J., Sutton, G.G., Smith, H.O., Yandell, M., Evans, C.A., Holt, R.A., Gocayne, J.D., Amanatides, P., Ballew, R.M., Huson D.H., Wortman J.R., Zhang Q., Kodira C.D., Zheng X.H., Chen L., Skupski M, Subramanian G, Thomas PD, Zhang J, Gabor Miklos G.L., Nelson, C,

Broder, S., Clark, A.G., Nadeau, J., McKusick, V.A., Zinder, N., Levine, A.J., Roberts, R.J., Simon, M., Slayman, C., Hunkapiller, M., Bolanos, R., Delcher, A., Dew, I., Fasulo, D., Flanigan, M., Florea, L., Halpern, A., Hannenhalli, S., Kravitz, S., Levy, S., Mobarry, C., Reinert, K., Remington, K., Abu-Threideh, J., Beasley, E., Biddick, K., Bonazzi, V., Brandon, R., Cargill, M., Chandramouliswaran, I., Charlab, R., Chaturvedi, K., Deng, Z., Di Francesco, V., Dunn, P., Eilbeck, K., Evangelista, C., Gabrielian, A.E., Gan, W., Ge, W., Gong, F., Gu, Z., Guan, P., Heiman, T.J., Higgins, M.E., Ji, R.R., Ke, Z., Ketchum, K.A., Lai, Z., Lei, Y., Li, Z., Li, J., Liang, Y., Lin, X., Lu, F., Merkulov, G.V., Milshina, N., Moore, H.M., Naik, A.K., Narayan, V.A., Neelam, B., Nusskern, D., Rusch, D.B., Salzberg, S., Shao, W., Shue, B., Sun, J., Wang, Z., Wang, A., Wang, X., Wang, J., Wei, M., Wides, R., Xiao, C., Yan, C., Yao, A., Ye, J., Zhan, M., Zhang, W., Zhang, H., Zhao, Q., Zheng, L., Zhong, F., Zhong, W., Zhu, S., Zhao, S., Gilbert, D., Baumhueter, S., Spier, G., Carter, C., Cravchik, A., Woodage, T., Ali, F., An, H., Awe, A., Baldwin, D., Baden, H., Barnstead, M., Barrow, I., Beeson, K., Busam, D., Carver, A., Center, A., Cheng, M.L., Curry, L., Danaher, S., Davenport, L., Desilets, R., Dietz, S., Dodson, K., Doup, L., Ferriera, S., Garg, N., Gluecksmann, A., Hart, B., Haynes, J., Haynes, C., Heiner, C., Hladun, S., Hostin, D., Houck, J., Howland, T., Ibegwam, C., Johnson, J., Kalush, F., Kline, L., Koduru, S., Love, A., Mann, F., May, D., McCawley, S., McIntosh, T., McMullen, I., Moy, M., Moy, L., Murphy, B., Nelson, K., Pfannkoch, C., Pratts, E., Puri, V., Qureshi, H., Reardon, M., Rodriguez, R., Rogers, Y.H., Romblad, D., Ruhfel, B., Scott, R., Sitter, C., Smallwood, M., Stewart, E., Strong, R., Suh, E., Thomas, R., Tint, N.N., Tse, S., Vech, C., Wang, G., Wetter, J., Williams, S., Williams, M., Windsor, S., Winn-Deen, E., Wolfe, K., Zaveri, J., Zaveri, K., Abril, J.F., Guigo, R., Campbell, M.J., Sjolander, K.V., Karlak, B., Kejariwal, A., Mi, H., Lazareva, B., Hatton, T., Narechania, A., Diemer, K., Muruganujan, A., Guo, N., Sato, S., Bafna, V., Istrail, S., Lippert, R., Schwartz, R., Walenz, B., Yooseph, S., Allen, D., Basu, A., Baxendale, J., Blick, L., Caminha, M., Carnes-Stine, J., Caulk, P., Chiang, Y.H., Coyne, M., Dahlke, C., Mays, A., Dombroski, M., Donnelly, M., Ely, D., Esparham, S., Fosler, C., Gire, H., Glanowski, S., Glasser, K., Glodek, A., Gorokhov, M., Graham, K., Gropman, B., Harris, M., Heil, J., Henderson, S., Hoover, J., Jennings, D., Jordan, C., Jordan, J., Kasha, J., Kagan, L., Kraft, C., Levitsky, A., Lewis, M., Liu, X., Lopez, J., Ma, D., Majoros, W., McDaniel, J., Murphy, S., Newman, M., Nguyen, T., Nguyen, N., Nodell, M., Pan, S., Peck, J., Peterson, M., Rowe, W., Sanders, R., Scott, J., Simpson, M., Smith, T., Sprague, A., Stockwell, T., Turner, R., Venter, E., Wang, M., Wen, M., Wu, D., Wu, M., Xia, A., Zandieh, A. and Zhu, X. (2001) The sequence of the human genome. *Science* **291**(5507): 1304-51.

Verheijen, F.W., Verbeek, E., Aula, N., Beerens, C.E.M.T., Havelaar, A.C., Joosse, M., Peltonen, L., Aula, P., Galjaard, H., van der Spek, P.J. and Mancini, G.M.S. (1999) A new gene, encoding an anion transporter, is mutated in sialic acid storage diseases. *Nat. Genet.* **23**(4): 462-465.

Vervoort, R., Lennon, A., Bird, A.C., Tulloch, B., Axton, R., Miano, M.G., Meindl, A., Meitinger, T., Ciccodicola, A. and Wright, A.F. (2000) Mutational hot spot within a new RPGR exon in X-linked retinitis pigmentosa. *Nat. Genet.* **25**(4): 462-466.

Wang, D.G., Fan, J.B., Siao, C.J., Berno, A., Young, P., Sapolsky, R., Ghandour, G., Perkins, N., Winchester, E., Spencer, J., Kruglyak, L., Stein, L., Hsie, L., Topaloglou, T., Hubbell, E., Robinson, E., Mittmann, M., Morris, M.S., Shen, N., Kilburn, D., Rioux, J., Nusbaum, C., Rozen, S., Hudson, T.J., Lipshutz, R., Chee, M. and Lander, E.S. (1998) Large-scale identification, mapping, and genotyping of single-nucleotide polymorphisms in the human genome. *Science* **280**(5366): 1077-1082.

Wang, L., Xu, J., Zeng, L., Ye, X., Wu, Q., Dai, J., Ji, C., Gu, S., Zhao, C., Xie, Y. and Mao, Y. (2002) Cloning and characterization of a novel human STAR domain containing cDNA KHDRBS2. *Mol. Biol. Rep.* **29**(4): 369-375.

Waterston, R.H., Lander, E.S. and Sulston, J.E. (2002) On the sequencing of the human genome. *Proc. Natl. Acad. Sci. U S A.* **99**(6): 3712-3716.

Weber JL. (1990) Human DNA polymorphisms and methods of analysis. *Curr. Opin. Biotechnol.* **1**(2): 166-171.

Weleber RG. (1994) *Retinitis pigmentosa and allied disorders*; in: Ryan SJ, 335 ed. Retina. 2nd ed. St. Louis: Mosby, pp 335-466.

Weleber, R.G., Carr, R.E., Murphey, W.H., Sheffield, V.C. and Stone, E.M. (1993) Phenotypic variation including retinitis pigmentosa, pattern dystrophy, and fundus flavimaculatus in a single family with a deletion of codon 153 or 154 of the peripherin/*RDS* gene. *Arch. Ophthalmol.* **111**(11): 1531–1542.

Wells, J., Wroblewski, J., Keen, J., Inglehearn, C., Jubb, C., Eckstein, A., Jay, M., Arden, G., Bhattacharya, S., Fitzke, F. and Bird, A. (1993) Mutations in the human retinal degeneration slow (*RDS*) gene can cause either retinitis pigmentosa or macular dystrophy. *Nat. Genet.* **3**(3): 213–218.

West, K.L., Ito, Y., Birger, Y., Postnikov, Y., Shirakawa, H. and Bustin, M. (2001) HMGN3a and HMGN3b, two protein isoforms with a tissue-specific expression pattern, expand the cellular repertoire of nucleosome-binding proteins. *J. Biol. Chem.* **276**(28): 25959-25969.

Witkorsky, P. (1994) Functional Anatomy of the Retina. In W Tasman, EA Jaeger (eds), *Duane's Foundations of Clinical Ophthalmology* (Vol **1**). Philadelphia: Lippincott, p. 1.

Woods, C.G., Valente, E.M., Bond, J. and Roberts, E. (2004) A new method for autozygosity mapping using single nucleotide polymorphisms (SNPs) and excludeAR. *J. Med. Genet.* **41**(8): e101.

Xie, J., Zhu, H., Larade, K., Ladoux, A., Seguritan, A., Chu, M., Ito, S., Bronson, R. T., Leiter, E. H., Zhang, C.Y., Rosen, E.D. and Bunn, H.F. (2004) Absence of a reductase, NCB5OR, causes insulin-deficient diabetes. *Proc. Nat. Acad. Sci.* **101**(29): 10750-10755.

Yagi T. and Takeichi, M. (2000) Cadherin superfamily genes: functions, genomic organization, and neurologic diversity. *Genes Dev.* **14**(10): 1169-1180.

Yamada-Okabe, T., Doi, R., Shimmi, O., Arisawa, M. and Yamada-Okabe, H. (1998) Isolation and characterization of a human cDNA for mRNA 5'-capping enzyme. *Nucleic Acids Res.* 26**(7)**: 1700-1706.

Yamamoto, H., Simon, A., Eriksson, U., Harris, E., Berson, E.L. and Dryja, T.P. (1999) Mutations in the gene encoding 11-cis retinol dehydrogenase cause delayed dark adaptation and fundus albipunctatus. *Nat. Genet.* **22**(2): 188-191.

Yamamoto, S., Sippel, K.C., Berson, E.L. and Dryja, T.P. (1997) Defects in the rhodopsin kinase gene in the Oguchi form of stationary night blindness. *Nat. Genet.* **15**(2): 175-178.

Yi, C.H., Terrett, J.A., Li, Q.Y., Ellington, K., Packham, E.A., Armstrong-Buisseret, L., McClure, P., Slingsby, T. and Brook, J.D. (1999) Identification, mapping, and phylogenomic analysis of four new human members of the T-box gene family: EOMES, TBX6, TBX18, and TBX19. *Genomics* **55**(1): 10-20.

Zagon, I., Verderame, M.F. and McLaughlin, J. (2002) The biology of the opioid growth factor receptor (OGFr). *Brain Res. Rev.* **38**(3): 351-376.

Zangerl, B., Goldstein, O., Philp, A.R., Lindauer, S.J.P., Pearce-Kelling, S.E., Mullins, R.F., Graphodatsky, A.S., Ripoll, D., Felix, J.S., Stone, E.M., Acland, G.M. and Aguirre, G.D. (2006) Identical mutation in a novel retinal gene causes progressive rod-cone degeneration in dogs and retinitis pigmentosa in humans. *Genomics* **88**(5): 551-563.

Zhang, K., Kniazeva, M., Han, M., Li, W., Yu, Z., Yang, Z., Li, Y., Metzker, M.L., Allikmets, R., Zack, D.J., Kakuk, L.E., Lagali, P.S., Wong, P.W., MacDonald, I.M., Sieving, P.A., Figueroa, D.J., Austin, C.P., Gould, R.J., Ayyagari, R. and Petrukhin, K. (2001) A 5-bp deletion in ELOVL4 is associated with two related forms of autosomal dominant macular dystrophy. *Nat. Genet.* **27**(1): 89-93.

Zhang, Q., Zulfiqar, F., Riazuddin, S.A., Xiao, X., Ahmad, Z., Riazuddin, S. and Hejtmancik, J.F. (2004) Autosomal recessive retinitis pigmentosa in a Pakistani family mapped to CNGA1 with identification of a novel mutation. *Mol. Vis.* **10**: 884-889.

Zhang, Q., Zulfiqar, F., Xiao, X., Riazuddin, S.A., Ayyagari, R., Sabar, F., Caruso, R., Caruso, R., Sieving, P.A., Riazuddin, S. and Hejtmancik, J.F. (2005) Severe autosomal recessive retinitis pigmentosa maps to chromosome 1p13.3-p21.2 between D1S2896 and D1S457 but outside ABCA4. *Hum. Genet.* **118**(3-4): 356-365.

APPENDIX 1

Table 1 Gene-specific STSs primers for *OGFRL1*, *KHDRBS2*, *KIAA1411* and *PTP4A1* genes

Genes	Primer Sequence	Product size
OGFRL1	(F) AAAAGTGGCACCAAAAGAGC	395 bp
	(R)CAAACAACAAAATGCTTATGACAG	
KHDRBS2	(F)AGAAGAATGGGCCACAACC	486 bp
	(R) CAACCCTAAACAAAGTTTCTGC	
KIAA1411	(F) AATGATCCACAACTTGCTTCG	656 bp
	(R) GCAGCCATAATTTTATTTCCAG	
PTP4A1	(F)CGTGGAGCTTTTAACAGCAAG	925 bp
	(R)TTGCACAAGACAAAGGCAAC	

Table 2 Primers designed and amplification conditions for the genes studied in this work

Gene	Exon No	Sequence (5`..... 3`)	Product size (bp)	$MgCl_2$	Temp
KIAA1586	Exon 1 F Exon 1 R	GAACTACCATCCCAGCATCC GGGTTCCTCGCTCAGACAC	448	1.5 mM	64.0 °C
	Exon 2 F Exon 2 R	TTCCGTGAAATTGTGCTCAG AACATTAAATGACCAGGTGAGG	300	1.5 mM	57.0 °C
	Exon 3 F Exon 3 R	TGCCACTTGCAAGATTTTCTC CTGGCCTCAAGTGATCCAAC	376	1.5 mM	57.0 °C
	Exon 4A F Exon 4A R	TGGGTTTTTCAAGAAATAGCAAG TCTTGCCCCCTCAATATCAG	798	3.5 mM	62.0 °C
	Exon 4B F Exon 4B R	AGCCCATGGTAAAATTCAGG ATCTCTTCGCCAAACCAGAG	908	3.5 mM	57.0 °C
	Exon 4C F Exon 4C R	TCGATTACAATTGTCACTTGATG TTACAAACGGTGTTGCATCC	995	1.5 mM	60.0 °C
	Exon 4D F Exon 4D R	AATTACTTTGATTTGCTGGAACC AAAATATTTCACATTGTTTCAGTTTTC	996	2.5 mM	57.0 °C
PRIM2A	Exon 1 F Exon 1 R	ACACCTTGAATTCCCAGACG CTACTGCTGCCTGCAAAGTG	300	1.5 mM	60.0 °C
	Exon 2 F Exon 2 R	AGGACATCACCCAGGAATTG TGTTGAATGGATTGCTGAATG	427	1.5 mM	60.0 °C
	Exon 3 F Exon 3 R	GGCAATTACCTGTCATGTTCTG CATCTGACTTCATGTCAATCACC	388	1.5 mM	63.0 °C
	Exon 4 F Exon 4 R	CTGGGTGGTAGAGCAAGACC GTTCAACCCCATGATCAACC	360	1.5 mM	63.0 °C

Table 2 (continued).

Gene	Exon No	Sequence (5`..... 3`)	Product size (bp)	$MgCl_2$	Temp
	Exon 5 F Exon 5 R	TGGCATCTTGCTGATGTTTG AAGTGATCTGCCCACCACAG	681	2.5 mM	57.0 °C
	Exon 6 F Exon 6 R	TTCAGAAATTGGCAGGGTTG CATTGGCACACCATTAGTGC	485	1.5 mM	57.0 °C
	Exon 6 new F Exon 6 new R	TTCAGAAATTGGCAGGGTTG CAATGCGACATATTTAACAAAACC	378	1.5 mM	57.0 °C
	Exon 7 F Exon 7 R	GCCACTGTTTGCTAATGCTG CCTAGGAATTTTGGGATTAACAG	473	3.5 mM	57.0 °C
	Exon 8 F Exon 8 R	TGCCCTTCAGCTCGTTTTAC AATTGAAGCGGTTTCACCAC	245	1.5 mM	57.0 °C
	Exon 9 F Exon 9 R	TTGGCTATGTTTCTGCTAAGG TCTATCTCCTCACCCAAAAGTC	300	1.5 mM	58.5 °C
	Exon 10 F Exon 10 R	AAAGCAGCACTTTCTTATGGTG AGACCGTTTCATTTTCAGACC	381	1.5 mM	63.0 °C
KHDRBS2	Exon 1 F Exon 1 R	CTACCGCCCAATGAGAGC CTAAGGCGAGCATCTTCAGG	594	1.5 mM	58.5 °C
	Exon 2 F Exon 2 R	CACATAACTGTTGGTGAGATGCTG CCCTATGTCAGTATCATGTGCTTG	436	1.5 mM	62.0 °C
	Exon 3 F Exon 3 R	TGGCATGACTCTCTTCTCAGTG ACAGGGTGATCCCAGGAAAT	368	1.5 mM	60.8 °C
	Exon 4 F Exon 4 R	TAGCAGATTTTTATTTCTCAAAGGG TTTTAGCTTTGTATCGACCTGTGG	443	1.5 mM	58.5 °C
	Exon 5 F Exon 5 R	ATATTTTTGCATATAAAGTTCCAGG GGTAGTGATTGTGGCTGATGTT	381	2.5 mM	60.0 °C
	Exon 6F Exon 6 R	TTTTATTTCATTGTATGGAGGCTGTG CACGGTATATGAACAGTTTGAGAC	384	2.5 mM	60.0 °C
	Exon 7 F Exon 7 R	AAATGTGATATATGGATACTTACCC GTAAGCAACTTGATAATTCAGAAAG	359	3.5 mM	60.0 °C
	Exon 8 F Exon 8 R	GTTTTATGCCTTGAAGTTCCTGG TACTAGCTGTGTAAGTCAAATCTC	340	2.5 mM	60.0 °C
	Exon 9 F Exon 9 R	CGGTGTTGAGATCTTTTGTTTTC GGACTATTACTTGTCTTGTTGCTG	297	2.5 mM	57.0 °C
PTP4A1	Exon 1 F Exon 1 R	CGCTTAGCCATTCATCAACC CTCCGAACAAAGGCGACAG	499	0795 mix	57.0 °C
	Exon 2 F Exon 2 R	ACTCACCCCTTGAGTTTTGC TCTGGGAACTGGAATTGTAGG	834	1.5 mM	65.2 °C
	Exon 3 F Exon 3 R	AGTGTATGAAGGGGGCACAC TCCTTGCTTAGCTTTTCACC	361	1.5 mM	62.0 °C
	Exon 4 F Exon 4 R	TTGAGCATTTAGTCACATTTGG TTCTCCAAACATTCCCCAAC	464	1.5 mM	57.0 °C
	Exon 5 F Exon 5 R	AGGCCTTGGGAGGTAAATG ATGAGCAACTGCATGAAATG	487	1.5 mM	57.0 °C
	Exon 6 F Exon 6 R	TTGCCACAAGAGAGGTGATG GCCAAATCTGTCTAGCTTGAGG	366	1.5 mM	64.0 °C
PHF3	Exon 1 F Exon 1 R	GCGGAGGTGTGAGCTAGAAGC GGAGAAAAGCGCGGAGAGTCC	649	2.5 mM	68.0 °C
	Exon 2 F Exon 2 R	CACATTCCAGATTTTCAAGAGTATG CGAATGGATTAGCAAAACATCA	480	2.5 mM	52.0 °C

Table 2 (continued).

Gene	Exon No	Sequence (5`..... 3`)	Product size (bp)	$MgCl_2$	Temp
	Exon 3A F Exon 3A R	CAGAATAAAGAAGTGATATATTC CTCAAGAATATGGTCATCTTCATGG	840	2.5 mM	57.0 °C
	Exon 3B F Exon 3B R	GAAGCTTTGATGGAATGTAAAGC CATCTGTGGTCATGTTTTGCTTAG	843	3.5 mM	64.6 °C
	Exon 3C F Exon 3C R	GAGTCCCATGAAACAGCAAAC CAGGTCTCTGTGTATCAAATAATG	1080	3.5 mM	51.0 °C
	Exon 4 F Exon 4 R	CAGATATTGAAAATTTAATTTAGCC CAAAATTATTGCAGTCAGTCC	560	2.5 mM	57.0 °C
	Exon 5 F Exon 5 R	GTTTAGTTATTTTCATTCTAATG CCTAAGTATACTAATTAATTGTATC	366	2.5 mM	52.0 °C
	Exon 6-7 F Exon 6-7 R	CTTTTAATCAGTTTTGTTTGTAAAC CTACTGTATTACAATCTGAGATACC	660	2.5 mM	52.0 °C
	Exon 8 F Exon 8 R	GATTTCAGTGTCAGGAATATTTCAA CAAAAGCAAATTATAATCTCACTCCA	657	1.5 mM	57.0 °C
	Exon 9 F Exon 9 R	CAGGCTGTCATTTAATCTCTGTG TACCCAATGGCTGAAAAACATAG	334	1.5 mM	57.0 °C
	Exon 10 F Exon 10 R	GGAAAATATAAATTGATTTTGAT CAATATTGGGAAAACAAAACCATC	375	2.5 mM	52.0 °C
	Exon 11 F Exon 11 R	CAGCAATTGAATCATAGAACCTG GAAGACTTGCAAGTATAATCTGGC	441	1.5 mM	57.0 °C
	Exon 12 F Exon 12 R	AACCCCAGGAAATGTATGGTTAC ATGAGAGGTTCCCAAAATGTCAC	430	1.5 mM	57.0 °C
	Exon 13 F Exon 13 R	AATAGCCTCATATTTTGGCCTTC AGTACATCTTGGGAAAAGTGCAG	492	1.5 mM	57.0 °C
	Exon 14 F Exon 14 R	GAGAAATAGTTTTAAAACCAAGC CTCTAGAGGGCTGGATCCTGAG	447	1.5 mM	57.0 °C
	Exon 15 F Exon 15 R	AGTTGGTAAACCACGTTATTTGG GAAGGCAGAATCAGTCTTTTCAC	410	1.5 mM	57.0 °C
	Exon 16A F Exon 16A R	GACGCAGAGACAGAAGCCAA CGATATTTACCAATTAAGGAATAAAAC	720	1.5 mM	58.4 °C
	Exon 16B F Exon 16B R	CTGTGTGTTGGTACAGAGTGCT GTTTTTCCCCTCATCTAATGCCTG	900	2.5 mM	58.4 °C
Q9NQ15	Exon 1A F Exon 1A R	TCCAACTTGGCCAGAAACAG GGTTACATGTATTTCCAGCCC	540	1.5 mM	63.0 °C
	Exon 1B F Exon 1B R	GGTTTTCAAGGCTGTATCCG TTGAATTACAACTACATGGTGCC	420	1.5 mM	63.0 °C
	Exon 1C F Exon 1C R	AGAAACCTCCAGTTCACTACTATATCC CCCCGTAAGCAATGTATCAAAG	540	1.5 mM	62.0 °C
Q5T669	Exon 1A F Exon 1A R	GTTGGAGCTCTGAAAACACG TAGTATTGGTGGAGTGGATTGTC	350	1.5 mM	52.0 °C
	Exon 1B F Exon 1B R	CCACGGATAAGAGCTGAGAC AGAGAAGGAGAGATGCGCTG	540	1.5 mM	58.4 °C
EGFL11	Exon 1 F Exon 1 R	CCATCCTCTGGATTATCATAAAAG CTTTGGGAAAGAAGGCCAAG	377	1.5 mM	57.0 °C
	Exon 2A F Exon 2A R	GCTGCTGGTGACACTATCTTTG GAAGTCCAAGCAGATGTTTTCTG	479	1.5 mM	57.0 °C
	Exon 2B F Exon 2B R	GCCTGATGGTTTTTCACAGC AAAATGGAGGCTGGCAATG	591	1.5 mM	57.0 °C
	Exon 2C F Exon 2C R	GCAGTTCTGCCAGGAATCTC GTGCTGGGATTACAGGTGTG	464	1.5 mM	57.0 °C

Table 2 (continued).

Gene	Exon No	Sequence (5'..... 3')	Product size (bp)	$MgCl_2$	Temp
	Exon 3 F	TTTCAATTTAAATGCATCATCG	505	2.5 mM	57.0 °C
	Exon 3 R	TGAAAAGCATGTGAACTGTTG			
	Exon 4 F	TTTGCAAAAGTTACTGTAGAATTGC	520	1.5 mM	57.0 °C
	Exon 4 R	GACCGTTCTTGTTCGTCTGAG			
	Exon 5 F	TGAGATGGGAGATGGTGTTG	473	1.5 mM	57.0 °C
	Exon 5 R	CAACAATTAACCCAAAACATGC			
	Exon 6 F	GCTTTTTGGCTAAGATCACAGG	363	2.5 mM	57.0 °C
	Exon 6 R	TGGCTAAGATTAATAAGAGCATTTG			
	Exon 7 F	GGCTTTTGAACATGGATATGAC	574	1.5 mM	57.0 °C
	Exon 7 R	TCTCTTGCACCAAGTAGATTTCC			
	Exon 8 F	GGAACTTATTTTGTGGCAGATG	492	1.5 mM	57.0 °C
	Exon 8 R	TGATTCTTCAAAATTTTTACTTTCC			
	Exon 9 F	CAAGCTTTGAACCCTTGTCC	545	1.5 mM	57.0 °C
	Exon 9 R	TTCTTCCCTCCTTTTATTGTGC			
BAI3	Exon 1A F	TTTTCTCAATGCACGTAGACTC	560	1.5 mM	57.0 °C
	Exon 1A R	TTGGGCTGACCTTGTTCAATACC			
	Exon 1B F	TTTTCACTCCTGGCTTATCAGTTTG	600	1.5 mM	54.0 °C
	Exon 1B R	GATAAATAATTAGGCCTGTGTG			
	Exon 2 F	CTAGGTATGTATAGGAACATATTGC	320	1.5 mM	54.0 °C
	Exon 2 R	ATCAGCTCCAAAAACTGACAAATG			
	Exon 3 F	GCATGTCATAATGTCAGTTTGGTA	342	1.5 mM	54.0 °C
	Exon 3 R	ACCCGTTTCATATGAAAATAACAA			
	Exon 4 F	CATTTGTCTATTTAATGAGTTTTGC	371	1.5 mM	54.0 °C
	Exon 4 R	CCAACGTGACTGAATGAAGGTTGTA			
	Exon 5 F	CATTCATAGTCCATTGATTGG	370	1.5 mM	52.0 °C
	Exon 5 R	CATGACCCTCTGGCATAGTTCTG			
	Exon 6 F	GAATAAGGTTTATTCACAGTAGTAG	381	1.5 mM	52.0 °C
	Exon 6 R	GAGGAATATGACCCTTAACCAATTG			
	Exon 7 F	CTAAAGAGCTCTGCAGTTAGAGGCTTA	323	1.5 mM	52.0 °C
	Exon 7 R	TTGGACAGACTTATTTATGG			
	Exon 8 F	AATATCAATTTCATGTGCATGTTT	340	1.5 mM	52.0 °C
	Exon 8 R	GATGTTACTGATTTGATTGTACAGC			
	Exon 9 F	GGCTATTTTAAGTTAATTGAGCAA	435	1.5 mM	54.0 °C
	Exon 9 R	GCATAACTTGGATGAGCATT			
	Exon 10 F	GCAATATTGCAAAGTGCTTATACC	309	1.5 mM	57.0 °C
	Exon 10 R	CTAGGATATAACCTAGACTGAC			
	Exon 11 F	GGCAGCTGTA GATTTTTTTGAAGTG	349	1.5 mM	54.0 °C
	Exon 11 R	GCTCACATGCAGTTAAACATATG			
	Exon 12 F	GAATATACTGCAAGATTTACCTTG	347	2.5 mM	57.0 °C
	Exon 12 R	CAGACTATTTCTAAACTGTTTAAT			
	Exon 13 F	CTTTGCCTAAGGAAGTACTGG	260	1.5 mM	54.0 °C
	Exon 13 R	CCTTCATATTACCACAGCTTGTTTG			
	Exon 14 F	GGATGCATTTATTTGAAACCATCCC	290	1.5 mM	52.0 °C
	Exon 14 R	GCAACTATAAAAGTCTAGAAAATG			
	Exon 15 F	CCACAAGATAAGAAATCTTCCATTC	234	1.5 mM	57.0 °C
	Exon 15 R	CACTGACTTATATTCCTGTTAAC			
	Exon 16 F	CAGTAGACGACTCTCTCAATTAAA	337	1.5 mM	57.0 °C
	Exon 16 R	GTACCCTGCAACATTTTCCATT			
	Exon 17 F	CAACTATATAGGCTATTTTTGAG	322	1.5 mM	57.0 °C
	Exon 17 R	CTGCTTTCAGTAAATTAAGAAGAC			
	Exon 18 F	CAGATGAATGCCATCAGTTTG	293	2.5 mM	62.0 °C
	Exon 18 R	GTCAGAAGTTCTCCATTTTAG			

Table 2 (continued).

Gene	Exon No	Sequence (5`..... 3`)	Product size (bp)	$MgCl_2$	Temp
	Exon 19 F Exon 19 R	GAAATAAAAGCAATGAATCAGAG CACAAAGTAGCCTGTGTCTAATC	351	1.5 mM	57.0 °C
	Exon 20 F Exon 20 R	GCACCTGGAGTTTGTTCTGG CTACCATTGTTAATGATTCCATGATAA	270	1.5 mM	57.0 °C
	Exon 21 F Exon 21 R	GCCAAAATTCCAAGGCAAAA CTACACAAGAACTACATTATC	277	1.5 mM	57.0 °C
	Exon 22 F Exon 22 R	TACTAGTGATACGGTGGTTATGAATT CAGAGTCAAACGCAGTCAGTG	283	1.5 mM	57.0 °C
	Exon 23 F Exon 23 R	CGTATTTAAAAGCTAACTTGAAGC GGTCTTGTATTAGAAAACACAAT	287	2.5 mM	57.0 °C
	Exon 24 F Exon 24 R	CCAAGTTAATGGTCTTGGAACCAC CCAGCTTTAATCTGAACATCAAG	385	1.5 mM	57.0 °C
	Exon 25 F Exon 25 R	GATAGTAAAATCAGTGATAACC GCCAAAGTCAATCAAAATGAAAA	303	1.5 mM	57.0 °C
	Exon 26 F Exon 26 R	TACTGCCAAGTTAGATATCTGTAA GCCCTTTCACAGAACAATATGTAA	261	1.5 mM	57.0 °C
	Exon 27 F Exon 27 R	CTTTAATGTTTAGTAGAAAGCGAGAC CCAGTGTCACATCAATCAAT	824	1.5 mM	52.0 °C
	Exon 28 F Exon 28 R	CAAGCAGGATTATCTTTAATGAA CCCTTACATGGCTGCATAGAGTAA	237	1.5 mM	52.0 °C
	Exon 29 F Exon 29 R	GCCAAACTTGATTACCCTTATT CCCACCATTAGGAGGTCCTGG	295	1.5 mM	52.0 °C
	Exon 30 F Exon 30 R	GCATCACAGAAACTGGATTAAGATT GGATGGTCAGAACTGTACACCTGG	500	1.5 mM	52.0 °C
C6orf209	Exon 1 F Exon 1 R	GGTGATGTCACTGCGTCC GCGAAGAGGGTCTCCGGGG	409	1.5 mM	55.0 °C
	Exon 2 F Exon 2 R	CAACTAAAATAACCTTTACTTCAC CCATTCTCATTCATTCCCAGATAC	411	3.5 mM	50.0 °C
	Exon 3 F Exon 3 R	GGAAGTGATATTCAGTCGTATTAA TAATTCGACCCAAGAGGAAGAACC	256	1.5 mM	55.0 °C
	Exon 4 F Exon 4 R	GGAATCAGATAGGGGAGTGAA GCTAACATTGTATTTCTATTAGA	335	1.5 mM	55.0 °C
	Exon 5 F Exon 5 R	GCATGTATCTGATGTGAAGGTACTGTT GGCTATTGTTCCTTGGAGATTT	316	1.5 mM	55.0 °C
	Exon 6 F Exon 6 R	CCTCTGTGCATAGTACAGATTTT CCAGCTGGGGTTAAATTCTTAAAAC	318	1.5 mM	55.0 °C
	Exon 7 F Exon 7 R	GCAGCTCAGCTTTCTATGTTGATT GAAAAAGAATCAAAATATTATAAAGG	280	3.5 mM	51.0 °C
	Exon 8 F Exon 8 R	CACAACTGCTGACTCTTATGAC GGTTGACAATGTCTAAGTCATATC	316	1.5 mM	61.0 °C
	Exon 9 F Exon 9 R	GAGTGTCCATCCTGAAAAGG CCATGCTGTAATGCCTCAAAAGG	355	3.5 mM	55.5 °C
	Exon 10-11 F Exon 10-11 R	CATTGTCATATTCTAGCAACTCA GCAACAGGATGTCAGAATGTTT	691	1.5 mM	61.0 °C
	Exon 12 F Exon 12 R	CACAGTAGCCTAATCTAAATCAAGG GCTACTATATTCTAAATCTAAGAT	345	3.5 mM	55.5 °C
	Exon 13 F Exon 13 R	GGTTGATTGAACTGTGTAAATC GAGCTAATATCTTATGCTAACC	352	3.5 mM	55.5 °C
	Exon 14 F Exon 14 R	GGAATGTTAGATAGATGTAGTT CCACGTAGTAAAACAAATGC	299	1.5 mM	61.0 °C
	Exon 15 F Exon 15 R	GCCATATGATCTTAGTCATTAGC TACTATGATACAAATGGCCTAGTAAG	301	3.5 mM	62.3 °C

Table 2 (continued).

Gene	Exon No	Sequence (5`..... 3`)	Product size (bp)	$MgCl_2$	Temp
	Exon 16 F Exon 16 R	CTTACTAGGCCATTTGTATCATAGTA GCTATATTGTAAATATTATTTGG	660	3.5 mM	55.5 °C
COL19A1	Exon 1F Exon 1R	GGCGACATCGCTGTCATTAAA CCATGTGTAGCACAGTTTTTACA	354	1.5 mM	64.6 °C
	Exon 2 F Exon 2 R	TAACGTTGATTGGTTTTGCTTTGG CTGTTATAGTACATTAATCTATGGCCTT	310	2 mM	61.2 °C
	Exon 3 F Exon 3 R	CCTCATTTTACAGAAATTTAATAAATG CGTTAATGCTATGATCTTAAATTGCAG	315	2 mM	61.2 °C
	Exon 4 F Exon 4 R	CAAGAAATTTTGCTGATCCCA AACACGTTTACCACTGCATTCC	373	1.5 mM	61.2 °C
	Exon 5 F Exon 5 R	GCATAAGTTACACATTTACTGAG CTAGATCTACTCGCAAATTTG	347	1.5 mM	61.2 °C
	Exon 6 F Exon 6 R	GCCTCAGTTATACTAATATGCATC AAAATTGATGAGAAGGGAATCTA	492	1.5 mM	61.2 °C
	Exon 7 F Exon 7 R	CAGTAATTTATTTATATTAGCTTCC CCTTACTAGGAATAAATTACCCAC	334	1.5 mM	58.4 °C
	Exon 8 F Exon 8 R	CCTCAGCAATCCCTAGTTTAGTGG CTGAATGGCAAGACACATTCT	320	1.5 mM	61.2 °C
	Exon 9 F Exon 9 R	GCGTTATCTTGCTAGTGCCAG GTCTCTATTTCAGTAATCAGC	303	2 mM	61.2 °C
	Exon 10 F Exon 10 R	GGAAAGTCCCTATGCATGATAGATAT CCACAAGTTCTCTTTGAAAAG	337	1.5 mM	61.2 °C
	Exon 11 F Exon 11 R	GAGCTTACATGTTAGAAATGGTTGTTA TGTCTATAAAATTATTGAATTGC	302	1.5 mM	58.4 °C
	Exon 12 F Exon 12 R	GCCTTTCAAGGGTTTAGCAAA GATTCTTAATTTTGTTGGATCATGG	303	1.5 mM	58.4 °C
	Exon 13 F Exon 13 R	GGAAGAATGAGATTTGGAGGTT GGTTAATTTTAGAATGCTTTTAGG	275	1.5 mM	61.2 °C
	Exon 14 F Exon 14 R	GCAGAGACTTTTATCAGGATGAAG CTCTGTGACTTAAATTCTGGTTT	276	1.5 mM	61.2 °C
	Exon 15 F Exon 15 R	GTTCAACCTTGAAAGAGCTCAAATTAC TTTCAGCCTTTGGATAATTGATAC	324	1.5 mM	58.4 °C
	Exon 16 F Exon 16 R	GTCATGTGGAATTGGAATTGTTTC GCTGAAACCAGTCATTCTAAACAGTAG	265	1.5 mM	61.2 °C
	Exon 17 F Exon 17 R	CAGAATATTTGACTAAATAGACAAG GGAAAGATGTTTAAATACATGTGA	325	1.5 mM	58.4 °C
	Exon 18 F Exon 18 R	CCTAGTATCCATAAAAAGCGG GGAGAATCACTTGAACCTGGG	275	1.5 mM	61.2 °C
	Exon 19 F Exon 19 R	GCATTGTCTGTTGGATGCTAATAG CTTGCTTGAAGATCTGATCTGTTG	330	1.5 mM	61.2 °C
	Exon 20 F Exon 20 R	GAATCTGAGTTTGGCCTATAGG GGACCTTATTTAATCAAATCTATT	242	1.5 mM	64.6 °C
	Exon 21-22 F Exon 21-22 R	GAATGAACTCTCCTTGATTTTATTGTG GGAGAGCATTTGTGAAGAAAATGAG	434	1.5 mM	61.2 °C
	Exon 23 F Exon 23 R	GAAAAGTGGGATGGTGGAAAGTT CATAGATGACCCATGTCTTTGG	309	1.5 mM	61.2 °C
	Exon 24 F Exon 24 R	CCAAAATCAATCCAACTCCTTC CTGTCCTTTCATCTCCCTTATG	274	1.5 mM	58.4 °C
	Exon 25 F Exon 25 R	GAATGAAGTTTGACTGGCTATGAT CTTGTGATCTGAAACTAGGAACC	285	1.5 mM	58.4 °C
	Exon 26-27 F Exon 26-27 R	CCGTTCCTTATTCTTTTATAGAAA GTATTTCCGTCTCTGACCTTTCTAT	471	1.5 mM	64.6 °C

Table 2 (continued).

Gene	Exon No	Sequence (5`..... 3`)	Product size (bp)	$MgCl_2$	Temp
	Exon 28-30 F Exon 28-30 R	GCAGTTTTCCACGTGTGTAC GGATAAACAAAATCACCAAGC	607	1.5 mM	58.4 °C
	Exon 31 F Exon 31 R	CTAAAGTGAGACACCAGAAGCTTC CCAGCTAAGCAATTGACTCAATTT	261	1.5 mM	64.6 °C
	Exon 32-34 F Exon 32-34 R	CACTCATCTCCAGAGGTTCCAA TTATTGGTTATAGCATCAGATCTGAGC	815	1.5 mM	64.6 °C
	Exon 35 F Exon 35 R	GACAAACATTATGTTTCTCGATTAGC GCTTGGATGAGGCTACTTTTCC	328	1.5 mM	64.6 °C
	Exon 36 F Exon 36 R	GAAGAAACATAAGCTTCTAGGGC CCATCATTTCTACTTTTAGGCTTTGC	308	1.5 mM	64.6 °C
	Exon 37 F Exon 37 R	AAGACTACAAGGCTGAAACAAC GCTACATTGGCTAACATTTATATTT	326	1.5 mM	61.2 °C
	Exon 38-39 F Exon 38-39 R	CTTAGAGTATTAAATTCCCTTTGTAACT GTATTCATAACATGCGTTTTTCA	445	1.5 mM	58.2 °C
	Exon 40 F Exon 40 R	CAAGTTATATTTATTCATCTTATCTT CCAGCATGTTAATTGATGAACACC	305	1.5 mM	61.2 °C
	Exon 41 F Exon 41 R	GGCATATCATTTCCTTGCTAAATT GCTAGAATGTAAGTCCCATGAGTACAT	287	1.5 mM	54.2 °C
	Exon 42 F Exon 42 R	CACACTAGCTTCACCCCATCTAATA GGTGGCATTATTTATGAAAGTAGAA	345	1.5 mM	54.2 °C
	Exon 43-44 F Exon 43-44 R	GATTCCAGACATGAGCCACC CCATCTGTGCATTCTTCTTACTCC	498	1.5 mM	61.2 °C
	Exon 45-46 F Exon 45-46 R	CCATTTTACCACCTTTCTTTACCAA CCTTTATAGATTTGGTGATTTGCAGG	461	1.5 mM	54.2 °C
	Exon 47 F Exon 47 R	GACACAGAGGAGTTTAAGTTATT GGGACCAGTTTAGGTTTGTTTTATTT	419	1.5 mM	54.2 °C
	Exon 48 F Exon 48 R	GCATCCCTACAGAAGTTTCAAA TAAAATGGGCTGCCCCTTAA	313	1.5 mM	61.2 °C
	Exon 49 F Exon 49 R	CAGCAGTCAGACCAGTTGGTAA AACCATTTTATATATTGCATATATT	417	1.5 mM	50.6 °C
	Exon 50-51 F Exon 50-51 R	GCAAAACAGTTAGCTAATATACTAT CAAACGGTTGCTTTTAATGCC	666	1.5 mM	66.3 °C
KIAA1411	Exon 1 F Exon 1 R	ATCTCAGTTGGCGCTGGAG TCCCCACCGACCTTCAAC	600	Buffer 3.5% +5%DMSO	57.0 °C
	Exon 2 F Exon 2 R	TTGAGCAGAAGAACTTTCTAAACG TCTCAAAGAAGTGTGGTTTGATG	388	1.5 mM	57.0 °C
	Exon 3 F Exon 3 R	CAAAACATAGGTTTCCTTAAGACAG GCTTGCAAGTGGGGTAAAATC	286	1.5 mM	57.0 °C
	Exon 4 F Exon 4 R	CTCAGAGAGGGGAGGGAAG GTCCCCACCGACCTTCAAC	337	2.5 mM	57.0 °C
	Exon 5 F Exon 5 R	TGGATACAAATGTGGAAGTCG ACATTCTTTGATGTGCTCATTG	375	2.5 mM	57.0 °C
	Exon 6-7 F Exon 6-7 R	TTTCAGAAATGTTCCAATACTGC TTTAAGAGGAAAATGGGCAATC	553	3.5 mM	57.0 °C
	Exon 8 F Exon 8 R	TTGCTTCTAATGCAACTTTGATG CAGCCTGAAGAACCATGACC	446	1.5 mM	57.0 °C
	Exon 9 F Exon 9 R	ACTTGCAAAACCCTTGCTGT GATCTATAAGTTGCTGAGCTGAAA	356	1.5 mM	57.0 °C
	Exon 10 F Exon 10 R	AGAAATTACTAGGGCCACATTTC AGAAGTGAAGCACACAAACACTG	472	1.5 mM	57.0 °C
	Exon 10A F Exon 10A R	TGAAATGTTGAGTGGCACATAC TTCAGAATGGTGGAAACATACC	410	1.5 mM	57.0 °C

Table 2 (continued).

Gene	Exon No	Sequence (5`..... 3`)	Product size (bp)	$MgCl_2$	Temp
	Exon 11 F Exon 11 R	TCATTGAATACAGTCCAGATCATTC CATGATCAACCATTTTATCTTTGC	293	2.5 mM	57.0 °C
	Exon 12 F Exon 12 R	GCATGCACATACAAATGCAC GCAGGGATTGTGATTGAAATAG	500	1.5 mM	57.0 °C
	Exon 13 F Exon 13 R	GATTGTGGAAGGCGTAATGG CAATTTGATTATAGATGGGATTTCTG	463	1.5 mM	60.0 °C
	Exon 14 F Exon 14 R	GGAAGGGGAAAGGGTAGATTC CCACATTAGGGAATGGTTTTATG	327	1.5 mM	57.0 °C
	Exon 15A F Exon 15A R	CATAAAACCATTCCCTAATGTGG TGAACATTTTCAATATCTGGAGAC	678	3.5 mM	57.0 °C
	Exon 15B F Exon 15B R	AAGGTCTGGATCCCACAATATG CGCAAAAGAACTCGGTTCAC	698	2.5 mM	57.0 °C
	Exon 15C F Exon 15C R	GAAGTAATCTACCTGCCCCTTC TCAGGACTCTGGAAGCCTTTAC	667	2.5 mM	62.0 °C
	Exon 15D F Exon 15D R	CAGGGAACTTGGACAATGAAAC TCCTGCTCTTCCTCCTCATC	574	1.5 mM	61.0 °C
	Exon 15E F Exon 15E R	TTTTGGTTCTCAAAGCAGTACG CGGATAGTCATCAAAGAAGCAC	689	1.5 mM	61.0 °C
	Exon 16 F Exon 16 R	TGATGCCACATATTTTCATGG AAGCATATTTCTGTTTCAGAATGC	449	1.5 mM	58.5 °C
	Exon 17 F Exon 17 R	TTGCCTGGCTAATAGAAATCAG TGTGAAGAGATCATAAGTCAAAATG	463	1.5 mM	61.0 °C
	Exon 18 F Exon 18 R	CCCCTAGAAATTTACTCTCTTTGC TCAGAATAGGACAACCCTATCACA	372	1.5 mM	61.0 °C
	Exon 19 F Exon 19 R	TTTTCAAATTGTTAGTATTCACATCC TTTTATTTCACGAAATTTCCAGTATG	377	2.5 mM	57.0 °C
	Exon 20 F Exon 20 R	GGCAATGTCATCTTTTGAAGTG TTTCAGTTCTGAGTTTGCTGTTTC	373	1.5 mM	62.0 °C
	Exon 21 F Exon 21 R	AAATTTGGAGAAAGGATCATCAAG GGGTGGAAAGGAAGTAACAGG	386	1.5 mM	57.0 °C
	Exon 22 F Exon 22 R	TTTAAAAAGAGCCATTTTTCTGC TATTGCACAGCCACATTACC	536	1.5 mM	60.0 °C
	Exon 10-12 F Exon 10-12 R	AAGGCCAACATGCAGCTC CCATCCAGGGTGCATCTAAG	753	1.5 mM	60.0 °C
OGFRL1	Exon 1 F Exon 1 R	CTGTGGGGAGGAGAAGGAG CACCGGGAGACAGGTCAG	633	1.5 mM +5% DMSO	58.5 °C
	Exon 2 F Exon 2 R	TTTGTTCTGGAAATTTCTTTGTG TCATGCATGTTTTCTCAGTGG	247	1.5 mM	57.0 °C
	Exon 3 F Exon 3 R	TGCATGAAGGGTCCTTGTATC TCCAATCAATGAAACAAACCAC	239	1.5 mM	57.0 °C
	Exon 4 F Exon 4 R	TTCGAATCTTAAAATGCCTTCAC AAAATTTTTCTATTAACGTTGTCTGG	226	2.5 mM	57.0 °C
	Exon 5 F Exon 5 R	AAAACTGGAGCACAACCACAC TAGCTACAAGGACAGTGAAATAGC	265	1.5 mM	58.5 °C
	Exon 6 F Exon 6 R	TGAAATTGAGGTAATGCAAGC TGAAATTGAGGTAATGCAAGC	370	1.5 mM	57.0 °C
	Exon 7A F Exon 7A R	TCCCAATAGTTTTCATTCTCCTG TTGAAATTGACCTCATCTCTGTTC	829	1.5 mM	58.5 °C
	Exon 7B F Exon 7B R	GAAGCAAAGCCCAGAAAATG CTGGGCCTGTCTGTCTCTTC	178	1.5 mM	58.5 °C
C6orf155	Exon 1A F Exon 1A R	GGTTCCCCAGGATTCTTGAC GCATTGGTCTGCGCGGCCTCG	480	3.5 mM	50.0 °C

Table 2 (continued).

Gene	Exon No	Sequence (5`..... 3`)	Product size (bp)	$MgCl_2$	Temp
	Exon 1B F	CACAAAGAACGCGGTGGGCG	540	3.5 mM	50.0 °C
	Exon 1B R	GCTCCATAAAGTATTAAAGG			
	Exon 2 F	GTACTTTGTCAGTAGTGTATACAGG	270	3.5 mM	50.0 °C
	Exon 2 R	GCATGATCATCATTCTCTTTAAGG			
KCNQ5	Exon 1F	TCTGCAGCCCCTCCTTTC	687	1.5 mM	58.5 °C
	Exon 1R	GGAGCACGCCCCAGGG			
	Exon 2 F	TTCATTTGAAGCAAGAAATTAAGTC	288	1.5 mM	50.0 °C
	Exon 2 R	GTAGGATAAGATGCATAGTATAA			
	Exon 3 F	GCCTAAATGTCCAAAAATATGC	307	1.5 mM	50.0 °C
	Exon 3 R	TTTTAATATTAATCAAATATTGC			
	Exon 4 F	GGTCAAAGTGAACCTTTTGGAA	356	1.5 mM	58.5 °C
	Exon 4 R	CTTGTGACAGGTTTATTAACTATT			
	Exon 5 F	GTGAATAGAATCCTCATAGAATTC	306	1.5 mM	58.5 °C
	Exon 5 R	CCATAGGAACCATTACGTTGTAT			
	Exon 6 F	GATTTGTTGAATAATGATTTAGTGG	300	1.5 mM	58.5 °C
	Exon 6 R	CAAGCATACGAATTTGTGAGAGC			
	Exon 7 F	GGACAGGTTACATACCGTTTGTC	296	1.5 mM	58.5 °C
	Exon 7 R	GTTCTACCAAGCAATGAAGCACAG			
	Exon 8 F	GATTCTTCATGTGTAGTAACTTAA	275	1.5 mM	58.5 °C
	Exon 8 R	GTGTGTGTGGGTATGGTTTGTTTAAC			
	Exon 9 F	CCAATCTCCAATTTGGCCATTATC	207	1.5 mM	58.5 °C
	Exon 9 R	GTTGATCGATTTTACTCACATGAG			
	Exon 10 F	GACCACATGAGCTTCATCAAATTAC	402	1.5 mM	58.5 °C
	Exon 10 R	CAAGTGGCACTATGGAGAATTAA			
	Exon 11 F	GTATCCCGCCATTTCCACGTGAG	299	1.5 mM	58.5 °C
	Exon 11 R	GGAAAGTGGTTATTCCAGGATA			
	Exon 12 F	CAGAGTTTCTTATTATATTTACTGG	312	1.5 mM	58.5 °C
	Exon 12 R	GGAGTTCAGAGGTTTACTCTACTA			
	Exon 13 F	CATCTTACATAAATTGAAGATAAC	331	1.5 mM	55.0 °C
	Exon 13 R	CACTGGAATACATACAATTCGG			
	Exon 14A F	GTGTTGGCACACCTTGACTTC	660	1.5 mM	58.0 °C
	Exon 14A R	GGTGAGATTTGACTGTGCAAC			
	Exon 14B F	TCTGCCCAGGCCAGAAACT	666	1.5 mM	54.0 °C
	Exon 14B R	GCTTATAAACTGCCTTTCATGTTC			
	Exon 14C F	GTCAAACTGAAATAAGTTCTT	660	1.5 mM	55.0 °C
	Exon 14C R	GCACACAAATTGACATTCAAA			
EEF1A1	Exon 1A F	GGCCAAGATCTGCACACTG	620	1.5 mM	59.0 °C
	Exon 1A R	TTTCACGACACCTGAAATGG			
	Exon 1B F	AGGGGTTTTATGCGATGGAG	425	1.5 mM	58.0 °C
	Exon 1B R	TCACTAGTTCTGGGGAAATCAC			
	Exon 2 F	AAGTGGAAACTGCCAATTAAGG	358	1.5 mM	58.0 °C
	Exon 2 R	TCCCTGTCAACTCTCCAAATG			
	Exon 3 F	CTTTATCCCAAAAGGCTTGC	496	1.5 mM	58.0 °C
	Exon 3 R	TTACGGGTGACTTTCCATCC			
	Exon 4 F	AACATGCTGGAGCCAAGTG	396	1.5 mM	58.0 °C
	Exon 4 R	CGGGTTTGAGAACACCAGTC			
	Exon 5 F	TGGTGGTAAGTTGGCTGTAAAC	454	1.5 mM	58.0 °C
	Exon 5 R	GGTTCAGGATAATCACCTTGG			
	Exon 6 F	AAATGACCCACCAATGGAAG	483	1.5 mM	58.0 °C
	Exon 6 R	TCATATCACGAACAGCAAAGC			
	Exon 7 F	TCCACCTTTGGGTAAGGATG	395	1.5 mM	58.0 °C
	Exon 7 R	TGGTCCACAAAACATTCTCC			

Table 2 (continued).

Gene	Exon No	Sequence (5`..... 3`)	Product size (bp)	$MgCl_2$	Temp
SLC17A5	Exon 1F Exon 1R	CCTACGAGAACTCCCAGAACTC CCACTTAATGTCCCCTCGCA	482	0795 mix	58.5 °C
	Exon 2 F Exon 2 R	CCAGCCTAAGCAACATGGCAAAA CAAAGTATAGTTTCTGTAGGATG	277	2.5 mM	57.0 °C
	Exon 3 F Exon 3 R	GTGGTTCAAAATCTCATTTAT CCAAAGAATGACATCTTT	414	0795 mix	58.5 °C
	Exon 4 F Exon 4 R	CGTTTGATTCTTATCCAGAAA CATTGCATCGTTCTGGTATGC	278	1.5 mM	57.0 °C
	Exon 5 F Exon 5 R	CAGGAATGAGCCACTGTG GTGGTTCAGTGATTTGGAAGA	277	2.5 mM	57.0 °C
	Exon 6 F Exon 6 R	TTGTTGGTGCTTTCTAATTTTG TTCTACTTTGTCTAGAGCATGC	309	1.5 mM	57.0 °C
	Exon 7 F Exon 7 R	GGAGTTTACTAATTAAGGTGA AATCTCTAAAATTTAGGACAGC	399	2.5 mM	57.0 °C
	Exon 8 F Exon 8 R	TTAGGGACTGCCTTGGACTG TTGGTGATTAGAGCGAGGTG	313	1.5 mM	58.5 °C
	Exon 9 F Exon 9 R	ATTACGCCCATGTTTTCCAG TCATGCCTGGCTAATTTTTG	388	1.5 mM	58.5 °C
	Exon 10 F Exon 10 R	AAAGAAGGAAAGAATGAAGC AAGAACATTTAGAATTTTAAAC	271	0795 mix	58.5 °C
	Exon11 F Exon 11 R	GGCTTTTATGAATAATGTGGC AACTAGTGATATTTCATGATTATAG	420	1.5 mM	57.0 °C
MYO6	Exon 1F Exon 1R	GCCATGGGAAGAACAAGAAC CATCCATCACCTGCTTCTCC	600	1.5 mM	58.5 °C
	Exon 2 F Exon 2 R	CATGGGCAGATGTGTTTGTTAG TGCTTTCCCAAATATCTACCTC	390	1.5 mM	58.5 °C
	Exon 3 F Exon 3 R	TTGTTCTGTTTTGGGGTTAATG GAACCCGCACAGTGTATCAG	337	1.5 mM	57.0 °C
	Exon 4 F Exon 4 R	CAGCTTCTAGGGTTTACATCAGC TCACACTCTATTCAAGAGGCTCAG	369	1.5 mM	57.0 °C
	Exon 5 F Exon 5 R	GGGAATATTTAGGACTGATTTGG TAAGCCTGCCCCATTAGTTG	483	2.5 mM	57.0 °C
	Exon 6 F Exon 6 R	AAATGATTTGAACACTTTTGAATGAC AGGTGGAACAGTGGCTTGAG	422	2.5 mM	57.0 °C
	Exon 7 F Exon 7 R	CCACACCTGACCCCAAATAG GAAACAAAAATCCCTGCCTTC	452	1.5 mM	57.0 °C
	Exon 8 F Exon 8 R	GACGGGGTTTCATCATCTTG GGACACATATATTCCTGCAACC	477	2.5 mM	57.0 °C
	Exon 9 F Exon 9 R	TGGGGATGTTTAAAATGAAGG AGGCTCAAGCAATCCATCC	468	3.5 mM	60.0 °C
	Exon 10 F Exon 10 R	TCATGGTTGGCACTATTTGG TGATGCCCAACCAGAAGAAC	497	3.5 mM	58.5 °C
	Exon 11 F Exon 11 R	AGTGCATTAATTGACCTGGTG TTCTTCATTTGGGAGATTCAAC	421	0795 mix	55.3 °C
	Exon 12 F Exon 12 R	CAGTACGGGTGTTTGACAAGG CAGCAAGGAACAACTTTAAGAGC	497	1.5 mM	57.0 °C
	Exon 13 F Exon 13 R	CCCCATTTATCTGTGCCTATTC ATCCCCACGAGTCTTTCCTC	497	1.5 mM	57.0 °C
	Exon 14 F Exon 14 R	TGAAATGAGAACATTTGGGAAG CATCCATCCACACCAATCAG	350	2.5 mM	60.0 °C
	Exon 15 F Exon 15 R	GTGCCTGTCTGCAAGTGTTC TCAATTAAAAAGCACAGAAAAAGC	331	2.5 mM	57.0 °C

Table 2 (continued).

Gene	Exon No	Sequence (5`..... 3`)	Product size (bp)	$MgCl_2$	Temp
	Exon 16 F Exon 16 R	GAATCACATGCTATGTTGTTTCTG TCAGACTACAGGCACATTGTACG	500	3.5 mM	57.0 °C
	Exon 17 F Exon 17 R	TGTGAAAAGTGTGAAAATTTCCTG GCACCTGAAGTGTGGCTAGTG	379	1.5 mM	60.0 °C
	Exon 18 F Exon 18 R	ACACTTCAGGTGCCCAGTG GAACCAAGAATGAACACATTCAG	555	1.5 mM	60.0 °C
	Exon 19 F Exon 19 R	CCAGGAGGTTGTTAAACTGG CAGGGTTACTATGCCTACTTGC	267	1.5 mM	57.0 °C
	Exon 20 F Exon 20 R	GCCAAGCTGGTCTTGAACTC CAGGCTGAAACAGTCCTCTTG	550	3.5 mM	57.0 °C
	Exon 21-22 F Exon 21-22 R	TTCTCATAAATTGCCCGTTTC AGCAATTCATGTTGTTAGTGACC	542	0795 mix	55.3 °C
	Exon 23 F Exon 23 R	TGCCAAGGCCTATGTAATTG GTTGCTCAGCATCACCTCTG	361	0795 mix	55.3 °C
	Exon 24 F Exon 24 R	GGTGTTAAAACTTTGTTTTTGATGTC GAAAACCTGAGTATCCAAACTGC	350	2.5 mM	57.0 °C
	Exon 25 F Exon 25 R	CCTTCAACAAGAGATCTGAAAAAG AGCATGTACTTGCCATCATTG	437	1.5 mM	57.0 °C
	Exon 26 F Exon 26 R	CGGACGTATTGCTTACCATC GCAAGACCCTGTCACAAAAAC	530	1.5 mM	62.0 °C
	Exon 27 F Exon 27 R	GTGGCCAGGAGGTTAATTTG TCCCAAAGAGCTGGGATTAC	295	3.5 mM	57.0 °C
	Exon 28 F Exon 28 R	TTGTATGGGGGCAGTTATGC TCCTATTCCCTTCTGCATGG	353	1.5 mM	57.0 °C
	Exon 29 F Exon 29 R	AAAATTCTGAGTGATCTCATGTTG TGTGATTGAGCACCATACAAG	350	2.5 mM	57.0 °C
	Exon 30 F Exon 30 R	CTGTGTGTTACGGCTAGATTTG AACAGGTTCTGGTCCAAATAATC	306	2.5 mM	57.0 °C
	Exon 31 F Exon 31 R	TTCCGGTTTTCAAACTTATGC GTGCATTCATGGACCAAAAG	368	2.5 mM	57.0 °C
	Exon 32 F Exon 32 R	TCAGAGTTCTTCTGTGGAGCAG GGCCATCAAGGCTGTATTAGG	520	1.5 mM	57.0 °C
	Exon 33 F Exon 33 R	TTCAGTCACCACCTCGATTG TTCCACTGAAAATTGTAGCAAAAC	236	1.5 mM	57.0 °C
	Exon 34 F Exon 34 R	GTGTGTTTGTGTTGGCAATG TTAACCGCAAGACTCCATCC	578	2.5 mM	57.0 °C
	Exon 35 F Exon 35 R	GGTATTTCAGGCATACAACTGG TGGGAATTACAGCGGGATAC	493	2.5 mM	57.0 °C
IMPG1	Exon 1F Exon 1R	CACCTGAGGGAAAGACAAGC TCAATTGGTAGCCTTGTTGG	368	1.5 mM	57.0 °C
	Exon 2 F Exon 2 R	TAGCAGTTGCACCACGGTAG TGTGGCTAAATGACAGAACTGG	480	1.5 mM	57.0 °C
	Exon 3 F Exon 3 R	TTTCCCAAATGGCTCAAAAG AACCCTTACGTTGTGGAAACC	584	1.5 mM	57.0 °C
	Exon 4 F Exon 4 R	TGCAAAATAATATGGTACAGTCAGG GTGGCTGACATAAAATCCTACAG	261	1.5 mM	57.0 °C
	Exon 5 F Exon 5 R	TTTTTGCATTTTTCCTCAATG CATGATGGTTGTTTCCAAACTG	498	2.5 mM	57.0 °C
	Exon 6 F Exon 6 R	GAAAAAGCATATTGAATTTTGACC TGGTTTATCCATTCTCTTTTCCTG	274	3.5 mM	57.0 °C
	Exon 7 F Exon 7 R	GCCTTCATAATCCACTTCTTGAG TCGCCGTAAGGGGTTTTATGTC	330	3.5 mM	57.0 °C

Table 2 (continued).

Gene	Exon No	Sequence (5`..... 3`)	Product size (bp)	$MgCl_2$	Temp
	Exon 8 F Exon 8 R	CATTTTCAGCTGTTCCCCTAAC GTTTCCAGGATTTGGCAGAG	296	1.5 mM	57.0 °C
	Exon 9 F Exon 9 R	TGAACAAACAAAAGAGACAATGG CATCAAAAAGTAATGGGCTTATCC	274	3.5 mM	57.0 °C
	Exon 10 F Exon 10 R	GATATTCTCTCCGAGCCCATC TGATCGACTTTAGAAGACCCAAG	487	1.5 mM	57.0 °C
	Exon 11 F Exon 11 R	CCGCATATTTCAACCTGGAC AAAGGGGATTTTGCTCTGTTC	268	1.5 mM	57.0 °C
	Exon 12 F Exon 12 R	TCAATGGATGTTATCCTTTTAGAAC GGATGGCTTTGTCACTGGTC	358	1.5 mM	57.0 °C
	Exon 13 F Exon 13 R	AAATGATCTACGCAAATGCTATG GCTTGGCGGTTTGTTTCTAC	771	3.5 mM	57.0 °C
	Exon 14 F Exon 14 R	AAAATCACAGCCATCCATCTC TTTGATTTTTGTGGCCTAAAG	563	1.5 mM	57.0 °C
	Exon 15 F Exon 15 R	TGGTCTCTTGCCTTTGACTG AAAACCATGGGTTGAAAGGAC	384	1.5 mM	57.0 °C
	Exon 16 F Exon 16 R	TCCAACTCAAACGGAAGACACA AAATGTCACCCCCTTAAAACAG	364	1.5 mM	57.0 °C
	Exon 17 F Exon 17 R	CATAAATGGCAAGCACATCC TTTCAGGGAAGGTGGAAGC	492	1.5 mM	57.0 °C
HMGN3	Exon 1F Exon 1R	CCTCGTGGAATTTAGAACGTT GCAGAATTTGAAGGCTTTTGAAATC	313	2 mM	54.2 °C
	Exon 2 F Exon 2 R	GGCTTGTCTTGTCCTGGGAAT CCTTGATCATTCATATTAAACTTT	271	2 mM	54.2 °C
	Exon 3 F Exon 3 R	GGAATCATACATTATAGTCATTCAA ATGAGGACCCTAGGTAATTTCAAA	290	1.5 mM	57.2 °C
	Exon 4 F Exon 4 R	AAAGCCATGTCAAAATGGATAG GTTTGGATCATTAAATACGGCCTT	260	1.5 mM	57.2 °C
	Exon 5 F Exon 5 R	GGTAACGGTTGTACTTCACCTT CGGCTGAAGGATTGAGAAATTT	283	1.5 mM	57.2 °C
	Exon 6 F Exon 6 R	CCTGCCTTGTCTTCTTCACTCAG CATGAAAAATTCAAATATGCACAG	510	1.5 mM	57.2 °C
SH3BGRL2	Exon 1 F Exon 1 R	CCAGGGAGAGACGGAAACTACA TTGTTGTCGGAGTGTGATGG	464	1.5 mM	57.2 °C
	Exon 2 F Exon 2 R	GGACAGTGCATGACACCTACATAAA TTAGACATGTGGATCAGAATGG	449	1.5 mM	57.2 °C
	Exon 3 F Exon 3 R	CCTGATCTGGACAGAGCAAT GGTAGTCTCTAATTATGCATCAGA	348	1.5 mM	57.2 °C
	Exon 4 F Exon 4 R	GCTGAAACCCAGGATTTTCTCTT GCAATTCTCATTATAGCCACATCTTTC	354	1.5 mM	57.2 °C
TTK	Exon 1 F Exon 1 R	AACTGGAAAGACCAGGAAAGC CGACCAGCGCTAACAATGAG	383	2.5 mM	64.0 °C
	Exon 2 F Exon 2 R	CCTTGTTGTTGTGCACTTACC CAGACAAAAACCCTGCCATC	463	1.5 mM	59.0 °C
	Exon 3 F Exon 3 R	GCAATTTGGCATTTGTTTTATG TGTTGTGGAAACGTGCATAG	461	2.5 mM	57.0 °C
	Exon 4 F Exon 4 R	TTTTTGGAAAATTGAATGAAGC GGCATTTTCTCCCCATATTC	336	2.5 mM	57.0 °C
	Exon 5 F Exon 5 R	TGAAATAAAATACATGAGCCTTGG TTTGCATGGGGTTGTAGAGAC	462	1.5 mM	57.0 °C
	Exon 6-8 F Exon 6-8 R	CTTGGTATCATCTTCATGTCTGC TCATTCCTTTGTTCCTGACAAC	850	1.5 mM	57.0 °C

Table 2 (continued).

Gene	Exon No	Sequence (5`..... 3`)	Product size (bp)	$MgCl_2$	Temp
	Exon 9 F Exon 9 R	CTTTTGTCATTGCCCAGCAC CCTTTCCCCAGAAAAAGCTC	376	1.5 mM	57.0 °C
	Exon 10 F Exon 10 R	TTCAGGCAGTTAACCTTTGC ATTTCCTTTGCTGCGGATTC	469	1.5 mM	57.0 °C
	Exon 11 F Exon 11 R	TGCTAAAAGCAAATTGTTAAGCAG GCACCAGTCTATCGGCAATC	557	1.5 mM	57.0 °C
	Exon 12 F Exon 12 R	CTTGCCATCAGTTTGAGCAG TGCATTATTGCAACCACTTCC	553	1.5 mM	57.0 °C
	Exon 13 F Exon 13 R	ATATCCGGTGGTGGCATATC AACCTCTCAAAGCCACAAGG	474	1.5 mM	57.0 °C
	Exon 14 F Exon 14 R	CAAAATGGGGAGCAGTTGAC AAAGGAAAAGCAGCCCTCAC	272	2.5 mM	66.0 °C
	Exon 15-16 F Exon 15-16 R	CACTCAAAATAGGCCCAGAAAC CGTTAAAGACACCAATAACCAATG	687	2.5 mM	57.0 °C
	Exon 17 F Exon 17 R	TGCCTGGCACATAACAAGTG TCAAATCCTTTGAAGAATGAGG	411	2.5 mM	57.0 °C
	Exon 18 F Exon 18 R	CCCAAGTTTCCAAGGATCTG CCAGCAATGTCTCTGTAATGG	367	1.5 mM	57.0 °C
	Exon 19 F Exon 19 R	TGATGGAATAACCAACTGAAATG CAAAATCCCCAAGTATTTACAAGC	523	2.5 mM	57.0 °C
	Exon 20-21 F Exon 20-21 R	TGCCTTGGGAGAAATAATCTTG TGATTGGACCAACTTTTCTTCAG	755	2.5 mM	57.0 °C
	Exon 22 F Exon 22 R	GGTAATGCTTAAGGCCAAGC TTGCTATCCACCCACTATTCC	544	2.5 mM	57.0 °C
C6orf165	Exon 1 F Exon 1R	TCTCTGCCTGAAATTCCTTTG GCAGCCTAAAGGATCGAGAC	382	1.5 mM	57.0 °C
	Exon 2 F Exon 2 R	TCCCAATCGTTGTCTGTCTTC CACAGAATTTAAAGGGGAAAATG	403	1.5 mM	57.0 °C
	Exon 3 F Exon 3 R	CCAACCCCAACGTAATCAAG GGAAGCCAGGAAGAATGGTC	389	1.5 mM	57.0 °C
	Exon 4 F Exon 4 R	TCAGGAACCACTGCTTTTCC TTCATTGTCAACCAAATGAAGC	278	1.5 mM	57.0 °C
	Exon 5 F Exon 5 R	TTGTCTTGAGGCTACATGCTG GGGTACATTTTAACTCATTTGTGC	512	1.5 mM	57.0 °C
	Exon 6 F Exon 6 R	AACTCAGACCCTTAACTTGCTG AGAATGCCAGTGGTGTGTTG	358	1.5 mM	57.0 °C
	Exon 7 F Exon 7 R	TTTGATTGGGGAGAAAAACC AAACCGAGCAGTTACTGAGG	443	1.5 mM	57.0 °C
	Exon 8 F Exon 8 R	GAGGATCTTGCGGAGAACAG CGGCAAAGTAACCATAAAGAAC	407	1.5 mM	57.0 °C
	Exon 9 F Exon 9 R	TTCGTAAGACTTTTGCTTAGGG CTGGGATTACAGGCGTGAG	697	1.5 mM	57.0 °C
	Exon 10 F Exon 10 R	TATCAAGTTTTTGCCCATCG ACCAGAGCACCTCCAAAATG	446	1.5 mM	57.0 °C
	Exon 11 F Exon 11 R	TCAGGCTGGTCTTGAACTCC GAATCCCTTTCAGACAACCTG	637	1.5 mM	63.0 °C
	Exon 12 F Exon 12 R	ACATGTGCCCCCTTGAATC GATTAAAGGAAGTTGGGAGTGC	690	1.5 mM	57.0 °C
	Exon 13 F Exon 13 R	TGGAATTAATTTCTTGTGGATTG AACAGAGCTGAAAATATTGATTAGG	719	1.5 mM	58.5 °C
SLC35A1	Exon 1 F Exon 1 R	TTGGGGTGTAGCTTGGATTC CTCCACGCAAACTCCTGAC	340	1.5 mM	58.5 °C

Table 2 (continued).

Gene	Exon No	Sequence (5`..... 3`)	Product size (bp)	$MgCl_2$	Temp
	Exon 2 F Exon 2 R	GTGCACGCTCATGTAATTGG TAGCAGCATCCTTGGTCTCC	560	1.5 mM	58.5 °C
	Exon 3 F Exon 3 R	TGTTGTCATATTTTCCCAAACAG TGGCCAACATAGTGAAACCTC	664	1.5 mM	58.5 °C
	Exon 4 F Exon 4 R	CCAAAGTTCTGGGATTACAGG CTGCATGCATCAATGTAACTG	389	1.5 mM	58.5 °C
	Exon 5 F Exon 5 R	GCTGTGATTTGAGGGACACA TTTACTGGAAAAACAGCTGACA	445	1.5 mM	58.5 °C
	Exon 6 F Exon 6 R	TGCTCTAATAAAGGCAGAAACTG GATATTTTGGGGCATTGCTATC	663	1.5 mM	58.5 °C
	Exon 7 F Exon 7 R	TGGCTCCTTCTAAGGAAAACAG TTAGCCACATCCCACACAAC	445	1.5 mM	58.5 °C
	Exon 8 F Exon 8 R	AAACACTGCCTTGATTTTACCC GTTTCCACATAACCGCACTG	463	1.5 mM	58.5 °C
CNR1	Exon 1 F Exon 1 R	ACCCCTTCCTTCTCCACTTC AGTGCATACAGAGCCAGGTG	445	1.5 mM	62.5 °C
	Exon 2A F Exon 2A R	GGTCCTTCCTGGATTCACAC GGTTCAGGACCATGAAACACTC	680	2.5 mM	68.0 °C
	Exon 2B F Exon 2B R	AGCTAGTCCCAGCAGACCAG TCACAATGGCTATGGTCCAC	534	1.5 mM	58.5 °C
	Exon 2C F Exon 2C R	CCGCAACGTGTTTCTGTTC TGCCTTCACAAGAGGGAAAC	698	2.5 mM	68.0 °C
	Exon 2D F Exon 2D R	TTTGGGAAGATGAACAAGCTC TTGTGTAGCCAAAGGTTTCC	597	2.5 mM	58.5 °C

Table 3 Primers designed for SNP analysis of arRP genes

Gene	SNPs	Sequence (5`..... 3`)	Product size (bp)	$MgCl_2$	Temp	IC
ABCA4	1. rs3945204	ATGCGTGGCATTCAGTTTTG CTTACTTCCACGCGGTCTG	187	2.5 mM	57.0 °C	0.49
	2. rs1191231	AATCAACTCCTTGGGCTCTG ATGGGAGATGAATGCAAAGG	341	2.5 mM	57.0 °C	0.495
	3. rs2151848	TTCTCAAAGGCCAGAGATTTG CTGTGCTCTTTCTCACGATCC	289	2.5 mM	57.0 °C	0.49
CRB1	1. rs3790380	AAAAAGTGCCAAACTGTACCTG TCAGTTCCTAAAAGCCTGGAG	234	1.5 mM	57.0 °C	0.497
	2. rs949571	AGCACTTGTCAAATGTTCTGTTAC TTACCCACTGTTCTCTCTGCTC	288	1.5 mM	57.0 °C	0.46
	3. rs1345529	TTCTCCAAACGTGCTCAGTG TGAGGTGATTTCTGCTCAGG	266	1.5 mM	57.0 °C	0.496
CNGA1	1. rs1012844	TCAATGCCAGTAACTCCCAAC AGTTGTGAAAACTTCAGATACCG	240	2.5 mM	57.0 °C	0.476
	2. rs1440224	CAACCTCTTTGGCAAACTGTC TGCTTCCTGTTTGGGACTTC	371	2.5 mM	57.0 °C	0.46
	3. rs1371729	CATAAGCTGCACACCTTTGTC TGCAAGAATGGGAAACATACC	250	1.5 mM	57.0 °C	0.412
	4. rs1371732	CCTTTCCCCAATTTCTGAG TGGCTGATTTCTGATTCACTG	250	1.5 mM	57.0 °C	0.45
	5. rs4695318	TCATATGACAATATCACGTGTGC TCTCTTTAAAGGCCTTGTCTCC	298	2.5 mM	57.0 °C	0.473
	6. rs3889306	CTGGCACCTTTCCGTCTG GGAGGAGGAACATTCACCAC	228	1.5 mM	57.0 °C	0.477
CERKL	1. rs1047307	GTGGCCGAATTTTGAACATC AAATCGGGGCTTGATTTTTC	355	1.5 mM	58.0 °C	0.486
	2. rs763860	TCCCCACTAGCAAATGTGAG AGAATCTCACCCTTCCAAACC	389	1.5 mM	58.0 °C	0.467
	3. rs6433926	TCCATTAGGGCAAGGCTATC TCTTGGGGAATCCAGATGAG	398	2.5 mM	58.5 °C	0.419
	4. rs1372119	TCCTGCCTTGACTTATCTTCAG GGCAGCATGAGAAATTCTTG	378	1.5 mM	57.0 °C	0.499
	5. rs1473295	GCAAAAGCTCGTGGGTGTAG CTCCACCTCCTTCTCCAAAG	386	1.5 mM	63.0 °C	0.50
CNGB1	1. rs2033249	AAGAGTGGGCCACACATTTAG AAGCAGAGATGACACGATGG	212	1.5 mM	57.0 °C	0.492
	2. rs376270	TGTGGCAGAAACCACATCTC ATTGCTCCACAGGGTCAGAG	222	1.5 mM	57.0 °C	0.499
	3. rs691897	CCAAAGTGTTGGGATTACGG ATGATCCTGTTGCCTTCTGC	232	1.5 mM	65.0 °C	0.43
	4. rs2241771	CCCTAGGACACCCTGGAAAC AGGCTGTGCAACACACACAG	260	1.5 mM	57.0 °C	0.50
	5. rs8055820	TTGTGTCCCAACATGCTGAC GATAAAGGGCCACCGTAGTG	274	1.5 mM	58.5 °C	0.477
LRAT	1. rs1061100	CTCGACGGCCATAAAAAGTC GAAGAGGGCGTCTTGGAGAG	359	1.5 mM	65.0 °C	ND
	2. rs201825	TCTCTGGGGAACCCATAAAC CGCTGCTTGCAACTTTAACC	359	1.5 mM	57.0 °C	0.352

Table 3 (continued).

Gene	SNPs	Sequence (5`..... 3`)	Product size (bp)	$MgCl_2$	Temp	IC
	3. rs201823	TGTTGGCCTATTTTTCTATCAGAC TGAGAAAAATCTGCTTTTGTGG	261	1.5 mM	60.8 °C	0.406
	4. rs201822	ATTCCTCCAATCTGCCATTC ACATAGCCAATAAGAGCTGGAG	300	2.5 mM	60.8 °C	0.389
	5. rs12507608	CATGTAAATTGATTCTGCTGAGG TGTTGTGGGCAAATTAGTGG	290	2.5 mM	57.0 °C	ND
MERTK	1. rs1400323	TTTCGCCACTCATGCTTATC AAAAGCAAAGGACCCAGTACC	365	1.5 mM	57.0 °C	0.473
	2. rs1113418	CCATAAAGACTTATTTTCATTGAGG GCCACGGAAAGTATGTATGACAC	300	1.5 mM	57.0 °C	0.50
	3. rs1554215	TCACAATGCTGAATGCTTGG TAGTGCACAAGGCTCTCCAG	280	1.5 mM	57.0 °C	0.498
	4. rs6710591	TTGTTGGATATGTGGTTTCCAG GCAACTCAATGGATTAAGGACAG	367	1.5 mM	57.0 °C	0.498
	5. rs869016	AAAATTAGCCAGGCATGGTG ATTGTAAACATCTTCCCAGAGG	344	1.5 mM	57.0 °C	0.499
	6. rs2230515	TTATCCCTGCACACGGTTG CCGACAGAAGGATTTCTTTGC	236	1.5 mM	57.0 °C	0.497
NR2E3	1. rs2723343	GTGTCGTCCTGACCCTTCC ATAAGGCTGGCCATGAAGTG	214	2.5 mM	57.0 °C	0.383
	2. Exon 6F Exon 6R	ACAGCACTTCCATTCCTTGG AGGCCTACACACATCTGCAC	454	1.5 mM	57.0 °C	ND
PDE6A	1. rs10515637	TGTTTCCTCACAGGACATGG GGAGTTGTGCAAAGCATAAAC	205	1.5 mM	58.5 °C	0.437
	2. rs10040588	TAAGTGGCCCCTACATTTGC GTGGTCATGGTTCTGCCTTC	283	1.5 mM	65.2 °C	0.489
	3. rs251346	CAAAATGGGATACCCTCCAG GAGCAGTGAAGGGGAATAATG	290	1.5 mM	58.5 °C	0.482
	4. rs152951	TCCTCCCCAAAGAGCATTAG TCATGAAACTTTGGAGCTTTTG	347	1.5 mM	58.5 °C	0.46
	5. rs308126	TAATTCGGTTCGTGGGAGAG TTTAACCCAGGAGGTGGAAG	395	1.5 mM	60.8 °C	0.408
	6. rs2277926	AATGTCCACAAGGATGCTGTC AAGCACCATGTTGTCACCAG	250	1.5 mM	60.0 °C	0.347
PDE6B	1. rs1135375	AAAGTGGAATCTGTCGCTTTG AGAAAGGTGGCCCAAGGAG	299	1.5 mM	57.0 °C	0.365
RGR	1. rs738786	CCCCACAAGAGGCAAATAGT CGGGGGCTGATAGTAAACTG	571	1.5 mM	57.0 °C	0.490
RHO	1. rs7984	CCAATCTCCCAGATGCTGAT GGCCAGCATGGAGAACTG	297	1.5 mM	65.0 °C	0.499
RLBP1	1. rs2070780	GCTGTCCAAGGAGAGAGCTG GCCTAGCAACCTGCTAAGTCC	342	1.5 mM	60.8 °C	0.430
RPE65	1. rs3125891	GCTTGACCTAGCAGTGCCTAA ACCCAACACTTGGTTTGCTC	381	1.5 mM	57.0 °C	ND
	2. rs3125898	TTTCTTCAGGCAGTGATAACCA CAATCTTAGCAAAGCATTCCA	330	1.5 mM	57.0 °C	0.488
SAG	1. rs1978921	TGCCACAATCATAGCTCACC ACAGTATGTCCCGCCTTCAC	323	1.5 mM	62.0 °C	ND
	2. rs12623795	CGATCTCTGCTCACTGCAAC TGAAAGGTAGCCCCTCTTTG	277	3.5 mM	65.0 °C	ND

Table 3 (continued).

Gene	SNPs	Sequence (5`..... 3`)	Product size (bp)	$MgCl_2$	Temp	IC
	3. rs2304777	ACCCTGGACAATGACTTTGC TTGCCTTAGATGGTGTCGTG	284	1.5 mM	57.0 °C	0.499
	4. rs11891546	CTGGTGGGATGTGTGTTGAG TTTTGTAGAGATGGGGTCTCG	291	1.5 mM	62.0 °C	0.48
	5. rs3792100	TGCAAGCCCTTTGTATACCTC TGAGAGAAGTGCCTGAATGC	341	1.5 mM	57.0 °C	0.494
	6. rs1000141	ATCCTACCATCTGGGTCCTG GCTTTAGTGGGAGGCTTC	276	3.5 Mm	65.0 °C	0.5
	7. rs1046974	GGCGTGCAATGATCAAAATG GACCCAGGGGAGAACAAAC	290	1.5 mM	62.0 °C	0.449
	8. rs3792097	GGGAGAGCCCATTTAGGAC CTACCTTCCCAGGCTTTGTG	387	1.5 mM	65.2 °C	0.493
TULP1	1. rs2273000	ACCATCACAGCATTGATTCAT AGAGCTCACAGGGAAGCAGA	349	1.5 mM	57.0 °C	0.436
USH2A	1. rs1324330	GACCCTTGGTCTGGGAAAAC GGCTCAAAGTGTGATGCTTG	363	1.5 mM	57.0 °C	0.484
	2. rs4078266	GGTGGGTACCATCCAATCAG AAGGCTGAAAGCCTGAGAAC	239	1.5 mM	57.0 °C	0.417
	3. rs3767687	CAGGATACTTTGCCAACATGG AAAACTCCTGCATCGCATAG	236	2.5 mM	58.5 °C	ND
	4. rs773498	AGACCTGGCAAATCTAACTGAG ACACAGGCCCCTTTATCTTC	217	1.5 mM	57.0 °C	ND

IC: Information content

Table 4 ABI and custom made (CM) microsatellite markers used to investigate known recessive RP loci

Gene	Markers /heterozygosity	Panel /CM	Colour/size	Distance from the gene (Mb)	Optimisation Condition	Annealing Temp
ABCA4	D1S2868/0.76	2	FAM/206-220	1.1 proximal	Multiplex PCR with D1S413	55.3 °C
	D1S2849/0.79	CM	HEX/174	1.2 proximal	Multiplex PCR	55.3 °C
	D1S2819/0.77	CM	FAM/166	1.2 distal	Multiplex PCR	55.3 °C
CRB1	D1S2816/0.64	CM	FAM/210	0.6 proximal	Multiplex PCR	55.3 °C
	D1S413/0.76	2	FAM/249-265	1.2 distal	Multiplex PCR with D1S2868	55.3 °C
CNGA1	D4S3002/0.71	CM	HEX/216	0.7 distal	Multiplex PCR	59 °C
CERKL	D2S2310/ 0.79	CM	FAM/244-260	0.2 proximal	Multiplex PCR	55.3 °C
	D2S364 /0.80	3	NED/230-256	0.6 distal	St PCR	55.0 °C
CNGB1	D16S3140 /0.82	73	VIC/283-321	1.6 proximal	Multiplex PCR	55.3 °C
	D16S3057 /0.72	72	NED/192-210	0.39 proximal	St PCR	55.0 °C
	D16S3038/0.47	CM	FAM/217	0.50 distal	Multiplex PCR	55.3 °C
LRAT	D4S3049/0.83	CM	FAM/210-236	0.8 proximal	Multiplex PCR	59.0 °C
	D4S3021/0.76	CM	HEX/223-245	0.73 proximal	Multiplex PCR with D4S2976& D2S1896	55.0 °C
	D4S2883/ND	CM	HEX/177	0.17 proximal	Multiplex PCR	55.0 °C
	D4S1285/ ND	CM	FAM/208	0.1 proximal	Multiplex PCR	55.0 °C
	D4S2976/0.67	CM	FAM/109-135	0.1 distal	Multiplex PCR with D4S3021& D2S1896	59.0 °C
	D4S3016/0.70	CM	FAM/198	0.9 distal	Multiplex PCR	55.3 °C
MERTK	D2S1896/0.79	CM	FAM/145-193	On the gene at 112.4	Multiplex PCR with D4S3021& D4S2976	59.0 °C
	D2S2269/0.89	CM	HEX/252-280	0.2 distal	Multiplex PCR with D1S227	55.3 °C
	D2S160/0.78	3	FAM/206-224	0.29 distal	Multiplex PCR	59.0 °C
NR2E3	D15S131/ 0.83	21	VIC/238-274	1.0 proximal	St PCR 3.5 mM $MgCl_2$	55.3 °C

Table 4 (continued).

Gene	Markers /heterozygosity	Panel if from ABI	Colour/size	Distance from the gene	Condition	Temp
	D15S204/ 0.77	CM	FAM/116	0.2 distal	Multiplex PCR	59.0 °C
PDE6A	D5S2090/0.83	44	FAM/189-205	2.0 proximal	St PCR	55.0 °C
PDE6B	D4S3360/0.67	CM	FAM/175-199	0.5 Proximal	St PCR	55.0 °C
	D4S3038/0.79	CM	HEX/207-229	0.47 distal	St PCR	55.0 °C
	D4S412/ 0.77	7	VIC/158-176	2.7 distal	Multiplex with D10S1686	55.0 °C
	D4S2936/0.83	43	VIC/172-190	0.02 distal	St PCR	55.0 °C
RGR	D10S1686/0.86	14	VIC/243-281	0.44 proximal	Multiplex with D4S412	55.0 °C
	D10S1717/0.83	CM	FAM/187-223	0.20 proximal	St PCR	55.0 °C
	D10S1774/0.70	CM	HEX/234-254	On the gene	St PCR	55.0 °C
	D10S573/0.65	CM	HEX/167-175	0.2 distal	Multiplex with D15S202& D15S1045	55.0 °C
RLBP1	D15S979/0.85	70	FAM/139-171	1.0 proximal	Multiplex with D1S198& D6S291	55.0 °C
	D15S1045/ 0.63	CM	FAM/176-224	0.3 proximal	Multiplex with D15S202& D10S573	55.0 °C
	D15S202/0.84	CM	HEX/226-247	0.2 Distal	Multiplex with D15S1045& D10S573	55.0 °C
RPE65	D1S198/0.79	32	FAM/313-327	1.9 proximal	Multiplex with D15S979& D6S291	55.0 °C
	D1S410/0.86	CM	FAM/317-351	0.8 proximal	Multiplex with D1S219	55.0 °C
	D1S219/0.82	CM	FAM/154-176	0.9 distal	Multiplex with D1S410	55.0 °C
	D1S2829/0.86	CM	??/177-225	0.7 proximal	St PCR	55.0 °C
SAG	D2S2344/0.78	35	NED /278-298	0.7 proximal	Multiplex with D2S206	55.0 °C
	D2S206/0.80	3	VIC/125-163	0.4 proximal	Multiplex with D2S2344	55.0 °C
TULP1	D6S1611/0.64	CM	FAM/222-240	0.2 proximal	St PCR 3.5 mM	59.0 °C
	D6S291/0.7	48	FAM/202-214	0.7 Distal	Multiplex with D1S198& D15S979	55.0 °C

Table 4 (continued).

Gene	Markers /heterozygosity	Panel if from ABI	Colour/size	Distance from the gene	Condition	Temp
USH2A	D1S2703/0.88	CM	FAM/211	2.71 proximal	St PCR	55.0 °C
	D1S2827/0.78	CM	FAM/214	On the gene at 214.2	St PCR	55.0 °C
	D1S227/0.71	31	NED/111-125	1.4 distal	Multiplex PCR with D2S2269	55.3 °C
RP22	1. D16S3103/0.81	22	VIC/315-343	17.4	1,2&4 with multiplex PCR	58.0 °C
	2. D16S3041/0.82	73	NED/247-277	19.3	1,2&4 with multiplex PCR	58.0 °C
	3. D16S3046/0.74	22	FAM/83-109	20.7	3,5&6 with multiplex PCR	57.0 °C
	4. D16S403/0.85	73	VIC/138-157	22.9	1,2&4 with multiplex PCR	58.0 °C
	5. D16S3068/0.77	21	FAM/219-235	25.4	3,5&6 with multiplex PCR	57.0 °C
	6. D16S3100/0.66	72	FAM/270-284	26.48	3,5&6 with multiplex PCR	57.0 °C
RP25	1. D6S452/0.84	49	NED/265-284	47.0	1,2, 15 &3 with multiplex PCR	57.4 °C
	2. D6S272/0.71	49	NED/182-200	50.9	1,2, 15& 3 with multiplex PCR	57.4 °C
	3. D6S294/0.81	CM	FAM/249-270	55.2	1,2, 15&3 with multiplex PCR	57.4 °C
	4. D6S257/0.87	9	NED/167-195	56.00	4 & 14 with multiplex PCR	57.4 °C
	5. D6S402/0.86	CM	FAM/108-126	63.00	5 & 6 with multiplex PCR	57.4 °C
	6. D6S430/0.88	CM	FAM/207-244	67.00	6&7 with multiplex PCR	57.4 °C
	7. D6S1557/0.79	CM	HEX/126-142	71.00	7 & 8 with multiplex PCR	57.4 °C
	8. D6S1681/0.87	CM	HEX/234-284	72.2	7 & 8 with multiplex PCR	57.4 °C
	9. D6S1596/0.79	CM	HEX/175-225	74.4	9 & 10 with multiplex PCR	57.4 °C
	10. D6S460/0.81	10	FAM/179-303	80.0	9 &15 with multiplex PCR	57.4 °C
	11. D6S445/0.69	CM	FAM/205-233	82.5	10 &12 with multiplex PCR	57.4 °C
	12. D6S1627/0.81	CM	FAM/98-114	85.4	10 & 12 with multiplex PCR	57.4 °C
	13. D6S1004/0.64	CM	HEX/201-231	88.2	11, 13 and 14 with multiplex	57.4 °C
	14. D6S462/0.68	10	VIC/104-121	90.5	11, 13& 14 with multiplex PCR	57.4 °C
	15. D6S300/0.75	47	FAM/187-213	94.8	1,2, 15& 3 with multiplex PCR	57.4 °C

Table 4 (continued).

Gene	Markers /heterozygosity	Panel if from ABI	Colour/size	Distance from the gene	Condition	Temp
RP25	15. D6S1671/0.88	47	NED/258-284	100.6	16, 17,18 with multiplex PCR	57.4 °C
	16. D6S434/0.86	9	VIC/202-246	102.5	16, 17,18 with multiplex PCR	57.4 °C
	17. D6S1698/0.81	49	VIC/167-193	111.4	16, 17,18 with multiplex PCR	57.4 °C
RP28	1. D2S147/0.70	CM	FAM/126-144	64.02	1, 2 and 4 with multiplex PCR	55.3 °C
	2. D2S380/0.83	CM	FAM/229-253	65.50	1, 2 and 4 with multiplex PCR	55.3 °C
	3. D2S2293/0.67	CM	HEX/112	65.80	St PCR	55.3 °C
	4. D2S136/0.74	CM	FAM/91-111	65.9	1, 2 and 4 with multiplex PCR	55.3 °C
RP29	1. D4S1597/0.76	5	NED/274-300	170.20	1, 2 and 3 with multiplex PCR	57.8 °C
	2. D4S1595/0.72	43	FAM/202-212	174.55	1, 2 and 3 with multiplex	57.8 °C
	3. D4S1539/0.68	7	FAM/316-326	175.92	1, 2 and 3 with multiplex PCR	57.8 °C
	4. D4S415/0.80	6	NED/264-300	178.94	4 and 5 with multiplex PCR	57.8 °C
	5. D4S2920/0.68	43	FAM/109-119	184.70	4 and 5 with multiplex PCR	57.8 °C
RP32	1. D1S206/0.82	1	NED/205-223	101.4	1, 2 and 3 with multiplex	55.3 °C
	2. D1S495/0.87	31	NED/143-169	102.2	1, 2 and 3 with multiplex PCR	55.3 °C
	3. D1S2726/0.75	1	NED/280-294	110.8	1, 2 and 3 with multiplex PCR	55.3 °C
20p11-q12	1. D20S871/0.74	80	VIC/130-162	23.3	1, 2 and 3 with multiplex PCR	60.0 °C
	2. D20S486/0.78	CM	FAM/231-251	24.5	1, 2 and 3 with multiplex PCR	60.0 °C
	3. D20S484/0.82	CM	FAM/181-209	29.5	1, 2 and 3 with multiplex PCR	60.0 °C
	4. D20S195/0.81	27	FAM/128-154	31.3	4 and 8 with multiplex PCR	60.0 °C
	5. D20S847/0.82	CM	FAM/113-145	34.3	5, 6 and 7 with multiplex PCR	60.0 °C
	6. D20S884/0.86	CM	HEX/135-157	35.5	5, 6 and 7 with multiplex PCR	60.0 °C
	7. D20S478/0.81	CM	HEX/243-275	36.6	5, 6 and 7 with multiplex PCR	60.0 °C
	8. D20S107	26	FAM/197-221	38.3	4 and 8 with multiplex PCR	60.0 °C

Table 5 Primers designed to screen genes that could not be excluded by SNPs or markers

Gene	Exon No	Sequence (5`..... 3`)	Product size (bp)	$MgCl_2$	Temp
MERTK	Exon 1 F Exon 1 R	CCCTCCCTTTCCCCTTTAC TTTGCAAACTTGTCCAGCAG	494	0795 mix	55.3 °C
	Exon 2 F Exon 2 R	GGCCTAAGAAGTTGGGAACC CAGCCTGGGCTACAGAATG	592	2.5 mM	67.0 °C
	Exon 3 F Exon 3 R	GGGTTTGACCAAACAACTGC TTGCAAGGTTTGCATACAGAG	383	1.5 mM	57.0 °C
	Exon 4 F Exon 4 R	ACATCAGGCCACTGCACTC ACCTGGTCCCATAACTTTGC	486	1.5 mM	63.0 °C
	Exon 5 F Exon 5 R	AATCCCAGGTTTGTTTCTCC TGTCCAAGGTCACAAAGAACC	386	1.5 mM	57.0 °C
	Exon 6 F Exon 6 R	GGGAGGCTCCTCTTGAAAAC ATGCATGCTGGACACTGAAG	410	1.5 mM	57.0 °C
	Exon 7 F Exon 7 R	CTGACATTCCCACCACCTTAC TTGGGGGCAATATACATTCTG	275	2.5 mM	57.0 °C
	Exon 8 F Exon 8 R	AGTTGAAAAGGTGAAAATGTGC TTCTTTATGTTCCCCTGAAAGG	446	2.5 mM	57.0 °C
	Exon 9 F Exon 9 R	GTGACAAAGGAATGCTGTGG CAAACTCCTCCTGCTTTTGC	451	1.5 mM	57.0 °C
	Exon 10 F Exon 10 R	CTTCCCTGTTACAAGCCAGTG TCTGGGAGCAATGTAAGCAG	327	1.5 mM	57.0 °C
	Exon 11F Exon 11R	TAGGGGGAAAGCTTTTGTTG TTCGACATCTTTGGCTTTTG	313	1.5 mM	57.0 °C
	Exon 12 F Exon 12 R	GAAAACACGCTGACAATTTTTG TCATGTGCCAGATCTGAGTTTC	328	2.5 mM	61.0 °C
	Exon 13 F Exon 13 R	TGGGTGAGTTGCTCTCATACC AAAGTAAGTCCCCCTTGGTG	337	1.5 mM	57.0 °C
	Exon 14F Exon 14R	TGGGTTTTAGAGAACAGAACTGC TTATGTTGGGGTTATACGAAGTG	299	1.5 mM	57.0 °C
	Exon 15F Exon 15R	AGTGTGAGTTAGGCGCTCTTG TCCTTCCTGGCTTCACTTTC	359	1.5 mM	57.0 °C
	Exon 16 F Exon 16 R	GATGTTTGCCAAGAAGTTTAAGG CACCCAGCCATATTTCCATC	473	1.5 mM	57.0 °C
	Exon 17 F Exon 17 R	AATGCAGCATGCTCACAGG TGCCATACCAGCTGAGGTC	383	1.5 mM	57.0 °C
	Exon 18 F Exon 18 R	CATAATTGCCAGCTTTGTGC ATCTCCCACATCAGGAATGG	437	1.5 mM	57.0 °C
	Exon 19A F Exon 19A R	GCCGCCATATAAAGAAAGAGAC ACAGCAGAAGAATTGGCTTG	850	1.5 mM	57.0 °C
	Exon 19B F Exon 19B R	GCCCGATGAACTTTTGTTTG CCCAAGGACCAGGCATTAAG	655	1.5 mM	57.0 °C
SAG	Exon 1F Exon 1R	GGGGTGTTGCTTAATGCTTAG CATACTGTCTGCAGGAAAACG	396	1.5 mM	57.0 °C
	Exon 2F Exon 2R	ATGTTGAAGCCGGTACAAGG CCCTCAAAGAGTTTTGATGTTG	346	1.5 mM	57.0 °C
	Exon 3F Exon 3R	TATTGGCCAGGCTCAAACTC TTGTTTCCAATCAGCCAGTG	381	1.5 mM	57.0 °C
	Exon 4F Exon 4R	TTCCCTTTGCCTGACTTTTC TTCCATGTAAATGCCCCTTC	273	1.5 mM	57.0 °C
	Exon 5F Exon 5R	ATCCCCTCCAGATGCTAAAG TCCTCTATCCCCTTTCCTTTG	390	1.5 mM	57.0 °C

Table 5 (continued).

Gene	Exon No	Sequence (5`..... 3`)	Product size (bp)	$MgCl_2$	Temp
	Exon 6F Exon 6R	AGGCAGGAAATTTTGGGAAG CCCAGCATTGGTGACAGAG	347	1.5 mM	57.0 °C
	Exon 7F Exon 7R	GTGCAACCCCGAATAGGAC TGTCCCACAGAGACAAGGTG	300	1.5 mM	57.0 °C
	Exon 8F Exon 8R	GGGAGCATTCCTGGAGAATC CTTGCAAGGCACCCATGTAG	349	1.5 mM	57.0 °C
	Exon 9F Exon 9R	TGTTTCAGGCCCTTCCTTAG CAGTTCCAAGGACCCAGAAG	363	1.5 mM	57.0 °C
	Exon 10F Exon 10R	GGAAGTGGAGGGAAACCATC TTCCTTCTTCAGCAATAAACG	277	1.5 mM	57.0 °C
	Exon 11F Exon 11R	AAGCACTGTTCTGCTTCTCG AGAGTGGGATCCTTGTGTGG	473	1.5 mM	57.0 °C
	Exon 12&13F Exon 12&13R	AGGACTTTGGAAGCTCAGTG AAGTGGCGCTAAGAATGCAC	461	1.5 mM	57.0 °C
	Exon 14F Exon 14R	TGCATTGTCTTTCAGCTTGG CTCTTACACCTGGCCACTCC	296	1.5 mM	57.0 °C
	Exon 15F Exon 15R	ACGAAGCCTTGAGGAAAATG ACGCAGCATAACTCCAAAGG	346	1.5 mM	57.0 °C
CERKL	Exon 1F Exon 1R	CTCCACCTCCTTCTCCAAAG GCAAAAGCTCGTGGGTGTAG	386	1.5 mM	57.0 °C
	Exon 2F Exon 2R	TTGATCCTCTCCCTTTGCTC CAACACTTTCTCACGACAAAAAC	494	1.5 mM	57.0 °C
	Exon 3F Exon 3R	TGCCTAATATTCACAAAGTTGC TTTGCATTAAGGACAAATTCAG	500	1.5 mM	57.0 °C
	Exon 4F Exon 4R	AAATGCTGTTTTATGACTTGACC TGCTTTCCTATGCCAGATCC	385	1.5 mM	57.0 °C
	Exon 5F Exon 5R	TGTGTTGTCTTACCCATTGACAC TCATTAATTCTGTGTTGTGCTGTC	400	1.5 mM	57.0 °C
	Exon 6F Exon 6R	ATCTGAACATTGAAGAATGACATC TGCCTTTTCTTAAAGTCTGATGG	269	1.5 mM	57.0 °C
	Exon 7&8F Exon 7&8R	TTCTCCTATAAGCCAATAAATATGC GATCCTAAGTCTGATCAATTGTTTG	493	1.5 mM	57.0 °C
	Exon 9F Exon 9R	GGCAGCAACAAAATTGTACG ACTGACCCTGGATCATTTGC	325	1.5 mM	57.0 °C
	Exon 10F Exon 10R	CTCCCAAATCTGGTGAGTCG CAGTTCAACAGTTGTTCTCAACC	387	1.5 mM	57.0 °C
	Exon 11F Exon 11R	CGGTTTATGAATTTTAGGTAAACG ATGAGGCAGGATTCGATGTC	345	1.5 mM	57.0 °C
	Exon 12F Exon 12R	TTGTGAGAGAGGGCTCAGTG CTAACCAACTGCCTGCTTTG	361	1.5 mM	57.0 °C
	Exon 13F Exon 13R	TGTTGGGAATGCTGTGTTTG TTAAAGCATGGCCACATTTC	250	2.5 mM	57.0 °C
LRAT	Exon 1F Exon 1R	TGTTGACCAGGAAAGTCCAG TCCTACCTGCCTCAATTTTAGC	286	1.5 mM	57.0 °C
	Exon 2AF Exon 2AR	TTGCCTTCCTCTCTCCTCAG TGGCCACTTTGACAATAACG	480	1.5 mM	57.0 °C
	Exon 2BF Exon 2BR	ACCTGACCCACTATGGCATC AAGTGGTAGGGGAGGTGTCC	487	1.5 mM	57.0 °C
	Exon 3F Exon 3R	TTGCCTAAGGGATCATTTCTG GCCTTTGTTCTTGGGCTTAC	532	1.5 mM	57.0 °C

Table 6 Primers designed for mutation screening of *RGR* and *LRRC21* genes

Gene	Exon No	Sequence (5`..... 3`)	Product size (bp)	$MgCl_2$	Temp
RGR	Exon 1 F Exon 1 R	TTCACAAAGGCTGCATTGTC CAGGTTCAATTGTCAGAACACC	467	1.5 mM	58.50 °C
	Exon 2 F Exon 2 R	GCATGAAGCATGCTACCCTA TCTGGAATTCAGCCCATTTT	449	2.5 mM	58.50 °C
	Exon 3 F Exon 3 R	CTCCAACGCCTCATAGGAAA GCCTATGCATGCACACTCAC	418	1.5 mM	57.0 °C
	Exon 4 F Exon 4 R	TCAATCCTGTAATCCCAGCAC TTTTTCCAGTCCCACTGTCC	474	1.5 mM	57.0 °C
	Exon 5 F Exon 5 R	TAGCTCCCTGGCTCCTAAAG GTCCACCCTCCCCTCTCTG	467	1.5 mM	61.0 °C
	Exon 6 F Exon 6 R	CCATCTGGTCCCAAGTTCC GAGACGAGGTGGGGGATTAG	448	1.5 mM	57.0 °C
	Exon 7 F Exon 7 R	CCAAGGCTGCAGAACTAAATG CTTGAGTGTAGGGGGCTGTG	464	2.5 mM	57.0 °C
LRRC21	Exon 1 F Exon 1 R	GGACTCCCCTCCCTAATCC CTCGGGCCCATGTGTATAG	508	1.5 mM	57.0 °C
	Exon 2 F Exon 2 R	ATGGCTTGGACTCTGGTGTG GTCTGGCTTGTGGATTGAGC	759	1.5 mM	57.0 °C
	Exon 3 F Exon 3 R	ACTAGCAAGGCAAGGAGCTG AAGCCCCTGTCAAACTCAAC	598	1.5 mM	57.0 °C
	Exon 4A F Exon 4A R	GTTGATACCCTTGGCTGGTC CACACGCCACATACTTGGTC	759	1.5 mM	57.0 °C
	Exon 4B F Exon 4B R	TGTCCTCTACGCGGTCTTTG ACCCCAGGGAAATGGAGAG	757	2.5 mM	61.0 °C

Table 7 microsatellite markers flanking the *PCDH21* gene used to study the haplotype of four members of family A and two sporadic patients

Markers /heterozygosity	Panel/ CM	Colour/size	Position (Mb)	Optimisation Condition	Annealing Temp
1. D10S580	61	FAM/133-143	77.728	1, 2, 3 and 6 with multiplex PCR	60.0 °C
2. D10S1730	59	FAM/232-266	78.601	1, 2, 3 and 6 with multiplex PCR	60.0 °C
3. D10S1686	14	VIC/243-281	85.555	1, 2, 3 and 6 with multiplex PCR	60.0 °C
4. D10S1774	CM	HEX/234-254	86.000	4 and 5 with multiplex PCR	55.0 °C
5. D10S573	CM	HEX/167-175	86.291	4 and 5 with multiplex PCR	55.0 °C
6. D10S1765	59	VIC/169-191	89.591	1, 2, 3 and 6 with multiplex PCR	60.0 °C

Appendix 2

A
RP5
B
RP214
D6S282
D6S257
D6S1695
D6S1711
D6S1710
D6S402
D6S1628
D6S1551
D6S430
D6S1275
D6S1718
D6S254
D6S313
COL9A1
D6S1557
D6S455
D6S1673
stSG6479
D6S421
D6S1681
D6S280
D6S1596
D6S460
D6S445
D6S1609
D6S1627
D6S1595
D6S1601
D6S1644
D6S1613
D6S1570

C
RP167
D6S257
D6S1695
D6S1711
D6S1710
D6S402
D6S1628
D6S1551
D6S430
D6S1275
D6S1718
D6S254
D6S313
COL9A1
D6S1557
D6S455
D6S1673
stSG6479
D6S421
D6S1681
D6S280
D6S1596
D6S460
D6S445
D6S1609
D6S1627
D6S1595
D6S1601
D6S1644
D6S1613
D6S1570

D
RP73
D6S282
D6S257
D6S1695
D6S1711
D6S1710
D6S402
D6S1628
D6S1551
D6S430
D6S1275
D6S1718
D6S254
D6S313
COL9A1
D6S1557
D6S455
D6S1673
stSG6479
D6S421
D6S1681
D6S1609
D6S1627
D6S1595
D6S1601
D6S1644
D6S1613
D6S1570
E
RP299
D6S257
D6S1695
D6S1711
D6S1710
D6S402
D6S1628
D6S1551
D6S430
D6S1718
D6S254
D6S313
COL9A1
D6S1557
D6S455
D6S1673
stSG6479
D6S421
D6S1681
D6S1609
D6S1627
D6S1595
D6S1601
D6S1644
D6S1613
D6S1570

P

P

Pa